Investigating the effects of human Carbonic Anhydrase 1 expression in mammalian cells

Thesis submitted in accordance with the requirements of the University of Liverpool

for the degree of Doctor in Philosophy

by

Xiaochen Liu, BSc, MSc

January 2016

ABSTRACT

Amyotrophic Lateral Sclerosis (ALS) is one of the most common motor neuron diseases with a crude annual incidence rate of ~2 cases per 100,000 in European countries, Japan, United States and Canada. The role of Carbonic Anhydrase 1 (CA1) in ALS pathogenesis is completely unknown. Previous unpublished results from Dr. Jian Liu have shown in the spinal cords of patients with sporadic amyotrophic lateral sclerosis (SALS) there is a significant increased expression of CA1 proteins. The purpose of this study is to examine the effect of CA1 expression in mammalian cells, specifically, whether CA1 expression will affect cellular viability and induce apoptosis. To further understand whether such effect is dependent upon CA1 enzymatic activity, three CA1 mutants (Thr199Val, Glu106Ile and Glu106Gln) were generated using two-step PCR mutagenesis. Also, a fluorescence-based assay using the pH-sensitive fluorophore Pyranine (8-hydroxypyrene-1,3,6-trisulfonic acid) to measure the anhydrase activity was developed. The assay has been able to circumvent the requirement of the specialized equipment by utilizing a sensitive and fast microplate reader and demonstrated that three mutants are enzymatically inactive under the physiologically relevant HCO_3^- dehydration reaction which has not been tested before by others. The data show that transient expression of CA1 in Human Embryonic Kidney 293 (HEK293), African Green Monkey Kidney Fibroblast (COS7) and Human Breast Adenocarcinoma (MCF7) cell lines did not induce significant changes to the cell viability at 36hrs using the Water Soluble Tetrazolium-8 (WST8) assay. Wild-type CA1 significantly reduced cell viability in HEK293 using a virally transduced inducible stable expression system at 96hrs and 144hrs of protein induction whereas out of the two mutants used only Thr199Val induced significant toxicity at 144hrs. Wild-type CA1 has also been found

to protect COS7 cells against doxycycline-induced toxicity at 96hrs and 144hrs of protein induction whereas no protective effect was seen by the mutants. Using flow cytometry analysis the results has shown wild-type CA1 expression significantly increased Caspase-3 activation and its downstream molecule Poly (ADP-Ribose) Polymerase 1 (PARP-1) cleavage at 96hrs whereas Glu106Ile only significantly increased Caspase-3 activation. In conclusion, this study marks the first time where CA1 expression has shown to directly cause significant apoptotic toxicity in HEK293 cells and protect against doxycycline-induced toxicity in COS7 cells. Although the implication of this study in ALS requires further investigation, the results here suggest in healthy cells increased levels of CA1 expression may cause onset of toxicity, whereas when cells undergo stress, increased CA1 expression can be protective to prevent further loss in cell viabilities. Despite numerous previous studies that have examined CA1 as potential diseases marker, these results represent for the first time in understanding the effect of CA1 in mammalian cells.

ACKNOWLEDGEMENTS

First and foremost, I would like to express my gratitude to my supervisors, Dr. Jian Liu and Prof. Samar Hasnain. This thesis would not have been possible without their guidance, suggestions, as well as patience in the past four years. Thank you sincerely for giving me the opportunity to undertake this journey in science.

I would like to express sincerest gratitude to Dr. Tatsuhiko Kadowaki for his time and patience during the past four years in helping me during the experimental stages.

I am grateful for Dr. Ferdinand Kappes for his invaluable help for providing me the DNA plasmids for setting up the inducible stable cell lines as well as his guidance throughout this process.

I am grateful for the help of Dr. Meng Huee Lee for allowing me to conduct experiments using his equipment, his guidance during the experimental stage, as well as lending his valuable reagents and DNA plasmids that were crucial for my experiments. I would like to say thank you to Dr. Minyan Wang for her kindness and allowing me to use her equipment. I would like to express gratitude to Dr. David Ruiz-Carillo, Prof. Zhiliang Lv, and Dr. Hebin Liu for their help and suggestions.

I want to say thank you to the technicians Mr. Deyi Lu, Miss. Qiaoli Feng, Mrs. Yan Zhang, Mr. Ziwen Xie, Mr. Zhongkai Huang and Mrs. Sijing Meng for their time and help.

I want to thank my PhD colleagues in the lab Miss. Xiaoyang Zhang, Mr. Hao Zhang, Mr. Xiaofeng Dong as well as all the other PhD students for their company and help.

I would like to express appreciation for the PhD Scholarship provided by XJTLU and the University of Liverpool which allowed me to pursue this PhD.

Last but not least, I want to thank my parents, Dr. Bo Liu and Dr. Naixia Wang for their love, care and support over the past 26 years and their support during the PhD process. I would also like to thank Miss. Yiran Qian for her love and encouragements when I needed it the most.

TABLE OF CONTENTS

LIST OF FIGURES AND TABLE

SUPPLEMENTARY FIGURE AND LIST OF APPENDICES

GLOSSARY OF ABBREVIATIONS

Abbreviation	Full name
AAZ	Acetazolamide
ALS	Amyotrophic Lateral Sclerosis
bCA2	Bovine Carbonic Anhydrase 2
C9ORF72	Chromosome 9 Open Reading Frame 72
CA	Carbonic Anhydrase
CNS	Central Nervous System
Glu106Ile	Substitution at Glutamine 106 for Isoleucine
Glu106Gln	Substitution at Glutamine 106 for Glycine
FALS	Familial Amyotrophic Lateral Sclerosis
FTLD	Front-temporal Lobe Dementia
FUS	Fused in Sarcoma
LMN	Lower Motor Neuron
PARP-1	Poly (ADP-Ribose) Polymerase 1
Pyranine	8-Hydroxypyrene-1,3,6-Trisulfonic acid
SALS	Sporadic Amyotrophic Lateral Sclerosis
Thr199Val	Substitution at Threonine 199 for Valine
TDP-43	TAR-DNA Binding Protein 43
UMN	Upper Motor Neuron
WST8	Water Soluble Tetrazolium 8
WT	Wild-Type

Theoretical background

Part One: Background to ALS and the proteins involved

Etiology of ALS

Amyotrophic lateral sclerosis (ALS), also known as Lou Gehrig's disease, is the most common and fatal progressive motor neuron diseases (Bruijn et al., 2004). It affects both the upper motor neurons (UMNs) originating from the motor cortex as well as the lower motor neurons (LMNs) in the brainstem and spinal cord (Byrne et al., 2012). ALS is different from other motor neuron diseases which involve only the UMNs (primary lateral sclerosis, hereditary spastic paraplegia) or LMNs (progressive muscular atrophy, spinobulbar muscular atrophy, spinal muscular atrophy) (Gordon et al., 2006, Salinas et al., 2008, Parboosingh et al., 1997, Rowland, 2010). The functions of the LMNs and UMNs are to relay signals from the central nervous system to the skeletal muscles; in humans this is crucial to conduct the everyday functions such as speaking, swallowing, walking and breathing.

Initially, ALS patients show signs of axonal retraction or the denervation of motor neurons, and their axons produce re-innervations as a compensatory mechanism (Hardiman et al., 2011). However, as the disease progresses, this compensatory mechanism fails due to the relentless nature of the disease. At the onset of disease, patients display symptoms of failing to relay signals from the motor cortex, brainstem, and spinal cord to the skeletal muscle tissues resulting in paralysis (Hardiman et al., 2011).

From clinical observations, there is a large variability in the phenotypic displays of ALS. This can be seen from differences in the locations of onset in ALS (Swinnen and Robberecht, 2014). ALS can start in the bulbar region (associated nerves in the medulla oblongata of the brainstem) in some patients (~20% of patients) affecting swallowing and speech due to impairment of the jaw and tongue muscles (Chio et al., 2011). In majority of patients ALS-like symptoms can be first seen in the limbs (~75%) characterized by weakness or atrophy in the arms or the legs, and in few cases (~5%) patients have respiratory onset characterized by shortness of breath affected by atrophy of the intercostal muscles (Rowland and Shneider, 2001). However, as the disease progresses, most patients will have developed all of the ALS-related symptoms including inability to speak or use their upper and lower limbs and eventually death commonly due to the loss of ability to breath (Rowland and Shneider, 2001).

Although ALS was long believed to be a neurodegenerative disorder affecting the motor neurons in isolation, it has increasingly been recognized that other neurological systems can be affected with cognitive impairment being the most common one (Phukan et al., 2007). This cognitive impairment can be caused by degeneration of layer V neurons in the frontal-temporal lobe which is termed front-temporal lobe dementia (FTLD); however, some patients also exhibit cognitive impairment without dementia (Rippon et al., 2006). The clinical manifestation of FTLD is most frequently characterized by delusions, apathy, disinhibition, and language abnormalities (Strong and Yang, 2011). Approximately 25% of all ALS patients have FTLD and patients with ALS-FTLD have worse prognosis than those with pure ALS mainly due to the difficulty in therapeutic compliance (Olney et al., 2005). In other instances, 5-15% of ALS patients have mild parkinsonism characteristics exhibiting postural instability (Manno et al., 2013) and although

rare, some inherited cases of ALS show prominent sensory neurological defect (Andersen et al., 1996), bladder disturbances (Andersen et al., 1996, Battistini et al., 2005) and neuralgic pain syndrome involving severe cramps and joint pains (Andersen et al., 2003) .

The median survival period for ALS is 3 years (with ~60% patients die within 10 years); however, there is a variation in ALS patients' survival times with 15-20% patients surviving between 5 to 10 years after prognosis and a smaller percentage of patients surviving more than 10 years (Kiernan et al., 2011). Prediction of the survival time is dependent on the age of onset (with older ages having worse prognosis outcomes) as well as the presence of bulbar and respiratory onset (Chio et al., 2011, Talbot, 2009). Subjects between ages of 50 to 75 years are within the high risk group for developing ALS, and evidence has suggested above the age of 75 there is reduction in number of patients to develop the disease (Huisman et al., 2011, Logroscino et al., 2010, O'Toole et al., 2008). Incidences of ALS cases with patients below the age of 40 is low (<1.5 cases/100,000 population), an evidence to suggest having significant better prognosis than older patients (Eisen et al., 1993, Sabatelli et al., 2008).

In the western world, the incidence for ALS amongst countries are fairly consistent with a rate of 2-3 cases per 100,000 general population (Mehta et al., 2014, Wolfson et al., 2009, Cetin et al., 2015, Chio et al., 2013, Huisman et al., 2011, Logroscino et al., 2010, O'Toole et al., 2008). Evidence has suggested reduced incidence in mixed race populations with non-European descents (Zaldivar et al., 2009, Cronin et al., 2007). There also exist regions of particularly high incidences of ALS often in the presence of dementia and Parkinsonism in the Pacific island of Guam and the Kii peninsula of Honshu island, Japan (Steele, 2005, Kuzuhara and Kokubo, 2005).

However, there is no clear explanation for the pockets of high ALS incidences (Steele and McGeer, 2008).

Currently the only drug that is approved by the US Food and Drug Administration (FDA) and the European Medicine Agency (EMA) is Riluzole, which has a slight positive effect on the disease prolonging 2-3 months of the patients' survival (Miller et al., 2012). Despite more than 50 randomized clinical trials taken place in the past half century and 18 drugs tested in phase II and III trials, the main form of ALS management is through symptom control to support patients' quality of life (Mitsumoto et al., 2014). These include ventilation support for patients who suffer from respiratory failure as well as nutritional support for patients who are malnourished due to difficulties in swallowing and chewing (Hardiman et al., 2011).

ALS genetics

Superoxide dismutase 1 (*SOD1*)

The SOD1 protein is known as an anti-oxidative enzyme, catalyzing the dismutation of superoxide to hydrogen peroxide and oxygen as well as acting as a nuclear transcription factor activating the expression of anti-oxidative genes (McCord and Fridovich, 1969, Fridovich, 1975, Huang et al., 1992, Tsang et al., 2014, Miao and St Clair, 2009). Eleven missense mutations in *SOD1* were discovered in a linkage study in 1993 in 13 families with ALS (Rosen et al., 1993); so far, over a hundred of *SOD1* mutations have been discovered. SOD1 mutations are responsible for 20% of all FALS cases and 1% of all the SALS cases (Rowland and Shneider, 2001). The

discoveries of these mutations led to the development of *SOD1* transgenic animal models of ALS which has been used to elucidate the molecular mechanisms associated with mutant *SOD1* induced motor neuron degeneration (Bruijn et al., 1997, Wong et al., 1995, Jonsson et al., 2006, Wang et al., 2005). Most of the SOD1 mutations destabilize the protein's conformation through structural reconstruction, causing protein instability and increases the likelihood for it to form aggregates within the motor neurons (Wright et al., 2013, Hough et al., 2004, Prudencio et al., 2009).

Because SOD1 is an anti-oxidative enzyme, one would expect loss of SOD1 function may be central to ALS pathology. However, alterations in the SOD1 enzyme activity do not appear to correlate with ALS disease (Prudencio et al., 2009). This was first seen by knocking out the wild-type SOD1 gene in mice that do not display motor neuron disease characteristics (Reaume et al., 1996). In addition, another study has found both elevating and eliminating the level of wild-type SOD1 did not have an impact on motor neuron loss (Bruijn et al., 1998). High levels of mutant SOD1 proteins in the brain have been found in transgenic mice expressing the G93A mutant which developed ALS pathological and clinical patterns similar to human ALS (Gurney et al., 1994). These studies suggest mutant SOD1 proteins have a gain-of-function type of toxicity in ALS (Gurney et al., 1994).

The range of toxic mechanisms associated with mutant SOD1 is large and these associated pathways affect motor neurons and neighboring glial cells (Boilee et al., 2006, Yamanaka et al., 2008). Mutant protein production within the motor neurons appears to be the primary factor for inducing the onset of ALS. One of the earliest findings in mutant SOD1 mouse

model as well as samples from ALS patients is excessive motor neuron firing due to glutamate excitotoxicity. Overstimulation of the motor neurons can lead to depletion of intracellular ATP stores and upregulation of calcium influx both of which can potentially lead to downstream motor neuron death (Van Den Bosch et al., 2006, Henneberry et al., 1989). Mutant SOD1 also generate ER stress by binding to ER luminal polypeptide chain binding protein (BiP) activating downstream ER stress transducers as well as inhibiting ER-associated degradation by binding to ER luminal protein Derlin-1 (Nishitoh et al., 2008, Kikuchi et al., 2006). Within the mitochondria, mutant SOD1 proteins have been found to deposit onto the cytoplasmic surface of the mitochondrial outer membrane (Liu et al., 2004, Vande Velde et al., 2008). They associate with the mitochondrial protein Bcl-2, turning previously a non-toxic protein into a toxic one and compromising mitochondrial structural integrity by releasing cytochrome C (Pedrini et al., 2010, Pasinelli et al., 2004). Axonal transport of motor neuron cell body synthesized components to axons and synaptic junctions are also compromised by mutant SOD1 expression as it slows both retrograde and anterograde transports, but upregulates retrograde transport of cell death signaling factors (Williamson and Cleveland, 1999, Perlson et al., 2009). Within motor neurons, mutant SOD1 can inhibit the clearance of damaged proteins by “overloading” the proteasome degradation pathway in the ER which not only increases the level of mutant SOD1 aggregates but also sequesters important cellular components causing further toxicity (Bruijn et al., 1998, Kabashi et al., 2004). Apart from these mentioned pathways, mutant SOD1 have been found to interact with the components of motor neuron secretory vesicles causing the extracellular release of mutant SOD1 (Urushitani et al., 2006). This consequently activated nearby microglial cells, the macrophages responsible for the innate immunity in the spinal cord, releasing pro-

inflammatory cytokines and free radicals, which ultimately causes neuronal cell death (Zhao et al., 2010).

The damage occurring in motor neurons through these pathways are primarily responsible for the onset of the disease; however, toxicity induced by mutant SOD1 in the neighboring astrocytes and microglial cells are the culprits for ALS disease progression (Boilee et al., 2006, Yamanaka et al., 2008)). Removal or reduction in mutant SOD1 levels in the microglial cells greatly improved disease progression in transgenic mice (Beers et al., 2006, Boillée et al., 2006). Indeed, it has been found that increased reactive oxygen species production as well as activation of unfolded protein response within microglial cells are associated with mice expressing mutant SOD1 (Jaronen et al., 2013, Wu et al., 2006a). On the other hand, astrocytes expressing mutant SOD1 release reactive oxygen species which promote motor neuron death (Nagai et al., 2007, Marchetto et al., 2008). Furthermore, mutant SOD1 expression significantly reduces glutamate receptor subunit GluR2 expression in astrocytes in neighboring motor neurons which protect motor neuron from glutamate toxicity (Van Damme et al., 2007). Mutant SOD1 expression in the astrocytes can also disrupt mitochondrial functions within the astrocytes themselves as well as the neighboring motor neurons. There have been large advances in research surrounding the pathology of mutant SOD1 protein in ALS since its first discovery. The wide multitude of pathological pathways associated with mutant SOD1 in ALS has not only implicated motor neuron itself but also the surrounding glial cells which have helped the understanding the mechanism of ALS onset and progression.

TAR-DNA Binding protein (*TARDBP*)

TARDBP encodes for TDP-43 expression which localizes primarily in the nucleus but can also be found in the cytoplasm, shuttling between the two subcellular compartments (Chen-Plotkin et al., 2010). Studies have shown TDP-43 predominantly functions as a RNA pathway regulator (Lee et al., 2011). Indeed, it has been identified that TDP-43 binds to a large number of RNA species in the mouse brain transcriptome (6,304 protein encoding genes) (Polymenidou et al., 2011b, Tollervey et al., 2011). TDP-43 mediates the splicing of its RNA targets either by itself or interaction with other splicing proteins (Tollervey et al., 2011, Polymenidou et al., 2011a). Furthermore, TDP-43 has been shown to regulate mRNA stability and turn-over (Strong et al., 2007, Volkening et al., 2009), participate in axonal RNA transport (Alami et al., 2014), function as a part of the Drosha microRNA processing complex (Ling et al., 2010), and repressed transcription via its N-terminal RNA recognition motif (RRM) (Lalmansingh et al., 2011).

In 2006, it was found that TDP-43 protein aggregates are present in ubiquinated cytoplasmic inclusions in motor neurons of sporadic ALS and FTD patients (Neumann et al., 2006). This led to the discovery of mutations in *TARDP* in patients with FALS and SALS. Since then the current prevalence of ALS patients with *TARDBP* mutations is found to be ~3% of FALS cases and ~1.5% SALS cases (Kabashi et al., 2008, Iida et al., 2012, Daoud et al., 2009, Sreedharan et al., 2008). These breakthrough discoveries gave new ground to ALS research outside of mutant-SOD1 related pathogenesis and raised the question what impact RNA processing has on ALS disease mechanisms.

On the whole, TDP-43 accumulates in the cytoplasm of neurons as cleaved, phosphorylated, rounded inclusions and is associated with neurodegeneration (Brettschneider et al., 2013). The TDP-43 proteinopathy can be first seen in the brainstem, the spinal cord and the motor cortex; then it diffuses throughout the brain and CNS possibly through the axonal transport system (Brettschneider et al., 2013). The TDP-43-containing inclusions not only accumulated the normal, full length TDP-43, but also the phosphorylated 45kDa species, as well as ubiquitylated high molecular weight and C-terminal truncated low molecular fragments. In addition, neuronal cells containing these inclusion bodies are prone to degeneration (Neumann et al., 2006, Pamphlett and Kum Jew, 2008). However, further studies have shown there is no correlation between the numbers of TDP-43 aggregates with *in vivo* neuronal death (Igaz et al., 2011, Miguel et al., 2011). On the other hand, it has been postulated that conformation changes to TDP-43 within the inclusion bodies causes pathological changes in ALS (Neumann et al., 2006). Nonetheless, whether TDP-43 aggregates cause neuronal degeneration or simply a marker of neurotoxic stress is unclear.

Mutations in the TDP-43 nuclear localization signal (NLS) cause mislocalization of TDP-43 to the cytoplasm, and this has been linked to neurodegeneration in cells and transgenic mice (Barmada et al., 2010, Igaz et al., 2011, Winton et al., 2008). Furthermore, mutating the TDP-43 NLS motif in *Drosophila melanogaster* worsened the retinal degeneration and reduced the life-span that was associated accumulation of cytoplasmic TDP-43 aggregates (Miguel et al., 2011). Although cytoplasmic accumulation was more toxic in the *Drosophila* model, nuclear accumulation of TDP-43 was also toxic as a recent study has shown overexpression of nuclear TDP-43 can be responsible for neurotoxicity (Suzuki et al., 2015). Since TDP-43 normally

localizes to euchromatin domains, including perichromatin fibrils and nuclear speckles, some nuclear mislocalization could also confer possible neurotoxic effect due to overexpression of nuclear TDP-43 (Casafont et al., 2009). Therefore, both cytoplasmic and nuclear accumulation of overexpressed TDP-43 proteins can be toxic in animal models; however, the gain of toxic function requires further work to elucidate the associated mechanistic importance of cytoplasmic versus nuclear TDP-43.

Loss of TDP-43 function has also been linked to neurodegeneration in several studies. Knockdown of TDP-43 has been found to reduce neurite growth and cell viability as well as induce apoptosis in neuron-like cell lines (Ayala et al., 2008, Iguchi et al., 2009). Furthermore, TDP-43 knockout mice were embryonic lethal and post-natal knockout of TDP-43 resulted in rapid death of mice (Chiang et al., 2010, Sephton et al., 2010, Kraemer et al., 2010). In post-mitotic neurons, partial loss of TDP-43 due to heterozygous knockout and microRNA knockdown resulted in neurodegeneration which eventually led to paralysis and death (Yang et al., 2014, Kraemer et al., 2010). Due to the fact that TDP-43 binds to the 3' UTR within its own mRNA transcript and is able to downregulate the level of its mRNA transcripts, overexpression of TDP-43 in the cytoplasm and nucleus was found to decrease levels of TDP-43 protein in cells and transgenic mice (Polymenidou et al., 2011b, Tollervey et al., 2011, Igaz et al., 2011, Winton et al., 2008). Whether this contributes to nuclear clearance of TDP-43 in human is not known. On the other hand, depletion of nuclear TDP-43 can lead to increased aggregation of TDP-43 proteins which can further deplete nuclear TDP-43 by sequestering free TDP-43 and downregulate TDP-43 mRNA transcript from producing new TDP-43 in the nucleus, leading to a cycle of gain and loss of functions in the cell. Mutations in the TDP-43 nucleic acid binding RRM

domains has been found to prolong protein half-life and are resistant to both heat-induced unfolding and aggregation, and thus represent a more stable protein which lead to faster disease progression due to elevated protein longevity (Austin et al., 2014; Kabashi et al., 2008). This is in stark contrast with SOD1 mutant aggregates which are thought to arise from increased exposure of hydrophobicity regions due to protein instability (Wang et al., 2008; Tiwari et al., 2005; Münch and Bertolotti, 2010).

Due to the large number of RNA targets interacting with TDP-43, the possible toxicity requires the consideration of its normal function within the cell, and possible abnormal new activities from its abnormal mutants as well as its cellular localization. Thus, many pathways may be involved in TDP-43 mediated neurotoxicity by both gain and loss of functions. It is likely that they are not mutually exclusive.

Fused in sarcoma (*FUS*)

Following the discovery of *TARDBP* mutations in ALS, mutations in the *FUS* gene were identified in FALS patients. The mutated FUS proteins were found in cytoplasmic inclusions in lower motor neurons and in spinal cords of FALS patients (Kwiatkowski et al., 2009, Vance et al., 2009). The FUS proteins have been known to shuttle between the nucleus and cytoplasm; however, similar to TDP-43, it resides largely in the nucleus (Lagier-Tourenne et al., 2010). FUS plays similar roles as TDP-43 (Sephton et al., 2011), and is responsible for RNA alternative splicing (Rogelj et al., 2012), required for efficient mRNA translation (Schwartz et al., 2012) and regulates transcription (Yasuda et al., 2013). The gene accounts for 3-5% in FALS cases and 0.7-

0.9% in SALS (Rademakers et al., 2010, Chio et al., 2009, Ticozzi et al., 2009, Corrado et al., 2010). Although the percentage of ALS patients associated with *FUS* mutation may seem insignificant, the functional similarities it shares with TDP-43 generated excitement in the field.

Pathology studies have revealed patients carrying *FUS* mutations are characterized by FUS-positive immune-reactive inclusions within the cytoplasm with no indication of TDP-43-positive and ubiquitin-positive aggregates that are associated with large percentage of ALS cases (Kwiatkowski et al., 2009, Vance et al., 2009). Studies have also suggested that FUS may act in the downstream pathway of TDP-43 which may explain the lack of TDP-43 pathology in patients with *FUS* mutations as wild-type FUS proteins could rescue *TARDBP* knockout but not vice versa, supporting the consensus view that FUS plays similar roles as TDP-43 (Kabashi et al., 2011, Wang et al., 2011b). However, the picture is more complicated than it seems as it has been noted that RNA targets of FUS are distinct from TDP-43, suggesting their pathways may diverge during RNA process (Lagier-Tourenne et al., 2012).

Like TDP-43, whether FUS confers toxicity via a gain or loss of function is unclear as mutations within the *FUS* nuclear localization signal (NLS) causing accumulation of FUS proteins within the cytoplasm do not always correlate with its corresponding *FUS* mutations in ALS patients (Dormann et al., 2010, Mackenzie et al., 2010). Genome-wide association studies have identified thousands of RNA targets have shown large abnormal RNA processing patterns due to *FUS-knockdown* (Lagier-Tourenne et al., 2012, Colombrita et al., 2012). A recent study has highlighted a simultaneous gain and loss of RNA processing functions conferred by *FUS* mutations in cells (Sun et al., 2015). It has shown that *FUS* mutations enhanced its interaction

with the SMN (spinal muscular atrophy) protein affecting its localization and function both in the nucleus and the cytoplasm. On the other hand, the same corresponding *FUS* mutations lead to reduction in its interaction with the U1-snRNP complex, leading to the reduced RNA processing ability (Sun et al., 2015).

Hexanucleotide repeat expansion in *C9ORF72*

In 2011, it was discovered a long hexanucleotide repeat (GGGGCC) in the first intron of the *C9ORF72* (Chromosome 9 Open Reading Frame 72) was linked to both ALS and FTD (DeJesus-Hernandez et al., 2011, Renton et al., 2011). The locus was previously linked to ALS-FTD patients through linkage and genome-wide association studies (GWAS); however, it was only when next generation, deep sequencing was used in parallel with the linkage analysis that *C9ORF72* repeat expansion was discovered responsible (DeJesus-Hernandez et al., 2011). The number of repeats in healthy controls ranges between 2 to 19, whereas in the patients there can be as few as 20 repeats and as much as 1600 repeats (DeJesus-Hernandez et al., 2011). Recently, it appears that small sized expansion (around 70 repeats) may signify a "pre-mutation" which can expand in the offspring (Xi et al., 2015). The repeat expansion accounts for ~7% of SALS patients with European ancestry and ~40% of FALS patients, the largest percentages in all of ALS genetic etiologies (DeJesus-Hernandez et al., 2011, Renton et al., 2011).

The discovery of the *C9ORF72* locus sparked series of new research; however, its pathologic mechanism remains unknown. The formation of RNA foci has been found in the brain and spinal cord patients with the *C9ORF72* repeat expansion (DeJesus-Hernandez et al.,

2011). One study has suggested the repeat expansion may confer its toxicity through toxic gain of functions, as knocking down the *C9ORF72* gene has shown improvement in motor neuron survival *in vitro* (Sareen et al., 2013). A recent study has shown by knocking out the *C9ORF72* gene in mice do not cause motor neuron degeneration suggesting that the loss of protein function is not responsible for the toxicity (Koppers et al., 2015b). The formation of RNA foci found in ALS patients may cause toxicity through RNA splicing dysregulation (Cooper-Knock et al., 2015).

Furthermore, in the brain tissues of ALS patients with *C9ORF72* repeat expansions contain protein inclusions that contains dipeptide proteins produced from *C9ORF72* repeat-associated, non-ATG-mediated translation (RAN mediated, translation of all reading frames of the GGGGCC expansion) (Mori et al., 2013). These dipeptides can be toxic, inducing apoptosis in the neuronal cells causing neurodegeneration (May et al., 2014). Moreover, it was found that specifically the arginine containing peptides caused neurodegeneration as seen in *Drosophila* (poly-GR and poly-PR proteins), not the non-arginine containing dipeptides (poly-GA and poly-PA) (Mizielinska et al., 2014, Kwon et al., 2014, Wen et al., 2014). It has also been shown the dipeptides expression significantly reduced the levels of soluble Unc19 proteins and the amount of insoluble Unc19 proteins in patients with the *C9ORF72* repeat expansion increased (May et al., 2014). This may lead to loss of Unc19 function which is important in maintaining motor neuron integrity (Knobel et al., 2001). The presence of repeat expansions can also sequester RNA binding proteins hindering cellular RNA metabolism. One study showed the expression of the repeat expansion induced neurodegeneration in *Drosophila*, by interacting

with the RNA-binding protein Purα forming inclusions which can affect its role in RNA transport (Xu et al., 2013).

The current trending view regarding how *C9ORF72* orchestrated pathology in ALS comes from the recent reports showing that both *C9ORF72* RNA repeat expansions and dipeptide repeat proteins might contribute towards ALS pathology through disruption of the nucleocytoplasmic transport system. Zhang *et al* (2015) have shown the *C9ORF72* hexanucleotide RNA repeats preferentially bind to the RanGAP1 proteins in neuronal cells and brain tissues derived from *C9ORF72* ALS patients, this disrupts RanGAP1 function which are required for the efficient nucleocytoplasmic transport leading to impairment in nuclear transport of proteins and neurodegeneration in *Drosophila* (Zhang et al., 2015b). Similar results from the Freibaum *et al* (2015) study identified 18 genetic modifiers that are components of nucleocytoplasmic transport that strongly enhanced *C9ORF72* repeat expansion mediated neurodegeneration in *Drosophila* (Freibaum et al., 2015). Furthermore, defect in RNA export was identified in *Drosophila* models expressing the RNA repeat expansions, as well as *C9ORF72* ALS patients. Moreover, this study has identified the dipeptide proteins were also highly toxic in the *Drosophila* models. Study done by Jovicic *et al* (2015) supports that toxicity induced by *C9ORF72* expansions do not only come from RNA repeats by showing that arginine-containing dipeptide species confer toxicity in yeast models supporting the findings from the previous studies (Mizielinska et al., 2014, Jovicic et al., 2015, Wen et al., 2014, Kwon et al., 2014). Furthermore, using a yeast genetic screening approach they have identified significant enrichment of genes participating in nucleocytoplasmic transport which enhanced *C9ORF72*-mediated toxicity in yeast. Similarly to the Zhang *et al* study, they have identified genes

encoding components within the Ran-GTPase-dependent protein trafficking (as does RanGAP1) responsible for the marked decrease of protein nuclear import in neurons derived from *C9ORF72* repeat expansion carriers (Jovicic et al., 2015, Zhang et al., 2015b)

The aforementioned studies indicate a gain of toxicity conferred by *C9ORF72* repeat expansions and this has been further supported by the recent transgenic mouse model with 66 *C9ORF72* repeat expansions showing key features of ALS/FTD including TDP-43 pathology, motor deficits and behavioral abnormalities (Chew et al., 2015). Loss of C9ORF72 protein functions has also been suggested to contribute to ALS. Studies have suggested the C9ORF72 protein is involved in the endosomal trafficking of proteins particularly in autophagy and endocytosis (Farg et al., 2014). It was found that DNA hyper-methylation in the 5' end of repeat expansions can occur which may lead to loss of C9ORF72 protein expression (Xi et al., 2014). As the C9ORF72 autophagy function is crucial for cellular functions, its loss may lead to disturbances in the protein degradation pathways which can cause aggregation of TDP-43 proteins (Thomas et al., 2013). As C9ORF72 protein has been detected around the synaptic region in *C9ORF72* repeat expansion affected ALS brain tissues, its loss of function could affect synaptic vesicle transport (Snowden et al., 2012). Conversely, the data from neuronal specific *C9ORF72 knockout* mice has suggested loss of *C9ORF72* function on its own do not cause ALS as these mice did not display motor defects or other phenotypes associated with ALS (Koppers et al., 2015a). Although this suggests ablation of *C9ORF72* may not contribute to the onset of the disease, its loss of function in ALS disease progression is not known.

Other genes associated with ALS

Several other genes have been implicated in ALS that explain ≤2-3% of FALS and SALS cases. In 2010, through exome sequencing it was found that 1-2% of patients have mutations in *VCP* (Valosin containing protein) (Johnson et al., 2010). VCP protein is a chaperone which degrades abnormally folded and damaged proteins to ensure optimal protein quality in the cell, this in turn has been implicated in cellular pathways such as apoptosis, autophagy, and cell membrane fusion (Seguin et al., 2014, Wójcik et al., 2004, Asai et al., 2002, Ju et al., 2009, Latterich et al., 1995). Within the same year, mutations in *OPTN* (Optineurin) were found in FALS and SALS patients mainly restricted to Japanese and Italian ethnic groups (Maruyama et al., 2010). Recent evidence has shown optineurin is important in mitophagy of damaged mitochondria through induction of autophagosome formation (Wong and Holzbaur, 2014). However, whether this process is associated with ALS pathology remains unclear.

In 2011, *UBQLN2* (Ubiquilin 2) mutations were identified in X-linked FALS cases, where ubiquilin 2 mutants disrupts the ubiquitin-proteasome system leading to accumulation of ubiquitinated proteins as a result of the slower protein degradation (Deng et al., 2011). Similarly, another gene coding for *SQSTM1* (Sequestome 1) also known as ubiquitin-binding protein p62 which is also involved in the ubiquitin-proteasome system, has been linked to both SALS and FALS cases (Fecto et al., 2011). Sequestome 1 protein directly interacts with important mediators in the ubiquitin-proteasome degradation pathway, and inhibition of the sequestome 1 protein led to accumulation of ubiquitinated proteins (Seibenhener et al., 2004). Both ubiquilin 2 and sequestome 1 regulate proteasome degradation of ubiquitinated proteins which

shows similarities with the functions of VCP and optineurin proteins, highlighting the importance of this pathway in ALS (Seibenhener et al., 2007, Deng et al., 2011). Interestingly, like *VCP* and *OPTN,* mutations in *SQSTM1* have also been associated with Paget's disease of the bone; however, it is unclear whether there is any overlap with ALS (Hocking et al., 2002, Albagha et al., 2010, Weihl et al., 2009).

The discovery of *PFN1* (Profilin 1) mutations segregating with several large ALS families implicated the cytoskeletal pathway as a novel mechanism in ALS (Wu et al., 2012). Profilin 1 is essential for the monomeric conversion of (G)-actin to the filamentous (F)-actin and the expression of Profilin 1 mutants had significantly reduced actin conversion. This led to decreased axonal outgrowth and smaller growth cones with abnormal morphology (Wu et al., 2012). This cytoskeletal defect has also been implicated in mutation in the *DCTN1* (Dynactin 1) gene through the linkage study (Puls et al., 2003). Dynactin is required to activate and tether the motor protein dynein to vesicles, organelles, proteins and RNA for retrograde transporting these molecules along the microtubule from the synapses back to the neuronal cell bodies (Gill et al., 1991). Disruption of the dynactin-dynein relationship causes motor neuron degeneration and ALS characteristics such as muscular weakness, abnormal gait and trembling in transgenic mice (LaMonte et al., 2002).

Non-genetic causes of ALS

Although several clear genetic factors have been identified in ALS, the role which environmental risk factors play in ALS-related neurodegeneration is undeniable. Despite a large

amount of studies done on this subject, there has not been a clear causal relationship identified between environmental risk factors and ALS. However, despite the difficulties associated with identifying potential environmental factors (such as variability in their effects, study designs that require long-term follow-ups, high financial cost and time required, recall and referral biases), research has identified several potential environmental causes for ALS (Al-Chalabi and Hardiman, 2013). Among them, high level of fitness is the most discussed risk factor for ALS due to the popularity gained from Lou Gehrig – a famous professional baseball who developed ALS as well as media reports of professional athletes developing the disease (Brennan, 2012). A recent population-based study which recruited 636 SALS patients and 2166 controls shows that it is the predisposition to leisure time physical activity not occupational physical activity or vigorous physical activity (i.e. marathons and triathlons) is significantly associated with ALS (Huisman et al., 2013). Therefore, how significant physical activity is associated with ALS required further investigation.

On the other hand, occupational hazards linked ALS and Gulf War veterans due to the higher than expected ALS incidence in the veterans (Haley, 2003). Subsequent compilation of the literature shows that there is an association between Gulf War deployment and ALS (Medicine, 2006). Other evidence show an increased ALS risk in many branches of the US armed forces except the Marine Corps (Weisskopf et al., 2005).

Several studies have identified smoking as a risk factor for ALS (Nelson et al., 2000, de Jong et al., 2012). One case-control study has failed to find any association between smoking and ALS (Yu et al., 2014), and a meta-analysis only found an increased risk of ALS in female

smokers and weak overall association between smoking and ALS (Alonso et al., 2010). Furthermore, a pooled analysis of five population cohorts did not show dose-response relationship between smoking duration and amounts with risk of ALS (Wang et al., 2011a). Therefore, whether smoking is a true risk factor for ALS needs further studies.

Part Two: Carbonic Anhydrase – its biological function and role in human diseases

The biological functions of the carbonic anhydrases (CA)

Carbon dioxide (CO_2) is a key metabolite in all living organisms. It is generated by respiration which needs to be expelled from the lungs in mammals and a key resource for plants to produce energy via photosynthesis.

CO_2 is stored as the bicarbonate ion (HCO_3^-) during photosynthesis and carbonic acid (H_2CO_3) during respiration; this is due to the characteristic of CO_2 being easily diffusible and the need for it to be hydrated into H_2CO_3 or HCO_3^- to be trapped inside the cell for transportation (Coleman, 2000). Both photosynthesis and respiration processes need to convert HCO_3^- or H_2CO_3 back into CO_2 to be used either for energy production or to be released as waste. At 25^oC, the rate constant for the reversible CO_2 hydration is 3.5 X 10^{-2} /s which is relatively slow in the absence of a catalyst (Lindskog and Coleman, 1973). The enzyme carbonic anhydrase (CA) catalyzes both the hydration and dehydration reactions in the neutral pH range and increases the reaction constants to between 10^5 to 10^6/s without changing the equilibrium constant for the reactions (Lindskog and Coleman, 1973, Koenig and Brown, 1972). This function of CA is

crucial in maintaining the physiological metabolic states in organisms involving the processes that transport H_2CO_3 and HCO_3^- for energy production, or utilize CO_2 and HCO_3^- as substrates for enzymatic reactions for the generation of fluids to maintain the physiological pH of the organism.

CA was first discovered in 1933 in the red blood cells of cows (Meldrum and Roughton, 1933). Since then, it has been found to be ubiquitous in all mammalian tissues, algae, plants and bacteria (Smith et al., 1999). CA is a large group of zinc-metalloenzymes and catalyzes more than one chemical reaction; however, the most important physiological reaction is the reversible reaction of CO_2 hydration ($CO_2 + H_2O \leftrightarrows HCO_3^- + H^+$) as it directly influences the cellular pH equilibrium (Imtaiyaz Hassan et al., 2013). Other than the CO_2 hydration/HCO_3^- dehydration reaction that CA carry out, there are several other reactions catalyzed by CA (Supuran et al., 2003). However, the CO_2 hydration/HCO_3^- dehydration reaction is the only one that is known to have physiological relevance, therefore it is considered the only physiological reaction that CA are involved (Supuran et al., 2003).

Not only ubiquitous across a vast number of species, CA are abundant and concentrated in certain tissues. In mammals there is around 1 to 2g of CA per 1 liter of red blood cells (Keilin and Mann, 1940). These enzymes are relatively stable, water soluble, and retain activities over a pH range of 6 to 10 (Maren, 1967).

In mammalian tissues, CA participates in a large variety of biological functions including acid-base balance, respiration, calcification, and the formation of aqueous humor, saliva, cerebro-spinal fluid and gastric acid (Imtaiyaz Hassan et al., 2013). Since this enzyme catalyzes

the reactions involving HCO_3^- ions and H^+, it plays a key role in regulating pH in the body of the organism (Effros et al., 1978).

Members of the CA family

There are three evolutionary unrelated CA families designated α-, β-, and γ-CA. These families have no significant sequence homologies but all are zinc-bound enzymes carrying out the same reactions (Hewett-Emmett and Tashian, 1996). Sixteen genetically distinct α-CA isozymes have been discovered in mammals, thirteen of which are enzymatically active (Pan et al., 2007). Five of the thirteen isoforms are localized in the cytoplasm (CA1, CA2, CA3, CA7, CA13), five are GPI-anchored to plasma membranes of specialized epithelial and endothelial cells (CA4, CA9, CA12, CA14, CA15), two are located in the mitochondria (CA5A, CA5B), and one is secreted (CA6) (Pan et al., 2007). CA2 (previously known as CA C) is the most studied isoform. It is distributed widely across many different organs and cell types. It is one of the fastest acting CA isoforms with a CO_2 hydration turnover rate of 10^6/s at 25^{o}C (Sly and Hu, 1995).

Two major forms of CA are found in humans: CA1 (previously known as CA B) and CA2. With a maximal CO_2 hydration turnover at $2.2x10^5$/s at 25^{o}C, CA1 is of lower activity than CA2; however, CA1 is the major non-hemoglobin protein in the human red blood cells where it was estimated to contain six times the amount of CA1 compared to CA2(Ren and Lindskog, 1992). CA have been implicated in a wide variety of physiological and pathological processes. They contribute to the acid-base balance in renal tubular cells by supporting H^+ secretions during urinary acidification (Sato et al., 1990), H^+ generation in the gastric parietal cells to generate

gastric acid (Rangachari, 2007), HCO_3^- secretion in the pancreatic juice from the pancreatic duct cells (Nishimori and Onishi, 2001, Nishimori et al., 1999) as well as contributing to the HCO_3^- content in salivary secretions (Parkkila et al., 1997). They also affect the CO_2 and HCO_3^- exchange associated with kidney HCO_3^- resorption (Purkerson and Schwartz, 2006), accelerate the removal of CO_2 in the pulmonary capillaries in the lungs (Crandall and O'Brasky, 1978), promote organs such as the heart, brain and skeletal muscles to be rid of CO_2 waste from their metabolic processes (Ghandour et al., 1992, Geers and Gros, 2000). Furthermore, the mitochondrial CA are involved in lipogenesis and gluconeogenesis in the hepatocytes, and inhibition of these CA are possible drug targets for obesity (Dodgson and Cherian, 1990, Supuran et al., 2008, Lynch et al., 1995).

Indeed, the wide range of physiological roles that CA play allow them to be potential clinical targets for epilepsy, glaucoma, osteoporosis, obesity, cancer as well as their recent implications in infectious diseases and Alzheimer's disease (Supuran, 2011). At present, CA inhibitors are widely used in treating glaucoma, gastric ulcers, and osteoporosis; furthermore, they are used as diuretics as well as anti-epileptic agents (Supuran, 2008, Supuran, 2011). On the other hand, though CA activators have long been studied, their potential as therapeutic agents has yet to be investigated in clinical settings. However, studies have shown their possible roles in enhancing synaptic efficiency in Alzheimer's disease, aging and other diseases which require memory and spatial learning (Pastorekova et al., 2004, Sun and Alkon, 2002).

Although CA inhibitors can be very effective drugs, severe side effects can follow the treatment due to inhibition of CA in other tissues such as the kidney, stomach and red blood

cells (Tawil et al., 1993, Supuran and Scozzafava, 2002). However, several advances have been made in this field in which effective inhibitors have been developed that can be given at the site of affected area (i.e. topically) rather than given systematically (Mincione et al., 1999). Indeed, it is worth considering given the ubiquitous presence of CA across the human body the importance of using topically active CA inhibitors not just for the treatment of glaucoma but also for other diseases to prevent unwanted side-effects. Given the large number of CA isoforms in the human body, it is crucial to develop inhibitors that target specific CA isoforms. This is possible through better understanding of the similarities and differences between the different isoforms and more importantly, their catalytic inhibitory mechanisms.

CA1 gene expression and physiological function

CA1 is located on chromosome 8q22 with neighboring genes *CA2* and *CA3*, in the order of *CA1, CA3, and CA2.* These genes cluster together in a stretch of around 180kb of DNA, with *CA1* situated around 80kb away from the other two CA (Edwards et al., 1986, Andersson et al., 1972, Lowe et al., 1991). *CA1* differs from other *CA* genes (*CA2, CA3, CA4, CA7*) in that rather than being divided into seven exons, *CA1* contains two noncoding exons 1a and 1b, lying 5' to the translation start site (Lowe et al., 1990). The *CA1* gene codes for a protein of 261 amino acids. CA1-expressing cells show a high level of *CA1* gene methylation while non-expressing cells exhibit partial methylation. However, the differences in methylation may be coincidental and do not directly affect gene expression (Lowe et al., 1990). Polymorphic variants of *CA1* gene have been identified in populations from Japan, Australia, and Philippines with no abnormal

phenotypes reported with these individuals (Goriki et al., 1980, Kageoka et al., 1981, Jones and Shaw, 1982, Omoto et al., 1981).

CA1 is a cytosolic protein and has been found to be distributed ubiquitously in humans; however, it is particularly abundant in the red blood cells and the gastrointestinal (GI) tract (Supuran, 2008). Along with CA2, CA1 was found to be expressed at high levels in the epithelial cells in the human colon, as well as being expressed in the majority of sub-epithelial capillaries along the entire GI tract (Lonnerholm et al., 1985).

In the GI tract CA1 is believed to facilitate the CO_2 release from metabolic active cells (Christie et al., 1997), as well as play important roles in the alkalization/acidification of the luminal content of the colon by secreting HCO_3^- through the HCO_3^-/Cl^- exchanger (Lonnerholm et al., 1985, Parkkila et al., 1994). Interestingly, CA1 expression was found to be significantly reduced in patients with colorectal cancer, where better prognosis is associated with those with more CA1 present (Mori et al., 1993). Also, reduced levels of CA1 have also been found in the colons of patients with ulcerative colitis, possibly affecting the Na^+/Cl^- ion absorption and HCO_3^- secretions (Fonti et al., 1998). CA1 was also found to be the only CA isoform expressed in the α-cells of the endocrine Langerhans islets in the pancreas; however, its function in the pancreas remains unknown (Parkkila et al., 1994).

The highest amount of CA1 in humans is found in the red blood cells. Though being more than five times the amount of CA2 in these cells (Supuran et al., 2003), CA1 contributes to 50% of the total CA activity in red blood cells due to being the much less active isoform (Supuran et al., 2003). The physiological role of CA1 in red blood cells appears to be uncertain.

In the 1970s, individuals with trace amounts of CA1 (inherited deficiency of CA1) were identified and they appeared healthy at the time of investigation with no abnormal phenotypes (Kendall and Tashian, 1977). Under normal physiological levels of chloride and HCO_3^-, the CO_2 hydration activity of CA1 is reduced by 92% (Maren et al., 1976), with CA1 being one of the isozymes with comparatively low enzyme activity the importance of CA1 function under physiological conditions remains unclear (Sly and Hu, 1995, Supuran et al., 2005). It has been presumed that other CA isoforms can compensate for its lack in CA1 deficient cases (Sly and Hy, 1995, Supuran et al., 2005).

CA1 and CA2 are the only isoforms known to be present in erythrocytes sharing 62.3% sequence identity (Supuran, 2008) (Figure 1.1). It can be presumed that CA1 possible can compensate for the loss of CA2 when CA2 are absent. Indeed, in patients with CA2-deficiency, it was found that they do not express abnormal erythrocyte functions and expresses a higher level of CA1 which can be attributed to CA1 compensating for the absence of CA2 in the red blood cells (Sly et al., 1983). However, in tissues where CA1 levels are low and CA2 functions are more significant, the absence of CA2 is much more critical to the cellular functions, with patients presenting osteoporosis, renal tubular acidosis and brain calcification as the primary symptoms in CA2-deficient individuals (Sly et al., 1983).

```
CA1       MASPDWGYDDKNGPEQWSKLYPIANGNNQSPVDIKTSETKHDTSLKPISVSYNPATAKEI
CA2       -MSHHWGYGKHNGPEHWHKDFPIAKGERQSPVDIDTHTAKYDPSLKPLSVSYDQATSLRI
            * .*** .:****:* * :***:*:.******.*  :*:* ****:****: **: .*

CA1       INVGHSFHVNFEDNDNRSVLKGGPFSDSYRLFQFHFHWGSTNEHGSEHTVDGVKYSAELH
CA2       LNNGHAFNVEFDDSQDKAVLKGGPLDGTYRLIQFHFHWGSLDGQGSEHTVDKKKYAAELH
          :* **:*.*:*:*.::::******:. :***:******** : :*******  **:****

CA1       VAHWNSAKYSSLAEAASKADGLAVIGVLMKVGEANPKLQKVLDALQAIKTKGKRAPFTNF
CA2       LVHWNT-KYGDFGKAVQQPDGLAVLGIFLKVGSAKPGLQKVVDVLDSIKTKGKSADFTNF
          :.***: **.:.:*..: *****:*:::***.*:* ****:*.*::****** * ****

CA1       DPSTLLPSSLDFWTYPGSLTHPPLYESVTWIICKESISVSSEQLAQFRSLLSNVEGDNAV
CA2       DPRGLLPESLDYWTYPGSLTTPPLLECVTWIVLKEPISVSSEQVLKFRKLNFNGEGEPEE
          **  ***.***:******** *** *.****: ** *******: :**.*  * **:

CA1       PMQHNNRPTQPLKGRTVRASF-
CA2       LMVDNWRPAQPLKNRQIKASFK
           * .* **:**** * ::***
```

Figure 1.1 Protein sequence alignment between CA1 and CA2. Identity match is at 62.3% between the two isoforms. Clustal Omage was used for the alignment. ***** indicates positions with fully conserved residue. **:** indicates strong conservation between groups. **.** Indicates weak conservation between groups

The enzymatic mechanism of CA1

The crystal structure of CA1 molecule is approximately ellipsoidal, with a dimension of 41 X 41 X 47 Å measured from the extreme points of the backbone (Kannan et al., 1975). The active site comprises a funnel-shaped dead-end cavity about 12 Å deep leading to the center of the molecule where the zinc ion is located (Kannan et al., 1975).

The predominant make-up for the CA1 secondary structure is the large β-pleated sheet, consisting of 10 chain-segments which take up about 40% of all the CA1 residues. The core of CA1 is formed by 5 chains, with the active site and zinc ligand situated in them (Figure 1.2) (Kannan et al., 1984).

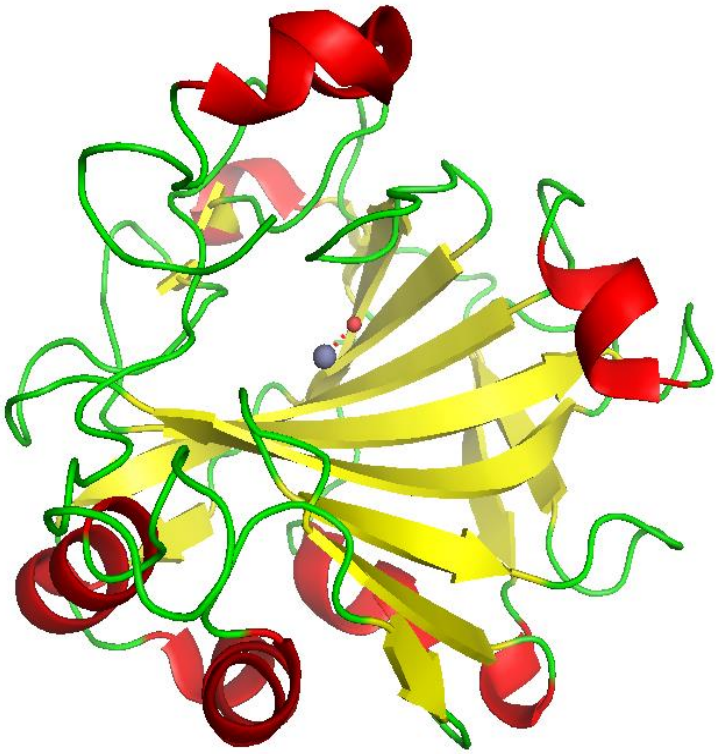

Figure 1.2. Schematic drawing of the CA1 protein. Red and yellow colors represent the helices and β-structure, respectively. The grey sphere in the middle is the zinc ion essential for CA1 catalytic activity and is coordinated to a water molecule represented by the red sphere. Red dashed lines represent co-ordinations around zinc. Image drawn from Brookhaven protein data bank file (file name – 3W6I). The figure was generated and rendered using Pymol.

The zinc is coordinated to the three nitrogen atoms from His94, His96, and His119, with the fourth ligand site filled by a water or hydroxide ion (OH^-) (Figure 1.3) (Kannan et al., 1984). The three histidine residues and the hydroxide ion form a distorted tetrahedral geometry around the zinc molecule with the zinc-bound hydroxide ion (Zn^{2+}-OH^-) as the eliciting a nucleophilic attack on CO_2. The histidine ligands are further hydrogen-bonded to the "second shell" of residues as the indirect ligands surrounding the protein-metal binding sites (Lesburg and Christianson, 1995). These indirect ligands contribute to the protein-metal affinity in the

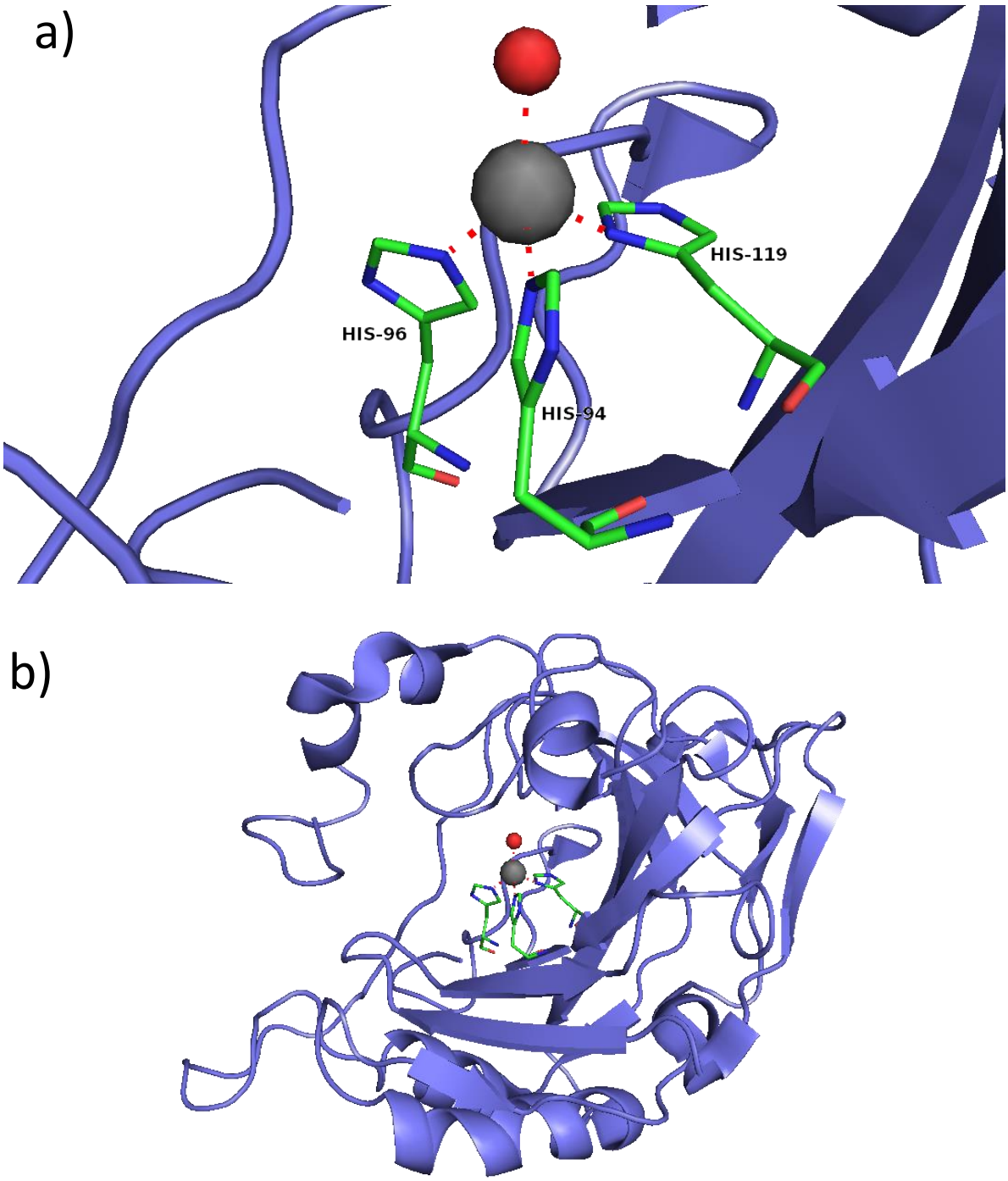

Figure 1.3. Zinc-bound histidines and water in the CA1 active site. a) The histidines and water form tetrahedral geometry around the zinc molecule; b) zoomed out drawing showing centrally placed CA1 active site. Grey and red spheres represent zinc and water, respectively. Red dashed lines represent co-ordinations around zinc. Image drawn from Brookhaven protein data bank file (file name – 3W6I). The figure was generated and rendered using Pymol.

tetra-cooridinate metal site. The metal-binding ligands and the "second shell" residues which include 10 amino acids are invariant across all α-CA. They either contribute directly to the catalytic activity of CA or help to stabilize the protein structure and that of the catalytic core (Lindskog, 1997).

The mechanism of mammalian CA activity has been studied in depth and is believed to involve three distinct steps (Silverman and Lindskog, 1988, Lindskog et al., 1984). In the first two steps, CO_2 bound to the active site and the zinc-bound OH^- elicit nucleophilic attacks on the CO_2 which then forms the metal bound HCO_3^- and eventually gets replaced by H_2O and released into the reaction medium. In the third step, the active site is regenerated by an intramolecular proton transfer from zinc-bound H_2O to the edge of the protein generating OH^-, resuming nucleophilicity of the active site (Figure 1.4).

$$\text{Step 1: E-Zn}^{2+}\text{-OH}^- + CO_2 \leftrightarrows \text{E-Zn}^{2+}\text{-HCO}_3^-$$

$$\text{Step 2: E-Zn}^{2+}\text{-HCO}_3^- + H_2O \leftrightarrows \text{E-Zn}^{2+}\text{-H}_2O + HCO_3^-$$

$$\text{Step 3: E-Zn}^{2+}\text{-H}_2O \leftrightarrows \text{E-Zn}^{2+}\text{-OH}^- + H^+$$

Figure 1.4. Equations showing the principles of the CA reversible hydration of CO_2. Note that the above reactions can be reversed in the other direction using protons and HCO_3^- ions as substrate to generate CO_2. "E-Zn^{2+}" representing the enzyme.

The proton transfer from the active site to the reaction medium is the rate-limiting step of the process (Steiner et al., 1975), though other studies have suggested the rate limiting step is when the nucleophilic zinc-bound OH^- ion attacks CO_2 (Mauksch et al., 2001). The residues

Glu106, Thr199, Tyr7, His64, His67, His200, and H243 in CA1 play an important role in mediating the proton transfer as well as the preceding step by forming a hydrogen-bond network (Kumar and Kannan, 1994, Kannan et al., 1977).

CA1 possesses four histidine residues for the proton transfer process (His64, His67, His200 and His243) (Briganti et al., 1997) (Figure 1.5). These four histidine residues are buried deep within the active site (unlike CA2 which has a "histidine cluster" that assists the proton transfer) which explains it being one of the low-activity CA in the family (Briganti et al., 1997).

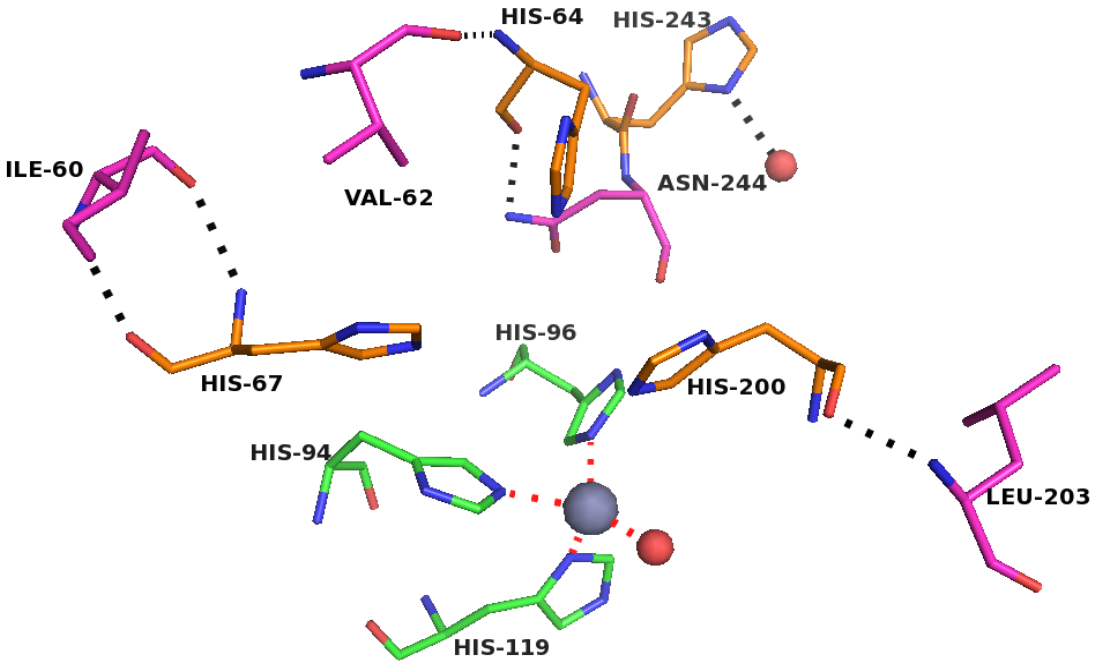

Figure 1.5. The four histidines assisting proton transfer in CA1. Schematic drawing of the four histidines are colored orange/blue/red alongside the zinc-bound histidines and water. Residues hydrogen bonded to the four histidines are colored pink/blue/red. Blue and red spheres represent zinc and water, respectively. Red and black dashed lines represent co-ordinations around zinc and hydrogen bonds between residues and a water molecules, respectively. Image drawn from Brookhaven protein data bank (file name – 3W6I). The figure was generated and rendered using Pymol.

As mentioned above, the zinc ion is bound to three histidine residues, and further bonded to a water molecule under low pH (pH less than 7) or to a OH^- ion in high pH (pH greater than 7) (Eriksson et al., 1988a, Eriksson et al., 1988b). The hydrogen bond is formed between zinc-bound water (or OH^- ion) and Thr199 as well as between Thr199 and Glu106 (Kannan et al., 1984, Merz, 1990) (Figure 1.6). Studies have shown that Thr199 is known to stabilize the correct orientation of the hydrogen atom in the zinc-bound OH^- ion to allow CO_2 moving to the active site (Merz, 1990). Glu106 further stabilizes Thr199 which allows CO_2 to react with the OH^- ion.

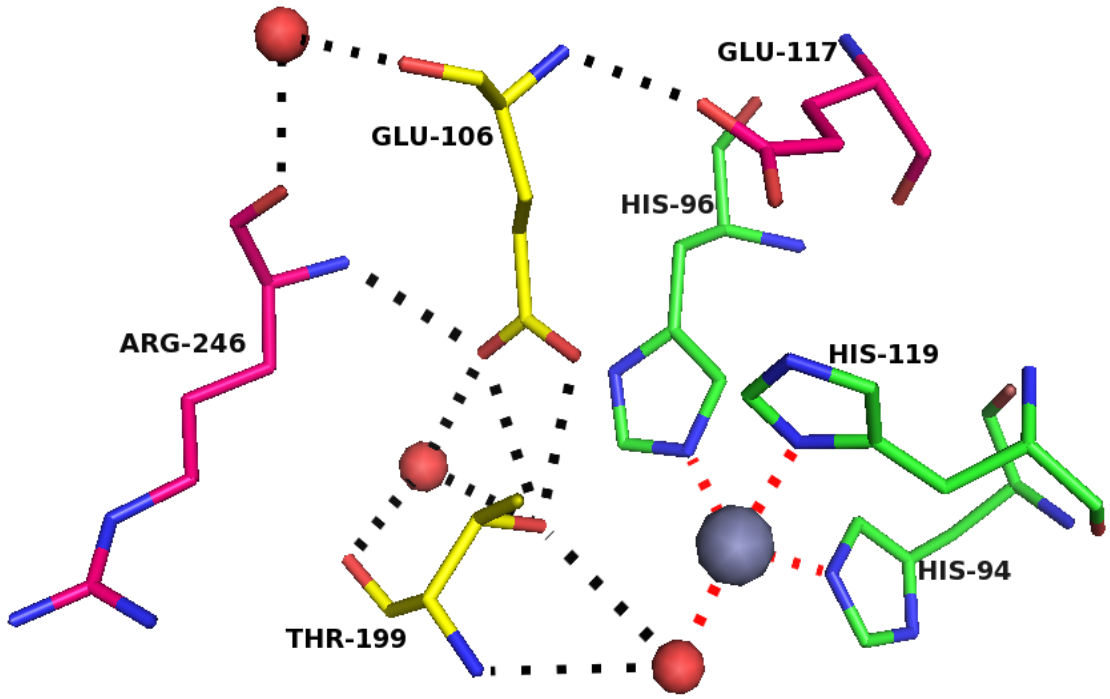

Figure 1.6. Thr199 and Glu106 residues in CA1. The two residues are colored yellow/blue/red alongside its hydrogen bonded waters, zinc-bound histidines and water. Residues hydrogen bonded to the four histidines are colored pink/blue/red. Blue and red spheres represent zinc and water molecules, respectively. Red and black dashed lines represent co-ordinations around zinc and hydrogen bonds between residues and water molecules, respectively. Image drawn from Brookhaven protein data bank (file name – 3W6I). The figure was generated and rendered using Pymol.

There is evidence demonstrates that Thr199-Glu106 residues are important in the CA catalytic function. Both Glu106 and Thr199 residues play important roles in helping the transition of the HCO_3^- ion into a much more stabilized intermediate while bound to the zinc ion after the reaction between CO_2 and the OH^- ion has occurred (Bottoni et al., 2004). On the other hand, Tyr7 does not seem to have a large effect on the activity of CO_2 reversible hydration (Mikulski et al., 2011, Liang et al., 1993).

As indicated by the above reactions, HCO_3^- ions and the OH^-/water bound to the active site are interchangeable (Xue et al., 1993b). When HCO_3^- replaces OH^-/H_2O, it accepts a hydrogen bond from the Thr199 residue which in turn is hydrogen bonded to Glu106 (Kumar and Kannan, 1994, Xue et al., 1993b). In this way, Thr199 and Glu106 act as hydrogen-bond donors and select the HCO_3^- ions as substrates to bind to the zinc ion.

Role of CA in the nervous system

The presence of CA activity in the nervous system was found many years ago, where it held important physiological roles (Ashby, 1948). These roles include HCO_3^- transport and metabolism to maintain neuronal extracellular (Shah et al., 2005) and intracellular pHs (Casey et al., 2009, Svichar et al., 2009) regulation of extracellular (Fedirko et al., 2007) and intracellular ion concentrations (Ghandour et al., 2000), propagation of neuronal activity through CO_2 metabolism (Sapirstein et al., 1984), and generation of HCO_3^- to be utilized for fatty acid biosynthesis used for neuronal function (Tansey et al., 1988) (Table 1.1).

CA isoform	Localization in nervous system cell types	Roles in the nervous system	Citations
CA2	Astrocytes, oligodendrocytes, sensory neurons, myelin	Removal of CO_2/HCO_3^- waste, maintenance of neuronal chloride levels, regulation of intracellular pH	Kumpulainen et al., 1983, Langley et al., 1980, Roussel et al., 1979, Kimelberg et al., 1982, Snyder et al., 1983, Neubauer et al., 1991, Kazimierczak et al., 1986, Peyonnard et al., 1986, Robertson and Grant, 1989, Aldskogius et al., 1988, Wong et al., 1983
CA4	Cerebral capillary endothelial cells	Regulate CO_2/HCO_3^- exchange between brain and plasma	Ghandour et al., 1992
CA5	Astrocytes, neurons	Fatty acid synthesize, gluconeogenesis, calcium homeostasis	Ghandour et al., 2000, Panov et al., 2014, Yu et al., 1983
CA14	Neurons	Modulates excitatory synaptic transmissions	Parkkila et al., 2001

Table 1.1 Distribution and role CA in the nervous system

CA2 appears to be the predominant isoform of CA in the central nervous system due to its abundancy and presence in various neuronal cell types (Giacobini, 1962). Indeed, when individuals with CA2-deficiency were discovered, one of their key characteristics was mental

retardation due to cerebral calcification (Sly et al., 1983). It was first suggested that the CA2 enzymes are mainly situated in the glial cells, with very little activity in the neurons, showing 120 times more CA activity in the glial cells than neurons (Giacobini, 1961, Giacobini, 1962). The localization of CA2 in the subtypes of glia cells has been controversial. Subsequent studies have shown that CA2 reside exclusively in the oligodendrocyte cells (Kumpulainen et al., 1983, Langley et al., 1980), whereas others have shown that CA2 activity can be seen in both astrocytes and oligodendrocytes (Roussel et al., 1979, Kimelberg et al., 1982). However, it appears that the CA activity in astrocytes is much lower than that of oligodendrocytes (Snyder et al., 1983).

Although it was believed human neuronal cells do not contain CA proteins (Maren, 1967), studies have shown otherwise (Ghandour et al., 2000, Parkkila et al., 2001, Neubauer et al., 1991). Evidences have suggested presence of CA2 in the human, mice and rat sensory neurons of the peripheral nervous system and detected overall CA activity in the sensory neurons (Neubauer et al., 1991, Kazimierczak et al., 1986, Peyonnard et al., 1986, Robertson and Grant, 1989, Aldskogius et al., 1988, Wong et al., 1983). Although the exact neurophysiological function of CA2 in the neurons is unknown, it has been postulated that it is used for removal of CO_2 and HCO_3^- produced in the decarboxylation reactions when making neurotransmitters (Severinghaus et al., 1969), maintaining levels of chloride ions in neuronal cells for GABA neurotransmission (Pasternack et al., 1993), and more importantly regulation of intracellular pH due to changes in high glycolytic activities as well as in calcium influx in the neurons (Deitmer et al., 2014, Wong et al., 1983).

The mitochondrial isoform CA5 was found in neuronal and astrocytic cells of the cerebellum, cerebral cortex, hippocampus, sciatic nerve and the spinal cord (Ghandour et al., 2000). In the astrocytes, the mitochondrial CA5 provides HCO_3^- for the pyruvate carboxylase to carry out fatty acid synthesize and gluconeogenesis which are important for energy metabolism in the brain (Panov et al., 2014, Supuran et al., 2008, Yu et al., 1983). Similarly, CA2 in the oligodendrocytes assists acetyl-CoA carboxylase to synthesize fatty acids used in myelin formation which is the primary function of oligodendrocytes (Tansey et al., 1988, Baumann and Pham-Dinh, 2001). Due to the absence of pyruvate carboxylase in the neurons fatty acid synthesis and gluconeogenesis might not be its main roles, the function of CA5 in the neurons have been postulated (Ghandour et al., 2000). Similar to CA2, CA5 was thought to regulate calcium ion concentration in neurons as well as assist GABA transmission through the production of HCO_3^- (Ghandour et al., 2000). Furthermore, this study has also highlighted that the different subcellular localized CA isoforms have their specific roles in the nervous system. Indeed, the membrane-associated CA4 was shown to be located in the endothelial cells of the cerebral capillaries which is associated with the blood-brain barrier (Ghandour et al., 1992). The functional significance of CA4 at this specific site may be to assist exchanges of CO_2 and HCO_3^- between the brain and its circulating blood plasma (Ghandour et al., 1992).

A more recent study demonstrated the presence of CA14 in the mouse brain and similar patterns of expression were seeing in the human brain (Parkkila et al., 2001). This study shows strong staining of CA14 in the pons medulla as well as positive staining in the hippocampus, cerebellar cortex, pyramidal tract, choroid plexus and corpus callosum, therefore a widespread expression pattern is seen. This study has further suggested CA14 modulates the excitatory

synaptic transmissions (Parkkila et al., 2001). Interestingly, this study implicates the expression of a CA isozyme within the motor system as CA14 is found to express in the midbrain and pyramidal tract. Another study has shown administration of sulthiame, a relative CA14-sensitive inhibitor, significantly increased the motor cortex motor threshold in humans reducing the axonal excitability (Siniatchkin et al., 2006).

There have been studies focusing on the presence of CA activity in the motor system (neurons involved in the innervation of muscle fibers); these studies observed the overall CA activity therefore there was no indication which CA isoform was responsible for the observed activity. In the spinal nerves as well as nerves of the peripheral nervous system innervating the muscle fibers, the majority of these studies using animal tissues (mice, rabbits and rats) show CA reside primarily in the sensory neurons rather than the motor neurons, and have shown actual immuno-staining of CA in sensory neurons that have been widely used to distinguish these nerves from motor neurons (Szabolcs et al., 1991, Riley et al., 1988, Oswald and Riley, 1987, Sanger et al., 1991, Wilke et al., 1992, Macias et al., 1998). However, these studies also show a less degree of the CA presence in the motor neurons. The difference between the distribution of CA in motor and sensory neurons varied across studies, with some reporting proportionally more CA in the motor neurons (Riley and Lang, 1984, Riley et al., 1988, Sanger et al., 1991, Oswald and Riley, 1987) than other studies (Szabolcs et al., 1991, Macias et al., 1998, Wilke et al., 1992). In a few studies it has been found that CA primarily reside in the small gamma motor neurons (Riley et al., 1984, Peyronnard et al., 1986).

Furthermore, CA activities found in the cytoplasm of intramuscular nerves in rat soleus muscles (Riley et al., 1982). They also play important roles in skeletal muscle contraction in frogs (Scheid and Siffert, 1985). Human subjects treated with the non-competitive CA inhibitor, acetazolamide (Verpoorte et al, 1967), were found to display diminished neuromuscular reflex (Brechue et al., 1997).

There have been very few studies that have indicated that CA1 is expressed in the nervous system; however, their presence in the mammalian nervous system is clear. It was shown that CA1 is present in the nerve fibers of the rat carotid body – a chemoreceptor which senses changes in CO_2 as well as pH in the environment (Yamamoto et al., 2003). This finding is consistent with the previous evidence showing CA activity in the sensory nerves in the peripheral nervous system and nerves of the dorsal root ganglia (Riley et al., 1988, Oswald and Riley, 1987, Szabolcs et al., 1991, Sanger et al., 1991). Further evidence linking CA1 to neuronal sensory functions comes from a study in a family with inactive erythrocyte CA1 (Shapira et al., 1974). The individuals in the family presented nerve deafness as well as renal tubular acidosis which was in contrast with a previous study showing individuals with no erythrocyte CA1 activity was asymptomatic (Kendall and Tashian, 1977). In addition, it the study also demonstrated that inactive CA1 was associated with functional defects of sensory nerves as nerve deafness is directly affected by the vestibulocochlear nerve – a cranial nerve within the peripheral nervous system (Sanders and Gillig, 2010).

Direct evidence of the presence of CA1 in the central nervous system comes from a study showing an increased expression of CA1 in the frontal cortex of patients with depression

using a proteomic approach (Johnston-Wilson et al., 2000). Due to the nature of the techniques used it was not possible to highlight the localization of CA1 within the specific cell-types (Johnston-Wilson et al., 2000). This result sheds light on the pathway in which the use of CA inhibitor acetazolamide significantly improves patients with bipolar disorder in clinical trial (Hayes, 1994). This study also highlights the need for determining the presence of CA1 activity in other areas of the brain for potential therapeutic targets.

Furthermore, a recent study has shown an increased expression of CA1 in the cerebral astrocytic inclusions from resected tissues of patients with pediatric epileptic seizures (Visanji et al., 2012). Thus, it appears that similar to CA2, CA1 could be present among multiple subtypes of neuronal and non-neuronal cells within the nervous system.

CA1 and human disease

CA1 has been implicated in a variety of diseases which include Alzheimer's disease (Korolainen et al., 2006), epilepsy (Visanji et al., 2012), thyroid diseases (Yoshida et al., 1991, Mondrup, 1980), colorectal cancer (Bekku et al., 2000, Wang et al., 2012, Mori et al., 1993), ulcerative colitis (Fonti et al., 1998), lung cancer (Chiang et al., 2002), ankylosing spondylitis (Chang et al., 2012, Chang et al., 2010, Zheng et al., 2012), diabetes (Gambhir et al., 2007, Torella et al., 2014), pancreatitis (Kino-Ohsaki et al., 1996, Frulloni et al., 2000), prostate cancer (Takakura et al., 2012), and chronic myeloid disorder (Bonapace et al., 2004). Among these studies, the levels and activities of CA1 in the affected individuals compared to their corresponding healthy individuals vary amongst different diseases (i.e. in some diseases CA1

levels are higher and in others lower), therefore it is not known what the role of CA1 is in disease pathology as a whole. The variety and number of affected tissue types implicated with changes in CA1 expression indicate that it is possible that CA1 plays much more significant roles in disease than it appears and therefore deserves closer attention.

In 2007, a study has shown that there was significant elevated CA1 expression in the vitreous fluid samples collected from patients with diabetic related retinopathy (Gao et al., 2007). Injecting CA1 into rat vitreous fluid increased retinal vascular permeability via activation of kallikrein-kinin pathway and the contact pathway (Gao et al., 2007). Furthermore, it was found injecting CA1 into the subdural space of the rat brain induced blood-brain barrier permeability (Gao et al., 2007). These are significant findings in that: 1) it has implied CA1 and its downstream pathway as potential new drug targets for treating diabetic related retinopathy; 2) it has identified a previously unknown link between CA1 and the contact system which suggests there are significant roles of CA1 that are yet to be discovered which will directly affect human pathophysiology; 3) it has been suggested the presence of CA1 can be destructive to tissue function specifically activating the inflammatory contact system due to CA1-induced alkalinization. As indicated by the authors, using CA1-selective inhibitors may be one viable therapeutic approach (Supuran et al., 2003).

Potential role of CA1 in motor neuron degeneration in ALS

The increased level of serum CA3 protein has been reported in many studies in patients with ALS and other neuromuscular disorders (Ohta et al., 1991, Osterman et al., 1985, Hibi et al.,

1984, Vaananen et al., 1988). CA3 has the lowest enzyme activity in the CA family (Krishnamurthy et al., 2008) and shares 54.05% and 58.46% sequence identity to CA1 and CA2, respectively (Figure 1.7). However, as CA3 is a cytosolic form of CA which resides primarily in the type I muscle fibers (Shima et al., 1983), this phenomenon is likely due to muscular damage associated with the neuromuscular diseases and thereby leakage of CA3 proteins into the blood stream rather than neurodegeneration.

```
CA3       -MAKEWGYASHNGPDHWHELFPNAKGENQSPVELHTKDIRHDPSLQPWSVSYDGGSAKTI
CA1       MASPDWGYDDKNGPEQWSKLYPIANGNNQSPVDIKTSETKHDTSLKPISVSYNPATAKEI
CA2       -MSHHWGYGKHNGPEHWHKDFPIAKGERQSPVDIDTHTAKYDPSLKPLSVSYDQATSLRI
            : .*** .:***::* : :* *:*:.****::.*   ::* **:* ****: .::  *

CA3       LNNGKTCRVVFDDTYDRSMLRGGPLPGPYRLRQFHLHWGSSDDHGSEHTVDGVKYAAELH
CA1       INVGHSFHVNFEDNDNRSVLKGGPFSDSYRLFQFHFHWGSTNEHGSEHTVDGVKYSAELH
CA2       LNNGHAFNVEFDDSQDKAVLKGGPLDGTYRLIQFHFHWGSLDGQGSEHTVDKKKYAAELH
          :* *:: .* *:*. ::::*:***:   *** ***:**** : :*******  **:****

CA3       LVHWNP-KYNTFKEALKQRDGIAVIGIFLKIGHENGEFQIFLDALDKIKTKGKEAPFTKF
CA1       VAHWNSAKYSSLAEAASKADGLAVIGVLMKVGEANPKLQKVLDALQAIKTKGKRAPFTNF
CA2       LVHWNT-KYGDFGKAVQQPDGLAVLGIFLKVGSAKPGLQKVVDVLDSIKTKGKSADFTNF
          :.***  **  : :* .: **:**:*:::*:*  :  :* .:*.*: ****** * **:*

CA3       DPSCLFPACRDYWTYQGSFTTPPCEECIVWLLLKEPMTVSSDQMAKLRSLLSSAENEPPV
CA1       DPSTLLPSSLDFWTYPGSLTHPPLYESVTWIICKESISVSSEQLAQFRSLLSNVEGDNAV
CA2       DPRGLLPESLDYWTYPGSLTTPPLLECVTWIVLKEPISVSSEQVLKFRKLNFNGEGEPEE
          **  *:* . *:*** **:* **  *.:.*:: ** ::***:*: ::*.*  . * :

CA3       PLVSNWRPPQPINNRVVRASFK
CA1       PMQHNNRPTQPLKGRTVRASF-
CA2       LMVDNWRPAQPLKNRQIKASFK
           :  * ** **:: * ::***
```

Figure 1.7 Protein sequence alignment between human CA3 to CA1 and CA2. CA3 shares 54.05% identity with CA1 and 58.46% with CA2. Clustal Omage was used for the alignment. * indicates positions with fully conserved residue. : indicates strong conservation between groups. . indicates weak conservation between groups

Other studies linking CA with motor defects include mice deficient in CA8 or alternatively name carbonic anhydrase-related protein (CARP) show motor dysfunctions

(Lamont and Weber, 2015) and movement ataxia (Aspatwar et al., 2014). Despite CA8 localize to the cytoplasm, it has no CA enzyme activity due to its lacks histidines to coordinate the zinc ion (Aspatwar et al., 2014). It shares around 30-40% amino acid sequence identity with other mammalian CA (Skaggs et al., 1993) (Figure 1.8). The motor dysfunction associated with CA8 is

Figure 1.8 Protein sequence alignment between CA8 to CA3, CA1 and CA2. CA8 shares 39.61% identity with CA1, 41.43% with CA2 and 38.98% with CA3. Clustal Omage was used for the alignment. * indicates positions with fully conserved residue. : indicates strong conservation between groups. . indicates weak conservation between groups

due to increased intracellular store calcium release as faulty CA8 unable to inhibit inositol 1,4,5-triphosphate (IP_3) binding to its receptor (Lamont and Weber, 2015). Due to the lack of

literature on the activities of CA enzymes in the motor neurons the question of whether the CA enzyme has a pathophysiological role in ALS is unknown.

In an investigation in 2007, Gruzman et al used the biotinylation technique to detect structural conformers of SOD1; subsequently, CA1 was identified as the protein recognized by the anti-SOD1 antibody after biotinylation (Liu et al, 2010). This study identified the change in CA1 in human ALS spinal cords which has not been previously reported.

Preliminary western blot data shows there is a significantly higher level of CA1 present in ALS patients' spinal cords (Figure 3.1). This indicates that CA1 is possibly involved in the pathogenesis of ALS. In addition, expressing human wild-type CA1 in *Drosophila melanogaster* motor neurons showed deficiencies in locomotion as well as reduced lifespan (Liu et al, unpublished results).

One study conducted in 2013 has shown mice with familial ALS symptoms have progressive acidosis in the CNS tissues during disease development (Dodge et al., 2013). Since CA modulates pH levels in the mammalian CNS, the role of CA was investigated through acetazolamide (the most widely used CA inhibitor) administration in these mice (Chesler, 2003). Acetazolamide significantly decreased limb strength in the ALS mice up to ~75 days from the beginning of the experiment; however, the limp strengths were similar between acetazolamide administered and untreated group from ~80 days to ~120 days (Dodge et al., 2013). There was also a significant earlier onset of paralysis and decrease in rate of survival in acetazolamide treated ALS mice (Dodge et al., 2013). Since acetazolamide has been established to be

membrane permeable, it likely inhibited intracellular CA including but not limited to CA1 (Maren, 1967).

There has been little indication from the literature regarding the role CA1 expression in the mammalian nervous system. It has been shown that there was a strong immunostaining for CA1 in rat carotid nerve bundles (Yamamoto et al., 2003). However, no evidence has been shown whether CA1 proteins are expressed in human motor neurons or its possible roles in the nervous system. It has been shown that CA is involved in the formation and flow of cerebrospinal fluid and high CO_2 hydration activity in the glial cells of mammalian central nervous system, but whether CA1 is specifically involved in these processes is unknown (Maren, 1967, Giacobini, 1962).

The aim of this project is to bring further understanding into the effect of CA1 in mammalian cells - whether CA1 expression will modify the cellular viability and survival. To accomplish this, transient CA1 expression system was used to monitor changes to cell viability changes in three mammalian cell lines. The straightforward nature of the transient expression system was done to test whether CA1 expression is able to induce significant effect in cell survival within a shorter time period in the initial study.

Virally transduced inducible stable CA1 expression was also used to observe whether CA1 caused changes to cell viability in a longer time period, and the inducible expression prevented any potential CA1-associated toxicity during setting up the stable cell lines.

To observe whether CA1 enzyme activity is involved in any cell viability changes, a fluorescence-based enzyme assay was developed utilizing a sensitive and fast micro-plate

reader and the pH-sensitive fluorescent dye Pyranine to monitor CA1 activity. This was done to avoid the use of specialized equipment needed in other CA activity assays and to monitor the activity changes in the previously untested CA1 mutants using this technique.

The basis for this study comes from a lack of understanding in the role of CA1 in ALS and previously unpublished results from Dr. Liu showing increased CA1 expression in the spinal cords of ALS patients. By observing whether CA1 expression has an effect on mammalian cell viability takes the first step in understanding the role of CA1 in ALS and human.

References:

AL-CHALABI, A. & HARDIMAN, O. 2013. The epidemiology of ALS: a conspiracy of genes, environment and time. *Nat Rev Neurol,* 9**,** 617-628.

ALAMI, N. H., SMITH, R. B., CARRASCO, M. A., WILLIAMS, L. A., WINBORN, C. S., HAN, S. S. W., KISKINIS, E., WINBORN, B., FREIBAUM, B. D., KANAGARAJ, A., CLARE, A. J., BADDERS, N. M., BILICAN, B., CHAUM, E., CHANDRAN, S., SHAW, C. E., EGGAN, K. C., MANIATIS, T. & TAYLOR, J. P. 2014. Axonal transport of TDP-43 mRNA granules in neurons is impaired by ALS-causing mutations. *Neuron,* 81**,** 536-543.

ALBAGHA, O. M., VISCONTI, M. R., ALONSO, N., LANGSTON, A. L., CUNDY, T., DARGIE, R., DUNLOP, M. G., FRASER, W. D., HOOPER, M. J., ISAIA, G., NICHOLSON, G. C., DEL PINO MONTES, J., GONZALEZ-SARMIENTO, R., DI STEFANO, M., TENESA, A., WALSH, J. P. & RALSTON, S. H. 2010. Genome-wide association study identifies variants at CSF1, OPTN and TNFRSF11A as genetic risk factors for Paget's disease of bone. *Nat Genet,* 42**,** 520-4.

ALDSKOGIUS, H., ARVIDSSON, J. & HANSSON, P. 1988. Carbonic anhydrase enzyme histochemistry of cranial nerve primary sensory afferent neurons in the rat. *Histochemistry,* 88**,** 151-154.

ALONSO, A., LOGROSCINO, G. & HERNAN, M. A. 2010. Smoking and the risk of amyotrophic lateral sclerosis: a systematic review and meta-analysis. *J Neurol Neurosurg Psychiatry,* 81**,** 1249-52.

ANDERSSON, B., NYMAN, P. O. & STRID, L. 1972. Amino acid sequence of human erythrocyte carbonic anhydrase B. *Biochem Biophys Res Commun,* 48**,** 670-7.

ANDERSEN, P. M., FORSGREN, L., BINZER, M., NILSSON, P., ALA-HURULA, V., KERANEN, M. L., BERGMARK, L., SAARINEN, A., HALTIA, T., TARVAINEN, I., KINNUNEN, E., UDD, B. & MARKLUND, S. L. 1996. Autosomal recessive adult-onset amyotrophic lateral sclerosis associated with homozygosity for Asp90Ala CuZn-superoxide dismutase mutation. A clinical and genealogical study of 36 patients. *Brain,* 119**,** 1153-72.

ANDERSEN, P. M., SIMS, K. B., XIN, W. W., KIELY, R., O'NEILL, G., RAVITS, J., PIORO, E., HARATI, Y., BROWER, R. D., LEVINE, J. S., HEINICKE, H. U., SELTZER, W., BOSS, M. & BROWN JR, R. H. 2003. Sixteen novel mutations in teh Cu/Zn superoxide dismutase gene in amyotrophic lateral sclerosis: a decade of discoveries, defects and disputes. *Amyotrophic Lateral Sclerosis & Other Motor Neuron Disorders,* 4**,** 62.

ASAI, T., TOMITA, Y., NAKATSUKA, S.-I., HOSHIDA, Y., MYOUI, A., YOSHIKAWA, H. & AOZASA, K. 2002. VCP (p97) Regulates NFKB Signaling Pathway, Which Is Important for Metastasis of Osteosarcoma Cell Line. *Japanese Journal of Cancer Research,* 93**,** 296-304.

ASHBY, W. 1948. Distribution pattern of carbonic anhydrase in the fetal central nervous system. *Fed Proc,* 7**,** 144.

ASPATWAR, A., TOLVANEN, M. E., ORTUTAY, C. & PARKKILA, S. 2014. Carbonic anhydrase related proteins: molecular biology and evolution. *Subcell Biochem,* 75**,** 135-56.

AUSTIN, J. A., WRIGHT, G. S., WATANABE, S., GROSSMANN, J. G., ANTONYUK, S. V., YAMANAKA, K. & HASNAIN, S. S. 2014. Disease causing mutants of TDP-43 nucleic acid binding domains are resistant to aggregation and have increased stability and half-life. *Proc Natl Acad Sci U S A,*111**,** 4309-14.

AYALA, Y. M., MISTELI, T. & BARALLE, F. E. 2008. TDP-43 regulates retinoblastoma protein phosphorylation through the repression of cyclin-dependent kinase 6 expression. *Proc Natl Acad Sci U S A,* 105**,** 3785-9.

BARMADA, S. J., SKIBINSKI, G., KORB, E., RAO, E. J., WU, J. Y. & FINKBEINER, S. 2010. Cytoplasmic mislocalization of TDP-43 is toxic to neurons and enhanced by a mutation associated with familial amyotrophic lateral sclerosis. *J Neurosci,* 30**,** 639-49.

BATTISTINI, S., GIANNINI, F., GRECO, G., BIBBO, G., FERRERA, L., MARINI, V., CAUSARANO, R., CASULA, M., LANDO, G., PATROSSO, M. C., CAPONNETTO, C., ORIGONE, P., MAROCCHI, A., DEL CORONA, A., SICILIANO, G., CARRERA, P., MASCIA, V., GIAGHEDDU, M., CARCASSI, C., ORRU, S., GARRE, C. & PENCO, S. 2005. SOD1 mutations in amyotrophic lateral sclerosis. Results from a multicenter Italian study. *J Neurol,* 252**,** 782-8.

BAUMANN, N. & PHAM-DINH, D. 2001. Biology of Oligodendrocyte and Myelin in the Mammalian Central Nervous System. *Physiological Reviews,* 81**,** 871-927.

BEERS, D. R., HENKEL, J. S., XIAO, Q., ZHAO, W., WANG, J., YEN, A. A., SIKLOS, L., MCKERCHER, S. R. & APPEL, S. H. 2006. Wild-type microglia extend survival in PU.1 knockout mice with familial amyotrophic lateral sclerosis. *Proc Natl Acad Sci U S A,* 103**,** 16021-6.

BEKKU, S., MOCHIZUKI, H., YAMAMOTO, T., UENO, H., TAKAYAMA, E. & TADAKUMA, T. 2000. Expression of carbonic anhydrase I or II and correlation to clinical aspects of colorectal cancer. *Hepatogastroenterology,* 47**,** 998-1001.

BOILLEE, S., YAMANAKA, K., LOBSIGER, C. S., COPELAND, N. G., JENKINS, N. A., KASSIOTIS, G., KOLLIAS, G. & CLEVELAND, D. W. 2006. Onset and progression in inherited ALS determined by motor neurons and microglia. *Science,* 312**,** 1389-92.

BONAPACE, G., IULIANO, F., MOLICA, S., PETA, A. & STRISCIUGLIO, P. 2004. Cytosolic carbonic anhydrase activity in chronic myeloid disorders with different clinical phenotype. *Biochimica et Biophysica Acta (BBA) - Molecular Basis of Disease,* 1689**,** 179-181.

BOTTONI, A., LANZA, C. Z., MISCIONE, G. P. & SPINELLI, D. 2004. New Model for a Theoretical Density Functional Theory Investigation of the Mechanism of the Carbonic Anhydrase: How Does the Internal Bicarbonate Rearrangement Occur? *Journal of the American Chemical Society,* 126**,** 1542-1550.

BOILLÉE, S., YAMANAKA, K., LOBSIGER, C. S., COPELAND, N. G., JENKINS, N. A., KASSIOTIS, G., KOLLIAS, G. & CLEVELAND, D. W. 2006. Onset and Progression in Inherited ALS Determined by Motor Neurons and Microglia. *Science,* 312**,** 1389-1392.

BRECHUE, W. F., KOCEJA, D. M. & STAGER, J. M. 1997. Acetazolamide reduces peripheral afferent transmission in humans. *Muscle Nerve,* 20**,** 1541-8.

BRENNAN, F. 2012. The 70th anniversary of the death of Lou Gehrig. *Am J Hosp Palliat Care,* 29**,** 512-4.

BRETTSCHNEIDER, J., DEL TREDICI, K., TOLEDO, J. B., ROBINSON, J. L., IRWIN, D. J., GROSSMAN, M., SUH, E., VAN DEERLIN, V. M., WOOD, E. M., BAEK, Y., KWONG, L., LEE, E. B., ELMAN, L., MCCLUSKEY, L., FANG, L., FELDENGUT, S., LUDOLPH, A. C., LEE, V. M. Y., BRAAK, H. & TROJANOWSKI, J. Q. 2013. Stages of pTDP-43 pathology in amyotrophic lateral sclerosis. *Annals of Neurology,* 74**,** 20-38.

BRIGANTI, F., MANGANI, S., ORIOLI, P., SCOZZAFAVA, A., VERNAGLIONE, G. & SUPURAN, C. T. 1997. Carbonic Anhydrase Activators: X-ray Crystallographic and Spectroscopic Investigations for the Interaction of Isozymes I and II with Histamine. *Biochemistry,* 36**,** 10384-10392.

BRUIJN, L. I., HOUSEWEART, M. K., KATO, S., ANDERSON, K. L., ANDERSON, S. D., OHAMA, E., REAUME, A. G., SCOTT, R. W. & CLEVELAND, D. W. 1998. Aggregation and Motor Neuron Toxicity of an ALS-Linked SOD1 Mutant Independent from Wild-Type SOD1. *Science,* 281**,** 1851-1854.

BRUIJN, L. I., MILLER, T. M. & CLEVELAND, D. W. 2004. Unraveling the mechanisms involved in motor neuron degeneration in ALS. *Annual Review of Neuroscience,* 27**,** 723-749.

BYRNE, S., ELAMIN, M., BEDE, P., SHATUNOV, A., WALSH, C., CORR, B., HEVERIN, M., JORDAN, N., KENNA, K., LYNCH, C., MCLAUGHLIN, R. L., IYER, P. M., O'BRIEN, C., PHUKAN, J., WYNNE, B., BOKDE, A. L., BRADLEY, D. G., PENDER, N., AL-CHALABI, A. & HARDIMAN, O. 2012. Cognitive and clinical characteristics of patients with amyotrophic lateral sclerosis carrying a C9orf72 repeat expansion: a population-based cohort study. *The Lancet Neurology,* 11**,** 232-240.

CASAFONT, I., BENGOECHEA, R., TAPIA, O., BERCIANO, M. T. & LAFARGA, M. 2009. TDP-43 localizes in mRNA transcription and processing sites in mammalian neurons. *J Struct Biol,* 167**,** 235-41.

CASEY, J. R., SLY, W. S., SHAH, G. N. & ALVAREZ, B. V. 2009. Bicarbonate homeostasis in excitable tissues: role of AE3 Cl-/HCO3- exchanger and carbonic anhydrase XIV interaction. *Am J Physiol Cell Physiol,* 297**,** 19.

CETIN, H., RATH, J., FUZI, J., REICHARDT, B., FULOP, G., KOPPI, S., ERDLER, M., RANSMAYR, G., WEBER, J., NEUMANN, K., HAGMANN, M., LOSCHER, W. N., AUFF, E. & ZIMPRICH, F. 2015.Epidemiology of amyotrophic lateral sclerosis and effect of riluzole on disease course.*Neuroepidemiology,*44**,**6-15.

CHEN-PLOTKIN, A. S., LEE, V. M. Y. & TROJANOWSKI, J. Q. 2010. TAR DNA-binding protein 43 in neurodegenerative disease. *Nature reviews. Neurology,* 6**,** 211-220.

CHEW, J., GENDRON, T. F., PRUDENCIO, M., SASAGURI, H., ZHANG, Y.-J., CASTANEDES-CASEY, M., LEE, C. W., JANSEN-WEST, K., KURTI, A., MURRAY, M. E., BIENIEK, K. F., BAUER, P. O., WHITELAW, E. C., ROUSSEAU, L., STANKOWSKI, J. N., STETLER, C., DAUGHRITY, L. M., PERKERSON, E. A., DESARO, P., JOHNSTON, A., OVERSTREET, K., EDBAUER, D., RADEMAKERS, R., BOYLAN, K. B., DICKSON, D. W., FRYER, J. D. & PETRUCELLI, L. 2015. C9ORF72 repeat expansions in mice cause TDP-43 pathology, neuronal loss, and behavioral deficits. *Science,* 348**,** 1151-1154.

CHIANG, P. M., LING, J., JEONG, Y. H., PRICE, D. L., AJA, S. M. & WONG, P. C. 2010. Deletion of TDP-43 down-regulates Tbc1d1, a gene linked to obesity, and alters body fat metabolism. *Proc Natl Acad Sci U S A,* 107**,** 16320-4.

CHANG, X., HAN, J., ZHAO, Y., YAN, X., SUN, S. & CUI, Y. 2010. Increased expression of carbonic anhydrase I in the synovium of patients with ankylosing spondylitis. *BMC Musculoskelet Disord,* 11**,** 1471-2474.

CHANG, X., ZHENG, Y., YANG, Q., WANG, L., PAN, J., XIA, Y., YAN, X. & HAN, J. 2012. Carbonic anhydrase I (CA1) is involved in the process of bone formation and is susceptible to ankylosing spondylitis. *Arthritis Res Ther,* 14.

CHAPMAN, S. K. & MAREN, T. H. 1978. A search for the function of human carbonic anhydrase B. *Biochimica et Biophysica Acta (BBA) - Enzymology,* 527**,** 272-276.

CHESLER, M. 2003. Regulation and Modulation of pH in the Brain. *Physiological Reviews,* 83**,** 1183-1221.

CHIANG, W. L., CHU, S. C., YANG, S. S., LI, M. C., LAI, J. C., YANG, S. F., CHIOU, H. L. & HSIEH, Y. S. 2002. The aberrant expression of cytosolic carbonic anhydrase and its clinical significance in human non-small cell lung cancer. *Cancer Lett,* 188**,** 199-205.

CHIO, A., CALVO, A., MOGLIA, C., MAZZINI, L. & MORA, G. 2011. Phenotypic heterogeneity of amyotrophic lateral sclerosis: a population based study. *J Neurol Neurosurg Psychiatry,* 82**,**740-6.

CHIO, A., LOGROSCINO, G., TRAYNOR, B. J., COLLINS, J., SIMEONE, J. C., GOLDSTEIN, L. A. & WHITE, L. A. 2013. Global epidemiology of amyotrophic lateral sclerosis: a systematic review of the published literature. *Neuroepidemiology,* 41**,** 118-30.

CHIO, A., RESTAGNO, G., BRUNETTI, M., OSSOLA, I., CALVO, A., MORA, G., SABATELLI, M., MONSURRO, M. R., BATTISTINI, S., MANDRIOLI, J., SALVI, F., SPATARO, R., SCHYMICK, J., TRAYNOR, B. J. & LA BELLA, V. 2009. Two Italian kindreds with familial amyotrophic lateral sclerosis due to FUS mutation. *Neurobiol Aging,* 30**,** 1272-5.

CHRISTIE, K. N., THOMSON, C., XUE, L., LUCOCQ, J. M. & HOPWOOD, D. 1997. Carbonic anhydrase isoenzymes I, II, III, and IV are present in human esophageal epithelium. *J Histochem Cytochem,* 45**,** 35-40.

COLEMAN, J. 2000. Carbonic Anhydrase and Its Role in Photosynthesis. *In:* LEEGOOD, R., SHARKEY, T. & VON CAEMMERER, S. (eds.) *Photosynthesis.* Springer Netherlands.

COLOMBRITA, C., ONESTO, E., MEGIORNI, F., PIZZUTI, A., BARALLE, F. E., BURATTI, E., SILANI, V. & RATTI, A. 2012. TDP-43 and FUS RNA-binding Proteins Bind Distinct Sets of Cytoplasmic Messenger RNAs and Differently Regulate Their Post-transcriptional Fate in Motoneuron-like Cells. *The Journal of Biological Chemistry,* 287**,** 15635-15647.

COOPER-KNOCK, J., BURY, J. J., HEATH, P. R., WYLES, M., HIGGINBOTTOM, A., GELSTHORPE, C., HIGHLEY, J. R., HAUTBERGUE, G., RATTRAY, M., KIRBY, J. & SHAW, P. J. 2015. C9ORF72 GGGGCC Expanded Repeats Produce Splicing Dysregulation which Correlates with Disease Severity in Amyotrophic Lateral Sclerosis. *PLoS ONE,* 10**,** e0127376.

CORRADO, L., DEL BO, R., CASTELLOTTI, B., RATTI, A., CEREDA, C., PENCO, S., SORARU, G., CARLOMAGNO, Y., GHEZZI, S., PENSATO, V., COLOMBRITA, C., GAGLIARDI, S., COZZI, L., ORSETTI, V., MANCUSO, M., SICILIANO, G., MAZZINI, L., COMI, G. P., GELLERA, C., CERONI, M., D'ALFONSO, S. & SILANI, V. 2010. Mutations of FUS gene in sporadic amyotrophic lateral sclerosis. *J Med Genet,* 47**,** 190-4.

CRANDALL, E. D. & O'BRASKY, J. E. 1978. Direct evidence of participation of rat lung carbonic anhydrase in CO2 reactions. *J Clin Invest,* 62**,** 618-22.

CRONIN, S., HARDIMAN, O. & TRAYNOR, B. J. 2007. Ethnic variation in the incidence of ALS: a systematic review. *Neurology,* 68**,** 1002-7.

DAOUD, H., VALDMANIS, P. N., KABASHI, E., DION, P., DUPRE, N., CAMU, W., MEININGER, V. & ROULEAU, G. A. 2009. Contribution of TARDBP mutations to sporadic amyotrophic lateral sclerosis. *J Med Genet,* 46**,** 112-4.

DE JONG, S. W., HUISMAN, M. H., SUTEDJA, N. A., VAN DER KOOI, A. J., DE VISSER, M., SCHELHAAS, H. J., FISCHER, K., VELDINK, J. H. & VAN DEN BERG, L. H. 2012. Smoking, alcohol consumption, and the risk of amyotrophic lateral sclerosis: a population-based study. *Am J Epidemiol,* 176**,** 233-9.

DEITMER, J. W., THEPARAMBIL, S. M., RUMINOT, I. & BECKER, H. M. 2014. The role of membrane acid/base transporters and carbonic anhydrases for cellular pH and metabolic processes. *Frontiers in Neuroscience,* 8**,** 430.

DEJESUS-HERNANDEZ, M., MACKENZIE, I. R., BOEVE, B. F., BOXER, A. L., BAKER, M., RUTHERFORD, N. J., NICHOLSON, A. M., FINCH, N. A., FLYNN, H., ADAMSON, J., KOURI, N., WOJTAS, A., SENGDY, P., HSIUNG, G. Y., KARYDAS, A., SEELEY, W. W., JOSEPHS, K. A., COPPOLA, G., GESCHWIND, D. H., WSZOLEK, Z. K., FELDMAN, H., KNOPMAN, D. S., PETERSEN, R. C., MILLER, B. L., DICKSON, D. W., BOYLAN, K. B., GRAFF-RADFORD, N. R. & RADEMAKERS, R. 2011. Expanded GGGGCC hexanucleotide repeat in noncoding region of C9ORF72 causes chromosome 9p-linked FTD and ALS. *Neuron,* 72**,** 245-56.

DENG, H. X., CHEN, W., HONG, S. T., BOYCOTT, K. M., GORRIE, G. H., SIDDIQUE, N., YANG, Y., FECTO, F., SHI, Y., ZHAI, H., JIANG, H., HIRANO, M., RAMPERSAUD, E., JANSEN, G. H., DONKERVOORT, S., BIGIO, E. H., BROOKS, B. R., AJROUD, K., SUFIT, R. L., HAINES, J. L., MUGNAINI, E., PERICAK-VANCE, M. A. & SIDDIQUE, T. 2011. Mutations in UBQLN2 cause dominant X-linked juvenile and adult-onset ALS and ALS/dementia. *Nature,* 477**,** 211-5.

DODGE, J. C., TRELEAVEN, C. M., FIDLER, J. A., TAMSETT, T. J., BAO, C., SEARLES, M., TAKSIR, T. V., MISRA, K., SIDMAN, R. L., CHENG, S. H. & SHIHABUDDIN, L. S. 2013. Metabolic signatures of amyotrophic lateral sclerosis reveal insights into disease pathogenesis. *Proc Natl Acad Sci U S A,* 110**,** 10812-7.

DODGSON, S. J. & CHERIAN, K. 1990. Rat renal proximal tubular gluconeogenesis: possible involvement of nonmitochondrial carbonic anhydrase isozymes. *Arch Biochem Biophys,* 282**,** 1-7.

DORMANN, D., RODDE, R., EDBAUER, D., BENTMANN, E., FISCHER, I., HRUSCHA, A., THAN, M. E., MACKENZIE, I. R., CAPELL, A., SCHMID, B., NEUMANN, M. & HAASS, C. 2010. ALS-associated fused in sarcoma (FUS) mutations disrupt Transportin-mediated nuclear import. *EMBO J,* 29**,** 2841-57.

EDWARDS, Y. H., BARLOW, J. H., KONIALIS, C. P., POVEY, S. & BUTTERWORTH, P. H. 1986. Assignment of the gene determining human carbonic anhydrase, CAI, to chromosome 8. *Ann Hum Genet,* 50**,** 123-9.

EFFROS, R., CHANG, R. & SILVERMAN, P. 1978. Acceleration of plasma bicarbonate conversion to carbon dioxide by pulmonary carbonic anhydrase. *Science,* 199**,** 427-429.

EISEN, A., SCHULZER, M., MACNEIL, M., PANT, B. & MAK, E. 1993. Duration of amyotrophic lateral sclerosis is age dependent. *Muscle Nerve,* 16**,** 27-32.

ERIKSSON, A. E., JONES, T. A. & LILJAS, A. 1988a. Refined structure of human carbonic anhydrase II at 2.0 A resolution. *Proteins,* 4**,** 274-82.

ERIKSSON, A. E., KYLSTEN, P. M., JONES, T. A. & LILJAS, A. 1988b. Crystallographic studies of inhibitor binding sites in human carbonic anhydrase II: a pentacoordinated binding of the SCN- ion to the zinc at high pH. *Proteins,* 4**,** 283-93.

FARG, M. A., SUNDARAMOORTHY, V., SULTANA, J. M., YANG, S., ATKINSON, R. A. K., LEVINA, V., HALLORAN, M. A., GLEESON, P. A., BLAIR, I. P., SOO, K. Y., KING, A. E. & ATKIN, J. D. 2014. C9ORF72, implicated in amytrophic lateral sclerosis and frontotemporal dementia, regulates endosomal trafficking. *Human Molecular Genetics,* 23**,** 3579-3595.

FECTO, F., YAN, J., VEMULA, S. P., LIU, E., YANG, Y., CHEN, W., ZHENG, J. G., SHI, Y., SIDDIQUE, N., ARRAT, H., DONKERVOORT, S., AJROUD-DRISS, S., SUFIT, R. L., HELLER, S. L., DENG, H. X. & SIDDIQUE, T. 2011. SQSTM1 mutations in familial and sporadic amyotrophic lateral sclerosis. *Arch Neurol,* 68**,** 1440-6.

FEDIRKO, N., AVSHALUMOV, M., RICE, M. E. & CHESLER, M. 2007. Regulation of postsynaptic Ca2+ influx in hippocampal CA1 pyramidal neurons via extracellular carbonic anhydrase. *J Neurosci,* 27**,** 1167-75.

FONTI, R., LATELLA, G., CAPRILLI, R., FRIERI, G., MARCHEGGIANO, A. & SAMBUY, Y. 1998. Carbonic anhydrase I reduction in colonic mucosa of patients with active ulcerative colitis. *Dig Dis Sci,* 43**,** 2086-92.

FREIBAUM, B. D., LU, Y., LOPEZ-GONZALEZ, R., KIM, N. C., ALMEIDA, S., LEE, K. H., BADDERS, N., VALENTINE, M., MILLER, B. L., WONG, P. C., PETRUCELLI, L., KIM, H. J., GAO, F. B. & TAYLOR, J. P. 2015. GGGGCC repeat expansion in C9orf72 compromises nucleocytoplasmic transport. *Nature,* 525**,** 129-33.

FRIDOVICH, I. 1975. Superoxide dismutases. *Annu Rev Biochem,* 44**,** 147-59.

FRULLONI, L., BOVO, P., BRUNELLI, S., VAONA, B., DI FRANCESCO, V., NISHIMORI, I. & CAVALLINI, G. 2000. Elevated serum levels of antibodies to carbonic anhydrase I and II in patients with chronic pancreatitis. *Pancreas,* 20**,** 382-8.

GAMBHIR, K. K., ORNASIR, J., HEADINGS, V. & BONAR, A. 2007. Decreased total carbonic anhydrase esterase activity and decreased levels of carbonic anhydrase 1 isozyme in erythrocytes of type II diabetic patients. *Biochem Genet,* 45**,** 431-9.

GAO, B. B., CLERMONT, A., ROOK, S., FONDA, S. J., SRINIVASAN, V. J., WOJTKOWSKI, M., FUJIMOTO, J. G., AVERY, R. L., ARRIGG, P. G., BURSELL, S. E., AIELLO, L. P. & FEENER, E. P. 2007. Extracellular carbonic anhydrase mediates hemorrhagic retinal and cerebral vascular permeability through prekallikrein activation. *Nat Med,* 13**,** 181-8.

GEERS, C. & GROS, G. 2000. Carbon dioxide transport and carbonic anhydrase in blood and muscle. *Physiol Rev,* 80**,** 681-715.

GHANDOUR, M. S., LANGLEY, O. K., ZHU, X. L., WAHEED, A. & SLY, W. S. 1992. Carbonic anhydrase IV on brain capillary endothelial cells: a marker associated with the blood-brain barrier. *Proceedings of the National Academy of Sciences of the United States of America,* 89**,** 6823-6827.

GHANDOUR, M. S., PARKKILA, A. K., PARKKILA, S., WAHEED, A. & SLY, W. S. 2000. Mitochondrial carbonic anhydrase in the nervous system: expression in neuronal and glial cells. *J Neurochem,* 75**,** 2212-20.

GIACOBINI, E. 1961. Localization of carbonic anhydrase in the nervous system. *Science,* 134**,** 1524-5.

GIACOBINI, E. 1962. A cytochemical study of the localization of carbonic anhydrase in the nervous system. *J Neurochem,* 9**,** 169-77.

GILL, S. R., SCHROER, T. A., SZILAK, I., STEUER, E. R., SHEETZ, M. P. & CLEVELAND, D. W. 1991. Dynactin, a conserved, ubiquitously expressed component of an activator of vesicle motility mediated by cytoplasmic dynein. *The Journal of Cell Biology,* 115**,** 1639-1650.

GORDON, P. H., CHENG, B., KATZ, I. B., PINTO, M., HAYS, A. P., MITSUMOTO, H. & ROWLAND, L. P. 2006. The natural history of primary lateral sclerosis. *Neurology,* 66**,** 647-53.

GORIKI, K., KAWAMOTO, S. & TASHIAN, R. E. 1980. The new variant carbonic anhydrase in the Japanese: CAINagasaki 1(76 Arg replaced by Gln) and CAIHiroshima 2. *Hemoglobin,* 4**,** 653-7.

GURNEY, M. E., PU, H., CHIU, A. Y., DAL CANTO, M. C., POLCHOW, C. Y., ALEXANDER, D. D., CALIENDO, J., HENTATI, A., KWON, Y. W., DENG, H. X. & ET, A. 1994. Motor neuron degeneration in mice that express a human Cu,Zn superoxide dismutase mutation. *Science (Classic),* 264**,** 1772.

HALEY, R. W. 2003. Excess incidence of ALS in young Gulf War veterans. *Neurology,* 61**,** 750-6.

HARDIMAN, O., VAN DEN BERG, L. H. & KIERNAN, M. C. 2011. Clinical diagnosis and management of amyotrophic lateral sclerosis. *Nat Rev Neurol,* 7**,** 639-49.

HAYES, S. G. 1994. Acetazolamide in bipolar affective disorders. *Ann Clin Psychiatry,* 6**,** 91-8.

HENNEBERRY, R. C., NOVELLI, A., COX, J. A. & LYSKO, P. G. 1989. Neurotoxicity at the N-methyl-D-aspartate receptor in energy-compromised neurons. An hypothesis for cell death in aging and disease. *Ann N Y Acad Sci,* 568**,** 225-33.

HEWETT-EMMETT, D. & TASHIAN, R. E. 1996. Functional diversity, conservation, and convergence in the evolution of the alpha-, beta-, and gamma-carbonic anhydrase gene families. *Mol Phylogenet Evol,* 5**,** 50-77.

HIBI, N., SHIMA, K., TASHIRO, K., TSUZUKI, K., TSUKADA, Y. & HIRAI, H. 1984. Development of a highly sensitive enzyme-immunoassay for serum carbonic anhydrase-III. *J Neurol Sci,* 65**,** 333-40.

HOCKING, L. J., LUCAS, G. J., DAROSZEWSKA, A., MANGION, J., OLAVESEN, M., CUNDY, T., NICHOLSON, G. C., WARD, L., BENNETT, S. T., WUYTS, W., VAN HUL, W. & RALSTON, S. H. 2002. Domain-specific mutations in sequestosome 1 (SQSTM1) cause familial and sporadic Paget's disease. *Hum Mol Genet,* 11**,** 2735-9.

HOUGH, M. A., GROSSMANN, J. G., ANTONYUK, S. V., STRANGE, R. W., DOUCETTE, P. A., RODRIGUEZ, J. A., WHITSON, L. J., HART, P. J., HAYWARD, L. J., VALENTINE, J. S. & HASNAIN, S. S. 2004. Dimer destabilization in superoxide dismutase may result in disease-causing properties: Structures of motor neuron disease mutants. *Proceedings of the National Academy of Sciences of the United States of America,* 101**,** 5976-5981.

HUANG, T. T., CARLSON, E. J., LEADON, S. A. & EPSTEIN, C. J. 1992. Relationship of resistance to oxygen free radicals to CuZn-superoxide dismutase activity in transgenic, transfected, and trisomic cells. *The FASEB Journal,* 6**,** 903-10.

HUISMAN, M. H., DE JONG, S. W., VAN DOORMAAL, P. T., WEINREICH, S. S., SCHELHAAS, H. J., VAN DER KOOI, A. J., DE VISSER, M., VELDINK, J. H. & VAN DEN BERG, L. H. 2011. Population based epidemiology of amyotrophic lateral sclerosis using capture-recapture methodology. *J Neurol Neurosurg Psychiatry,* 82**,** 1165-70.

HUISMAN, M. H. B., SEELEN, M., DE JONG, S. W., DORRESTEIJN, K. R. I. S., VAN DOORMAAL, P. T. C., VAN DER KOOI, A. J., DE VISSER, M., SCHELHAAS, H. J., VAN DEN BERG, L. H. & VELDINK, J. H. 2013. Lifetime physical activity and the risk of amyotrophic lateral sclerosis. *Journal of Neurology, Neurosurgery & Psychiatry,* 84**,** 976-981.

IGAZ, L. M., KWONG, L. K., LEE, E. B., CHEN-PLOTKIN, A., SWANSON, E., UNGER, T., MALUNDA, J., XU, Y., WINTON, M. J., TROJANOWSKI, J. Q. & LEE, V. M. 2011. Dysregulation of the ALS-associated gene TDP-43 leads to neuronal death and degeneration in mice. *J Clin Invest,* 121**,** 726-38.

IGUCHI, Y., KATSUNO, M., NIWA, J., YAMADA, S., SONE, J., WAZA, M., ADACHI, H., TANAKA, F., NAGATA, K., ARIMURA, N., WATANABE, T., KAIBUCHI, K. & SOBUE, G. 2009. TDP-43 depletion induces neuronal cell damage through dysregulation of Rho family GTPases. *J Biol Chem,* 284**,** 22059-66.

IIDA, A., KAMEI, T., SANO, M., OSHIMA, S., TOKUDA, T., NAKAMURA, Y. & IKEGAWA, S. 2012. Large-scale screening of TARDBP mutation in amyotrophic lateral sclerosis in Japanese. *Neurobiol Aging,* 33**,** 786-90.

ILIEVA, H., POLYMENIDOU, M. & CLEVELAND, D. W. 2009. Non–cell autonomous toxicity in neurodegenerative disorders: ALS and beyond. *The Journal of Cell Biology,* 187**,** 761-772.

IMTAIYAZ HASSAN, M., SHAJEE, B., WAHEED, A., AHMAD, F. & SLY, W. S. 2013. Structure, function and applications of carbonic anhydrase isozymes. *Bioorg Med Chem,* 21**,** 1570-82.

JARONEN, M., VEHVILÄINEN, P., MALM, T., KEKSA-GOLDSTEINE, V., POLLARI, E., VALONEN, P., KOISTINAHO, J. & GOLDSTEINS, G. 2013. Protein disulfide isomerase in ALS mouse glia links protein misfolding with NADPH oxidase-catalyzed superoxide production. *Human Molecular Genetics,* 22**,** 646-655.

JOHNSON, J. O., MANDRIOLI, J., BENATAR, M., ABRAMZON, Y., VAN DEERLIN, V. M., TROJANOWSKI, J. Q., GIBBS, J. R., BRUNETTI, M., GRONKA, S., WUU, J., DING, J., MCCLUSKEY, L., MARTINEZ-LAGE, M., FALCONE, D., HERNANDEZ, D. G., AREPALLI, S., CHONG, S., SCHYMICK, J. C., ROTHSTEIN, J., LANDI, F., WANG, Y. D., CALVO, A., MORA, G., SABATELLI, M., MONSURRO, M. R., BATTISTINI, S., SALVI, F., SPATARO, R., SOLA, P., BORGHERO, G., GALASSI, G., SCHOLZ, S. W., TAYLOR, J. P., RESTAGNO, G., CHIO, A. & TRAYNOR, B. J. 2010. Exome sequencing reveals VCP mutations as a cause of familial ALS. *Neuron,* 68**,** 857-64.

JOHNSTON-WILSON, N. L., SIMS, C. D., HOFMANN, J. P., ANDERSON, L., SHORE, A. D., TORREY, E. F. & YOLKEN, R. H. 2000. Disease-specific alterations in frontal cortex brain proteins in schizophrenia, bipolar disorder, and major depressive disorder. The Stanley Neuropathology Consortium. *Mol Psychiatry,* 5**,** 142-9.

JONES, G. L. & SHAW, D. C. 1982. A polymorphic variant of human erythrocyte carbonic anhydrase I with a widespread distribution in Australian aborigines, CAI Australia-9 (8 Asp leads to Gly): purification, properties, amino acid substitution, and possible physiological significance of the variant enzyme. *Biochem Genet,* 20**,** 943-77.

JONSSON, P. A., GRAFFMO, K. S., ANDERSEN, P. M., BRANNSTROM, T., LINDBERG, M., OLIVEBERG, M. & MARKLUND, S. L. 2006. Disulphide-reduced superoxide dismutase-1 in CNS of transgenic amyotrophic lateral sclerosis models. *Brain,* 129**,** 451-64.

JOVICIC, A., MERTENS, J., BOEYNAEMS, S., BOGAERT, E., CHAI, N., YAMADA, S. B., PAUL, J. W., 3RD, SUN, S., HERDY, J. R., BIERI, G., KRAMER, N. J., GAGE, F. H., VAN DEN BOSCH, L., ROBBERECHT, W. & GITLER, A. D. 2015. Modifiers of C9orf72 dipeptide repeat toxicity connect nucleocytoplasmic transport defects to FTD/ALS. *Nat Neurosci,* 18**,** 1226-9.

JU, J. S., FUENTEALBA, R. A., MILLER, S. E., JACKSON, E., PIWNICA-WORMS, D., BALOH, R. H. & WEIHL, C. C. 2009. Valosin-containing protein (VCP) is required for autophagy and is disrupted in VCP disease. *J Cell Biol,* 187**,** 875-88.

KABASHI, E., AGAR, J. N., TAYLOR, D. M., MINOTTI, S. & DURHAM, H. D. 2004. Focal dysfunction of the proteasome: a pathogenic factor in a mouse model of amyotrophic lateral sclerosis. *J Neurochem,* 89**,** 1325-35.

KABASHI, E., BERCIER, V., LISSOUBA, A., LIAO, M., BRUSTEIN, E., ROULEAU, G. A. & DRAPEAU, P. 2011. FUS and TARDBP but not SOD1 interact in genetic models of amyotrophic lateral sclerosis. *PLoS Genet,* 7**,** 4.

KABASHI, E., VALDMANIS, P. N., DION, P., SPIEGELMAN, D., MCCONKEY, B. J., VANDE VELDE, C., BOUCHARD, J. P., LACOMBLEZ, L., POCHIGAEVA, K., SALACHAS, F., PRADAT, P. F., CAMU, W., MEININGER, V., DUPRE, N. & ROULEAU, G. A. 2008. TARDBP mutations in individuals with sporadic and familial amyotrophic lateral sclerosis. *Nat Genet,* 40**,** 572-4.

KAGEOKA, T., HEWETT-EMMETT, D., STROUP, S. K., YU, Y. S. & TASHIAN, R. E. 1981. Amino acid substitution and chemical characterization of a Japanese variant of carbonic anhydrase I: CA I Hiroshima-1 (86 Asp replaced by Gly). *Biochem Genet,* 19**,** 535-49.

KANNAN, K. K., NOTSTRAND, B., FRIDBORG, K., LOVGREN, S., OHLSSON, A. & PETEF, M. 1975. Crystal structure of human erythrocyte carbonic anhydrase B. Three-dimensional structure at a nominal 2.2-A resolution. *Proc Natl Acad Sci U S A,* 72**,** 51-5.

KANNAN, K. K., PETEF, M., FRIDBORG, K., CID-DRESDNER, H. & LOVGREN, S. 1977. Structure and function of carbonic anhydrases. Imidazole binding to human carbonic anhydrase B and the mechanism of action of carbonic anhydrases. *FEBS Lett,* 73**,** 115-9.

KANNAN, K. K., RAMANADHAM, M. & JONES, T. A. 1984. Structure, refinement, and function of carbonic anhydrase isozymes: refinement of human carbonic anhydrase I. *Ann N Y Acad Sci,* 429**,** 49-60.

KAZIMIERCZAK, J., SOMMER, E. W., PHILIPPE, E. & DROZ, B. 1986. Carbonic anhydrase activity in primary sensory neurons. I. Requirements for the cytochemical localization in the dorsal root ganglion of chicken and mouse by light and electron microscopy. *Cell Tissue Res,* 245**,** 487-95.

KEILIN, D. & MANN, T. 1940. Carbonic anhydrase. Purification and nature of the enzyme. *Biochem J,* 34**,** 1163-76.

KENDALL, A. G. & TASHIAN, R. E. 1977. Erythrocyte carbonic anhydrase I: inherited deficiency in humans. *Science,* 197**,** 471-2.

KIERNAN, M. C., VUCIC, S., CHEAH, B. C., TURNER, M. R., EISEN, A., HARDIMAN, O., BURRELL, J. R. & ZOING, M. C. 2011. Amyotrophic lateral sclerosis. *Lancet,* 377**,** 942-55.

KIKUCHI, H., ALMER, G., YAMASHITA, S., GUÉGAN, C., NAGAI, M., XU, Z., SOSUNOV, A. A., MCKHANN, G. M. & PRZEDBORSKI, S. 2006. Spinal cord endoplasmic reticulum stress associated with a microsomal accumulation of mutant superoxide dismutase-1 in an ALS model. *Proceedings of the National Academy of Sciences,* 103**,** 6025-6030.

KIMELBERG, H. K., STIEG, P. E. & MAZURKIEWICZ, J. E. 1982. Immunocytochemical and biochemical analysis of carbonic anhydrase in primary astrocyte cultures from rat brain. *J Neurochem,* 39**,** 734-42.

KINO-OHSAKI, J., NISHIMORI, I., MORITA, M., OKAZAKI, K., YAMAMOTO, Y., ONISHI, S. & HOLLINGSWORTH, M. A. 1996. Serum antibodies to carbonic anhydrase I and II in patients with idiopathic chronic pancreatitis and Sjogren's syndrome. *Gastroenterology,* 110**,** 1579-86.

KNOBEL, K. M., DAVIS, W. S., JORGENSEN, E. M. & BASTIANI, M. J. 2001. UNC-119 suppresses axon branching in C. elegans. *Development,* 128**,** 4079-92.

KOENIG, S. H. & BROWN, R. D., 3RD 1972. H 2 CO 3 as substrate for carbonic anhydrase in the dehydration of HCO 3. *Proc Natl Acad Sci U S A,* 69**,** 2422-5.

KOPPERS, M., BLOKHUIS, A. M., WESTENENG, H.-J., TERPSTRA, M. L., ZUNDEL, C. A. C., VIEIRA DE SÁ, R., SCHELLEVIS, R. D., WAITE, A. J., BLAKE, D. J., VELDINK, J. H., VAN DEN BERG, L. H. & PASTERKAMP, R. J. 2015a. C9orf72 ablation in mice does not cause motor neuron degeneration or motor deficits. *Annals of Neurology,* 78**,** 426-438.

KOPPERS, M., BLOKHUIS, A. M., WESTENENG, H. J., TERPSTRA, M. L., ZUNDEL, C. A., VIEIRA DE SA, R., SCHELLEVIS, R. D., WAITE, A. J., BLAKE, D. J., VELDINK, J. H., VAN DEN BERG, L. H. & JEROEN PASTERKAMP, R. 2015b. C9orf72 ablation in mice does not cause motor neuron degeneration or motor deficits. *Ann Neurol,* 5**,** 24453.

KOROLAINEN, M. A., GOLDSTEINS, G., NYMAN, T. A., ALAFUZOFF, I., KOISTINAHO, J. & PIRTTILÄ, T. 2006. Oxidative modification of proteins in the frontal cortex of Alzheimer's disease brain. *Neurobiology of Aging,* 27**,** 42-53.

KRAEMER, B. C., SCHUCK, T., WHEELER, J. M., ROBINSON, L. C., TROJANOWSKI, J. Q., LEE, V. M. & SCHELLENBERG, G. D. 2010. Loss of murine TDP-43 disrupts motor function and plays an essential role in embryogenesis. *Acta Neuropathol,* 119**,** 409-19.

KRISHNAMURTHY, V. M., KAUFMAN, G. K., URBACH, A. R., GITLIN, I., GUDIKSEN, K. L., WEIBEL, D. B. & WHITESIDES, G. M. 2008. Carbonic anhydrase as a model for biophysical and physical-organic studies of proteins and protein-ligand binding. *Chem Rev,* 108**,** 946-1051.

KUMAR, V. & KANNAN, K. K. 1994. Enzyme-substrate interactions. Structure of human carbonic anhydrase I complexed with bicarbonate. *J Mol Biol,* 241**,** 226-32.

KUMPULAINEN, T., DAHL, D., KORHONEN, L. K. & NYSTRÖM, S. H. 1983. Immunolabeling of carbonic anhydrase isoenzyme C and glial fibrillary acidic protein in paraffin-embedded tissue sections of human brain and retina. *Journal of Histochemistry & Cytochemistry,* 31**,** 879-86.

KUZUHARA, S. & KOKUBO, Y. 2005. Atypical parkinsonism of Japan: amyotrophic lateral sclerosis-parkinsonism-dementia complex of the Kii peninsula of Japan (Muro disease): an update. *Mov Disord,* 20**,** S108-13.

KWIATKOWSKI, T. J., JR., BOSCO, D. A., LECLERC, A. L., TAMRAZIAN, E., VANDERBURG, C. R., RUSS, C., DAVIS, A., GILCHRIST, J., KASARSKIS, E. J., MUNSAT, T., VALDMANIS, P., ROULEAU, G. A., HOSLER, B. A., CORTELLI, P., DE JONG, P. J., YOSHINAGA, Y., HAINES, J. L., PERICAK-VANCE, M. A., YAN, J., TICOZZI, N., SIDDIQUE, T., MCKENNA-YASEK, D., SAPP, P. C., HORVITZ, H. R., LANDERS, J. E. & BROWN, R. H., JR. 2009. Mutations in the FUS/TLS gene on chromosome 16 cause familial amyotrophic lateral sclerosis. *Science,* 323**,** 1205-8.

KWON, I., XIANG, S., KATO, M., WU, L., THEODOROPOULOS, P., WANG, T., KIM, J., YUN, J., XIE, Y. & MCKNIGHT, S. L. 2014. Poly-dipeptides encoded by the C9orf72 repeats bind nucleoli, impede RNA biogenesis, and kill cells. *Science,* 345**,** 1139-45.

LAGIER-TOURENNE, C., POLYMENIDOU, M. & CLEVELAND, D. W. 2010. TDP-43 and FUS/TLS: emerging roles in RNA processing and neurodegeneration. *Hum Mol Genet,* 19**,** 15.

LAGIER-TOURENNE, C., POLYMENIDOU, M., HUTT, K. R., VU, A. Q., BAUGHN, M., HUELGA, S. C., CLUTARIO, K. M., LING, S.-C., LIANG, T. Y., MAZUR, C., WANCEWICZ, E., KIM, A. S., WATT, A., FREIER, S., HICKS, G. G., DONOHUE, J. P., SHIUE, L., BENNETT, C. F., RAVITS, J., CLEVELAND, D. W. & YEO, G. W. 2012. Divergent roles of ALS-linked proteins FUS/TLS and TDP-43 intersect in processing long pre-mRNAs. *Nature neuroscience,* 15**,** 1488-1497.

LALMANSINGH, A. S., UREKAR, C. J. & REDDI, P. P. 2011. TDP-43 Is a Transcriptional Repressor: THE TESTIS-SPECIFIC MOUSE acrv1 GENE IS A TDP-43 TARGET IN VIVO. *Journal of Biological Chemistry,* 286**,** 10970-10982.

LAMONT, M. G. & WEBER, J. T. 2015. Mice deficient in carbonic anhydrase type 8 exhibit motor dysfunctions and abnormal calcium dynamics in the somatic region of cerebellar granule cells. *Behav Brain Res,* 286**,** 11-6.

LAMONTE, B. H., WALLACE, K. E., HOLLOWAY, B. A., SHELLY, S. S., ASCAÑO, J., TOKITO, M., VAN WINKLE, T., HOWLAND, D. S. & HOLZBAUR, E. L. F. 2002. Disruption of Dynein/Dynactin Inhibits Axonal Transport in Motor Neurons Causing Late-Onset Progressive Degeneration. *Neuron,* 34**,** 715-727.

LANGLEY, O. K., GHANDOUR, M. S., VINCENDON, G. & GOMBOS, G. 1980. Carbonic anhydrase: an ultrastructural study in rat cerebellum. *Histochem J,* 12**,** 473-83.

LATTERICH, M., FRÖHLICH, K.-U. & SCHEKMAN, R. 1995. Membrane fusion and the cell cycle: Cdc48p participates in the fusion of ER membranes. *Cell,* 82**,** 885-893.

LEE, E. B., LEE, V. M. & TROJANOWSKI, J. Q. 2011. Gains or losses: molecular mechanisms of TDP43-mediated neurodegeneration. *Nat Rev Neurosci,* 13**,** 38-50.

LESBURG, C. A. & CHRISTIANSON, D. W. 1995. X-ray crystallographic studies of engineered hydrogen bond networks in a protein-zinc binding site. *Journal of the American Chemical Society,* 117**,** 6838-6844.

LIANG, Z., XUE, Y., BEHRAVAN, G., JONSSON, B. H. & LINDSKOG, S. 1993. Importance of the conserved active-site residues Tyr7, Glu106 and Thr199 for the catalytic function of human carbonic anhydrase II. *Eur J Biochem,* 211**,** 821-7.

LINDSKOG, S. 1997. Structure and mechanism of carbonic anhydrase. *Pharmacol Ther,* 74**,** 1-20.
LINDSKOG, S. & COLEMAN, J. E. 1973. The catalytic mechanism of carbonic anhydrase. *Proc Natl Acad Sci U S A,* 70**,** 2505-8.
LINDSKOG, S., ENGBERG, P., FORSMAN, C., IBRAHIM, S. A., JONSSON, B.-H., SIMONSSON, I. & TIBELL, L. 1984. Kinetics and Mechanism of Carbonic Anhydrase Isoenzymesa. *Annals of the New York Academy of Sciences,* 429**,** 61-75.
LING, S.-C., ALBUQUERQUE, C. P., HAN, J. S., LAGIER-TOURENNE, C., TOKUNAGA, S., ZHOU, H. & CLEVELAND, D. W. 2010. ALS-associated mutations in TDP-43 increase its stability and promote TDP-43 complexes with FUS/TLS. *Proceedings of the National Academy of Sciences of the United States of America,* 107**,** 13318-13323.
LIU, J., LILLO, C., JONSSON, P. A., VELDE, C. V., WARD, C. M., MILLER, T. M., SUBRAMANIAM, J. R., ROTHSTEIN, J. D., MARKLUND, S., ANDERSEN, P. M., BRÄNNSTRÖM, T., GREDAL, O., WONG, P. C., WILLIAMS, D. S. & CLEVELAND, D. W. 2004. Toxicity of Familial ALS-Linked SOD1 Mutants from Selective Recruitment to Spinal Mitochondria. *Neuron,* 43**,** 5-17.
LOGROSCINO, G., TRAYNOR, B. J., HARDIMAN, O., CHIO, A., MITCHELL, D., SWINGLER, R. J., MILLUL, A., BENN, E. & BEGHI, E. 2010. Incidence of amyotrophic lateral sclerosis in Europe. *J Neurol Neurosurg Psychiatry,* 81**,** 385-90.
LONNERHOLM, G., SELKING, O. & WISTRAND, P. J. 1985. Amount and distribution of carbonic anhydrases CA I and CA II in the gastrointestinal tract. *Gastroenterology,* 88**,** 1151-61.
LOWE, N., BRADY, H. J., BARLOW, J. H., SOWDEN, J. C., EDWARDS, M. & BUTTERWORTH, P. H. 1990. Structure and methylation patterns of the gene encoding human carbonic anhydrase I. *Gene,* 93**,** 277-83.
LOWE, N., EDWARDS, Y. H., EDWARDS, M. & BUTTERWORTH, P. H. 1991. Physical mapping of the human carbonic anhydrase gene cluster on chromosome 8. *Genomics,* 10**,** 882-8.
LYNCH, C. J., FOX, H., HAZEN, S. A., STANLEY, B. A., DODGSON, S. & LANOUE, K. F. 1995. Role of hepatic carbonic anhydrase in de novo lipogenesis. *Biochemical Journal,* 310**,** 197-202.
MACIAS, M. Y., LEHMAN, C. T., SANGER, J. R. & RILEY, D. A. 1998. Myelinated sensory and alpha motor axon regeneration in peripheral nerve neuromas. *Muscle Nerve,* 21**,** 1748-58.
MACKENZIE, I. R., RADEMAKERS, R. & NEUMANN, M. 2010. TDP-43 and FUS in amyotrophic lateral sclerosis and frontotemporal dementia. *Lancet Neurol,* 9**,** 995-1007.
MANNO, C., LIPARI, A., BONO, V., TAIELLO, A. C. & LA BELLA, V. 2013. Sporadic Parkinson disease and amyotrophic lateral sclerosis complex (Brait-Fahn-Schwartz disease). *J Neurol Sci,* 326**,** 104-6.
MARCHETTO, M. C. N., MUOTRI, A. R., MU, Y., SMITH, A. M., CEZAR, G. G. & GAGE, F. H. 2008. Article: Non-Cell-Autonomous Effect of Human SOD1G37R Astrocytes on Motor Neurons Derived from Human Embryonic Stem Cells. *Cell Stem Cell,* 3**,** 649-657.
MAREN, T. H. 1967. Carbonic anhydrase: chemistry, physiology, and inhibition. *Physiol Rev,* 47**,** 595-781.
MAREN, T. H., RAYBURN, C. S. & LIDDELL, N. E. 1976. Inhibition by anions of human red cell carbonic anhydrase B: physiological and biochemical implications. *Science,* 191**,** 469-72.
MARUYAMA, H., MORINO, H., ITO, H., IZUMI, Y., KATO, H., WATANABE, Y., KINOSHITA, Y., KAMADA, M., NODERA, H., SUZUKI, H., KOMURE, O., MATSUURA, S., KOBATAKE, K., MORIMOTO, N., ABE, K., SUZUKI, N., AOKI, M., KAWATA, A., HIRAI, T., KATO, T., OGASAWARA, K., HIRANO, A., TAKUMI, T., KUSAKA, H., HAGIWARA, K., KAJI, R. & KAWAKAMI, H. 2010. Mutations of optineurin in amyotrophic lateral sclerosis. *Nature,* 465**,** 223-6.
MAUKSCH, M., BRAUER, M., WESTON, J. & ANDERS, E. 2001. New insights into the mechanistic details of the carbonic anhydrase cycle as derived from the model system [(NH(3))(3)Zn(OH)](+)/CO(2): how does the H(2)O/HCO(3)(-) replacement step occur? *Chembiochem,* 2**,** 190-8.
MAY, S., HORNBURG, D., SCHLUDI, M. H., ARZBERGER, T., RENTZSCH, K., SCHWENK, B. M., GRÄSSER, F. A., MORI, K., KREMMER, E., BANZHAF-STRATHMANN, J., MANN, M., MEISSNER, F. & EDBAUER, D.

2014. C9orf72 FTLD/ALS-associated Gly-Ala dipeptide repeat proteins cause neuronal toxicity and Unc119 sequestration. *Acta Neuropathologica,* 128**,** 485-503.
MCCORD, J. M. & FRIDOVICH, I. 1969. Superoxide dismutase. An enzymic function for erythrocuprein (hemocuprein). *J Biol Chem,* 244**,** 6049-55.
MEDICINE, I. O. 2006. *Amyotrophic Lateral Sclerosis in Veterans: Review of the Scientific Literature,* Washington, DC, The National Academies Press.
MEHTA, P., ANTAO, V., KAYE, W., SANCHEZ, M., WILLIAMSON, D., BRYAN, L., MURAVOV, O. & HORTON, K. 2014. Prevalence of amyotrophic lateral sclerosis - United States, 2010-2011. *MMWR Surveill Summ,* 7**,** 1-14.

MELDRUM, N. U. & ROUGHTON, F. J. 1933. Carbonic anhydrase. Its preparation and properties. *J Physiol,* 80**,** 113-42.
MERZ, K. M., JR. 1990. Insights into the function of the zinc hydroxide-Thr199-Glu106 hydrogen bonding network in carbonic anhydrases. *J Mol Biol,* 214**,** 799-802.
MIAO, L. & ST CLAIR, D. K. 2009. Regulation of superoxide dismutase genes: implications in disease. *Free Radic Biol Med,* 47**,** 344-56.
MIGUEL, L., FRÉBOURG, T., CAMPION, D. & LECOURTOIS, M. 2011. Both cytoplasmic and nuclear accumulations of the protein are neurotoxic in Drosophila models of TDP-43 proteinopathies. *Neurobiology of Disease,* 41**,** 398-406.
MIKULSKI, R., AVVARU, B. S., TU, C., CASE, N., MCKENNA, R. & SILVERMAN, D. N. 2011. Kinetic and Crystallographic Studies of the Role of Tyrosine 7 in the Active Site of Human Carbonic Anhydrase II. *Archives of biochemistry and biophysics,* 506**,** 181-187.
MILLER, R. G., MITCHELL, J. D. & MOORE, D. H. 2012. Riluzole for amyotrophic lateral sclerosis (ALS)/motor neuron disease (MND). *Cochrane Database Syst Rev,* 14.
MINCIONE, G., MENABUONI, L., BRIGANTI, F., MINCIONE, F., SCOZZAFAVA, A. & SUPURAN, C. T. 1999. Carbonic anhydrase inhibitors. Part 79. Synthesis of topically acting sulfonamides incorporating GABA moieties in their molecule, with long-lasting intraocular pressure-lowering properties. *Eur J Pharm Sci,* 9**,** 185-99.
MITSUMOTO, H., BROOKS, B. R. & SILANI, V. 2014. Clinical trials in amyotrophic lateral sclerosis: why so many negative trials and how can trials be improved? *The Lancet Neurology,* 13**,** 1127-1138.
MIZIELINSKA, S., GRÖNKE, S., NICCOLI, T., RIDLER, C. E., CLAYTON, E. L., DEVOY, A., MOENS, T., NORONA, F. E., WOOLLACOTT, I. O. C., PIETRZYK, J., CLEVERLEY, K., NICOLL, A. J., PICKERING-BROWN, S., DOLS, J., CABECINHA, M., HENDRICH, O., FRATTA, P., FISHER, E. M. C., PARTRIDGE, L. & ISAACS, A. M. 2014. C9orf72 repeat expansions cause neurodegeneration in Drosophila through arginine-rich proteins. *Science,* 345**,** 1192-1194.
MONDRUP, M. 1980. Isolation and quantitative immunoelectrophoresis of erythrocyte carbonic anhydrase B and C in subjects with thyroid disorders. *Ann Acad Med Singapore,* 9**,** 60-4.
MORI, M., STANIUNAS, R. J., BARNARD, G. F., JESSUP, J. M., STEELE, G. D., JR. & CHEN, L. B. 1993. The significance of carbonic anhydrase expression in human colorectal cancer. *Gastroenterology,* 105**,** 820-6.
MORI, K., WENG, S. M., ARZBERGER, T., MAY, S., RENTZSCH, K., KREMMER, E., SCHMID, B., KRETZSCHMAR, H. A., CRUTS, M., VAN BROECKHOVEN, C., HAASS, C. & EDBAUER, D. 2013. The C9orf72 GGGGCC repeat is translated into aggregating dipeptide-repeat proteins in FTLD/ALS. *Science,* 339**,** 1335-8.
MÜNCH, C. & BERTOLOTTI, A. 2010. Exposure of Hydrophobic Surfaces Initiates Aggregation of Diverse ALS-Causing Superoxide Dismutase-1 Mutants. *Journal of Molecular Biology,* 399**,** 512-525.

NAGAI, M., RE, D. B., NAGATA, T., CHALAZONITIS, A., JESSELL, T. M., WICHTERLE, H. & PRZEDBORSKI, S. 2007. Astrocytes expressing ALS-linked mutated SOD1 release factors selectively toxic to motor neurons. *Nature neuroscience,* 10**,** 615-622.

NELSON, L. M., MCGUIRE, V., LONGSTRETH, W. T., JR. & MATKIN, C. 2000. Population-based case-control study of amyotrophic lateral sclerosis in western Washington State. I. Cigarette smoking and alcohol consumption. *Am J Epidemiol,* 151**,** 156-63.

NEUBAUER, J. 1991. Carbonic Anhydrase and Sensory Function in the Central Nervous System. *In:* DODGSON, S., TASHIAN, R., GROS, G. & CARTER, N. (eds.) *The Carbonic Anhydrases.* Springer US.

NEUMANN, M., SAMPATHU, D. M., KWONG, L. K., TRUAX, A. C., MICSENYI, M. C., CHOU, T. T., BRUCE, J., SCHUCK, T., GROSSMAN, M., CLARK, C. M., MCCLUSKEY, L. F., MILLER, B. L., MASLIAH, E., MACKENZIE, I. R., FELDMAN, H., FEIDEN, W., KRETZSCHMAR, H. A., TROJANOWSKI, J. Q. & LEE, V. M. 2006. Ubiquitinated TDP-43 in frontotemporal lobar degeneration and amyotrophic lateral sclerosis. *Science,* 314**,** 130-3.

NISHIMORI, I., FUJIKAWAADACHI, K., ONISHI, S. & HOLLINGSWORTH, M. A. 1999. Carbonic anhydrase in human pancreas: hypotheses for the pathophysiological roles of CA isozymes. *Ann N Y Acad Sci,* 880**,** 5-16.

NISHIMORI, I. & ONISHI, S. 2001. Carbonic anhydrase isozymes in the human pancreas. *Dig Liver Dis,* 33**,** 68-74.

NISHITOH, H., KADOWAKI, H., NAGAI, A., MARUYAMA, T., YOKOTA, T., FUKUTOMI, H., NOGUCHI, T., MATSUZAWA, A., TAKEDA, K. & ICHIJO, H. 2008. ALS-linked mutant SOD1 induces ER stress- and ASK1-dependent motor neuron death by targeting Derlin-1. *Genes & Development,* 22**,** 1451-1464.

O'TOOLE, O., TRAYNOR, B. J., BRENNAN, P., SHEEHAN, C., FROST, E., CORR, B. & HARDIMAN, O. 2008. Epidemiology and clinical features of amyotrophic lateral sclerosis in Ireland between 1995 and 2004. *J Neurol Neurosurg Psychiatry,* 79**,** 30-2.

OHTA, M., ITAGAKI, Y., ITOH, N., HAYASHI, K., NISHITANI, H. & OHTA, K. 1991. Carbonic anhydrase III in serum in muscular dystrophy and other neurological disorders: relationship with creatine kinase. *Clin Chem,* 37**,** 36-9.

OMOTO, K., UEDA, S., GORIKI, K., TAKAHASHI, N., MISAWA, S. & PAGARAN, I. G. 1981. Population genetic studies of the Philippine Negritos. III. Identification of the carbonic anhydrase-1 variant with CA1 Guam. *Am J Hum Genet,* 33**,** 105-11.

OLNEY, R. K., MURPHY, J., FORSHEW, D., GARWOOD, E., MILLER, B. L., LANGMORE, S., KOHN, M. A. & LOMEN-HOERTH, C. 2005. The effects of executive and behavioral dysfunction on the course of ALS. *Neurology,* 65**,** 1774-7.

OSTERMAN, P. O., ASKMARK, H. & WISTRAND, P. J. 1985. Serum carbonic anhydrase III in neuromuscular disorders and in healthy persons after a long-distance run. *J Neurol Sci,* 70**,** 347-57.

OSWALD, T. & RILEY, D. A. 1987. Peripheral nerve carbonic anhydrase activity and chronic acetazolamide treatment of rats. *Brain Res,* 406**,** 379-84.

PAMPHLETT, R. & KUM JEW, S. 2008. *TDP-43 inclusions do not protect motor neurons from sporadic ALS*, Acta Neuropathol. 2008 Aug;116(2):221-2. doi: 10.1007/s00401-008-0392-0. Epub 2008 Jun 3.

PAN, P. W., RODRIGUEZ, A. & PARKKILA, S. 2007. A systematic quantification of carbonic anhydrase transcripts in the mouse digestive system. *BMC Mol Biol,* 8**,** 22.

PANOV, A., ORYNBAYEVA, Z., VAVILIN, V. & LYAKHOVICH, V. 2014. Fatty Acids in Energy Metabolism of the Central Nervous System. *BioMed Research International,* 2014**,** 22.

PARBOOSINGH, J. S., FIGLEWICZ, D. A., KRIZUS, A., MEININGER, V., AZAD, N. A., NEWMAN, D. S. & ROULEAU, G. A. 1997. Spinobulbar muscular atrophy can mimic ALS: the importance of genetic testing in male patients with atypical ALS. *Neurology,* 49**,** 568-72.

PARKKILA, S., PARKKILA, A.-K., RAJANIEMI, H., SHAH, G. N., GRUBB, J. H., WAHEED, A. & SLY, W. S. 2001. Expression of membrane-associated carbonic anhydrase XIV on neurons and axons in mouse and human brain. *Proceedings of the National Academy of Sciences,* 98**,** 1918-1923.

PARKKILA, S., PARKKILA, A. K., JUVONEN, T. & RAJANIEMI, H. 1994. Distribution of the carbonic anhydrase isoenzymes I, II, and VI in the human alimentary tract. *Gut,* 35**,** 646-650.

PARKKILA, S., PARKKILA, A. K., LEHTOLA, J., REINILA, A., SODERVIK, H. J., RANNISTO, M. & RAJANIEMI, H. 1997. Salivary carbonic anhydrase protects gastroesophageal mucosa from acid injury. *Dig Dis Sci,* 42**,** 1013-9.

PASINELLI, P., BELFORD, M. E., LENNON, N., BACSKAI, B. J., HYMAN, B. T., TROTTI, D. & BROWN, R. H., JR. 2004. Amyotrophic lateral sclerosis-associated SOD1 mutant proteins bind and aggregate with Bcl-2 in spinal cord mitochondria. *Neuron,* 43**,** 19-30.

PASTERNACK, M., VOIPIO, J. & KAILA, K. 1993. Intracellular carbonic anhydrase activity and its role in GABA-induced acidosis in isolated rat hippocampal pyramidal neurones. *Acta Physiologica Scandinavica,* 148**,** 229.

PASTOREKOVA, S., PARKKILA, S., PASTOREK, J. & SUPURAN, C. T. 2004. Carbonic anhydrases: current state of the art, therapeutic applications and future prospects. *J Enzyme Inhib Med Chem,* 19**,** 199-229.

PEDRINI, S., SAU, D., GUARESCHI, S., BOGUSH, M., BROWN, R. H., NANICHE, N., KIA, A., TROTTI, D. & PASINELLI, P. 2010. ALS-linked mutant SOD1 damages mitochondria by promoting conformational changes in Bcl-2. *Human Molecular Genetics,* 19**,** 2974-2986.

PERLSON, E., JEONG, G.-B., ROSS, J. L., DIXIT, R., WALLACE, K. E., KALB, R. G. & HOLZBAUR, E. L. F. 2009. A Switch in Retrograde Signaling from Survival to Stress in Rapid-Onset Neurodegeneration. *The Journal of Neuroscience,* 29**,** 9903-9917.

PEYRONNARD, J. M., MESSIER, J. P., CHARRON, L., LAVOIE, J., BERGOUIGNAN, F. X. & DUBREUIL, M. 1986. Carbonic anhydrase activity in the normal and injured peripheral nervous system of the rat. *Exp Neurol,* 93**,** 481-99.

PHUKAN, J., PENDER, N. P. & HARDIMAN, O. 2007. Cognitive impairment in amyotrophic lateral sclerosis. *Lancet Neurol,* 6**,** 994-1003.

POLYMENIDOU, M., LAGIER-TOURENNE, C., HUTT, K. R., HUELGA, S. C., MORAN, J., LIANG, T. Y., LING, S.-C., SUN, E., WANCEWICZ, E., MAZUR, C., KORDASIEWICZ, H., SEDAGHAT, Y., DONOHUE, J. P., SHIUE, L., BENNETT, C. F., YEO, G. W. & CLEVELAND, D. W. 2011a. Long pre-mRNA depletion and RNA missplicing contribute to neuronal vulnerability from loss of TDP-43. *Nature neuroscience,* 14**,** 459-468.

POLYMENIDOU, M., LAGIER-TOURENNE, C., HUTT, K. R., HUELGA, S. C., MORAN, J., LIANG, T. Y., LING, S.-C., SUN, E., WANCEWICZ, E., MAZUR, C., KORDASIEWICZ, H., SEDAGHAT, Y., DONOHUE, J. P., SHIUE, L., BENNETT, C. F., YEO, G. W. & CLEVELAND, D. W. 2011b. Long pre-mRNA depletion and RNA missplicing contribute to neuronal vulnerability from loss of TDP-43. *Nat Neurosci,* 14**,** 459-468.

PRUDENCIO, M., HART, P. J., BORCHELT, D. R. & ANDERSEN, P. M. 2009. Variation in aggregation propensities among ALS-associated variants of SOD1: correlation to human disease. *Hum Mol Genet,* 18**,** 3217-26.

PULS, I., JONNAKUTY, C., LAMONTE, B. H., HOLZBAUR, E. L., TOKITO, M., MANN, E., FLOETER, M. K., BIDUS, K., DRAYNA, D., OH, S. J., BROWN, R. H., JR., LUDLOW, C. L. & FISCHBECK, K. H. 2003. Mutant dynactin in motor neuron disease. *Nat Genet,* 33**,** 455-6.

PURKERSON, J. M. & SCHWARTZ, G. J. 2006. The role of carbonic anhydrases in renal physiology. *Kidney Int,* 71**,** 103-115.

RADEMAKERS, R., STEWART, H., DEJESUS-HERNANDEZ, M., KRIEGER, C., GRAFF-RADFORD, N., FABROS, M., BRIEMBERG, H., CASHMAN, N., EISEN, A. & MACKENZIE, I. R. A. 2010. *Fus Gene Mutations in Familial and Sporadic Amyotrophic Lateral Sclerosis*, Muscle Nerve. 42(2):170-6.

RANGACHARI, P. K. 2007. Texts in context: Horace Davenport, carbonic anhydrase, and gastric acid secretion. *Advances in Physiology Education,* 31**,** 140-144.

REAUME, A. G., ELLIOTT, J. L., HOFFMAN, E. K., KOWALL, N. W., FERRANTE, R. J., SIWEK, D. R., WILCOX, H. M., FLOOD, D. G., BEAL, M. F., BROWN, R. H., SCOTT, R. W. & SNIDER, W. D. 1996. Motor neurons in Cu/Zn superoxide dismutase-deficient mice develop normally but exhibit enhanced cell death after axonal injury. *Nat Genet,* 13**,** 43-47.

REN, X. & LINDSKOG, S. 1992. Buffer dependence of CO2 hydration catalyzed by human carbonic anhydrase I. *Biochim Biophys Acta,* 27**,** 81-6.

RENTON, A. E., CHIO, A. & TRAYNOR, B. J. 2014. State of play in amyotrophic lateral sclerosis genetics. *Nat Neurosci,* 17**,** 17-23.

RENTON, A. E., MAJOUNIE, E., WAITE, A., SIMON-SANCHEZ, J., ROLLINSON, S., GIBBS, J. R., SCHYMICK, J. C., LAAKSOVIRTA, H., VAN SWIETEN, J. C., MYLLYKANGAS, L., KALIMO, H., PAETAU, A., ABRAMZON, Y., REMES, A. M., KAGANOVICH, A., SCHOLZ, S. W., DUCKWORTH, J., DING, J., HARMER, D. W., HERNANDEZ, D. G., JOHNSON, J. O., MOK, K., RYTEN, M., TRABZUNI, D., GUERREIRO, R. J., ORRELL, R. W., NEAL, J., MURRAY, A., PEARSON, J., JANSEN, I. E., SONDERVAN, D., SEELAAR, H., BLAKE, D., YOUNG, K., HALLIWELL, N., CALLISTER, J. B., TOULSON, G., RICHARDSON, A., GERHARD, A., SNOWDEN, J., MANN, D., NEARY, D., NALLS, M. A., PEURALINNA, T., JANSSON, L., ISOVIITA, V. M., KAIVORINNE, A. L., HOLTTA-VUORI, M., IKONEN, E., SULKAVA, R., BENATAR, M., WUU, J., CHIO, A., RESTAGNO, G., BORGHERO, G., SABATELLI, M., HECKERMAN, D., ROGAEVA, E., ZINMAN, L., ROTHSTEIN, J. D., SENDTNER, M., DREPPER, C., EICHLER, E. E., ALKAN, C., ABDULLAEV, Z., PACK, S. D., DUTRA, A., PAK, E., HARDY, J., SINGLETON, A., WILLIAMS, N. M., HEUTINK, P., PICKERING-BROWN, S., MORRIS, H. R., TIENARI, P. J. & TRAYNOR, B. J. 2011. A hexanucleotide repeat expansion in C9ORF72 is the cause of chromosome 9p21-linked ALS-FTD. *Neuron,* 72**,** 257-68.

RILEY, D. A., ELLIS, S. & BAIN, J. 1982. Carbonic anhydrase activity in skeletal muscle fiber types, axons, spindles, and capillaries of rat soleus and extensor digitorum longus muscles. *J Histochem Cytochem,* 30**,** 1275-88.

RILEY, D. A., ELLIS, S. & BAIN, J. L. W. 1984. Ultrastructural cytochemical localization of carbonic anhydrase activity in rat peripheral sensory and motor nerves, dorsal root ganglia and dorsal column nuclei. *Neuroscience,* 13**,** 189-206.

RILEY, D. A. & LANG, D. H. 1984. Carbonic anhydrase activity of human peripheral nerves: A possible histochemical aid to nerve repair. *The Journal of Hand Surgery,* 9**,** 112-120.

RILEY, D. A., SANGER, J. R., MATLOUB, H. S., YOUSIF, N. J., BAIN, J. L. & MOORE, G. H. 1988. Identifying motor and sensory myelinated axons in rabbit peripheral nerves by histochemical staining for carbonic anhydrase and cholinesterase activities. *Brain Res,* 453**,** 79-88.

RIPPON, G. A., SCARMEAS, N., GORDON, P. H., MURPHY, P. L., ALBERT, S. M., MITSUMOTO, H., MARDER, K., ROWLAND, L. P. & STERN, Y. 2006. An observational study of cognitive impairment in amyotrophic lateral sclerosis. *Arch Neurol,* 63**,** 345-52.

ROBERTSON, B. & GRANT, G. 1989. Immunocytochemical evidence for the localization of the GM1 ganglioside in carbonic anhydrase-containing and RT 97-immunoreactive rat primary sensory neurons. *J Neurocytol,* 18**,** 77-86.

ROGELJ, B., EASTON, L. E., BOGU, G. K., STANTON, L. W., ROT, G., CURK, T., ZUPAN, B., SUGIMOTO, Y., MODIC, M., HABERMAN, N., TOLLERVEY, J., FUJII, R., TAKUMI, T., SHAW, C. E. & ULE, J. 2012. Widespread binding of FUS along nascent RNA regulates alternative splicing in the brain. *Sci. Rep.,* 2.

ROSEN, D. R., SIDDIQUE, T., PATTERSON, D., FIGLEWICZ, D. A., SAPP, P., HENTATI, A., DONALDSON, D., GOTO, J., O'REGAN, J. P., DENG, H. X. & ET AL. 1993. Mutations in Cu/Zn superoxide dismutase gene are associated with familial amyotrophic lateral sclerosis. *Nature,* 362**,** 59-62.

ROUSSEL, G., DELAUNOY, J.-P., NUSSBAUM, J.-L. & MANDEL, P. 1979. Demonstration of a specific localization of carbonic anhydrase C in the glial cells of rat CNS by an immunohistochemical method. *Brain Research,* 160**,** 47-55.

ROWLAND, L. P. 2010. Progressive muscular atrophy and other lower motor neuron syndromes of adults. *Muscle Nerve,* 41**,** 161-5.

ROWLAND, L. P. & SHNEIDER, N. A. 2001. Amyotrophic lateral sclerosis. *N Engl J Med,* 344**,** 1688-700.

SABATELLI, M., MADIA, F., CONTE, A., LUIGETTI, M., ZOLLINO, M., MANCUSO, I., LO MONACO, M., LIPPI, G. & TONALI, P. 2008. Natural history of young-adult amyotrophic lateral sclerosis. *Neurology,* 71**,** 876-81.

SALINAS, S., PROUKAKIS, C., CROSBY, A. & WARNER, T. T. 2008. Hereditary spastic paraplegia: clinical features and pathogenetic mechanisms. *Lancet Neurol,* 7**,** 1127-38.

SANDERS, R. D. & GILLIG, P. M. 2010. Cranial Nerve VIII: Hearing and Vestibular Functions. *Psychiatry (Edgmont),* 7**,** 17-22.

SANGER, J. R., RILEY, D. A., MATLOUB, H. S., YOUSIF, N. J., BAIN, J. L. & MOORE, G. H. 1991. Effects of axotomy on the cholinesterase and carbonic anhydrase activities of axons in the proximal and distal stumps of rabbit sciatic nerves: a temporal study. *Plast Reconstr Surg,* 87**,** 726-38.

SAPIRSTEIN, V. S., STROCCHI, P. & GILBERT, J. M. 1984. Properties and function of brain carbonic anhydrase. *Ann N Y Acad Sci,* 429**,** 481-93.

SAREEN, D., O'ROURKE, J. G., MEERA, P., MUHAMMAD, A., GRANT, S., SIMPKINSON, M., BELL, S., CARMONA, S., ORNELAS, L., SAHABIAN, A., GENDRON, T., PETRUCELLI, L., BAUGHN, M., RAVITS, J., HARMS, M. B., RIGO, F., BENNETT, C. F., OTIS, T. S., SVENDSEN, C. N. & BALOH, R. H. 2013. Targeting RNA foci in iPSC-derived motor neurons from ALS patients with C9ORF72 repeat expansion. *Science translational medicine,* 5**,** 208

SATO, S., ZHU, X. L. & SLY, W. S. 1990. Carbonic anhydrase isozymes IV and II in urinary membranes from carbonic anhydrase II-deficient patients. *Proc Natl Acad Sci U S A,* 87**,** 6073-6.

SCHEID, P. & SIFFERT, W. 1985. Effects of inhibiting carbonic anhydrase on isometric contraction of frog skeletal muscle. *J Physiol,* 361**,** 91-101.

SCHWARTZ, J. C., EBMEIER, C. C., PODELL, E. R., HEIMILLER, J., TAATJES, D. J. & CECH, T. R. 2012. FUS binds the CTD of RNA polymerase II and regulates its phosphorylation at Ser2. *Genes & Development,* 26**,** 2690-2695.

SEGUIN, S. J., MORELLI, F. F., VINET, J., AMORE, D., DE BIASI, S., POLETTI, A., RUBINSZTEIN, D. C. & CARRA, S. 2014. Inhibition of autophagy, lysosome and VCP function impairs stress granule assembly. *Cell Death Differ,* 21**,** 1838-1851.

SEIBENHENER, M. L., BABU, J. R., GEETHA, T., WONG, H. C., KRISHNA, N. R. & WOOTEN, M. W. 2004. Sequestosome 1/p62 Is a Polyubiquitin Chain Binding Protein Involved in Ubiquitin Proteasome Degradation. *Molecular and Cellular Biology,* 24**,** 8055-8068.

SEIBENHENER, M. L., GEETHA, T. & WOOTEN, M. W. 2007. Sequestosome 1/p62 – More than just a scaffold. *FEBS Letters,* 581**,** 175-179.

SEPHTON, C. F., CENIK, C., KUCUKURAL, A., DAMMER, E. B., CENIK, B., HAN, Y., DEWEY, C. M., ROTH, F. P., HERZ, J., PENG, J., MOORE, M. J. & YU, G. 2011. Identification of neuronal RNA targets of TDP-43-containing ribonucleoprotein complexes. *J Biol Chem,* 286**,** 1204-15.

SEPHTON, C. F., GOOD, S. K., ATKIN, S., DEWEY, C. M., MAYER, P., 3RD, HERZ, J. & YU, G. 2010. TDP-43 is a developmentally regulated protein essential for early embryonic development. *J Biol Chem,* 285**,** 6826-34.

SEVERINGHAUS, J. W., HAMILTON, F. N. & COTEV, S. 1969. Carbonic acid production and the role of carbonic anhydrase in decarboxylation in brain. *Biochem J,* 114**,** 703-5.
SHAH, G. N., ULMASOV, B., WAHEED, A., BECKER, T., MAKANI, S., SVICHAR, N., CHESLER, M. & SLY, W. S. 2005. Carbonic anhydrase IV and XIV knockout mice: Roles of the respective carbonic anhydrases in buffering the extracellular space in brain. *Proceedings of the National Academy of Sciences of the United States of America,* 102**,** 16771-16776.
SHAPIRA, E., BEN-YOSEPH, Y., EYAL, F. G. & RUSSELL, A. 1974. Enzymatically inactive red cell carbonic anhydrase B in a family with renal tubular acidosis. *J Clin Invest,* 53**,** 59-63.
SHIMA, K., TASHIRO, K., HIBI, N., TSUKADA, Y. & HIRAI, H. 1983. Carbonic anhydrase-III immunohistochemical localization in human skeletal muscle. *Acta Neuropathol,* 59**,** 237-9.
SILVERMAN, D. N. & LINDSKOG, S. 1988. The catalytic mechanism of carbonic anhydrase: implications of a rate-limiting protolysis of water. *Accounts of Chemical Research,* 21**,** 30-36.
SINIATCHKIN, M., GROPPA, S., SIEBNER, H. & STEPHANI, U. 2006. A single dose of sulthiame induces a selective increase in resting motor threshold in human motor cortex: A transcranial magnetic stimulation study. *Epilepsy Research,* 72**,** 18-24.
SKAGGS, L. A., BERGENHEM, N. C., VENTA, P. J. & TASHIAN, R. E. 1993. The deduced amino acid sequence of human carbonic anhydrase-related protein (CARP) is 98% identical to the mouse homologue. *Gene,* 126**,** 291-2.
SLY, W. S., HEWETT-EMMETT, D., WHYTE, M. P., YU, Y. S. & TASHIAN, R. E. 1983. Carbonic anhydrase II deficiency identified as the primary defect in the autosomal recessive syndrome of osteopetrosis with renal tubular acidosis and cerebral calcification. *Proceedings of the National Academy of Sciences of the United States of America,* 80**,** 2752-2756.
SLY, W. S. & HU, P. Y. 1995. Human carbonic anhydrases and carbonic anhydrase deficiencies. *Annu Rev Biochem,* 64**,** 375-401.
SMITH, K. S., JAKUBZICK, C., WHITTAM, T. S. & FERRY, J. G. 1999. Carbonic anhydrase is an ancient enzyme widespread in prokaryotes. *Proc Natl Acad Sci U S A,* 96**,** 15184-9.
SNOWDEN, J. S., ROLLINSON, S., THOMPSON, J. C., HARRIS, J. M., STOPFORD, C. L., RICHARDSON, A. M. T., JONES, M., GERHARD, A., DAVIDSON, Y. S., ROBINSON, A., GIBBONS, L., HU, Q., DUPLESSIS, D., NEARY, D., MANN, D. M. A. & PICKERING-BROWN, S. M. 2012. Distinct clinical and pathological characteristics of frontotemporal dementia associated with C9ORF72 mutations. *Brain,* 135**,** 693-708.
SNYDER, D. S., ZIMMERMAN JR, T. R., FAROOQ, M., NORTON, W. T. & CAMMER, W. 1983. Carbonic anhydrase, 5'-nucleotidase, and 2',3'-cyclic nucleotide-3'-phosphodiesterase activities in oligodendrocytes, astrocytes, and neurons isolated from the brains of developing rats. *Journal of Neurochemistry,* 40**,** 120-127.
SREEDHARAN, J., BLAIR, I. P., TRIPATHI, V. B., HU, X., VANCE, C., ROGELJ, B., ACKERLEY, S., DURNALL, J. C., WILLIAMS, K. L., BURATTI, E., BARALLE, F., DE BELLEROCHE, J., MITCHELL, J. D., LEIGH, P. N., AL-CHALABI, A., MILLER, C. C., NICHOLSON, G. & SHAW, C. E. 2008. TDP-43 mutations in familial and sporadic amyotrophic lateral sclerosis. *Science,* 319**,** 1668-72.
STEELE, J. C. 2005. Parkinsonism-dementia complex of Guam. *Mov Disord,* 20**,** S99-S107.
STEELE, J. C. & MCGEER, P. L. 2008. The ALS/PDC syndrome of Guam and the cycad hypothesis. *Neurology,* 70**,** 1984-1990.
STEINER, H., JONSSON, B. H. & LINDSKOG, S. 1975. The catalytic mechanism of carbonic anhydrase. Hydrogen-isotope effects on the kinetic parameters of the human C isoenzyme. *Eur J Biochem,* 59**,** 253-9.
STRONG, M. J., VOLKENING, K., HAMMOND, R., YANG, W., STRONG, W., LEYSTRA-LANTZ, C. & SHOESMITH, C. 2007. TDP43 is a human low molecular weight neurofilament (hNFL) mRNA-binding protein. *Mol Cell Neurosci,* 35**,** 320-7.

STRONG, M. J. & YANG, W. 2011. The frontotemporal syndromes of ALS. Clinicopathological correlates. *J Mol Neurosci,* 45**,** 648-55.
SUN, M. K. & ALKON, D. L. 2002. Carbonic anhydrase gating of attention: memory therapy and enhancement. *Trends Pharmacol Sci,* 23**,** 83-9.
SUN, S., LING, S.-C., QIU, J., ALBUQUERQUE, C. P., ZHOU, Y., TOKUNAGA, S., LI, H., QIU, H., BUI, A., YEO, G. W., HUANG, E. J., EGGAN, K., ZHOU, H., FU, X.-D., LAGIER-TOURENNE, C. & CLEVELAND, D. W. 2015. ALS-causative mutations in FUS/TLS confer gain and loss of function by altered association with SMN and U1-snRNP. *Nat Commun,* 6.
SUPURAN, C. T. 2008. Carbonic anhydrases: novel therapeutic applications for inhibitors and activators. *Nat Rev Drug Discov,* 7**,** 168-81.
SUPURAN, C. T. 2011. Carbonic anhydrase inhibitors and activators for novel therapeutic applications. *Future Med Chem,* 3**,** 1165-80.
SUPURAN, C. T., DI FIORE, A. & DE SIMONE, G. 2008. Carbonic anhydrase inhibitors as emerging drugs for the treatment of obesity. *Expert Opin Emerg Drugs,* 13**,** 383-92.
SUPURAN, C. T. & SCOZZAFAVA, A. 2002. Applications of carbonic anhydrase inhibitors and activators in therapy. *Expert Opinion on Therapeutic Patents,* 12**,** 217-242.
SUPURAN, C. T., SCOZZAFAVA, A. & CASINI, A. 2003. Carbonic anhydrase inhibitors. *Med Res Rev,* 23**,** 146-89.
SUPURAN, C. T., SCOZZAFAVA, A. & CONWAY, J. 2005. Carbonic Anhydrase: its inhibitors and activators. *In:* SMITH, J. T. & SIMONS, C. (eds.). MA: Taylor and Francis.
SUZUKI, H., SHIBAGAKI, Y., HATTORI, S. & MATSUOKA, M. 2015. Nuclear TDP-43 causes neuronal toxicity by escaping from the inhibitory regulation by hnRNPs. *Hum Mol Genet,* 24**,** 1513-27.
SVICHAR, N., WAHEED, A., SLY, W. S., HENNINGS, J. C., HUBNER, C. A. & CHESLER, M. 2009. Carbonic anhydrases CA4 and CA14 both enhance AE3-mediated Cl--HCO3- exchange in hippocampal neurons. *J Neurosci,* 29**,** 3252-8.
SWINNEN, B. & ROBBERECHT, W. 2014. The phenotypic variability of amyotrophic lateral sclerosis. *Nat Rev Neurol,* 10**,** 661-70.
SZABOLCS, M. J., WINDISCH, A., KOLLER, R. & PENSCH, M. 1991. Axon typing of rat muscle nerves using a double staining procedure for cholinesterase and carbonic anhydrase. *J Histochem Cytochem,* 39**,** 1617-25.
TAKAKURA, M., YOKOMIZO, A., TANAKA, Y., KOBAYASHI, M., JUNG, G., BANNO, M., SAKUMA, T., IMADA, K., ODA, Y., KAMITA, M., HONDA, K., YAMADA, T., NAITO, S. & ONO, M. 2012. Carbonic anhydrase I as a new plasma biomarker for prostate cancer. *ISRN Oncol,* 768190**,** 19.
TALBOT, K. 2009. Motor neuron disease: the bare essentials. *Pract Neurol,* 9**,** 303-9.
TANSEY, F. A., THAMPY, K. G. & CAMMER, W. 1988. Acetyl-CoA carboxylase in rat brain. II. Immunocytochemical localization. *Brain Res,* 471**,** 131-8.
TAWIL, R., MOXLEY, R. T., 3RD & GRIGGS, R. C. 1993. Acetazolamide-induced nephrolithiasis: implications for treatment of neuromuscular disorders. *Neurology,* 43**,** 1105-6.
THOMAS, M., ALEGRE-ABARRATEGUI, J. & WADE-MARTINS, R. 2013. RNA dysfunction and aggrephagy at the centre of an amyotrophic lateral sclerosis/frontotemporal dementia disease continuum. *Brain,* 136**,** 1345-60.
TICOZZI, N., SILANI, V., LECLERC, A. L., KEAGLE, P., GELLERA, C., RATTI, A., TARONI, F., KWIATKOWSKI, T. J., JR., MCKENNA-YASEK, D. M., SAPP, P. C., BROWN, R. H., JR. & LANDERS, J. E. 2009. Analysis of FUS gene mutation in familial amyotrophic lateral sclerosis within an Italian cohort. *Neurology,* 73**,** 1180-5.
TIWARI, A., XU, Z. & HAYWARD, L. J. 2005. Aberrantly increased hydrophobicity shared by mutants of Cu,Zn-superoxide dismutase in familial amyotrophic lateral sclerosis. *J Biol Chem,* 280**,** 29771-9.

TOLLERVEY, J. R., CURK, T., ROGELJ, B., BRIESE, M., CEREDA, M., KAYIKCI, M., KONIG, J., HORTOBAGYI, T., NISHIMURA, A. L., ZUPUNSKI, V., PATANI, R., CHANDRAN, S., ROT, G., ZUPAN, B., SHAW, C. E. & ULE, J. 2011. Characterizing the RNA targets and position-dependent splicing regulation by TDP-43. *Nat Neurosci,* 14**,** 452-8.

TORELLA, D., ELLISON, G. M., TORELLA, M., VICINANZA, C., AQUILA, I., IACONETTI, C., SCALISE, M., MARINO, F., HENNING, B. J., LEWIS, F. C., GARERI, C., LASCAR, N., CUDA, G., SALVATORE, T., NAPPI, G., INDOLFI, C., TORELLA, R., COZZOLINO, D. & SASSO, F. C. 2014. Carbonic anhydrase activation is associated with worsened pathological remodeling in human ischemic diabetic cardiomyopathy. *J Am Heart Assoc,* 3**,** 000434.

TSANG, C. K., LIU, Y., THOMAS, J., ZHANG, Y. & ZHENG, X. F. 2014. Superoxide dismutase 1 acts as a nuclear transcription factor to regulate oxidative stress resistance. *Nat Commun,* 5.

URUSHITANI, M., SIK, A., SAKURAI, T., NUKINA, N., TAKAHASHI, R. & JULIEN, J. P. 2006. Chromogranin-mediated secretion of mutant superoxide dismutase proteins linked to amyotrophic lateral sclerosis. *Nat Neurosci,* 9**,** 108-18.

VAANANEN, H. K., TAKALA, T. E., TOLONEN, U., VUORI, J. & MYLLYLA, V. V. 1988. Muscle-specific carbonic anhydrase III is a more sensitive marker of muscle damage than creatine kinase in neuromuscular disorders. *Arch Neurol,* 45**,** 1254-6.

VAN DAMME, P., BOGAERT, E., DEWIL, M., HERSMUS, N., KIRALY, D., SCHEVENEELS, W., BOCKX, I., BRAEKEN, D., VERPOORTEN, N., VERHOEVEN, K., TIMMERMAN, V., HERIJGERS, P., CALLEWAERT, G., CARMELIET, P., VAN DEN BOSCH, L. & ROBBERECHT, W. 2007. Astrocytes regulate GluR2 expression in motor neurons and their vulnerability to excitotoxicity. *Proc Natl Acad Sci U S A,* 104**,** 14825-30.

VAN DEN BOSCH, L., VAN DAMME, P., BOGAERT, E. & ROBBERECHT, W. 2006. The role of excitotoxicity in the pathogenesis of amyotrophic lateral sclerosis. *Biochimica et Biophysica Acta (BBA) - Molecular Basis of Disease,* 1762**,** 1068-1082.

VANCE, C., ROGELJ, B., HORTOBAGYI, T., DE VOS, K. J., NISHIMURA, A. L., SREEDHARAN, J., HU, X., SMITH, B., RUDDY, D., WRIGHT, P., GANESALINGAM, J., WILLIAMS, K. L., TRIPATHI, V., AL-SARAJ, S., AL-CHALABI, A., LEIGH, P. N., BLAIR, I. P., NICHOLSON, G., DE BELLEROCHE, J., GALLO, J. M., MILLER, C. C. & SHAW, C. E. 2009. Mutations in FUS, an RNA processing protein, cause familial amyotrophic lateral sclerosis type 6. *Science,* 323**,** 1208-11.

VANDE VELDE, C., MILLER, T. M., CASHMAN, N. R. & CLEVELAND, D. W. 2008. Selective association of misfolded ALS-linked mutant SOD1 with the cytoplasmic face of mitochondria. *Proc Natl Acad Sci U S A,* 105**,** 4022-7.

VERPOORTE, J. A., MEHTA, S. & EDSALL, J. T. 1967. Esterase activities of human carbonic anhydrases B and C. *J Biol Chem,* 242**,** 4221-9.

VISANJI, N. P., WONG, J. C., WANG, S. X., CAPPEL, B., KLEINSCHMIDT-DEMASTERS, B. K., HANDLER, M. H., OCHI, A., OTSUBO, H., RUTKA, J. T., GO, C., WEISS, S., VINTERS, H. V., HAWKINS, C. E., DESOUZA, L. V., SIU, K. W. & HAZRATI, L. N. 2012. A proteomic analysis of pediatric seizure cases associated with astrocytic inclusions. *Epilepsia,* 53**,** 1528-1167.

VOLKENING, K., LEYSTRA-LANTZ, C., YANG, W., JAFFEE, H. & STRONG, M. J. 2009. Tar DNA binding protein of 43 kDa (TDP-43), 14-3-3 proteins and copper/zinc superoxide dismutase (SOD1) interact to modulate NFL mRNA stability. Implications for altered RNA processing in amyotrophic lateral sclerosis (ALS). *Brain Res,* 11**,** 168-82.

WANG, J., XU, G., LI, H., GONZALES, V., FROMHOLT, D., KARCH, C., COPELAND, N. G., JENKINS, N. A. & BORCHELT, D. R. 2005. Somatodendritic accumulation of misfolded SOD1-L126Z in motor neurons mediates degeneration: alphaB-crystallin modulates aggregation. *Hum Mol Genet,* 14**,** 2335-47.

WANG, Q., JOHNSON, J. L., AGAR, N. Y. R. & AGAR, J. N. 2008. Protein Aggregation and Protein Instability Govern Familial Amyotrophic Lateral Sclerosis Patient Survival. *PLoS Biol,* 6**,** e170.
WANG, H., O'REILLY, E. J., WEISSKOPF, M. G., LOGROSCINO, G., MCCULLOUGH, M. L., THUN, M. J., SCHATZKIN, A., KOLONEL, L. N. & ASCHERIO, A. 2011a. Smoking and risk of amyotrophic lateral sclerosis: a pooled analysis of 5 prospective cohorts. *Arch Neurol,* 68**,** 207-13.
WANG, J.-W., BRENT, J. R., TOMLINSON, A., SHNEIDER, N. A. & MCCABE, B. D. 2011b. The ALS-associated proteins FUS and TDP-43 function together to affect Drosophila locomotion and life span. *The Journal of Clinical Investigation,* 121**,** 4118-4126.
WANG, N., CHEN, Y., HAN, Y., ZHAO, Y., LIU, Y., GUO, K. & JIANG, Y. 2012. Proteomic analysis shows down-regulations of cytoplasmic carbonic anhydrases, CAI and CAII, are early events of colorectal carcinogenesis but are not correlated with lymph node metastasis. *Tumori,* 98**,** 783-91.
WEIHL, C. C., PESTRONK, A. & KIMONIS, V. E. 2009. Valosin-containing protein disease: inclusion body myopathy with Paget's disease of the bone and fronto-temporal dementia. *Neuromuscul Disord,* 19**,** 308-15.
WEISSKOPF, M. G., O'REILLY, E. J., MCCULLOUGH, M. L., CALLE, E. E., THUN, M. J., CUDKOWICZ, M. & ASCHERIO, A. 2005. Prospective study of military service and mortality from ALS. *Neurology,* 64**,** 32-7.
WEN, X., TAN, W., WESTERGARD, T., KRISHNAMURTHY, K., MARKANDAIAH, S. S., SHI, Y., LIN, S., SHNEIDER, N. A., MONAGHAN, J., PANDEY, U. B., PASINELLI, P., ICHIDA, J. K. & TROTTI, D. 2014. Antisense proline-arginine RAN dipeptides linked to C9ORF72-ALS/FTD form toxic nuclear aggregates that initiate *in vitro* and in vivo neuronal death. *Neuron,* 84**,** 1213-25.
WILKE, R. A., RILEY, D. A. & SANGER, J. R. 1992. Histochemical discrimination of fibers in regenerating rat infraorbital nerve. *Microsurgery,* 13**,** 39-44.
WILLIAMSON, T. L. & CLEVELAND, D. W. 1999. Slowing of axonal transport is a very early event in the toxicity of ALS-linked SOD1 mutants to motor neurons. *Nat Neurosci,* 2**,** 50-6.
WINKLHOFER, K. F., TATZELT, J. & HAASS, C. 2008. The two faces of protein misfolding: gain- and loss-of-function in neurodegenerative diseases. *EMBO J,* 27**,** 336-49.
WINTON, M. J., IGAZ, L. M., WONG, M. M., KWONG, L. K., TROJANOWSKI, J. Q. & LEE, V. M. 2008. Disturbance of nuclear and cytoplasmic TAR DNA-binding protein (TDP-43) induces disease-like redistribution, sequestration, and aggregate formation. *J Biol Chem,* 283**,** 13302-9.
WÓJCIK, C., YANO, M. & DEMARTINO, G. N. 2004. RNA interference of valosin-containing protein (VCP/p97) reveals multiple cellular roles linked to ubiquitin/proteasome-dependent proteolysis. *Journal of Cell Science,* 117**,** 281-292.
WOLFSON, C., KILBORN, S., OSKOUI, M. & GENGE, A. 2009. Incidence and prevalence of amyotrophic lateral sclerosis in Canada: a systematic review of the literature. *Neuroepidemiology,* 33**,** 79-88.
WONG, V., BARRETT, C. P., DONATI, E. J., ENG, L. F. & GUTH, L. 1983. Carbonic anhydrase activity in first-order sensory neurons of the rat. *J Histochem Cytochem,* 31**,** 293-300.
WONG, Y. C. & HOLZBAUR, E. L. F. 2014. Optineurin is an autophagy receptor for damaged mitochondria in parkin-mediated mitophagy that is disrupted by an ALS-linked mutation. *Proceedings of the National Academy of Sciences of the United States of America,* 111**,** E4439-E4448.
WONG, P. C., PARDO, C. A., BORCHELT, D. R., LEE, M. K., COPELAND, N. G., JENKINS, N. A., SISODIA, S. S., CLEVELAND, D. W. & PRICE, D. L. 1995. An adverse property of a familial ALS-linked SOD1 mutation causes motor neuron disease characterized by vacuolar degeneration of mitochondria. *Neuron,* 14**,** 1105-1116.
WRIGHT, G. S. A., ANTONYUK, S. V., KERSHAW, N. M., STRANGE, R. W. & SAMAR HASNAIN, S. 2013. Ligand binding and aggregation of pathogenic SOD1. *Nat Commun,* 4**,** 1758.
WU, C.-H., FALLINI, C., TICOZZI, N., KEAGLE, P. J., SAPP, P. C., PIOTROWSKA, K., LOWE, P., KOPPERS, M., MCKENNA-YASEK, D., BARON, D. M., KOST, J. E., GONZALEZ-PEREZ, P., FOX, A. D., ADAMS, J.,

TARONI, F., TILOCA, C., LECLERC, A. L., CHAFE, S. C., MANGROO, D., MOORE, M. J., ZITZEWITZ, J. A., XU, Z.-S., VAN DEN BERG, L. H., GLASS, J. D., SICILIANO, G., CIRULLI, E. T., GOLDSTEIN, D. B., SALACHAS, F., MEININGER, V., ROSSOLL, W., RATTI, A., GELLERA, C., BOSCO, D. A., BASSELL, G. J., SILANI, V., DRORY, V. E., BROWN, R. H. & LANDERS, J. E. 2012. Mutations in the Profilin 1 Gene Cause Familial Amyotrophic Lateral Sclerosis. *Nature,* 488**,** 499-503.

WU, D.-C., RÉ, D. B., NAGAI, M., ISCHIROPOULOS, H. & PRZEDBORSKI, S. 2006. The inflammatory NADPH oxidase enzyme modulates motor neuron degeneration in amyotrophic lateral sclerosis mice. *Proceedings of the National Academy of Sciences of the United States of America,* 103**,** 12132-12137.

XI, Z., RAINERO, I., RUBINO, E., PINESSI, L., BRUNI, A. C., MALETTA, R. G., NACMIAS, B., SORBI, S., GALIMBERTI, D., SURACE, E. I., ZHENG, Y., MORENO, D., SATO, C., LIANG, Y., ZHOU, Y., ROBERTSON, J., ZINMAN, L., TARTAGLIA, M. C., ST. GEORGE-HYSLOP, P. & ROGAEVA, E. 2014. Hypermethylation of the CpG-island near the C9orf72 G4C2-repeat expansion in FTLD patients. *Human Molecular Genetics,* 23**,** 5630-5637.

XI, Z., VAN BLITTERSWIJK, M., ZHANG, M., MCGOLDRICK, P., MCLEAN, J. R., YUNUSOVA, Y., KNOCK, E., MORENO, D., SATO, C., MCKEEVER, P. M., SCHNEIDER, R., KEITH, J., PETRESCU, N., FRASER, P., TARTAGLIA, M. C., BAKER, M. C., GRAFF-RADFORD, N. R., BOYLAN, K. B., DICKSON, D. W., MACKENZIE, I. R., RADEMAKERS, R., ROBERTSON, J., ZINMAN, L. & ROGAEVA, E. 2015. Jump from Pre-mutation to Pathologic Expansion in C9orf72. *Am J Hum Genet,* 96**,** 962-70.

XU, Z., POIDEVIN, M., LI, X., LI, Y., SHU, L., NELSON, D. L., LI, H., HALES, C. M., GEARING, M., WINGO, T. S. & JIN, P. 2013. Expanded GGGGCC repeat RNA associated with amyotrophic lateral sclerosis and frontotemporal dementia causes neurodegeneration. *Proceedings of the National Academy of Sciences of the United States of America,* 110**,** 7778-7783.

XUE, Y., VIDGREN, J., SVENSSON, L. A., LILJAS, A., JONSSON, B. H. & LINDSKOG, S. 1993. Crystallographic analysis of Thr-200-->His human carbonic anhydrase II and its complex with the substrate, HCO3. *Proteins,* 15**,** 80-7.

YAMAMOTO, Y., FUJIMURA, M., NISHITA, T., NISHIJIMA, K., ATOJI, Y. & SUZUKI, Y. 2003. Immunohistochemical localization of carbonic anhydrase isozymes in the rat carotid body. *J Anat,* 202**,** 573-7.

YAMANAKA, K., CHUN, S. J., BOILLEE, S., FUJIMORI-TONOU, N., YAMASHITA, H., GUTMANN, D. H., TAKAHASHI, R., MISAWA, H. & CLEVELAND, D. W. 2008. Astrocytes as determinants of disease progression in inherited amyotrophic lateral sclerosis. *Nat Neurosci,* 11**,** 251-3.

YANG, C., WANG, H., QIAO, T., YANG, B., ALIAGA, L., QIU, L., TAN, W., SALAMEH, J., MCKENNA-YASEK, D. M., SMITH, T., PENG, L., MOORE, M. J., BROWN, R. H., JR., CAI, H. & XU, Z. 2014. Partial loss of TDP-43 function causes phenotypes of amyotrophic lateral sclerosis. *Proc Natl Acad Sci U S A,* 111**,** 10.

YASUDA, K., ZHANG, H., LOISELLE, D., HAYSTEAD, T., MACARA, I. G. & MILI, S. 2013. The RNA-binding protein Fus directs translation of localized mRNAs in APC-RNP granules. *J Cell Biol,* 203**,** 737-46.

YOSHIDA, K., KISO, Y., WATANABE, T., KAISE, K., KAISE, N., FUKAZAWA, H., MORI, K., ABE, K. & YOSHINAGA, K. 1991. Clinical utility of red blood cell carbonic anhydrase I and zinc concentrations in patients with thyroid diseases. *Metabolism,* 40**,** 1048-51.

YU, A. C., DREJER, J., HERTZ, L. & SCHOUSBOE, A. 1983. Pyruvate carboxylase activity in primary cultures of astrocytes and neurons. *J Neurochem,* 41**,** 1484-7.

YU, Y., SU, F. C., CALLAGHAN, B. C., GOUTMAN, S. A., BATTERMAN, S. A. & FELDMAN, E. L. 2014. Environmental risk factors and amyotrophic lateral sclerosis (ALS): a case-control study of ALS in Michigan. *PLoS ONE,* 9.

ZALDIVAR, T., GUTIERREZ, J., LARA, G., CARBONARA, M., LOGROSCINO, G. & HARDIMAN, O. 2009. Reduced frequency of ALS in an ethnically mixed population: a population-based mortality study. *Neurology,* 72**,** 1640-5.

ZHANG, K., DONNELLY, C. J., HAEUSLER, A. R., GRIMA, J. C., MACHAMER, J. B., STEINWALD, P., DALEY, E. L., MILLER, S. J., CUNNINGHAM, K. M., VIDENSKY, S., GUPTA, S., THOMAS, M. A., HONG, I., CHIU, S. L., HUGANIR, R. L., OSTROW, L. W., MATUNIS, M. J., WANG, J., SATTLER, R., LLOYD, T. E. & ROTHSTEIN, J. D. 2015. The C9orf72 repeat expansion disrupts nucleocytoplasmic transport. *Nature,* 525**,** 56-61.

ZHAO, W., BEERS, D. R., HENKEL, J. S., ZHANG, W., URUSHITANI, M., JULIEN, J. P. & APPEL, S. H. 2010. Extracellular mutant SOD1 induces microglial-mediated motoneuron injury. *Glia,* 58**,** 231-43.

ZHENG, Y., WANG, L., ZHANG, W., XU, H. & CHANG, X. 2012. Transgenic mice over-expressing carbonic anhydrase I showed aggravated joint inflammation and tissue destruction. *BMC Musculoskelet Disord,* 13**,** 1471-2474.

Fluorescence-based assay for measuring CA1 enzyme activity

Introduction

Observing the rate of CA1 enzyme activity is imperative to this project as it allows the ability to conclude if any effects obtained during later experiments were contributed by CA1 enzyme activity. Based on several well-established methods which are discussed below; this study shows the successful development of a unique and modified fluorescence-based technique which allowed measurements of the relative catalytic activities of CA1.

Establishing enzyme-inactive CA1 mutants was needed to be used in conjunction with wild-type CA1 to confirm any effects seen under CA1 protein expression can be attributed to CA1 enzyme activity. To accomplish this, mutations in Thr199 and Glu106 within the active site were generated for the inactive CA1 mutants.

The catalytic process of CA

The CA enzymes catalyze the reversible hydration of CO_2 giving rise to HCO_3^- and H^+:

$$CO_2 + H_2O \leftrightarrows HCO_3^- + H^+$$

The catalytic mechanism for this reaction is composed of essentially of three steps (Bottoni et al., 2004):

1) $EZn^{2+}\text{-}OH^- + CO_2 \leftrightarrows EZn^{2+}\text{-}HCO_3^-$

2) $EZn^{2+}\text{-}HCO_3^- + H_2O \leftrightarrows EZn^{2+}\text{-}OH_2 + HCO_3^-$

3) $EZn^{2+}\text{-}OH_2 \leftrightarrows EZn^{2+}\text{-}OH^- + H^+$

In the first step of the reaction, the zinc OH- ion carries out a nucleophilic attack on the CO2 molecule positioned in the CA reactive site – the result of this nucleophilic attack converts the OH- ion into HCO3- (Lindskog, 1997, Silverman and Lindskog, 1988, Bottoni et al., 2004). In step two, a water molecule substitutes the zinc bound HCO3- releasing it into the reaction medium (Lindskog, 1997, Silverman and Lindskog, 1988, Bottoni et al., 2004). In the final step, a proton transfer process occurs from the zinc-bound water molecule to the surrounding reaction media which will generate the enzymatically active CA reactive site with an OH- ion bound to the zinc for the process to repeat (Lindskog, 1997, Silverman and Lindskog, 1988, Bottoni et al., 2004). The proton transfer in the last step is believed to the rate-limiting reaction for CA catalysis (Briganti et al., 1997, Steiner et al., 1975, Silverman and Lindskog, 1988).

The importance of the Thr199 and Glu106 residues in CA1 catalysis

The zinc ion in the CA1 catalytic site is bound to three histidine residues, with its fourth coordination site occupied by water at the low pH (pH <7) or a OH^- ion at high pH (pH >7) (Eriksson et al., 1988). The hydrogen bond between the zinc-bound OH^- (or water molecule) and an oxygen atom of Thr199 which is further linked to a hydrogen atom of Glu106 (Merz et al., 1989) (Figure 2.1) forms the zinc-OH^- (water)-Thr199-Glu106 hydrogen-bond network which

is crucial in the CA-mediated CO_2 hydration. More importantly, this hydrogen-bond network is also conserved in CA1 (Merz et al., 1989, Kannan et al., 1977a, Liang et al., 1993).

There have been many studies on the functional role of the zinc-OH^--Thr199-Glu106 hydrogen-bond network. What is known is that the Thr199 residue is critical for positioning the hydrogen atom of hydroxide in the "down" position so as to allow CO_2 to gain access to the active site and react with the OH^- ion (Merz, 1990, Supuran et al., 2003). Also, Thr199 forms part of the "deep water pocket" where CO_2 binds in the active site, placing it in close proximity to the zinc-OH^- ion for the nucleophilic attack (Merz, 1990, Merz et al., 1989). The hydrogen bond between Thr199 and the hydrogen atom in the zinc-OH^- ion prevents the hydrogen atom from interacting with the water molecules within the catalytic site and blocks the CO_2 molecules from reaching the "deep water pocket" (Merz, 1990, Supuran and Scozzafava, 2002, Supuran et al., 2003). Also, the zinc OH^--Thr199 hydrogen bond would expose the oxygen atom towards the CO_2 molecules, which is a more energetically favorable position for reaction with CO_2 (Merz et al., 1989).

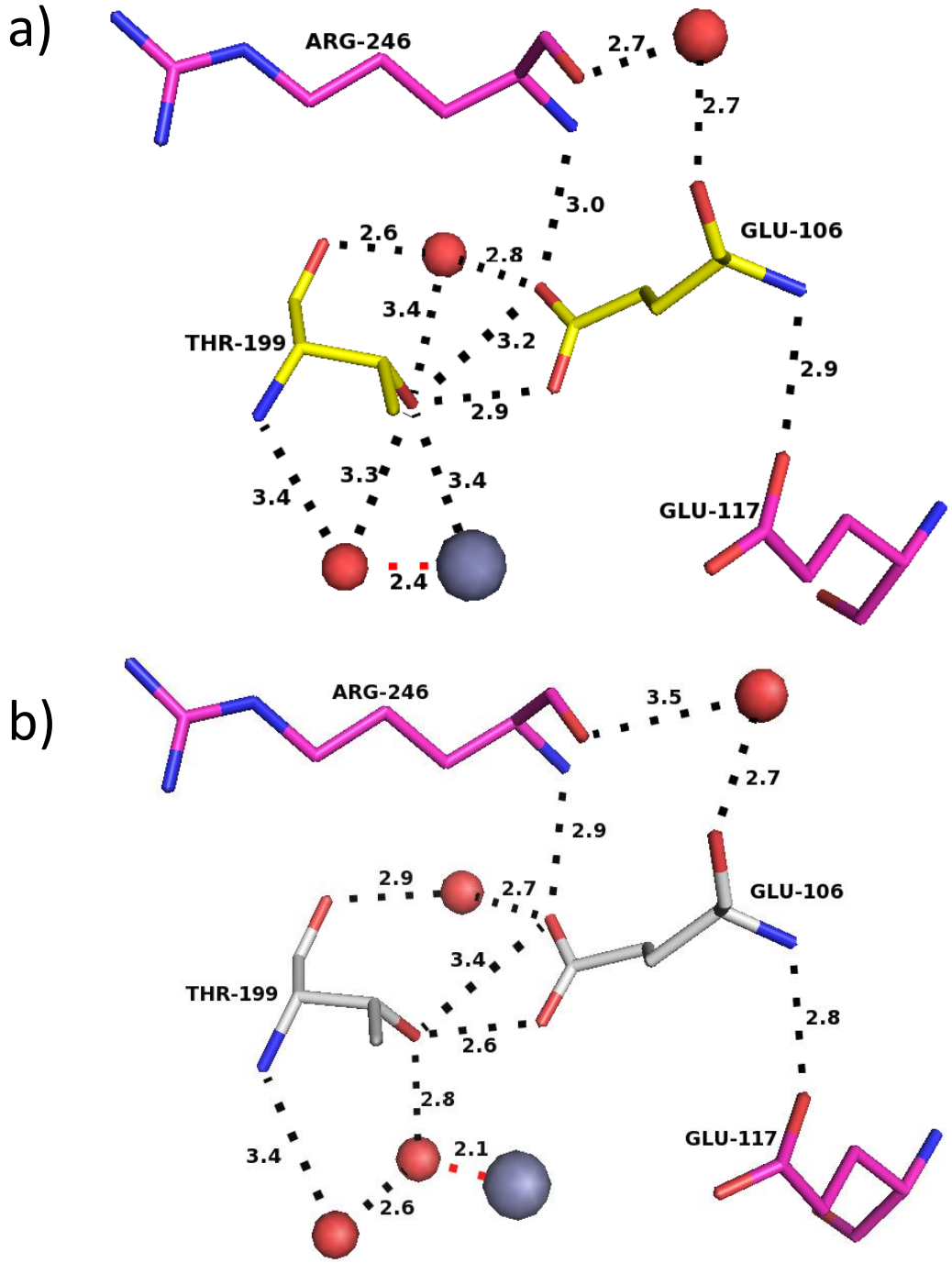

Figure 2.1. Thr199 and Glu106 comparison between CA1 and CA2. The two residues are critical across all stages of the enzymatic process in a) CA1 and b) CA2. The two residues are colored yellow/blue/red for CA1 and grey/blue/red for CA2, their outer hydrogen bonded residues are labelled pink/red/blue. Also shown are its hydrogen bonded waters, the catalytic zinc ion and zinc-bound water. Both residues share great similarities in CA1 and CA2. Grey and red spheres represent zinc and water molecules, respectively. Red and black dashed lines represent co-ordination between water molecule to the zinc ion and hydrogen bonds between residues and water molecules, respectively, with bond lengths labelled in angstroms. The image was generated from the x-ray structures of CA1 and CA2 from Brookhaven protein data bank (CA1 – file code 3W6I; CA2 – file code 2CBA). The figure was generated and rendered using Pymol.

Thr199 and Glu106 have also been found important in other stages of the CA catalytic process. It has been found that the zinc bound HCO_3^- ion undergoes structural rearrangements to stabilize itself after CO_2 nucleophilic attack (Liang and Lipscomb, 1989). The proposed mechanism involves an internal proton transfer within the HCO_3^- ion between its two oxygen atoms and allows the HCO_3^- to stabilize itself while bound to the zinc (Liang and Lipscomb, 1989). It has been found that this proton shift between the HCO_3^- oxygen atoms first requires a relay mechanism by transferring double protons to the Thr199 oxygen and then to the Glu106 oxygen (Miscione et al., 2007, Bottoni et al., 2004). The electrostatic effects of the protonated Glu106 on the zinc ion and the HCO_3^- oxygen atom stabilizes the structure of the intermediate molecules and lowers the energy required for the molecule to move between different transitional states during the proton transfer. The loss of Glu106 increases the amount of energy needed to carry out the proton transfer and causes weakening of the HCO_3^--zinc interaction (Bottoni et al., 2004, Miscione et al., 2007). Furthermore, Thr199 also plays an important role in the water molecule attacking the zinc bound HCO_3^- (Bottoni et al., 2004). As Thr199 interacts with the HCO_3^-, it stabilizes the intermediate transitional states of the enzyme, allowing more energy efficient removal of the HCO_3^- ion. These findings show that Thr199-Glu106 are directly involved in forming the stable zinc bound HCO_3^- intermediates as well as supporting the later transition from HCO_3^- to a water molecule within the active site.

Thr199-Glu106 are also involved in the deprotonation from the zinc-bound water to the reaction medium (Pullman, 1981, Merz et al., 1989, Kannan et al., 1977b). Studies have shown that the proton transfer process which produces the zinc-bound OH^- ion critical for further nucleophilic attack on CO_2 requires the existence of the Thr199-Glu106 proton relay network

(Pullman, 1981, Merz et al., 1989). In this case, the Thr199-Glu106 proton shuttle acts as the proton acceptor for the deprotonation of the zinc-bound water, while Thr199 acts as the immediate proton relay for further transfer to Glu106 (the deprotonation process is also facilitated by binding to the zinc ion). This process allows the formation of the OH^- to react with CO_2 in the active site without the need to overcome any energy barriers (Pullman, 1981).

Generating CA1 inactive mutants – what the studies have shown

There have been few reports studying the enzyme activities of CA1 mutants, while the majority has studied CA2 mutants. However, these existing CA1 studies which have been focusing on mutants generated by point mutations and their subsequent effects on the enzyme activity have highlighted a few important key amino acid residues within CA1. Residues that participate in the catalysis as well as those that support the catalysis-dependent residues structurally were examined to reproduce CA2 enzyme activity in CA1 and vice versa (Behravan et al., 1991, Engstrand et al., 1995). However, all of these studies have failed to show a near or complete ablation of CO_2 hydration/HCO_3^- dehydration activity (the reversible reaction that is believed to be physiologically important) after substituting the targeted CA1 residues. One study has looked at the residue Val62 within the CA1 active site, and His67 and His200, the two histidine residues that are important for the proton transfer during CA catalysis by mutating them to the corresponding amino acids at the three positions in CA2 (Engstrand et al., 1995). The results showed that the single mutation of Val62 or His67 only affected CA1 enzyme activity minimally, while mutations involving His200 increased the enzyme activity.

Furthermore, the triple mutations (i.e. containing point mutations at all three residues) surprisingly doubled the CA1 enzyme activity for CO_2 hydration.

On the other hand, Kockar *et al* found a mutation in amino acid 91 of CA1 near the substrate binding site in CA1 and previously thought non-essential for the catalysis, increases the CO_2 hydration activity by 16% (Kockar et al., 2010). Another finding made by Ferraroni *et al* in 2002 was the CA1 Michigan 1 variant (Ferraroni et al., 2002) which was first discovered in a Caucasian family in Michigan and has a single mutation in reside 67 (from Histidine to Arginine) (Shaw et al., 1962). This variant shows small overall conformation deviations from the wild-type and its CO_2 hydration and ester hydrolysis activities in absence of zinc are unchanged when compared to the wild-type.

Mohanty *et al* have studied the effects of substituting residues that form the hydrogen-bond network in CA1 (Tyr7, His107, Glu117, Thr199 and Glu106) on its esterase activity (Mohanty et al., 1998). Although these residues are believed to be important in either supporting CA1 structural integrity or directly participate in the enzyme reaction, Thr199 and Glu106 are conserved across different isozymes of CA in other mammalian species and believed to be most critical to CA1 enzyme function (Merz et al., 1989, Liang et al., 1993, Kannan et al., 1977a). Mohanty *et al* study also found that Thr199Val, Glu106Gln, and Glu106Ile mutants had the lowest esterase activity (5-10% of the wild-type). Although the study focused on the CA1 esterase activity, these three mutants provided the best candidates for the purpose of establishing CA mutants inactive of the reversible CO_2 hydration/ HCO_3^- dehydration (CA anhydrase) activity. As the previous results have shown the esterase activity of CA1 relative to

CA2 is of the same ratio as the reversible CA anhydrase activity between CA1 and CA2 (around 1:7 for both), it is likely that the three mutants would have absent/near-absent CA anhydrase activities (Verpoorte et al., 1967, Supuran et al., 2003).

Measuring CA enzyme activity

The natural reversible hydration of CO_2 reaction without the catalyst is fairly slow (Koenig and Brown, 1973). The CA-catalyzed reaction greatly enhances the rate of reaction and is both pH- and temperature-dependent, with faster reaction seen under the higher pH and temperatures for both CA1 and CA2 (Khalifah, 1971, Khalifah and Edsall, 1972).

CA anhydrase activity is generally measured using the manometric, colorimetric, spectrophotometric and electrometric methods (Henry, 1991).

The manometric method

The first CA activity measurement was developed by Meldrum and Roughton in 1933 (Meldrum and Roughton, 1933), using the buffer containing the CA enzyme shaken vigorously with the HCO_3^- solution in a boat-like vessel. The apparatus was connected to a manometer which measures the rate of CO_2 production at various times when the shaking occurred. Unlike the methods later developed which are based upon measuring pH changes, this method is more reliable in that it directly measures CO_2 production. However, its main disadvantage is the limitation factor of its maximal measuring ability due to gas diffusion when the reaction velocity

reaches higher levels and with the increased speed of shaking (Roughton, 1941). This in effect causes the slow response-rate one may encounter with manometers and it is amplified when enzyme activity rises to high levels. The effect which diffusion has on the observed reaction rate was later calculated by taking into account of the existence of stationary films in between liquid and gas governing the rate of their interchanges (Roughton, 1941). However, this was a theoretical correction that was not confirmed by experimental measures. Furthermore, the other major disadvantage associated with manometers is the possibility of forming air bubbles between the liquid-gas interphase in its pipe which can affect the reliabilities of the results (Daood et al., 2007).

The colorimetric method

The colorimetric and electrometric methods were developed later to measure the pH change when CO_2-saturated water was injected into the carbonic anhydrase-containing system producing protons and HCO_3^- ions (Wilbur and Anderson, 1948). These methods utilized a pH electrode or a pH indicator (e.g. bromothymol blue and phenol red) measuring the time for reaching an end-point pH or following the pH changes. The classic colorimetric method described by Maren in 1960 was simple to carry out (Maren, 1960). This method uses phenol red as the pH indicator and measures the pH change as CO_2 is pumped into the reaction medium followed by the addition of an alkali buffer: the time for phenol red to turn from red to yellow indicates the CA activity.

The colorimetric approach is inexpensive and simple to use; however, its main disadvantage comes from the inhibitory effects on the CA activity from the indicators which in some cases can inhibit the reaction by 30% (Wilbur and Anderson, 1948). Furthermore, the colorimetric methods used in the early developmental stages were relatively crude and unable to determine small differences in enzyme activities. Due to the fact that majority of the techniques relies upon human identification of the color change; they are sensitive to human errors.

The electrometric method

The electrometric method is similar to the colorimetric method, using a pH electrode is quick and simple. The pH electrode forms the basis for the classical Wilbur-Andersen method which is used commonly even today (Wilbur and Anderson, 1948). This method uses an apparatus which injects CO_2-saturated solution into the CA-containing solution. The pH electrode measures the time for the pH to drop from an alkaline state (~pH 8) to an acidic state (~pH 6.3). This method cannot measure the small changes in enzyme activity and there does not seem to be a good linear relationship between the time measured (time to reach the end-point pH) and the pH range (Wilbur and Anderson, 1948). Furthermore, using a pH electrode also comes with its own disadvantages. For example, some suggests pH electrodes are sensitive to pH changes in the 0.001 scale; however, taking account into the various layers surrounding the electrode its sensitivity is likely to be 0.01 after calibration (Cheng and Zhu, 2005). Due to the necessity of using a stir-bar in these experiments, disturbances in the liquid will affect the

readings. Furthermore, the thickness, composition, surface area, and electrical property of the solution will affect the readings, making the comparisons with data obtained with a different brand of electrode to be potentially inaccurate (Cheng and Zhu, 2005).

The inherent disadvantage of using these earlier techniques is the requirement of carrying out the experiments at 0 ˚C, far off the physiological temperature of 37 ˚C in which CA normally function. This temperature requirement also reduces the velocity of the reaction so that the delay in instrument response time and mixing (which could be problematic) will not be shown to be limiting factors in monitoring the enzyme activity.

The spectrophotometric method

The great improvement of the colorimetric method is the use of spectrophotometric measurement combined with a stop-flow rapid-mixing instrument (Khalifah, 1971). The use of spectrophotometric dyes allows the quick detection of pH change (within 0.001 pH change), and the stop-flow instrument allows monitoring the instantaneous pH change at the initial phase of the reaction (less than 0.001 sec) (Khalifah, 1971). The stop-flow instrument functions by forcing a small amount of reaction solution (around 80µl) into a mixing chamber, the flow of the solution is suddenly stopped within milliseconds (as low as 0.03 milliseconds) initiating the monitoring of the enzyme kinetics (Berger, 1978). Due to its ability to measure miniscule amounts of reactants in a rapid time-frame, the stop-flow system allows researchers to measure CA activity at 25˚C instead of 0˚C, making the experiment more practical to carry out (Khalifah, 1971). The stop-flow instrument can be linked to any rapid-responding device such as

a spectrophotometer, temperature recorder, nuclear magnetic resonance system which can be further connected to a computer designed to handle the large data output (Berger, 1978). Despite its advantages, many research laboratories are not equipped with this unusual system making it less widely used.

CA does not only catalyze the CO_2-HCO_3^- exchange reaction, it also catalyzes a host of other reactions (Supuran et al., 2003). One spectrophotometric method is to measure the esterase activity of the CA enzyme. This method uses nitrophenyl acetate as the substrate and measures the change in light absorbance once the substrate has been hydrolyzed (Verpoorte et al., 1967). Although the CO_2 hydration and esterase reactions share some similarities (i.e. the reaction K_m is independent of pH, the zinc ion central to both reactions and that CA2 is faster than CA1 for both reactions), there still exist some fundamental differences between the two reactions (Khalifah, 1971, Verpoorte et al., 1967). Namely, CA show different reactive behaviors under a pH range for both reactions, and the enzyme velocities between CA2 and CA1 are different for the two reactions (Verpoorte et al., 1967, Khalifah, 1971). Lastly, the method of measuring the esterase activity appears prone to errors as a close observation of the results shows the highly active CA2 enzyme the range of error is close to 30% (Verpoorte et al., 1967).

Other methods that do not measure the pH change as CA activity also exist. These include the measure of ^{18}O isotopes to be incorporated in the CO_2-HCO_3^- exchange using a mass spectrometer (Silverman, 1982). Similarly, another method uses the ^{13}C isotope which also measures the CO_2-HCO_3^- exchange using nuclear magnetic resonance (Simonsson et al., 1979). These methods have the advantages of being able to be carried out at physiological

temperatures, in native cells, without the use of a buffer, and require as little as 10^{-15} moles of CA enzyme for reaction. However, they are time-consuming and require the use of expensive equipment maintained by an expert. Furthermore, due to the nature of the output of the spectra data, the noise level can be very large.

Radioactively labelled tracers have also been used to detect CA activity, by incorporating ^{14}C radioisotopes into HCO_3^- ($H^{14}CO_3^-$) and CO_2 ($^{14}CO_2$) and measuring radioactive $^{14}CO_2$ and $H^{14}CO_3^-$ production respectively (Stemler, 1993). The diffused radioactive gases are further trapped and transferred into a scintillation counter where the radioactivity is measured. Unlike the other methods, this assay does not require the use of expensive equipment such a mass spectrometer or stop-flow equipment and is sensitive in the nano-gram range; however, it requires the use of radioactive substances which can difficult to both handle and discard. Further, the assay can take a relatively long time (up to 5 hours) to develop strong signals (Stemler, 1993).

Comparing the methods described above and taking into account convenience, sensitivity, experimental temperature and pH range, as well as speed, the most convincing approach to measure CA activity is through the spectrophotometric methods. One method used by Li and Ci but which was first described by Thompson and Jones showed that the compound 5-di methylaminonaphthalene-l-sulfonamide (dansylamide) was able to form a complex with the zinc ion in CA which increases the emission of fluorescence when excited (Li and Ci, 1995, Thompson and Jones, 1993). This method is sensitive in that it can detect trace amounts of CA (29ng/ml), and can be carried out at 20 ˚C in a pH range of 7.0-8.5. However, the

dansylamide is a CA inhibitor and cannot be directly used to measure the CA activity. In addition, it does not directly measure CA activity; rather it measures the degree of dansylamide association with the CA active site.

The method described by Shingle and Moroney used a fluorescence indicator, 8-hydroxy-pyrene-1,3,6-trisufonate (Pyranine) which can sense the pH changes between pH 6.5 and pH 8.0. This method measures the pH change when a buffer of pH 6.0 (more protons being present) is mixed with another buffer of pH 8.0 (containing HCO_3^-) that drives the dehydration of bicarbonates, consuming protons in the process forming CO_2 and H_2O (Shingles and Moroney, 1997). This is a sensitive method allowing detection of 65ng/ml of CA measured in the pH range of pH 6.5-8.0 at 25 ˚C. This method uses a spectrophotometer to measure the fluorescence change of Pyranine reflecting the pH changes. It is also equipped with a stop-flow apparatus that is able to stop the injection of the alkali solution (containing HCO_3^-) rapidly. The initial rate of the CA reaction rate can be determined at a high resolution of 2ms (milliseconds). Unlike the dansylamide method which does not measure the CA reaction itself but the concentration of zinc ion in the mixture, this method directly measures the physiological CA reaction. However, as mentioned previously, the stop-flow apparatus is fairly specialized and not widely available which is the apparent disadvantage to this technique.

Aim of the study

All of the methods described above offer their unique blend of advantages and disadvantages; however, the early methods (manometric, colorimetric, and electrometric) have proven to be fairly inaccurate or require undesirable experimental conditions (i.e. 0 ^{o}C). On the other hand, using the specialized equipment such as the stop-flow spectrophotometer, nuclear magnetic resonance, radio-isotope tracers are cumbersome to handle and require specialized techniques. What the study requires is a simplified, efficient, yet accurate method to measure the speed of the CA1-catalyzed reaction for comparing the relative activities of wild-type and mutant CA1.

For the purpose of this project, it was decided to develop a method using the fluorescence-indicator Pyranine to measure the rate of pH change of HCO_3^- hydration during the reversible CA anhydrase reaction using the Pherastar microplate reader which can handle very rapid and sensitive changes in fluorescent intensities (a modification for the use of the stop-flow device). The goal was to use bovine CA2 (bCA2) as the proof of principal test. Once a linear relationship between bCA2 concentrations and the rates of the initial pH changes during bCA2 catalyzed reaction can be obtained, this method will be valid to measure relative activities of wild-type and mutant CA1.

The objective for the study in this chapter is to develop a modified method for measuring CA activity. The new fluorescence-based technique uses a rapid injection of the reactant into the wells of a microplate to initiate the CA-catalyzed reaction and measure the changes in fluorescence via the Pherastar microplate reader. Pherastar can detect sensitive

fluorescent changes within short enough time intervals (<40ms) which allow the reliable measurement of the rate of the initial reaction. The validity of this method will be demonstrated by the linear relationship between the concentrations of the CA enzymes and the rates of the initial reactions as described by Shingles and Moroney (1997). Furthermore, the study will determine whether the two mutations in Thr199 and Glu106 amino acid residues are catalytically inactive.

Materials and methods

Mutagenesis to generate site directed CA1 mutants

Site-specific mutations were introduced into human wild-type CA1 gene at the position of Thr199 and Glu106. The Thr199Val, Glu106Ile and Glu106Gln mutations in the CA1 gene were made with appropriately designed primers using a two-round PCR method (Figure 2.2, and Appendix 1).

The first round of PCR produces two double-stranded DNA fragments with the mutation site near the 3' end of one fragment and the 5'end of the other fragment. The two fragments overlap with each other with the complementary sequences containing the mutation site. The F1 and R1 primers contain the 5' and 3' end wild-type CA1 sequences and KpnI and NotI restriction sites, respectively.

The F2 and R2 primers contain the Glu106Ile mutation in the 5' and 3' end of the primer sequences respectively. The F3 and R3 primers contain the Thr199Val mutation in the 5' and 3' end of the primers respectively. The F4 and R4 primers contain the Glu106Gln mutation in the 5' and 3' end of the primers, respectively. To produce each mutant, the pair of F1 and R1 primers was added along with the F2/R2 primers for making Glu106Ile mutant or the F3/R3 for making Thr199Val mutant or the F4/R4 for making Glu106Gln mutant. For the PCR reaction, 500ng of the *CA1*-pcDNA3.1(+)plasmid was used, 1µM of each upstream and downstream primer was used, along with 1mM dNTP mixture (#4030, Takara, Japan), 2.5 units of Pwo DNA polymerase (#11644947001, Roche Applied Science, Germany) and 1X Pwo PCR buffer with water added to a total of 50µl of the reaction volume. The PCR condition is as follows: 95˚C for 3mins, 30

rounds of: 95˚C for 30s 60˚C for 30s 72˚C for 60s 72˚C for 5mins, and placed at 4 ˚C. The PCR products were purified using the QIAquick PCR Purification kit (Qiagen, California, USA) and ran on a 1% agarose gel. For each mutant, two PCR fragments (for Glu106Ile 5' fragment size = 492bp, 3' fragment size = 979bp; for Thr199Val 5' fragment size = 771bp, 3' fragment size = 700bp; for Glu106Gln 5' fragment size = 492bp, 3' fragment size = 979bp) were gel-purified using the QIAquick gel extraction kit (Qiagen, California, USA).

The second round PCR reaction were conducted using the gel-extracted DNAs (two fragments per mutant) to anneal and DNA polymerase to fill in the gap DNA sequences. For this PCR reaction 500ng of total DNA was used with the two fragment added in a 1:1 molar ratio, along with 1mM dNTP mixture (#4030, Takara, Japan), 2.5 units of Pwo DNA polymerase (#11644947001, Roche Applied Science, Germany) and 1X Pwo PCR buffer with water added to a total reaction volume of 50µl . The PCR condition is as follows: 95˚C for 3 mins, 30 rounds of: 95˚C for 30 s 40˚C for 30 s 60˚C for 60 s and then 72 ˚C for 5 mins, and placed at 4 ˚C.

The PCR products were purified using the QIAquick PCR Purification kit (Qiagen, California, USA), and ran on a 1% agarose gel. The CA1 mutant DNAs were gel-purified using the QIAquick gel extraction kit (Qiagen, California, USA), with the band sizes of 1471bp. The extracted DNA was digested with KpnI (R0142S, NEB, Massachusetts, USA) and NotI (R0189S, NEB, Massachusetts, USA). The mutant CA1 inserts were then ligated to the KpnI and NotI-digested pcDNA3.1 (+) vector using T4 DNA ligase (M020S, NEB, Massachusetts, USA). All mutant DNAs were confirmed by s produced commercial sequencing company (Invitrogen sequencing services).

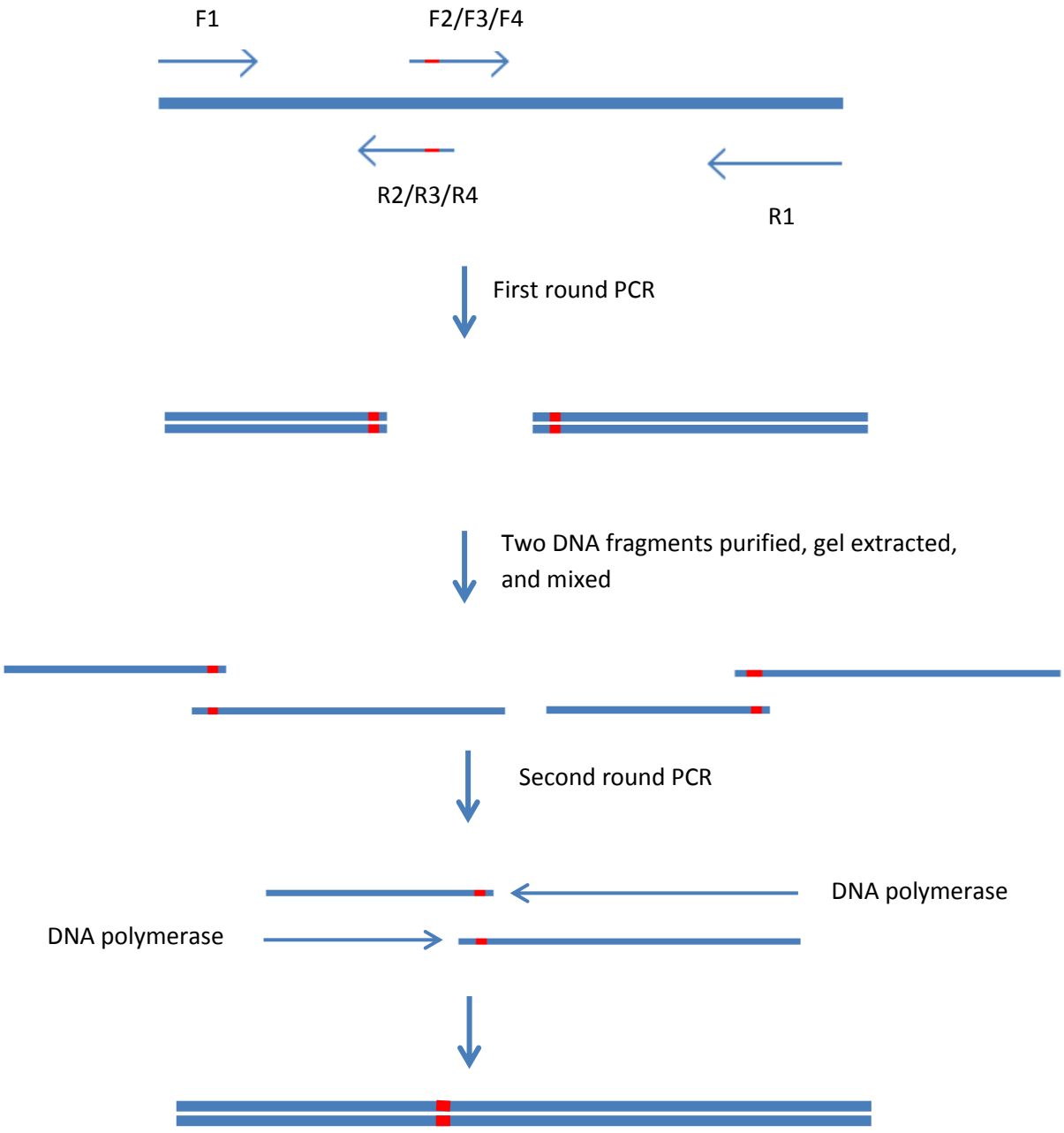

Figure 2.2. Schematic diagram of CA1 mutant production via two-round PCR method. The F1, R1, F2, R2, F3, R3, F4, R4 primers with their sequences are listed below. The red box depicts the mutant site only and is not drawn to scale relative to any of the mutant locations in the *CA1* gene. The technique used is based on the previous published method by Mohanty *et al* (Mohanty et al., 1998).

The wild-type and mutant *CA1* genes were cloned from the pcDNA3.1(+) vector into the bacterial expressing pRSET-C vector. The *CA1* genes were first replicated using PCR with the forward primer containing the NdeI restriction site (and 5' end of *CA1*) and the reverse primer containing HindIII restriction site sequence, 6X His-tag sequence (and 3' end of *CA1*) using the primer sequences as listed in Appendix 2.

For the PCR reaction, 500ng of each of the *CA1*-pcDNA3.1(+) DNA (wild-type *CA1* or mutant Thr199Val *CA1* or mutant Glu106Ile *CA1* or mutant Glu106Gln *CA1*) mutant plasmid was used, 1µM of F4 upstream and R4 downstream primer were used, along with 1mM dNTP mixture (#4030, Takara, Japan), 2.5 units of Pwo DNA polymerase (#11644947001, Roche Applied Science, Germany) and 1X Pwo PCR buffer with water added to a total of 50µl of the reaction volume. The PCR condition is as follows: 95˚C for 3mins, 30 rounds of: 95˚C for 30s 60˚C for 30s 72˚C for 60s 72˚C for 5mins, and placed at 4˚C.

The PCR products were purified using the QIAquick PCR Purification kit (Qiagen, California, USA) and ran on a 1% agarose gel. The CA1 mutant DNAs were gel purified using the QIAquick gel extraction kit (Qiagen, California, USA), with the band sizes of 1476bp. The extracted DNA was digested with NdeI (R0142S, NEB, Massachusetts, USA) and HindIII (R0189S, NEB, Massachusetts, USA). The wild-type and mutant *CA1* inserts were then ligated to the NdeI and HindIIII digested pRSET-C vector using T4 DNA ligase (M020S, NEB, Massachusetts, USA). All wild-type and mutants *CA1*-pRSET-C DNAs were confirmed by commercial sequencing company (Invitrogen sequencing services).

Protein expression and purification

The expression constructs were transformed into BL 21 (DE3) pLysS cells, plated on LB plates containing ampicillin (100µg/ml) and incubated o/n at 37°C. The next day colonies were collected and used to inoculate 500ml cultures of 2YT medium containing ampicillin. The cultures were grown at 37°C until the OD 600 was 0.5 and then induced by addition of IPTG to a final concentration of 0.5mM. Cultures were then grown at 30°C for 4hrs. The cells were pelleted by centrifugation at 5100 x g for 5mins at 4^{O}C. Cell pellets were re-suspended in 37.5ml of cold extraction buffer (50mM Tris pH 7.8, 20mM Imidazole). The cells were then sonicated (while being on ice) in 10x 10s cycles with 20s breaks to keep the cell suspension remains cold throughout. The sonicated solution was then centrifuged at 12,000g for 30mins at 4^{O}C. 5ml Nickel-Sepharose His-Trap columns (GE Healthcare, UK) were washed with 10 column volume of washing buffer (50mM Tris pH 7.8, 500mM NaCl, 20mM Imidazole, and 5% glycerol) before loading the protein supernatant to the column at approximately 1ml/1min loading speed using a peristaltic pump. After loading all the protein, the unbound protein was washed off from the column using washing buffer using approximately 20x column volume. The bound protein was eluted using approximately 20x column volume elution buffer (50mM Tris pH 7.8, 100mM NaCl, 200mM Imidazole, 5% glycerol) from the column. The eluted proteins were then purified and desalted by filtering through a centrifugal unit using the Amicon ultra-15 centrifugal unit (#UFC901024, Merck Millipore, Germany) and re-suspended in water. Final protein concentrations were quantified using the BCA method using bovine serum albumin to generate a protein standard curve (#23225, Pierce Biotechnology, USA). To visualize the proteins, 10µl of

2.5µM of the protein samples were ran on a SDS-PAGE gel and stained with the Instantblue – a coomasie protein stain dye (#ISB1L, Expedeon, San Diego, USA)

pH vs. fluorescence calibration and UV spectra profile for the enzyme assay

To select a suitable available optic probe on the Pherastar to measure changes in Pyranine fluorescences due to pH changes, increments of 10µl of 0.05M HCl solution were added into 8 tubes each containing a mixture of 0.5mM bicine-KOH at pH 6, 1mM $KHCO_3$, 0.5mM Hepes-KOH at pH 8, 200nm Pyranine dissolved in water (#H-348, Molecular Probes, Oregon, USA) in a total volume of 2.5ml. The testing of fluorescent emissions of the 8 samples at 480nm, 520nm, 530nm, 620nm, 665nm when excited with a range of excitation wavelengths between 250nm and 700nm were carried out on a Perkin Elmer LS 55 Fluorescence spectrophotometer (PerkinElmer, Massachusetts, USA) at room temperature. The emission intensities were then plotted as a spectral graph. After the spectra have been collected, the end-point pH of all the 8 reaction samples was measured using a PHM 92 Lab pH Meter (Radiometer Analytical, France).

To determine the relationship between pH and Pyranine fluorescence emission intensity at 530nm/430nm setting, increments of 1.5µl of 0.05M of HCl were added into 10 sample mixtures of 0.5mM bicine-KOH at pH 6, 2mM $ZnCl_2$, 1mM $KHCO_3$, 0.5mM Hepes-KOH at pH 8, and 200nM of Pyranine in a total volume of 1ml per sample. The pH was measured using the PHM 92 Lab pH Meter (Radiometer Analytical, France) and end-point fluorescence was measured using the Pherastar FS microplate reader (BMG Labtech, Germany). All of the pH and fluorescence measurements were taken at 25^{o}C. The relationship between Pyranine end-point

fluorescence emissions were plotted against the end-point pH of the solution mixtures for observations as well as calculating the formula for this relationship.

Three independent experiments were done for the calibration, and curves were plotted between the end-point pH values (y-axis) and the fluorescence emissions (x-axis). The slopes of the three curves were the same (7E-06) and the constants were averaged to give the mean value. The pH values were averages and the fluorescence values were calculated based on the final calibrated equation (y=7E-06x + 5.5156).

Fluorescence-based assay for measuring relative CA1 anhydrase activity

Bovine CA2 (bCA2) (#C3934, Sigma-Aldrich, St Louis) and lysozyme (#L687, Sigma-Aldrich, St. Louis) proteins dissolved in sterilized water were used as positive and negative controls respectively to test the enzyme assay. Increments of 20nM of the bCA2 and lysozyme proteins within a range of 0nM-100nM concentrations were used in the test enzyme assay (i.e 0nM, 20nM, 40nM, 60nM, 80nM and 100nM). Once the standard curves of the positive and negative controls were established, the enzyme assay observing the CA1 enzyme activities were carried out. When carrying out the enzyme assay, 2.5µM of wild-type, mutant Thr199Val, Glu106Ile and Glu106Gln CA1 proteins were used for the enzyme reaction.

The proteins were mixed with cold (placed on ice) buffer A at pH 6.0 (0.5mM HEPES-KOH, 200nM Pyranine, 2mM $ZnCl_2$) and added to black 96 well plate in total volume of 50µl per well and 6 replicate wells per protein concentration while on ice. Once the solutions have been added to the wells, the plate is placed in the PheraStar FS microplate reader (BMG Labtech, Germany) and gently shaken for 5mins at 25˚C. 50µl of buffer B with pH 8.0 (0.5mM Bicine-KOH,

1mM $KHCO_3$) was then injected per well into the 96 wells containing the buffer A and enzyme mixture at 260µl/s injection speed 1s after the initial start at 25^{o}C using the PheraStar FS microplate reader (BMG Labtech, Germany). pH changes when buffer A and B were mixed were monitored through fluorescence change using the pH-sensitive fluorescent dye Pyranine. Pyranine fluorescence changes were monitored using fluorescent optic probe with 430nm excitation wavelength and 530nm emission wavelength (tested as the most suitable optic from previous experiments using the fluorescence spectrophotometer). The change of fluorescence was monitored at every 0.04s for a total of 30s in duration. The emitted fluorescence was converted to pH using the pH vs. fluorescence formula derived from calibration as described above using Microsoft Excel.

Results

Establishing a modified method for measuring CA1 anhydrase activity

CA1-catalyzed dehydration of HCO_3^- ions requires protons to produce CO_2 and water. By mixing the solution containing HCO_3^- at an alkaline pH with the solution at an acidic pH will allow the reaction to happen naturally. In the presence of CA1, the rate of the reaction will be significantly increased due to the catalytic activity of the enzyme. The rate of the reaction can be measured by the change of the pH of the mixed solution. The fluorescence of the compound 8-hydroxy-pyrene-1,3,6-trisufonate (Pyranine) changes with the pH. Specifically, Pyranine is sensitive to the near-neutral pH range (between pH 5.5-7) (Verchère et al., 2012) and has largely been used to monitor transmembrane pH changes in bacteria (Damiano et al., 1984, Verchère et al., 2012, Straubinger et al., 1990) and liposomes (Kano and Fendler, 1978, Straubinger et al., 1990). It exhibits greater sensitivity than other popularly used pH probes (Zhu et al., 2005). By adding Pyranine in the reaction mix and measure the change of its fluorescent intensities, one can determine CA1 anhydrase activity.

The peak excitation and emission wavelengths of Pyranine are at ~455nm and ~520nm respectively (Gelatt, 2014). Using spectrophotometry, others have used emission wavelengths at 509nm, 513nm and 520nm for detection while testing the pH sensitive range of Pyranine with a range of excitation wavelengths (Aguedo et al., 2001, Verchère et al., 2012, Gan et al., 1998). These studies have found that Pyranine is sensitive to pH change in the range of 5.5-8 when excited between 420nm to 480nm.

In order to determine an alternative combination of excitation and emission wavelengths for Pyranine to be qualified as a pH-sensor, all the available fluorescent optic modules (ex430/em480, ex640/em680, ex485/em520, ex430/em530, ex337/em665, and ex337/em620) with fixed excitations and emissions wavelength on PherastarFS were tested. The goal was to find out which of the optic module will result in the most sensitive and pH-dependent change in Pyranine fluorescence. It was found that by fixing the emission wavelength at 530nm and testing the excitation wavelengths ranging from 250nm to 600nm, the excitation wavelength at 430nm was sensitive enough to differentiate the differences in Pyranine fluorescence between pH 6.34 to pH 7.47 (Figure 2.3). While fixing the emission wavelengths at 480nm, 520nm, 620nm, 665nm, 680nm and testing the same range of excitation wavelengths and the same pH levels, the ability to differentiate the fluorescence emissions were sub-optimal (results not shown).

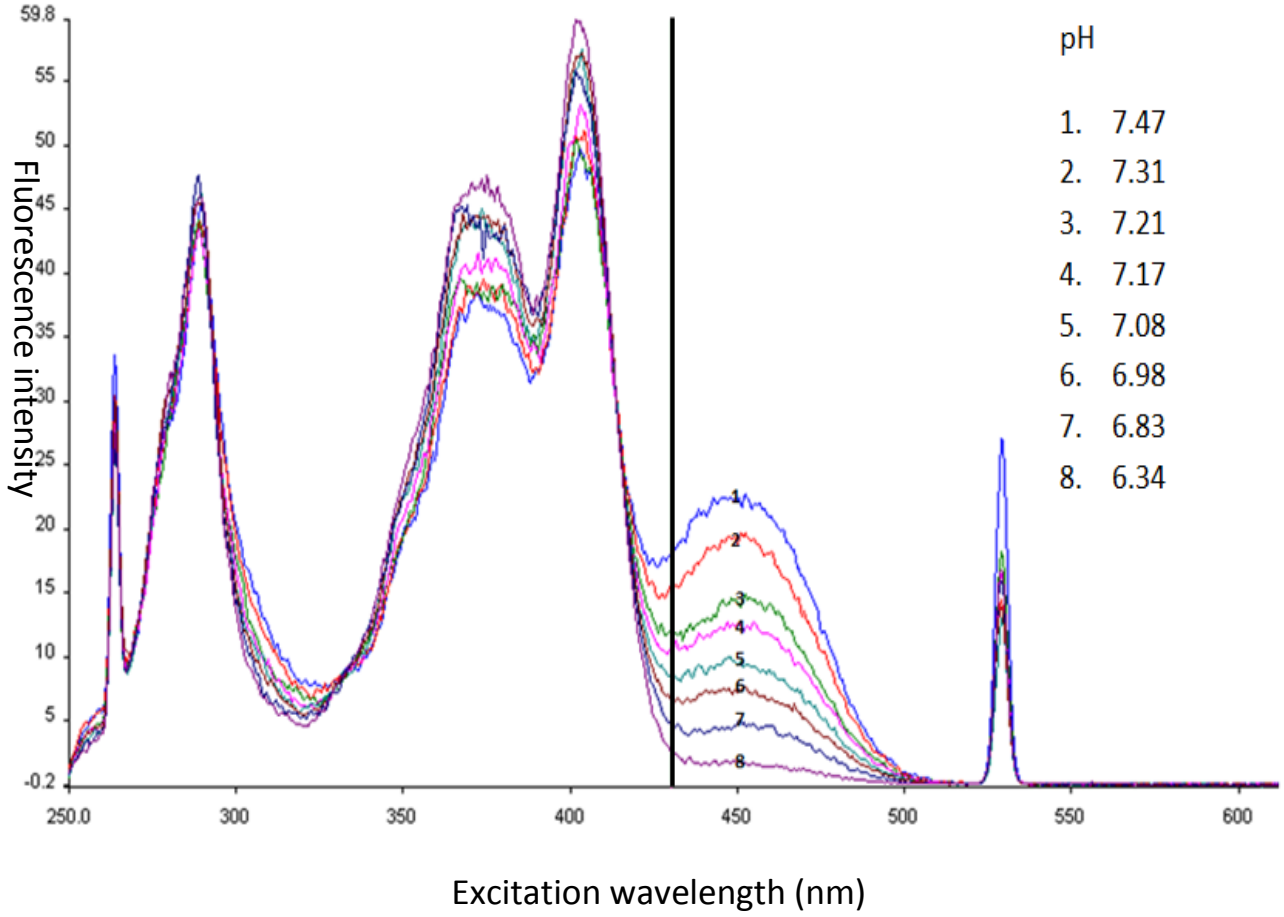

Figure 2.3. Fluorescent spectra of Pyranine. O.D. excitation wavelength at 430nm shows spectra of Pyranine fluorescence at different pH. 200nM of pyranine in eight mixed solutions used during enzyme assay at decreasing end-point pH: 1) **7.47** 2) **7.31** 3) **7.21** 4) **7.17** 5) **7.08** 6) **6.98** 7) **6.83** 8) **6.34** were excited using fluorescent wavelengths between 250nm-600nm while fixing the emission wavelength at 530nm. Black line shows excitation at 430nm used during the assay. This experiment was repeated for a total of two independent experiments, each showing the similar pattern of behavior, results from one of the experiment is shown in this figure.

The linear relationship between pH and Pyranine fluorescence

Once the pH-sensitive excitation and emission wavelengths were determined for Pyranine in the experiments, it was required to test whether the relationship between pH levels and Pyranine fluorescent intensities is linear. Ten samples containing Pyranine with different pH levels in the near-neutral pH range were prepared and their fluorescent intensities were obtained. It was found that between pH 5.6 to pH 6.7 and measured with 530/430 the relationship between Pyranine fluorescent intensities pH values is linear (Figure 2.4). The data-derived linear equation shown in the figure was used to convert the fluorescence readings to pH values for the data in this study.

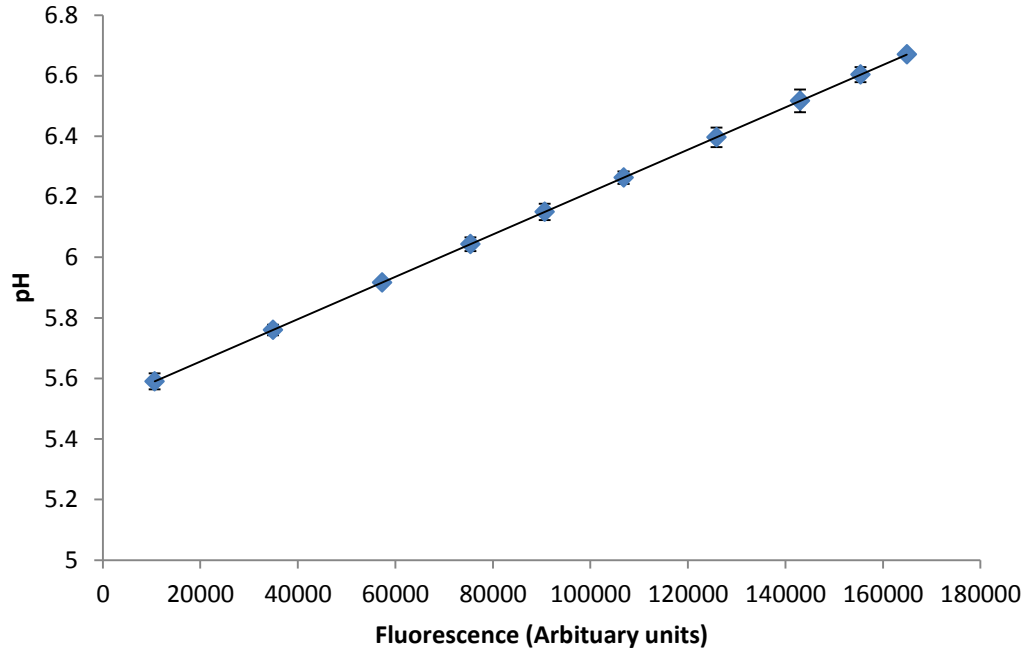

Figure 2.4. Change of pyranine fluorescence is linearly correlated with change in pH. Figure showing pyranine emissions at 530nm while excited at 430nm plotted against 10 assay solution mixtures with increasing pH in the ~pH5.6-~pH6.8 range. A total of three independent experiments were done, with the gradients staying the same for all three and the constants were averaged to give the final equation as shown in the figure. The corresponding pH values were calculated from the fluorescence data. The error bars show the standard deviation of the pH values.

bCA2 exhibits *in vitro* activity linearly correlated with the concentration

Once the pH-fluorescence relationship has been established, the next stage was to carry out the enzyme assay using a protein which has been shown to have CA enzyme activity as the positive control and another protein without known CA enzyme activity as the negative control for the validity of the modified assay method. For this purpose, the bovine CA2 (bCA2) protein was selected as the positive control and the lysozyme protein was selected as the negative control.

Six concentrations from 0nM to 100nM of the proteins were used for the experiment, based on the previous experiment done by Shingles and Moroney (Shingles and Moroney, 1997) (Figures 2.5 and 2.6). The protein samples were included in the acidic buffer of pH 6, the buffered alkaline solution of pH 8 containing the HCO_3^- were injected into the acidic-protein mixture. This allows the HCO_3^- ions to react with the protons in the acidic buffer, generating CO_2 and water during the process. The injection was then stopped at 1.24s and the changes in Pyranine-emitted fluorescence were recorded. The fluorescence data were then converted to pH values using the calibrated equation above (Figure 2.4).

The results showed the pH value steadily increased until it reached a near-plateau at later stage of the experiment (Figures 2.5 and 2.6). There are clear differences in rate of pH changes between bCA2 and lysozyme. Using same concentrations of bCA2 and lysozyme, the time for the reaction mixture to reach its pH equilibrium is more rapid in presence of bCA2 than with lysozyme which is not different from without adding any proteins (Figures 2.5 and 2.6).

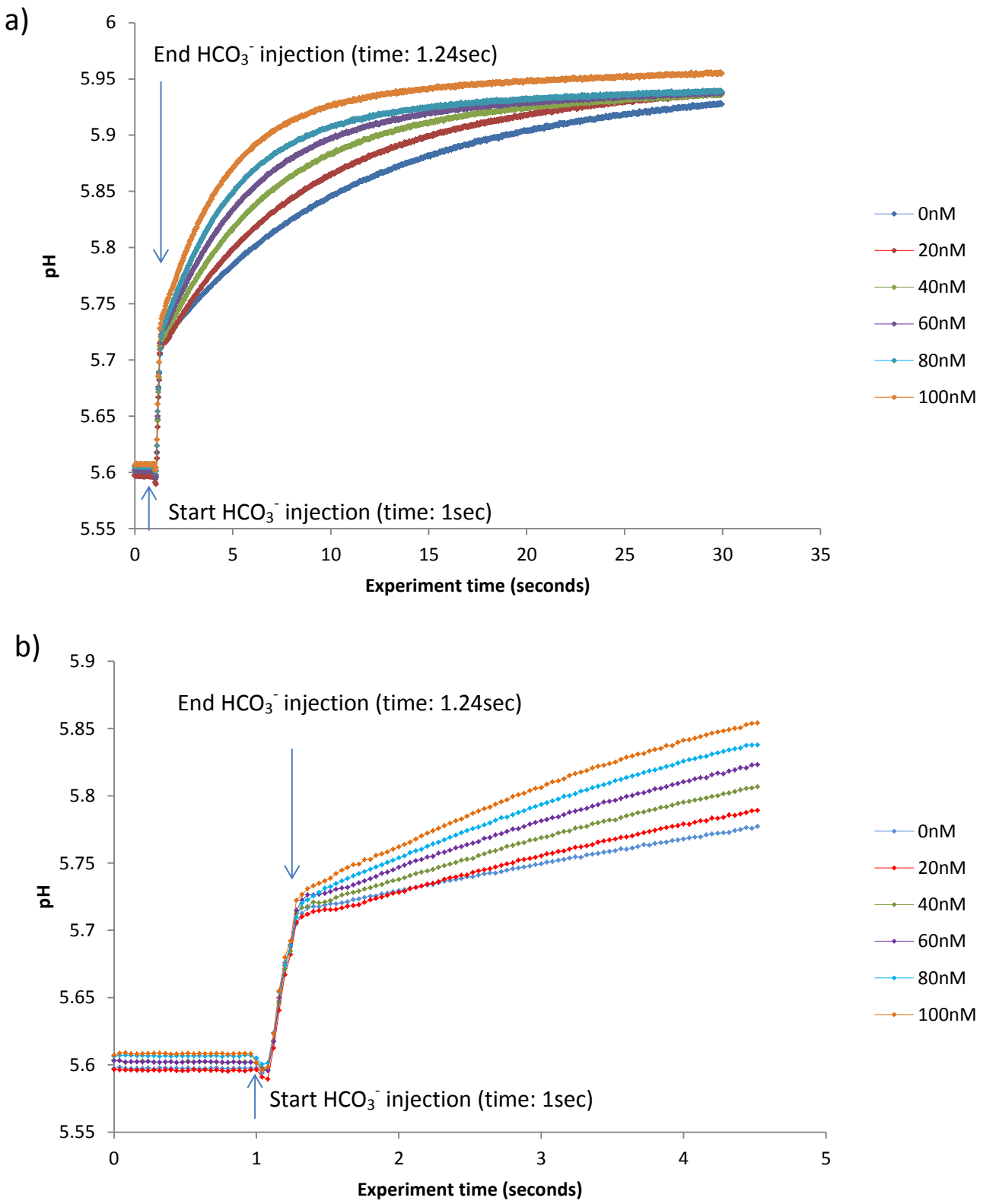

Figure 2.5. bCA2 exhibit enzyme activity *in vitro*. 0nM-100nM of bCA2 proteins were assayed in measuring the rate of pH change during HCO_3^- dehydration. A) Shows the complete reaction time course and b) shows the initial pH change when the HCO_3^- injection is stopped. The color coded curves represent the pH change for each protein concentration. A total of three independent experiments were done, the averages are shown in the figure.

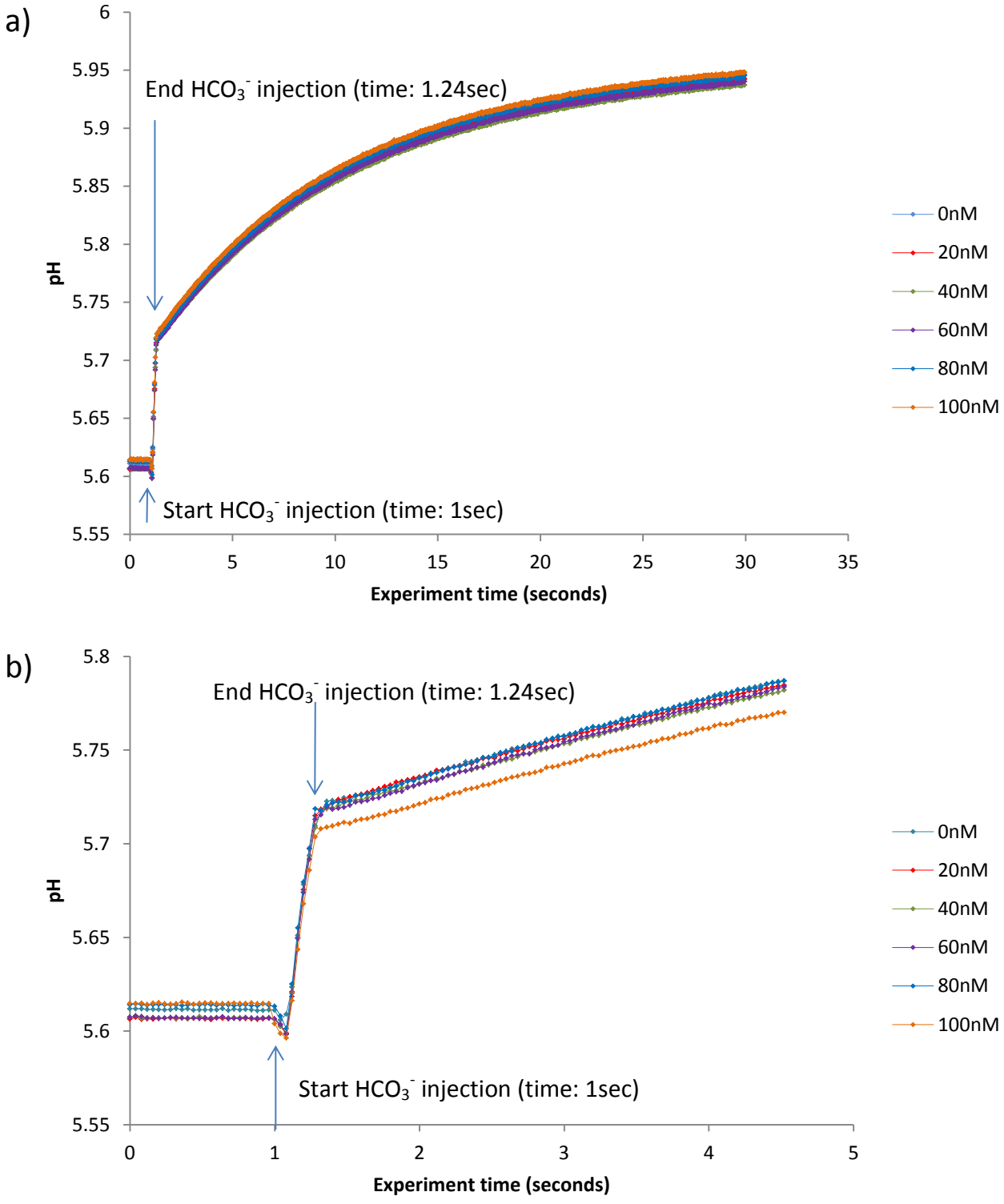

Figure 2.6. Lysozyme do not exhibit enzyme activity *in vitro*. 0nM-100nM of lysozyme proteins were assayed in measuring the rate of pH change during HCO_3^- dehydration. A) Shows the complete reaction time course and b) shows the initial pH change when the HCO_3^- injection is stopped. The color coded curves represent the pH change for each protein concentration. A total of three independent experiments were done, the averages are shown in the figure.

More importantly, the rate of the reaction is linearly and positively correlated with the concentration of bCA2, while it did not change with lysosome (Figure 2.7). The initial pH change after the HCO_3^- injection is linear from 1.24s to 4s of the experiment (Figure 2.7). In addition, the effect of acetazolamide (AAZ), a CA inhibitor was tested using this assay. In two different ranges of inhibitor concentrations (0-5 μM and 0-100 μM, respectively), AAZ inhibited bCA2 activity in a dose-dependent manner (Figure 2.8). The inhibition appeared to reach a saturation point when ≥1μM of AAZ was used as the ΔpH/s did not further decrease even using up 100μM of AAZ (Figures 2.8c and 2.8d).

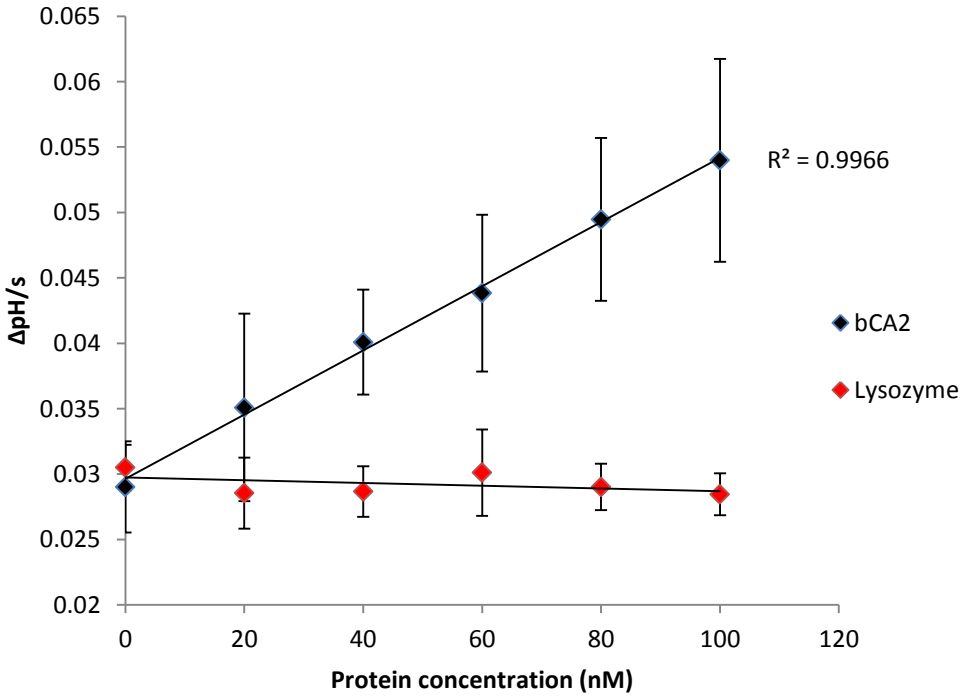

Figure 2.7. Linear relationship between bCA2 activity and concentration. Six increasing concentrations of bCA2 were used to observe enzyme activity: rate of change in reaction pH per second (ΔpH/s) between 1.24s to 4s with lysozyme used as negative control. A good linear relationship fit was seen (R^2>0.99) Total of three independent experiments were done with averages shown; error bars indicate the standard deviations between experiments

a)

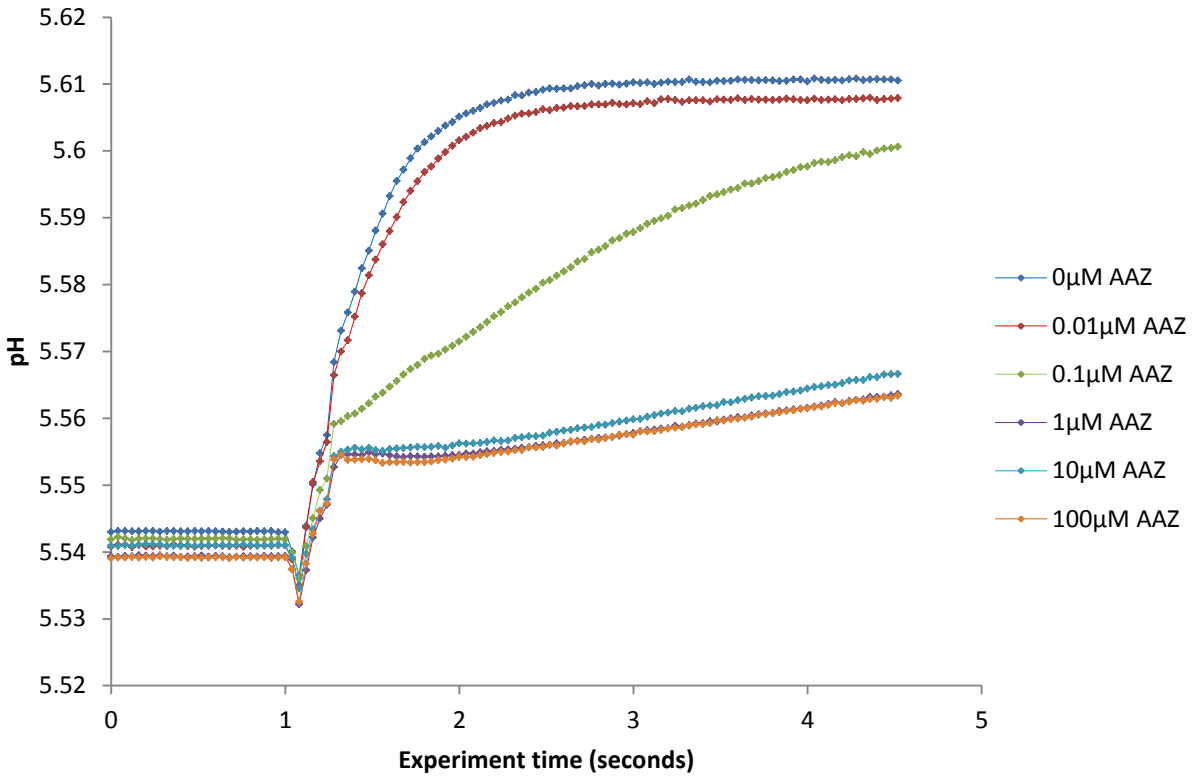
5.62
5.61
5.6
5.59
5.58
5.57
5.56
5.55
5.54
5.53
5.52
pH
0
1
2
3
4
5
Experiment time (seconds)
0μM AAZ
0.01μM AAZ
0.1μM AAZ
1μM AAZ
10μM AAZ
100μM AAZ

b)

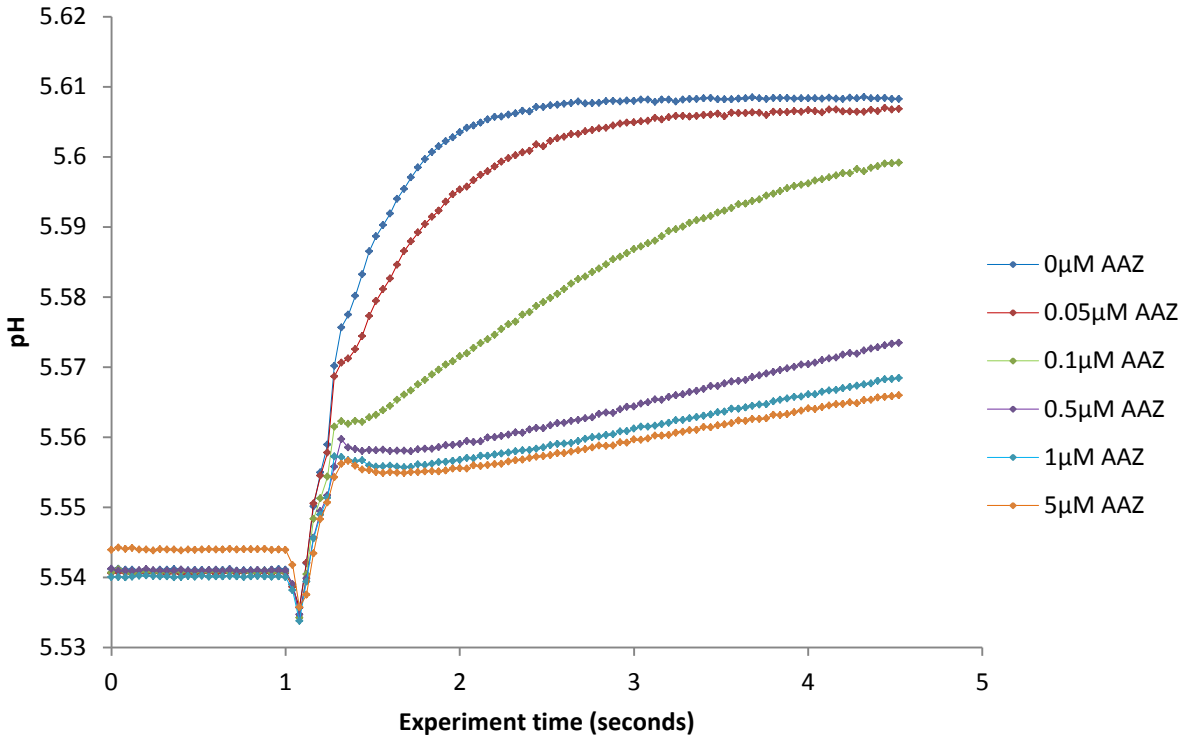
5.62
5.61
5.6
5.59
5.58
5.57
5.56
5.55
5.54
5.53
pH
0
1
2
3
4
5
Experiment time (seconds)
0μM AAZ
0.05μM AAZ
0.1μM AAZ
0.5μM AAZ
1μM AAZ
5μM AAZ

c)

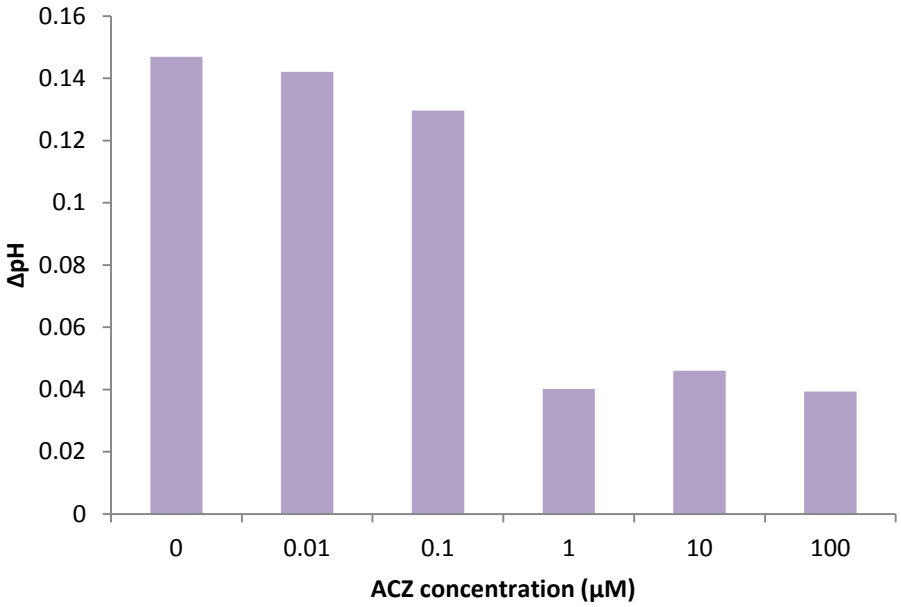

d)

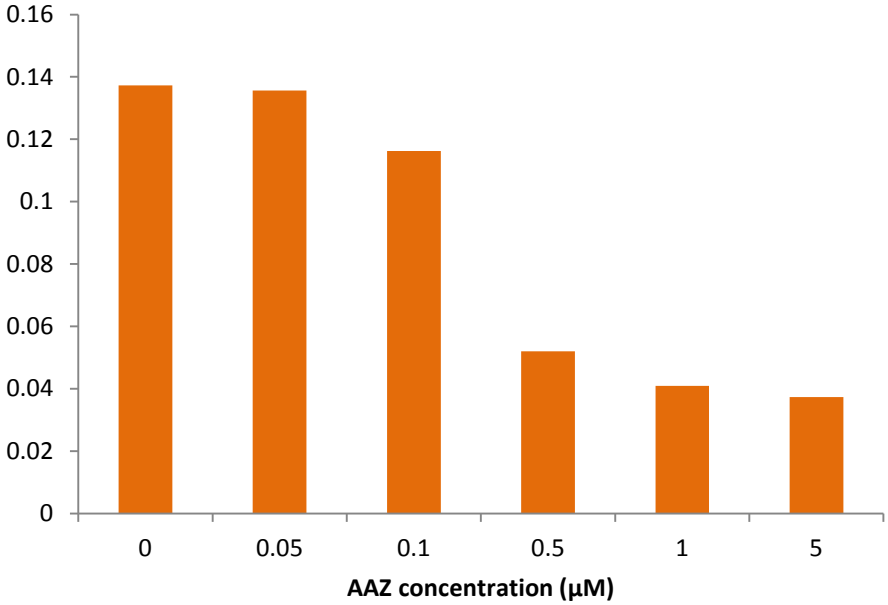

Figure 2.8. Acetazolamide inhibits bCA2 activity. a) 0-100µM and b) 0-5µM of CA1 inhibitor AAZ were added to inhibit bCA2 activity c) shows corresponding rate of change in pH per second (ΔpH/s) in a) between 1.24s to 4s ; d)shows corresponding ΔpH/s at the same interval from b). One independent experiment is done for each series of AAZ inhibition study

Mutant CA1 proteins do not retain activity *in vitro*

Once the assay has shown to be effective in measuring bCA2 activity, the same method was used to determine the activities for the three CA1 mutants: Thr199Val, Glu106Ile and Glu106Gln. The quality of *in vitro* expressed and purified CA1 proteins were visualized (Figure 2.9). The protein samples showed high purity and were of the expected molecular weight.

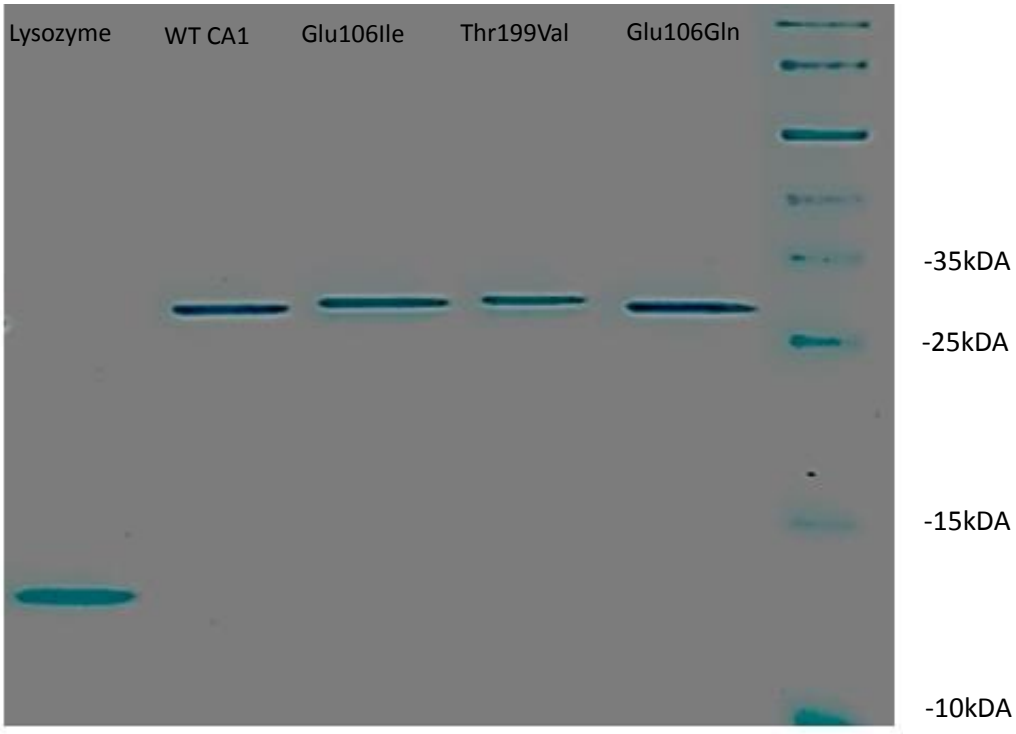

Figure 2.9. Protein purification of his-tagged wild-type and mutant CA1s. Coomassie based gel staining of SDS-PAGE gel of 2.5µM of purified and dialyzed wild-type and mutant his-tagged CA1 proteins, and 2.5µM of chicken egg lysozyme protein as a comparative control. Expected protein sizes - wild-type CA1 : 29.69kDa, Glu106Ile CA1 : 29.68kDa, Thr199Val CA1 : 29.69kDa, Glu106Gln CA1 : 29.69kDa, Lysozyme : 14.3kDa. Expected sizes of the purified proteins were generated using the ExPASy ComputPl/Mw software (Swiss institute of bioinformatics, Switzerland)

Using the same amount of either wild-type or mutant CA1, the obtained reaction curves viewed in both shorter and longer time intervals were shown in Figure 2.10a-2.10d. Figure 2.10a shows the initial reaction pH curve in CA1 after HCO_3^- injection as compared to the wild-type, the curves were zoomed in and overlaid in figure 2.10b. Figure 2.10c and 2.10d show the entire reaction pH curve for each individual CA1 sample.

Figure 2.10a and 2.10b show the initial reaction pH changes when HCO_3^- was injected into the reaction media. The figures show there was steady pH increases in all of the reaction samples between 1.24s to 4.5s. For wild-type CA1, the rate of initial pH increase is significantly higher than the other samples, i.e. reaching a higher pH value within the given period. The figures show great similarities in the initial pH change between the CA1 mutants and lysozyme negative control. These results suggest wild-type CA1 retained its enzyme activity in catalyzing the pH equilibrization reaction whereas mutant CA1 did not retain any enzyme activity as they have shown similar pH trends as the negative control.

Figure 2.10c and 2.10d show the pH changes during the entire course of the reaction. While the pH of all the samples reached a similar end-point at 30s, reaction involving wild-type CA1 reached its pH equilibrium at a much faster velocity compared to the mutants and the negative control.

Applying the same analysis to calculate the initial rates for all reactions i.e. measuring the pH changes between 1.24s (end of HCO_3^- injection) to 4s (the linear portion of initial pH change) the data have demonstrated that all three CA1 mutants in the experiments retained no

higher activities than a known protein without any anhydrase activity (lysozyme) (Figure 2.10e).

In other words, Thr199Val, Glu106Ile and Glu106Gln are inactive mutants of CA1.

a)

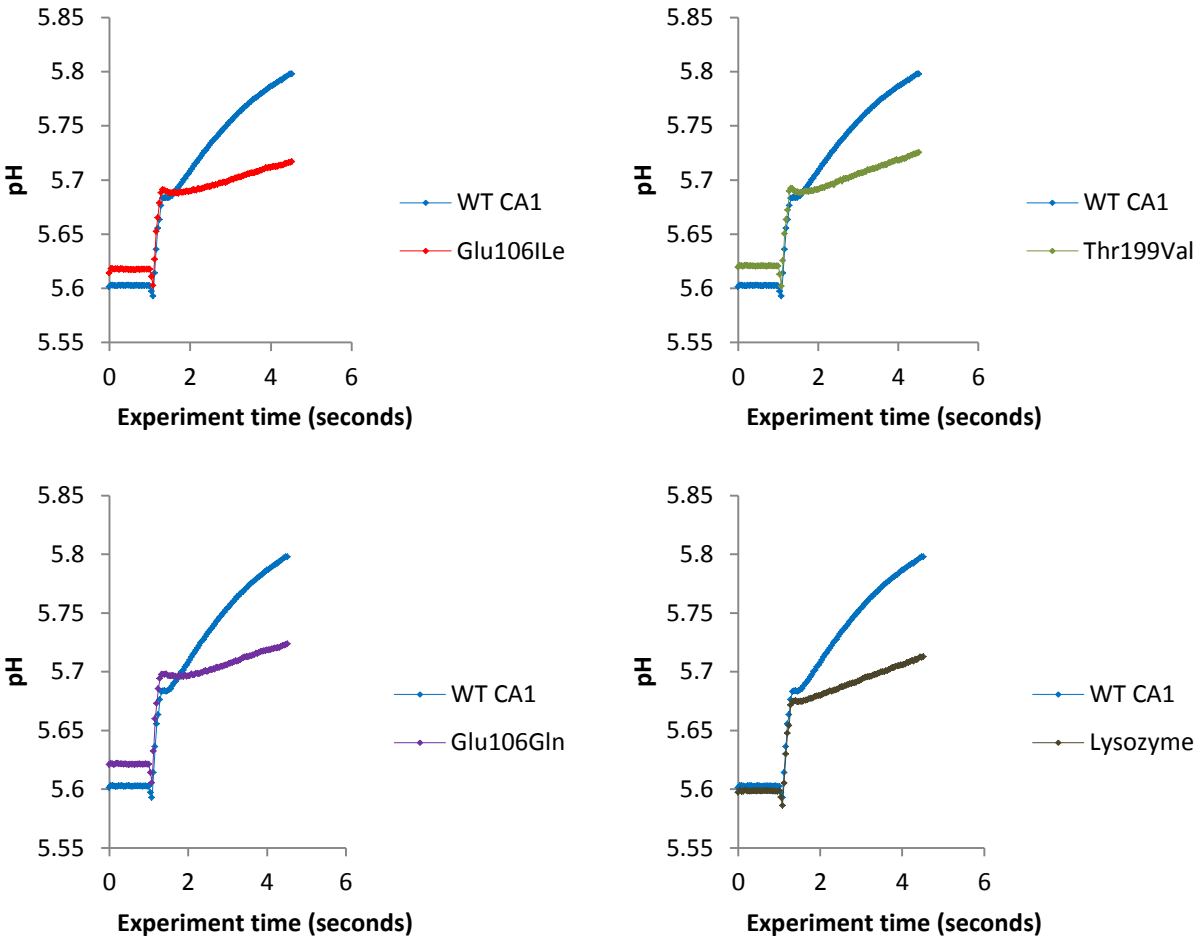

b)

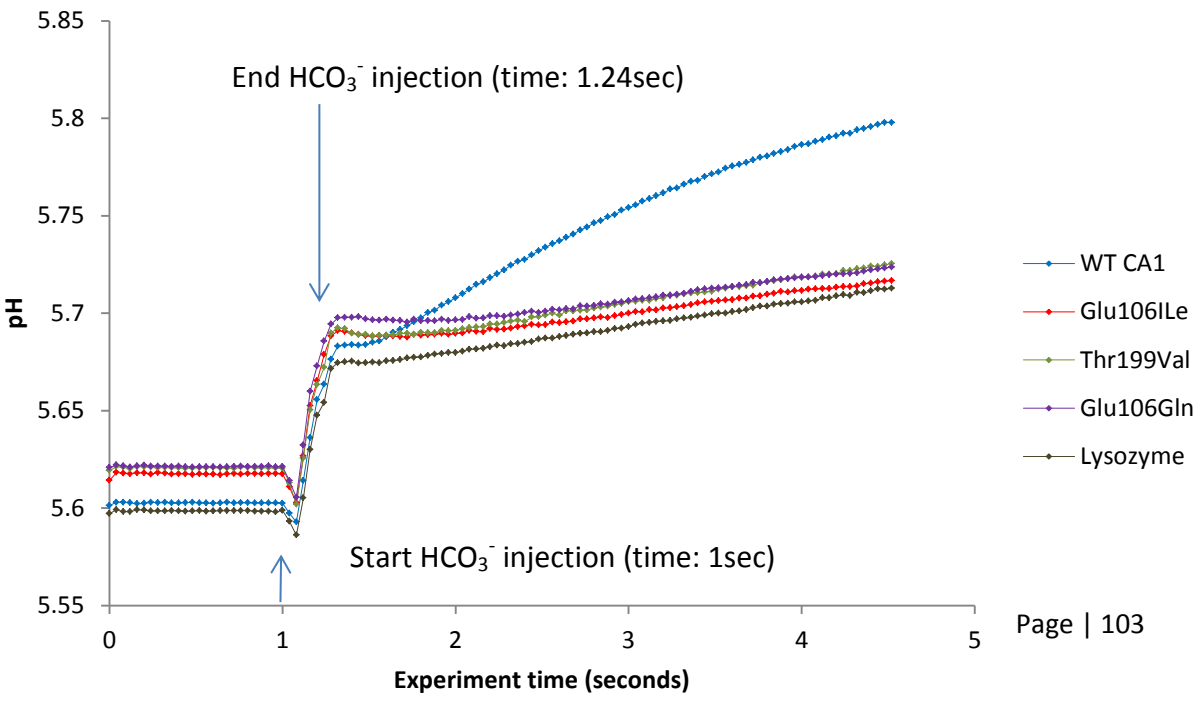

c)

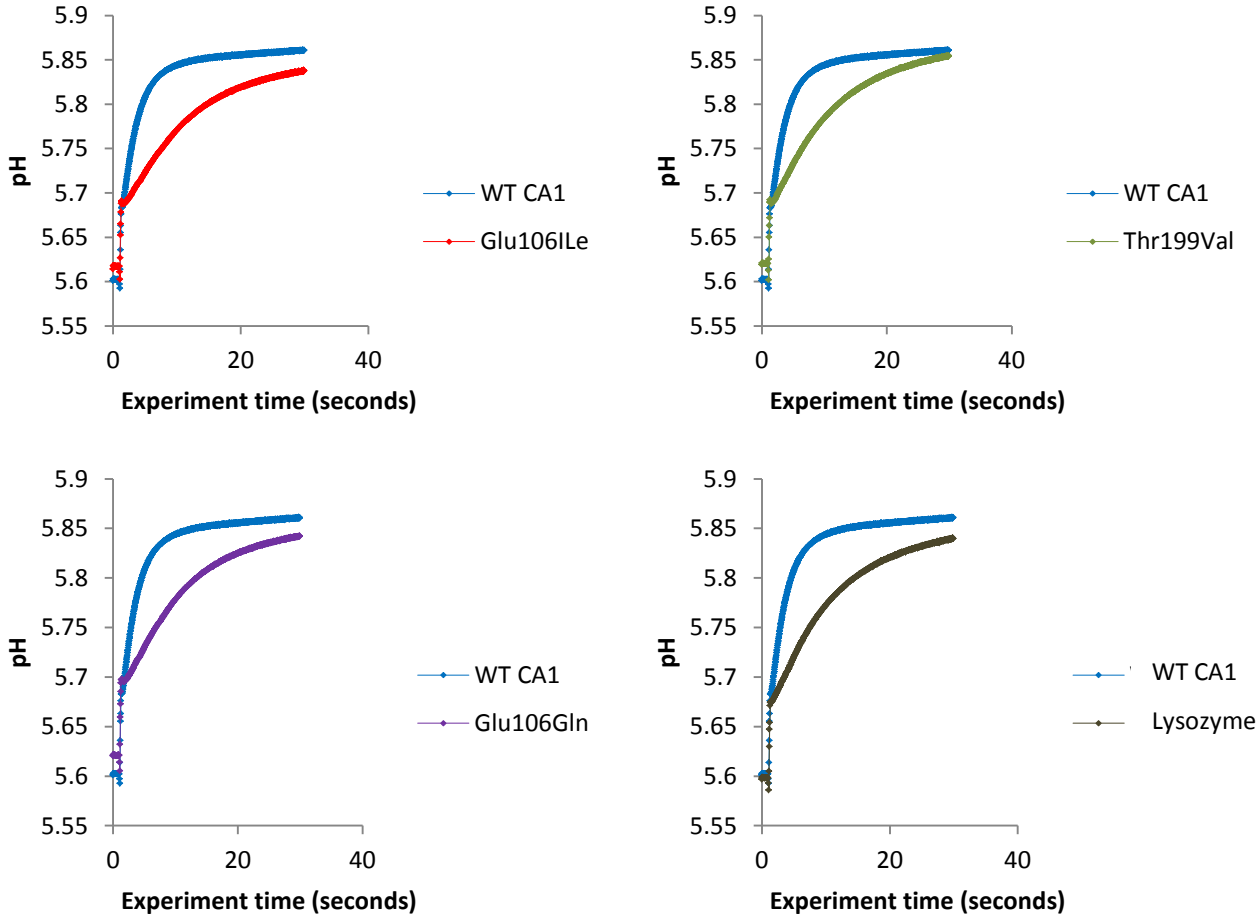
pH
Experiment time (seconds)
WT CA1
Glu106ILe
Thr199Val
Glu106Gln
Lysozyme

d)

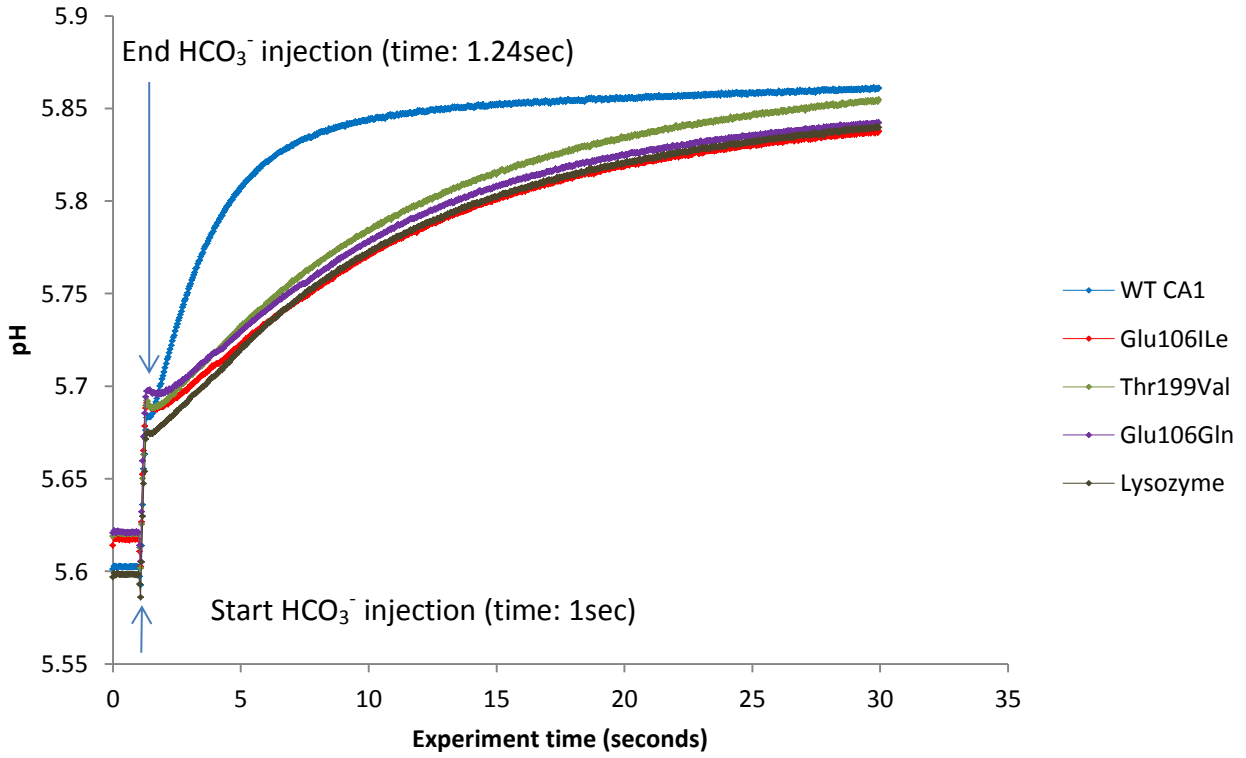
End HCO_3^- injection (time: 1.24sec)
Start HCO_3^- injection (time: 1sec)
pH
Experiment time (seconds)
WT CA1
Glu106ILe
Thr199Val
Glu106Gln
Lysozyme

e)

	Initial enzyme rate (ΔpH/s)	Initial enzyme rate with respect to wild-type CA1 (%)
Wild-type CA1	0.045±0.008	100.00±16.82
Glu106Ile	0.012±0.004	26.71±8.86
Thr199Val	0.017±0.002	37.4±3.83
Glu106Gln	0.012±0.005	26.69±11.16
Lysozyme	0.019±0.005	41.91±11.65

Figure 2.10. Mutant CA1 proteins do not exhibit activity *in vitro*. Wild-type and mutant CA1 proteins and lysozyme negative control were used to observe the rate of pH change during HCO_3^- dehydration. A) Shows initial reaction changes in individual samples in comparison with the wild-type CA1; b) overlays the pH curves from all samples; the interval used to calculate the initial enzyme activity was between 1.24s to 4s; c) Shows the complete reaction time course in individual samples in comparison with the wild-type; d) overlays the pH curves from all samples,; e) table shows the enzyme activity of all samples relative to wild-type CA1, calculated using the pH change from 1.24s to 4s of the experiment. Six independent experiments were done for each curve.

Discussion

Development of a modified fluorescence-based assay of measuring CA activities

The method in this study utilizes HCO_3^- as the CA1 enzyme substrate, which reacts with the protons in the acidic reaction environment. As HCO_3^- ions are injected into the mixture, the reaction pH will increase as the protons get consumed to produce CO_2 and water, eventually reaching its pH equilibrium. The presence of the wild-type CA1 will accelerate the rate of the pH change due to its catalytic activity. On the other hand, it is predicted that using mutant CA1 proteins with substituted Thr199 and Glu106 (Thr199Val, Glu106Gln and Glu106Ile) should have reduced and/or ablated CA1 activity in due to the roles the two residues play in CA1 enzyme activity (Merz, 1990, Bottoni et al., 2004, Miscione et al., 2007, Lindskog, 1997, Briganti et al., 1997, Xue et al., 1993).

The technique described here is essentially a modified pH-indicator method that follows the principles of the previous methods used to measure CA activity (Clark and Perrin, 1951, Khalifah, 1971). However, the main advantage of this technique is that it substitutes very specialized equipment (i.e. mass spectrometer or stop-flow equipment) with a microplate reader which is more widely used in biological research laboratories. The only requirement of this microplate reader is that it can measure the fluorescence change in a very fast way. In particular, it utilizes a fluorescence based pH-sensitive indicator Pyranine (instead of other dyes used in previous studies to measure the changes in absorbance) which has been reported to be very sensitive to pH changes in the near neutral range compared to other pH-sensitive fluorescent dyes in the near-neutral pH range (Zhu et al., 2005, Verchère et al., 2012).

Though this method did not utilize other HCO_3^- substrate concentrations to calculate the Michaelis-Menten kinetic parameters of wild-type CA1 proteins in the study, this can be done in future experiments. With regards to measuring the Pyranine fluorescence changes, probes with a more sensitive excitation wavelength (i.e. at 450nm) can be used to identify the pH changes instead of the wavelength used here (i.e. at 430nm) (Figure 2.3). Furthermore, the stop-flow equipment can be a useful addition as it allows more time-sensitive resolution of the pH change which was employed in previous studies (Khalifah, 1971, Clark and Perrin, 1951, Verpoorte et al., 1967). Nonetheless, the results presented here show another way to measure CA activity which is more convenient and simpler to operate. Its main purpose is not to replace the established methods, rather provide an alternative method to measure the CA enzyme activity if the specialized equipment was not present.

With regards to the reliability of the technique, the results obtained at present shows consistency with the CA2 and CA1 mutagenesis studies using the same mutants during CO_2-HCO_3^- interconversion reaction (Krebs et al., 1993, Liang et al., 1993, Mohanty et al., 1998). The results show dramatic decrease in the rate of initial pH change when using the CA1 mutants in the HCO_3^- dehydration reaction as compared to the wild-type CA1 protein, as well as the similarities in the initial pH change found between the CA1 mutants with the negative control sample. This is consistent with previous studies where the Thr199Val and Glu106Ile mutants show significant loss of enzyme activity as compared to the wild-type in CA2 and CA1.

Mutant CA1 are enzymatically inactive *in vitro*

As mentioned above, results from this study introduces a modified fluorescence based for measuring the enzyme activity of wild-type, Thr199Val, Glu106Ile, Glu106Gln mutant CA1 proteins. Using lysozyme as the negative control, the results demonstrate that wild-type CA1 protein significantly accelerates the rate of HCO_3^- dehydration seen by the rate of pH changes in the reaction; whereas mutant CA1 and lysozyme did not alter the rate of reaction compared with that in absence of any catalyst, suggesting the mutants do not retain CA1 enzyme activity *in vitro*.

Due to the overall lack of CA1 mutagenesis studies, evidence supporting how substituting Thr199 and Glu106 will specifically affect CA1 enzyme activity require inference from studies done in CA2 at these residues (Krebs and Fierke, 1993, Liang et al., 1993, Mohanty et al., 1998, Xue et al., 1993, Krebs et al., 1993). Results of these studies show: firstly, substitutions at Thr199 or Glu106 resulted in significant loss of CA2 and CA1 enzyme activity; secondly, patterns observed with regards to CA2 Thr199/Glu106 substituted mutants are consistent with results found in CA1. This is likely due to the zinc-OH^- (or water)-Thr199-Glu106 hydrogen bond network sequence being conserved and sharing similar orientations for both CA1 and CA2 (Figure 2.1). For instance, in CA2, the substitution Thr199Val caused the HCO_3^- dehydration activity to drop to ~1/2900th of the wild-type CA2 activity, which is similar to the near-ablation of activity in the CA1 mutant Thr199Val applied in this study, carried out in the similar reaction environment and approach as the method develop in this investigation (at pH 6.1, 25˚C using a pH indicator assay) (Krebs et al., 1993). Furthermore, mutations of the Glu106

residue in CA2 have shown similar results, where it was observed the Glu106Gln mutant retained only ~1/3000th of the original CA2 activity similar to the findings with CA1 in this study (Liang et al., 1993). Other studies that substituted Thr199 and Glu106 using other amino acids supports these observations highlighting their importance in CA catalysis (Liang et al., 1993, Krebs and Fierke, 1993, Xue et al., 1993).

On the other hand, the Thr199 and Glu106 residues have been substituted in the CA1 enzyme to study the effects of these mutations on the CA1 enzyme activity (Mohanty et al., 1998). To date, this is the only study reported on CA1 mutants with substituted amino acids at the Thr199 and Glu106 residues in studying the esterase activity CA1. This study has found Thr199Val mutant only retained 5-8% of wild-type CA1 esterase activity, the lowest out of all eight CA1 mutants studied. The same Thr199Val mutant in CA2 retained around 18% of its wild-type esterase activity (Krebs et al., 1993, Mohanty et al., 1998). The reported esterase activity for the CA2 mutant Glu106Gln was around 1/187th of the wild-type activity (Liang et al., 1993); whereas, in CA1 the Glu106Gln mutant appears to retain around 7% of the wild-type CA1 activity (Mohanty et al., 1998). Although the Mohanty *et al* study examines the esterase activity of the wild-type and mutant CA1, previous data have shown the results from the esterase assay done in CA1 and CA2 share great similarity in the enzyme kinetics and velocity as the reversible CO_2 hydration reaction (Khalifah, 1971, Verpoorte et al., 1967). Therefore, it appears the data are consistent with the same mutations from previous studies causing dramatic loss of enzyme activity in both CA1 and CA2 (Liang et al., 1993, Krebs and Fierke, 1993, Xue et al., 1993).

Crystallography studies of mutants at Thr199 and Glu106 have provided mechanistic changes as to how these mutations affect CA2 catalysis, which can be used to infer how they may affect CA1. Due to the Thr199Val substitution, the mutant has lost its hydrogen bonding between Glu106 and Val199 (Figure 2.11). It appears that there is also loss of hydrogen bonding between Val199 and the zinc-bound water if it was present (structure showing the Thr199Val mutant with the active site water present without displacement by an inhibitor is currently unavailable). Furthermore, the Val199 residue causes conformation changes in the Glu106 residue, though its position is held relatively similar to the Thr199 residue in the wild-type CA2 (Krebs et al., 1993, Krishnamurthy et al., 2008). The conformational change of Glu106 results in stabilization of the zinc-HCO_3^- complex requiring additional energy during the HCO_3^- dehydration reaction causing a significant drop in reaction velocity (Liang et al., 1993, Krebs et al., 1993).

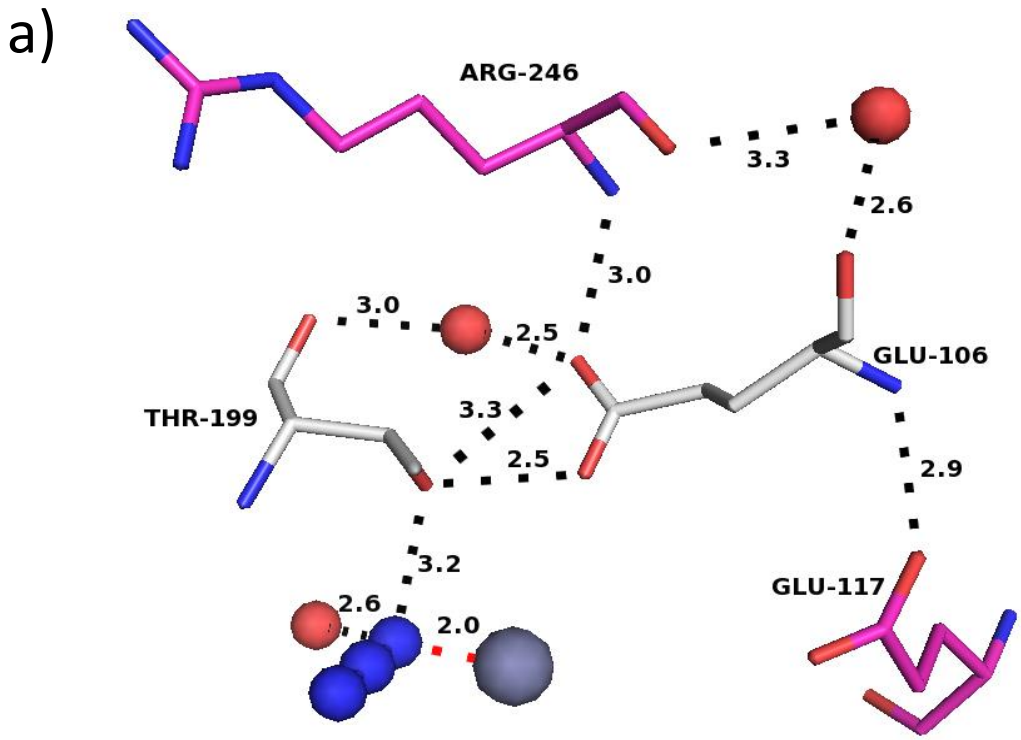

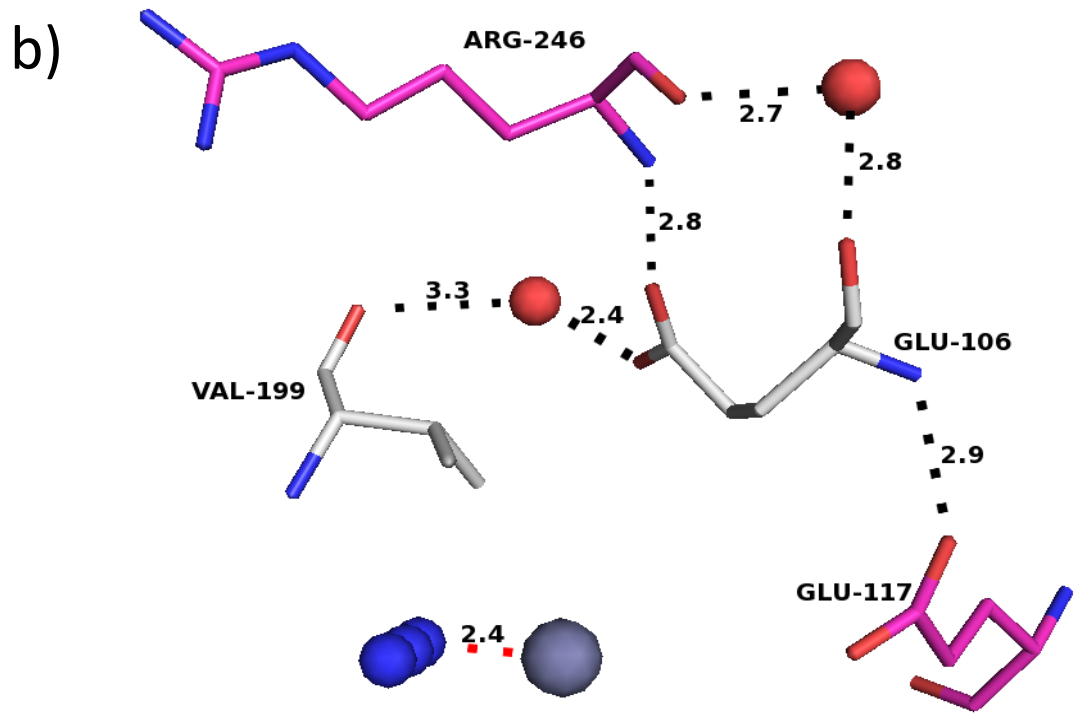

Figure 2.11. Comparison between wild-type and Thr199Val mutant CA2. A) shows the wild-type structure and b) shows the Thr199Val structure. The Thr199/Val199 and Glu106 residues are colored grey/blue/red, their outer hydrogen bonded residues are labelled pink/red/blue. Grey and red spheres represent zinc and water molecules, respectively. The dark blue spheres represent an azide ion inhibitor bound to the active site. Red and black dashed lines represent co-ordination between water molecule to the zinc ion and hydrogen bonds between residues and water molecules, respectively, with bond lengths labelled in angstroms. The image was generated from the x-ray structures from Brookhaven protein data bank (wild-type CA2 – file code 1RAY; Thr199Val CA2 – file code 1CVA). The figure was generated and rendered using Pymol.

Figure 2.12 shows the comparison between wild-type and Glu106Gln CA2 structures complexed with an acetate ligand (Glu106Gln structure without inhibitor present is unavailable). The figure shows a hydrogen bond is maintained between Gln106 and Thr199 (Figure 2.12). However, directionality of the hydrogen bonding in the Thr199-Glu106 interaction is reversed in the Glu106Gln mutant from the wild-type CA2 as the Gln106 amide NH_2 group now acts as the hydrogen bond donor to Thr199 (Liang et al., 1993, Xue et al., 1993). In the mutant, Thr199 acts

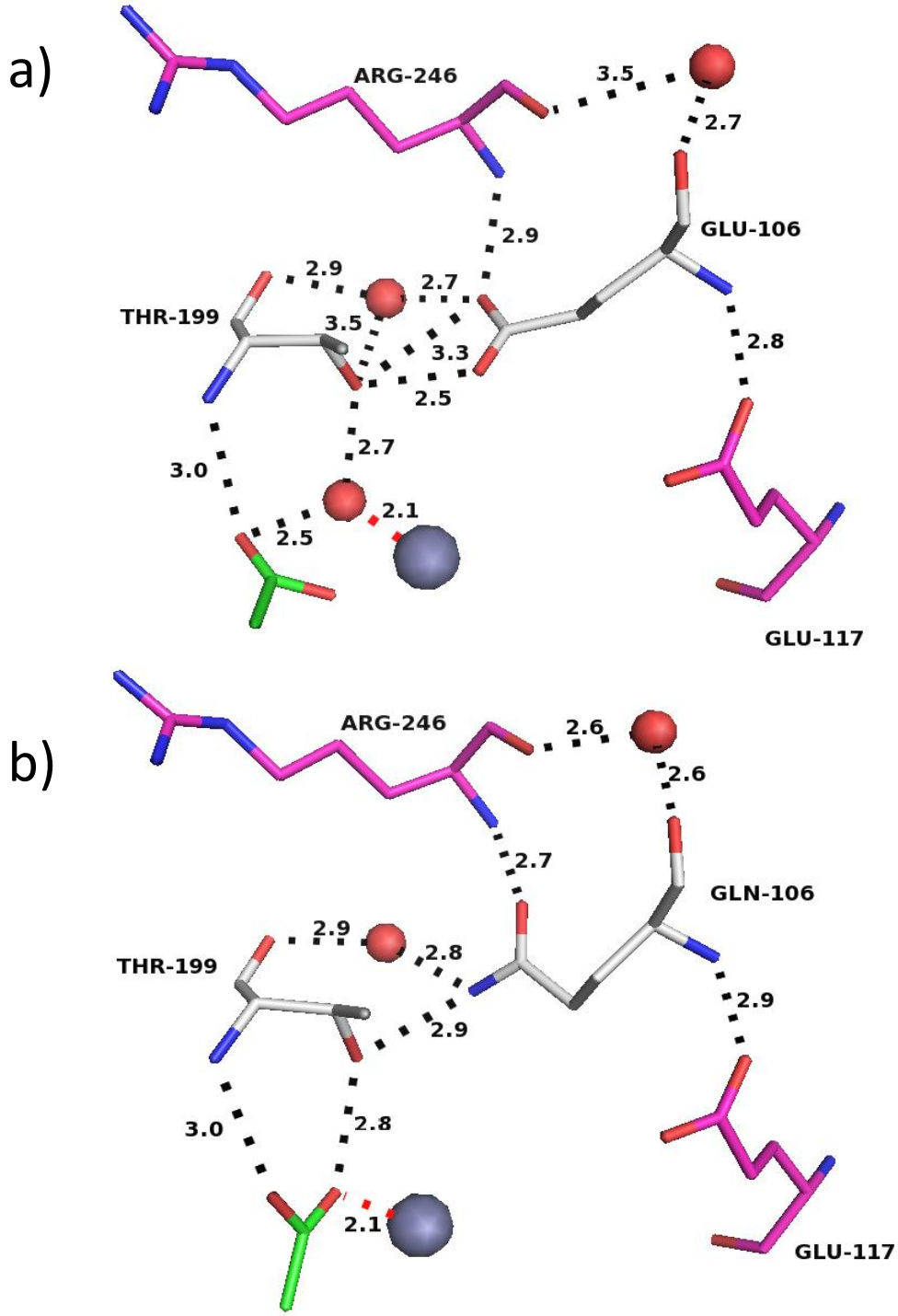

Figure 2.12. Comparison between wild-type and Glu106Gln mutant CA2. A) shows the wild-type structure and b) shows the Glu106Gln structure. The Thr199 and Glu106/Gln106 residues are colored grey/blue/red, their outer hydrogen bonded residues are labelled pink/red/blue. Grey and red spheres represent zinc and water molecules, respectively. The green/red sticks represent the acetate inhibitor bound to the active site. Red and black dashed lines represent co-ordination between water molecule to the zinc ion and hydrogen bonds between residues and water molecules, respectively, with bond lengths labelled in angstroms. The image was generated from the x-ray structures from Brookhaven protein data bank (wild-type CA2 – file code 1CAY; Glu106Gln CA2 – file code 1CAZ). The figure was generated and rendered using Pymol.

as the hydrogen bond donor to the acetate ligand which has displaced the zinc-bound water molecule (Hakansson et al., 1994). In the absence of inhibitors, it is likely that the zinc-bound water will remain hydrogen bonded to Thr199 with Thr199 acting as the hydrogen bond acceptor to Gln106 and donor to the zinc-bound water (Figure 2.12) (Hakansson et al., 1994, Xue et al., 1993). This reversed hydrogen bonding pattern is likely to alter the Thr199 interaction with the OH^- ion (Xue et al., 1993). The loss of activity could be due to decrease in the HCO_3^- dissociation efficiency from the zinc ion and a less efficient proton transfer process from the active site to the surrounding medium (Xue et al., 1993, Liang et al., 1993).

Currently, with regards to how the Glu106Ile mutant causes reduced activity in CA1 is unclear. However, the Glu106 mutant has been studied and as both Alanine and Isoleucine are hydrophobic amino acids, insights from Glu106Ala may shed light on the matter (Liang et al., 1993, Xue et al., 1993). First of all, the Glu106Gln and the Glu106Ala mutants share many similarities in the structure of their active site (Xue et al., 1993, Liang et al., 1993). The substitution of Glu106 with a hydrophobic amino acid such as Alanine will remove the negative charge previously present with the Glu106 residue. This loss of negative charge is partly responsible for the substantial increase in affinity for HCO_3^- ions by the zinc ion (Liang et al., 1993). This increase in affinity for HCO_3^- reduces the dissociation between the HCO_3^- and zinc, thus likely to inhibit the transition stage during 1) HCO_3^- dehydration reaction to produce the CO_2; and 2) to regenerate the active free enzyme during the proton transfer from the enzyme active site to the reaction medium.

The results from this study have shown that the three mutant CA1 proteins used (Thr199Val, Glu106Ile and Glu106Gln) share overlapping reaction pH changes with the lysozyme protein used as the negative control in the experiment suggesting an ablation of CA activity in the mutants. This technique has shown to be sensitive to 20ng increments of bCA2 enzyme activity, whereas using the lysozyme protein at the same concentrations no change in enzyme activity was seen using incremental concentrations of the protein. Lysozyme hydrolyzes the β(1–4) glycosidic linkage between *N*-acetylmuramic acid and *N*-acetylglucosamine in the bacterial cell wall peptidoglycan layer causing bacterial cell lysis (Li-Chan and Kim, 2007). Although the lysozyme hydrolysis activity was found to be increased in the presence of HCO_3^-, lysozyme do not participate in the HCO_3^- dehydration related reactions (Banerjee et al., 2011).

Results presented in this chapter represent for the first time the effect of substituting the Thr199 and Glu106 residues on the CA1 HCO_3^- dehydration enzyme activities. Although these residues are conserved across the CA family and have been shown to be critical during the CA catalytic process, they have not being studied within CA1 during the physiologically relevant CO_2-HCO_3^- interconversion reaction (Mohanty et al., 1998). The technique presented here offers a convenient alternative to quickly assess CA enzyme activity without the need for specialized equipment. Furthermore, these results indicate mutation at Thr199 or Glu106 is sufficient to cause an ablation of CA1 activity that can be applied as enzyme-inactive controls in future studies to assess CA1 function in cells and animals.

References

AGUEDO, M., WACHÉ, Y. & BELIN, J.-M. 2001. Intracellular pH-dependent efflux of the fluorescent probe pyranine in the yeast Yarrowia lipolytica. *FEMS Microbiology Letters,* 200**,** 185-189.

BANERJEE, P., KEENER, K. M. & LUKITO, V. D. 2011. Influence of carbon dioxide on the activity of chicken egg white lysozyme. *Poultry Science,* 90**,** 889-895.

BEHRAVAN, G., JONASSON, P., JONSSON, B.-H. & LINDSKOG, S. 1991. Structural and functional differences between carbonic anhydrase isoenzymes I and II as studied by site-directed mutagenesis. *European Journal of Biochemistry,* 198**,** 589-592.

BERGER, R. L. 1978. Some problems concerning mixers and detectors for stopped flow kinetic studies. *Biophys J,* 24**,** 2-20.

BOTTONI, A., LANZA, C. Z., MISCIONE, G. P. & SPINELLI, D. 2004. New Model for a Theoretical Density Functional Theory Investigation of the Mechanism of the Carbonic Anhydrase: How Does the Internal Bicarbonate Rearrangement Occur? *Journal of the American Chemical Society,* 126**,** 1542-1550.

BRIGANTI, F., MANGANI, S., ORIOLI, P., SCOZZAFAVA, A., VERNAGLIONE, G. & SUPURAN, C. T. 1997. Carbonic Anhydrase Activators: X-ray Crystallographic and Spectroscopic Investigations for the Interaction of Isozymes I and II with Histamine. *Biochemistry,* 36**,** 10384-10392.

CHENG, K. L. & ZHU, D.-M. 2005. On Calibration of pH Meters. *Sensors (Basel, Switzerland),* 5**,** 209-219.

CLARK, A. M. & PERRIN, D. D. 1951. A re-investigation of the question of activators of carbonic anhydrase. *Biochemical Journal,* 48**,** 495-502.

DAMIANO, E., BASSILANA, M., RIGAUD, J. L. & LEBLANC, G. 1984. Use of the pH sensitive fluorescence probe pyranine to monitor internal pH changes in Escherichia coli membrane vesicles. *FEBS Lett,* 166**,** 120-4.

DAOOD, S. S., IJAZ, A. & BUTT, M. A. 2007. Study on a Concentric Tube Bulb Manometer and its Performance Compared to U-shaped Manometer. *Sensors (Basel, Switzerland),* 7**,** 2835-2845.

ENGSTRAND, C., JONSSON, B. H. & LINDSKOG, S. 1995. Catalytic and inhibitor-binding properties of some active-site mutants of human carbonic anhydrase I. *Eur J Biochem,* 229**,** 696-702.

ERIKSSON, A. E., KYLSTEN, P. M., JONES, T. A. & LILJAS, A. 1988. Crystallographic studies of inhibitor binding sites in human carbonic anhydrase II: a pentacoordinated binding of the SCN- ion to the zinc at high pH. *Proteins,* 4**,** 283-93.

FERRARONI, M., TILLI, S., BRIGANTI, F., CHEGWIDDEN, W. R., SUPURAN, C. T., WIEBAUER, K. E., TASHIAN, R. E. & SCOZZAFAVA, A. 2002. Crystal structure of a zinc-activated variant of human carbonic anhydrase I, CA I Michigan 1: evidence for a second zinc binding site involving arginine coordination. *Biochemistry,* 41**,** 6237-44.

GAN, B. S., KRUMP, E., SHRODE, L. D. & GRINSTEIN, S. 1998. Loading pyranine via purinergic receptors or hypotonic stress for measurement of cytosolic pH by imaging. *American Journal of Physiology - Cell Physiology,* 275**,** C1158-C1166.

GELATT, K. N. 2014. Ophthalmic Structures. *Essentials of Veterinary Ophthalmology.* 3 ed.: John Wiley & Sons, Ltd.

HAKANSSON, K., BRIAND, C., ZAITSEV, V., XUE, Y. & LILJAS, A. 1994. Wild-type and E106Q mutant carbonic anhydrase complexed with acetate. *Acta Crystallogr D Biol Crystallogr,* 50**,** 101-4.

HENRY, R. P. 1991. Techniques for Measuring Carbonic Anhydrase Activity in Vitro. *In:* DODGSON, S. J., TASHIAN, R. E., GROS, G. & CARTER, N. D. (eds.) *The Carbonic Anhydrases: Cellular Physiology and Molecular Genetics.* Boston, MA: Springer US.

KANNAN, K. K., PETEF, M., FRIDBORG, K., CID-DRESDNER, H. & LO¨VGREN, S. 1977a. Structure and function of carbonic anhydrases: Imidazole binding to human carbonic anhydrase B and the mechanism of action of carbonic anhydrases. *FEBS Letters,* 73**,** 115-119.

KANNAN, K. K., PETEF, M., FRIDBORG, K., CID-DRESDNER, H. & LOVGREN, S. 1977b. Structure and function of carbonic anhydrases. Imidazole binding to human carbonic anhydrase B and the mechanism of action of carbonic anhydrases. *FEBS Lett,* 73**,** 115-9.

KANO, K. & FENDLER, J. H. 1978. Pyranine as a sensitive pH probe for liposome interiors and surfaces. pH gradients across phospholipid vesicles. *Biochimica et Biophysica Acta (BBA) - Biomembranes,* 509**,** 289-299.

KHALIFAH, R. G. 1971. The carbon dioxide hydration activity of carbonic anhydrase. I. Stop-flow kinetic studies on the native human isoenzymes B and C. *J Biol Chem,* 246**,** 2561-73.

KHALIFAH, R. G. & EDSALL, J. T. 1972. Carbon dioxide hydration activity of carbonic anhydrase: kinetics of alkylated anhydrases B and C from humans (metalloenzymes-isoenzymes-active sites-mechanism). *Proc Natl Acad Sci U S A,* 69**,** 172-6.

KOCKAR, F., MARESCA, A., AYDIN, M., ISIK, S., TURKOGLU, S., SINAN, S., ARSLAN, O., GULER, O. O., TURAN, Y. & SUPURAN, C. T. 2010. Mutation of Phe91 to Asn in human carbonic anhydrase I unexpectedly enhanced both catalytic activity and affinity for sulfonamide inhibitors. *Bioorg Med Chem,* 18**,** 5498-503.

KOENIG, S. H. & BROWN, R. D. 1973. Kinetic parameters of human carbonic anhydrase B as determined from NMR linewidths of 13 C in CO 2 and HCO 3. *Biochem Biophys Res Commun,* 53**,** 624-30.

KREBS, J. F. & FIERKE, C. A. 1993. Determinants of catalytic activity and stability of carbonic anhydrase II as revealed by random mutagenesis. *Journal of Biological Chemistry,* 268**,** 948-954.

KREBS, J. F., IPPOLITO, J. A., CHRISTIANSON, D. W. & FIERKE, C. A. 1993. Structural and functional importance of a conserved hydrogen bond network in human carbonic anhydrase II. *Journal of Biological Chemistry,* 268**,** 27458-27466.

LI-CHAN, E. C. Y. & KIM, H.-O. 2007. Structure and Chemical Compositions of Eggs. *Egg Bioscience and Biotechnology.* John Wiley & Sons, Inc.

LI, H.-N. & CI, Y.-X. 1995. A new rapid fluorimetric method for the determination of carbonic anhydrase. *Analytica Chimica Acta,* 317**,** 353-357.

LIANG, J.-Y. & LIPSCOMB, W. N. 1989. Theoretical study of carbonic anhydrase-catalyzed hydration of co2: A brief review. *International Journal of Quantum Chemistry,* 36**,** 299-312.

LIANG, Z., XUE, Y., BEHRAVAN, G., JONSSON, B. H. & LINDSKOG, S. 1993. Importance of the conserved active-site residues Tyr7, Glu106 and Thr199 for the catalytic function of human carbonic anhydrase II. *Eur J Biochem,* 211**,** 821-7.

LINDSKOG, S. 1997. Structure and mechanism of carbonic anhydrase. *Pharmacol Ther,* 74**,** 1-20.

MAREN, T. H. 1960. A simplified micromethod for the determination of carbonic anhydrase and its inhibitors. *J Pharmacol Exp Ther,* 130**,** 26-9.

MELDRUM, N. U. & ROUGHTON, F. J. 1933. Carbonic anhydrase. Its preparation and properties. *J Physiol,* 80**,** 113-42.

MERZ, K. M., HOFFMANN, R. & DEWAR, M. J. S. 1989. The mode of action of carbonic anhydrase. *Journal of the American Chemical Society,* 111**,** 5636-5649.

MERZ, K. M., JR. 1990. Insights into the function of the zinc OH^--Thr199-Glu106 hydrogen bonding network in carbonic anhydrases. *J Mol Biol,* 214**,** 799-802.

MISCIONE, G., STENTA, M., SPINELLI, D., ANDERS, E. & BOTTONI, A. 2007. New computational evidence for the catalytic mechanism of carbonic anhydrase. *Theoretical Chemistry Accounts: Theory, Computation, & Modeling,* 118**,** 193-201.

MOHANTY, KANNAN & MAHAJAN 1998. Human carbonic anhydrase I: Effect of specific site mutations on its function. *Journal of Biosciences* 23**,** 12.

PULLMAN, A. 1981. Carbonic anhydrase: theoretical studies of different hypotheses. *Ann N Y Acad Sci,* 367**,** 340-55.
ROUGHTON, F. J. W. 1941. A METHOD OF ALLOWING FOR THE INFLUENCE OF DIFFUSION IN MANOMETRIC MEASUREMENTS OF CERTAIN RAPID BIOCHEMICAL REACTIONS. *Journal of Biological Chemistry,* 141**,** 129-145.
SHAW, C. R., SYNER, F. N. & TASHIAN, R. E. 1962. New Genetically Determined Molecular Form of Erythrocyte Esterase in Man. *Science,* 138**,** 31-32.
SHINGLES, R. & MORONEY, J. V. 1997. Measurement of carbonic anhydrase activity using a sensitive fluorometric assay. *Anal Biochem,* 252**,** 190-7.
SILVERMAN, D. N. 1982. Carbonic anhydrase: oxygen-18 exchange catalyzed by an enzyme with rate-contributing proton-transfer steps. *Methods Enzymol,* 87**,** 732-52.
SILVERMAN, D. N. & LINDSKOG, S. 1988. The catalytic mechanism of carbonic anhydrase: implications of a rate-limiting protolysis of water. *Accounts of Chemical Research,* 21**,** 30-36.
SIMONSSON, I., JONSSON, B.-H. & LINDSKOG, S. 1979. A 13C Nuclear-Magnetic-Resonance Study of CO2-HCO3− Exchange Catalyzed by Human Carbonic Anhydrase C at Chemical Equilibrium. *European Journal of Biochemistry,* 93**,** 409-417.
STEINER, H., JONSSON, B. H. & LINDSKOG, S. 1975. The catalytic mechanism of carbonic anhydrase. Hydrogen-isotope effects on the kinetic parameters of the human C isoenzyme. *Eur J Biochem,* 59**,** 253-9.
STEMLER, A. 1993. An assay for carbonic anhydrase activity and reactions that produce radiolabeled gases or small uncharged molecules. *Anal Biochem,* 210**,** 328-31.
STRAUBINGER, R. M., PAPAHADJOPOULOS, D. & HONG, K. L. 1990. Endocytosis and intracellular fate of liposomes using pyranine as a probe. *Biochemistry,* 29**,** 4929-39.
SUPURAN, C. T. & SCOZZAFAVA, A. 2002. Applications of carbonic anhydrase inhibitors and activators in therapy. *Expert Opinion on Therapeutic Patents,* 12**,** 217-242.
SUPURAN, C. T., SCOZZAFAVA, A. & CASINI, A. 2003. Carbonic anhydrase inhibitors. *Med Res Rev,* 23**,** 146-89.
SUPURAN, C. T., SCOZZAFAVA, A. & CONWAY, J. 2005. Carbonic Anhydrase: its inhibitors and activators. *In:* SMITH, J. T. & SIMONS, C. (eds.). MA: Taylor and Francis.
THOMPSON, R. B. & JONES, E. R. 1993. Enzyme-based fiber optic zinc biosensor. *Analytical Chemistry,* 65**,** 730-734.
VERCHÈRE, A., BROUTIN, I. & PICARD, M. 2012. Photo-induced proton gradients for the *in vitro* investigation of bacterial efflux pumps. *Sci. Rep.,* 2.
VERPOORTE, J. A., MEHTA, S. & EDSALL, J. T. 1967. Esterase activities of human carbonic anhydrases B and C. *J Biol Chem,* 242**,** 4221-9.
WILBUR, K. M. & ANDERSON, N. G. 1948. ELECTROMETRIC AND COLORIMETRIC DETERMINATION OF CARBONIC ANHYDRASE. *Journal of Biological Chemistry,* 176**,** 147-154.
XUE, Y., LILJAS, A., JONSSON, B. H. & LINDSKOG, S. 1993. Structural analysis of the zinc OH^--Thr-199-Glu-106 hydrogen-bond network in human carbonic anhydrase II. *Proteins,* 17**,** 93-106.
ZHU, H., DERKSEN, R., KRAUSE, C., FOX, R., BRAZEE, R. & OZKAN, H. 2005. Fluorescent Intensity of Dye Solutions under Different pH Conditions. *Journal of ASTM International,* 2.

Investigating the effect of CA1 in mammalian cells by transient expression

Introduction

Effect of CA1 expression on cell survival

The physiological role of CA has been investigated for the past 80 years since its discovery in 1932 (Maren, 1967, Supuran et al., 2003, Chegwidden and Carter, 2000, Supuran, 2011). Its low activity relative to CA2 as well as it being strongly inhibited under physiological levels of chloride ions have cast questions regarding CA1's physiological importance in human (Chapman and Maren, 1978, Kendall and Tashian, 1977, Maren et al., 1976). CA1 is mainly expressed in the erythrocytes, kidney tubule cells, colon epithelial cells and sub-epithelail capillaries along the gastrointestinal tract (Supuran et al., 2003, Chegwidden and Carter, 2000, Parkkila et al., 1994, Lonnerholm et al., 1985). Although the role of CA1 in erythrocytes is unknown, it has been suggested that CA1 is involved in the ion change involving H^+ and HCO_3^- and luminal acidification and alkalinization in the kidney and colon cells, respectively (Parkkila etal., 1994, Chegwidden and Carter, 2000, Lonnerholm et al., 1985). However, the physiological role of CA1 has not been investigated in-depth with only a few expression studies at present which do not definitively address the physiological role of CA1 in cells.

CA1 has been implicated in a range of pathological diseases involving various tissues in human other than the cells mentioned above that has shown to express CA1 (Parkkila et al., 1994, Maren, 1967, Lonnerholm et al., 1985, Nigro et al., 2015, Peng et al., 2012, Takakura et al., 2012, Zheng et al., 2012, Torella et al., 2014). Most of the studies used proteomic and immunohistochemical approaches that have found irregular CA1 expression levels in diseased

tissues; however, these studies have not addressed how changes in CA1 expression levels affect cell survival. Due to the observations show that CA1 expression can be significantly elevated in one disease and reduced in another as well as a lack of cell and animal studies make it difficult to conclude whether CA1 is protective or toxic in cells.

Measuring CA1-induced cell viability changes

Effects of expression of other CA isoforms on cell viability have been studied using the tetrozolium salt MTT (monotetrozolium salts) assay as well as its more updated version – the WST (water soluble tetrozolium salt) assay (Kaluzová et al., 2004, Cianchi et al., 2010, Marques et al., 2010, Chang et al., 2012). These studies have been used to determine the effects of carbonic anhydrase inhibitors in cells expressing CA proteins (CA1, CA7, CA9, and CA12). The tetrazolium assays are colorimetric measurement of the activities of cellular metabolic enzymes such as NAD(P)H-dependent oxidoreductases and dehydrogenases (Mosmann, 1983, Berridge et al., 2005). These enzymes (along with other reported oxidases, peroxidases and dehydrogenases in the cell) reduce the weakly colored tetrozolium salts into the brightly colored formazan products which can be detected spectrophotometrically.

Microplate tetrazolium assays have been used widely to measure cell viability since they were first used in 1983 (Mosmann, 1983). The assays are able to measure both acute (hours) and long-term (days) effects on cell viability by the application of a chemical agent or protein expression. Previously, MTT formazan crystals needed to be solubilized prior to the spectrophotometric analysis on microplate readers. However, the development of water

soluble tetrazolium salts such as the most widely used WST8 eliminates this problem. In addition WST8 is more stable in the presence of its intermediate electron acceptors that facilitate the dye reduction (Berridge et al., 2005).

Aim of the study

There is an overall lack of studies observing the effects of CA expression in cells which either express endogenous CA or not despite numerous associations between changes in CA expression and disease. Moreover, many proteomic and histochemical studies showed elevated or reduced levels of CA1 expression in diseased tissues, but there have been few studies focusing on the effect of CA1 expression in tissues, which partly can be attributed to its relative slow enzyme activity and less ubiquitous tissue expression than the more studied CA2 isoform.

Recent preliminary results (Figure 3.1, via personal communication with Dr. Liu and unpublished data) have demonstrated that in the spinal cord protein extracts from sporadic ALS patients the expression of CA1 is higher than that of the controls using western blotting analysis; on the other hand, expression of SOD1 protein is unchanged, which is anticipated as SOD1 expression has not been linked to sporadic ALS. However, the physiological importance of this finding is not clear: whether the increase of CA1 indicates itself being the cause of motor neuron damage or acts as a compensatory protection to the damaged neurons, or it is an epiphenomenon from other pathways associated with the motor neuron damage. The purpose of this study is to observe whether CA1 expression has any beneficial or toxic effect on cellular viability using the WST8 assay.

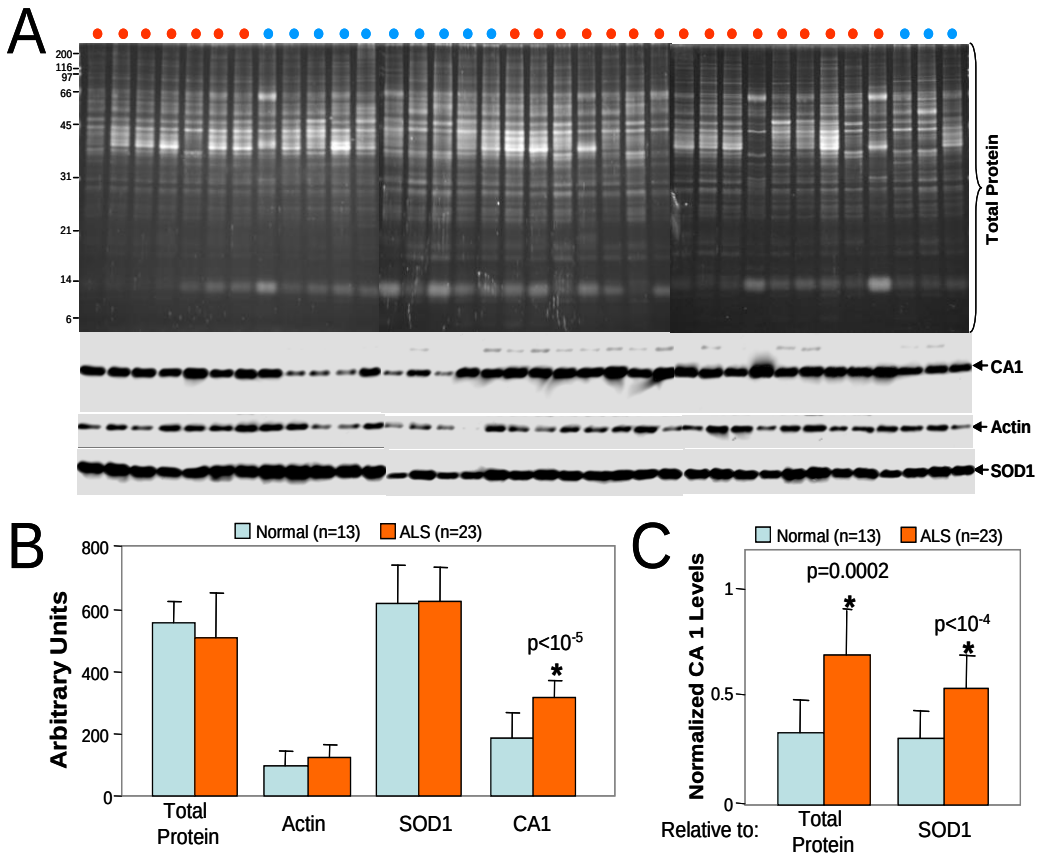

Figure 3.1. The CA1 protein levels are significantly increased in ALS spinal cord. Spinal cord proteins from normal and ALS subjects were prepared as previously described (Gruzman et al., 2007). Two sets of SDS/PAGE gels were prepared. In one set, a total of 5mg of proteins were loaded for each lane for Western analyses using antibodies towards CA1 (Rockland), actin (Sigma, A2066), and SOD1 (Stressgen, SOD-100). In another set, a total of 1 µg of proteins were loaded for each lane for SYPRO-staining for quantification of the total amount of proteins loaded for each sample. For quantitative Western analysis, the ECF substrate (GE Healthcare) was used to generate a fluorescent signal that can be captured using the Typhoon phosphoImager (Amersham). (***A***) Images of SYPRO-stained gels for total protein and Western blots for CA1, actin, and SOD1 proteins. Blue and red dots above the SYPRO image indicate normal and ALS samples, respectively. (***B***) ImageQuan software was used to quantify the intensities of antibody-generated signals for actin, SOD1 and CA1 as well as the total amount of proteins. (***C***) CA1 protein levels are presented after normalizations to either the total amount of proteins or the SOD1 Western signal. The results shown in this figure is through personal communication with Dr. Jian Liu and is unpublished data

Materials and Methods

Cell culture

COS7 (African green monkey kidney fibroblast-like cells), MCF-7 (human breast cancer cells), HEK293 (human embryonic kidney cells) were maintained at 37^{o}C and 5% carbon dioxide in 75cm^{2} flasks. The cells were grown in Dulbecco's Modified Medium containing 1% L-Glutamine, 1% Penicillin-Streptomycin (100U/ml and 100mg/ml, respectively) and 10% heat-inactivated fetal bovine serum. For passaging, the cells were detached from the cell culture flask by washing with phosphate-buffered saline (PBS) and brief incubation with trypsine (0.5g/L)/EDTA (0.2g/L) (Invitrogen). The cells were passaged every 3-4 days.

Transient transfection of human *CA1* into mammalian cells

Transient transfection experiments were done using Lipofectamine 2000 (Invitrogen). 0.5x10^{4} cells were seeded per well in 96 well plates 36-40hrs prior transfection. Lipofectamine was incubated with Opti-Mem I reduced serum media (Invitrogen) for 5 minutes at room temperature. 0.2μg of plasmid DNA were incubated with the Lipofectamine/Opti-Mem mixture for 20mins at room temperature before adding to the seeded cells in 100μl of growth media per well of cells in 96 well plates. Cell medium containing the transfection reagents were replaced with fresh medium 4hrs post transfection.

Cell viability via WST8 assay

Water Soluble Tetraolium-8 (WST8) assay was used for analyzing cell viability. Thirty six hours post transfection, the WST8 reagent are added to the cells according to the

manufacturer's instructions by using a multi-channel pipette to add 10µl of the WST8 reagent per well of cells in a 96 well plate containing 100µl of media per well (Dojindo Laboratories, Japan). After 2hrs incubation at 37^{o}C and 5% CO_2, absorbance readings at 450nm wavelength were read on a microplate reader (Biotek, Canada).

Western blot analysis

Immediately after WST8 experiments were done, COS7, HEK293 and MCF7 cells were lysed using 1X loading dye containing 5% beta-mercaptoethanol. Proteins were collected by centrifuging the lysed cell samples at 10,000G for 30mins at 4^{o}C and removing the supernatant. 30ul of the protein supernatants were loaded onto 12% SDS-Polyacrylamide for gel electrophoresis, which ran at 100 Volts for 120mins, and then the proteins were transferred onto nitrocellulose membranes. Membranes were blocked with 5% milk solution (skimmed milk powder in PBS solution with 0.05% Tween-20 added (Sigma)). Membranes were then incubated with primary antibodies: rabbit monoclonal anti-human/mouse CA1 antibody (#3567-1, Epitomics) for detecting CA1 expression. Membranes were then incubated with donkey anti-rabbit fluorescent secondary antibody (#9263223, Li-Cor Bioscience, Nebraska). Membranes were developed using the Odyssey Infra-red imager (Li-Cor Bioscience, Nebraska).

Results

Effect of transient CA1 expression in COS7 cell line

Wild-type CA1 and Glu106Ile mutant were transiently transfected in COS7 cells and cell viabilities was examined using the WST8 assay 36hrs post *CA1* transfection and compared to cells transfected with the vector-only control. In three independent experiments, the *CA1*-transfected cells have shown CA1 protein expression (and no endogenous expression of CA1) 36hrs post transfection (Figure 3.2a). There was a ~5% decrease in the WST8 reading in the samples expressing wild-type CA1 and ~4% decrease in the Glu106Ile samples compared to the vector control; however, these changes are not statically significant (Figure 3.2b).

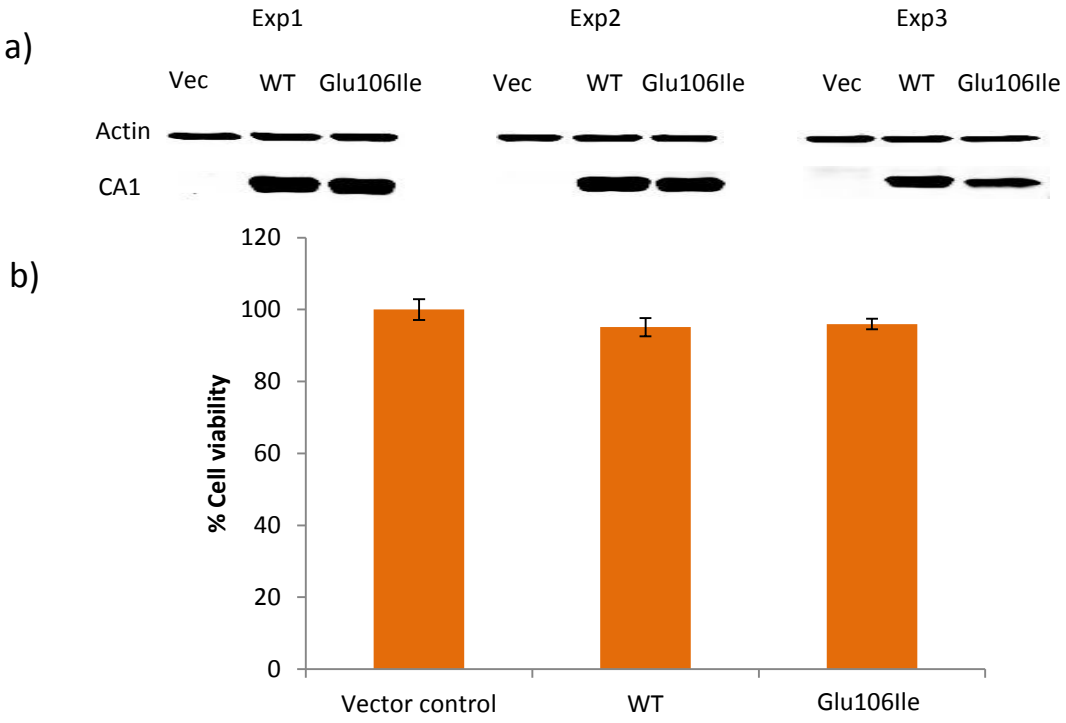

Figure 3.2. Transient expression of CA1 does not change cell viability in COS7 cells. 36hrs post human wild-type and Glu106Ile *CA1* transfection in COS7 cells, (a) whole cell proteins were extracted and the cells show wild-type (WT)CA1 protein expression in western blot analysis after WST8 analysis have been carried out in the cells (b) WST8 results showing percentage cell viabilities relative to the vector control 36 hrs post transfection. Vec = Vector control, protein expression of all three independent experiments are shown. Six replicates per sample in each experiment were used. Ws8 results comes from the averages combined three experiments, error bars are the standard deviation of the sample data.

Effect of transient CA1 expression in HEK293 cell line

Human wild-type *CA1* was transfected in HEK293 cells and its cell viability was examined using the WST8 assay 36hrs post *CA1* transfection. In all of the three independent experiments, the *CA1* transfected cells have shown CA1 protein expression (and no endogenous expression of CA1) 36hrs post transfection (Figure 3.3a). There was a ~6% decrease in the WST8 reading in the samples expressing CA1; however, this change is not statically significant (Figure 3.3b).

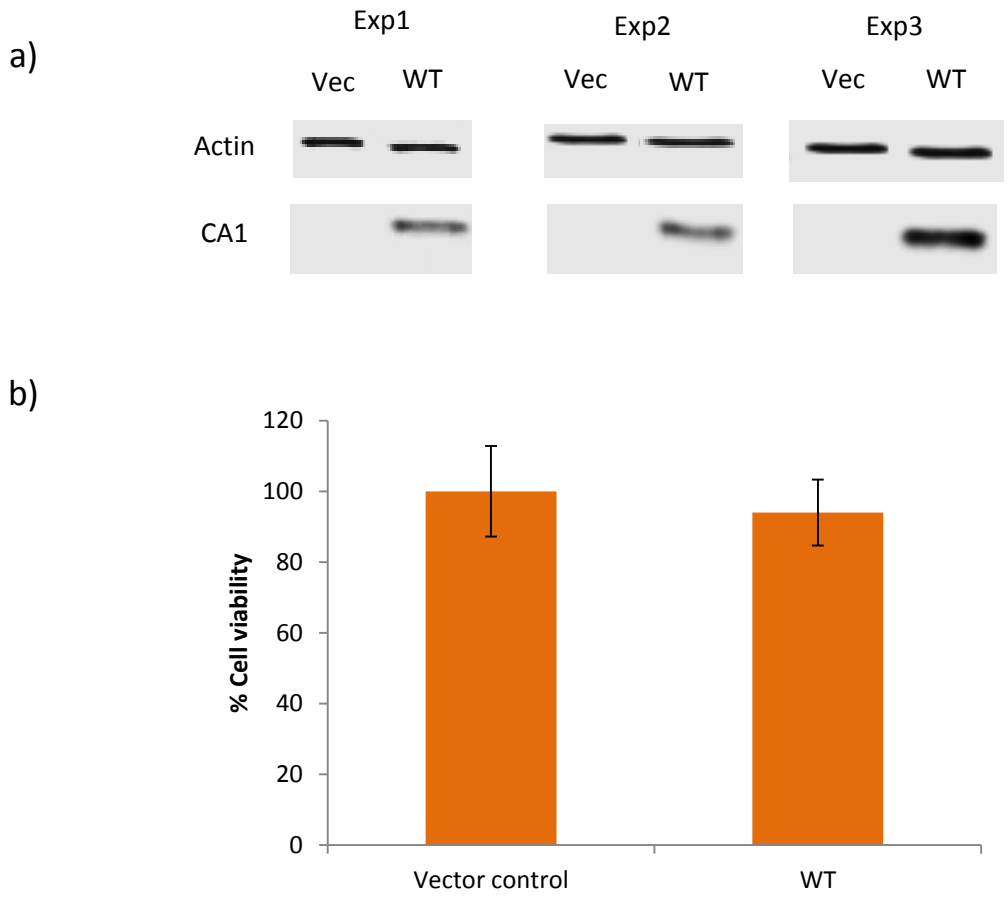

Figure 3.3. Transient expression of CA1 does not change cell viability in HEK293 cells. 36hrs post human wild-type *CA1* transfection in COS7 cells, (a) whole cell proteins were extracted and the cells show CA1 protein expression in western blot analysis after WST8 analysis have been carried out in the cells (b) WST8 results showing percentage cell viabilities relative to the vector control 36hrs post transfection. Vec = Vector control, protein expression of all three independent experiments are shown. Six replicates per sample in each experiment were used. WST8 results comes from the averages combined three experiments, error bars are the standard deviation of the sample data.

Effect of transient CA1 expression in MCF7 cell line

Human wild-type *CA1* was transfected in MCF7 cells and its cell viability was examined using the WST8 assay 36hrs post *CA1* transfection. The *CA1* transfected cells have shown CA1 protein expression (and no endogenous expression of CA1) 36hrs post transfection (Figure 3.4a) There was a ~4.5% decrease in the WST8 reading in the samples expressing CA1; however, this change is not statically significant (Figure 3.4b).

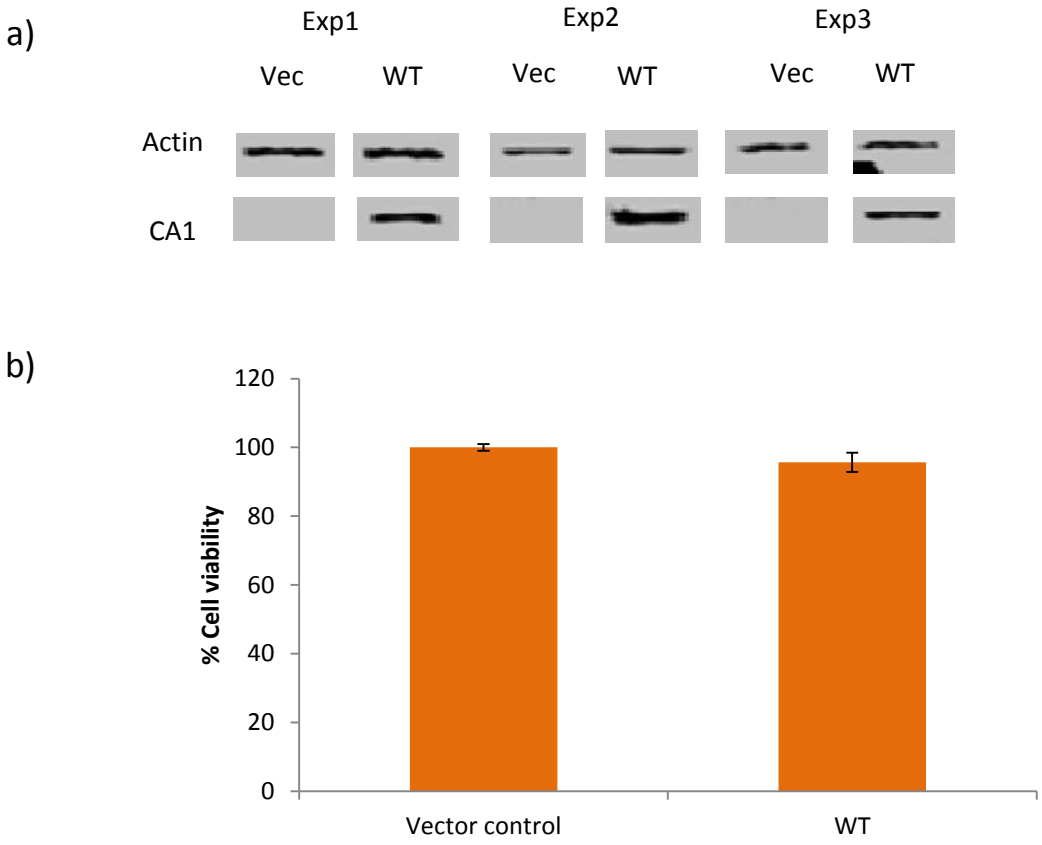

Figure 3.4. Transient expression of CA1 does not change cell viability in MCF7 cells. 36hrs post human wild-type *CA1* transfection in COS7 cells, (a) whole cell proteins were extracted and the cells show CA1 protein expression in western blot analysis after WST8 analysis have been carried out in the cells (b) WST8 results showing percentage cell viabilities relative to the vector control 36 hrs post transfection. Vec = Vector control, protein expression of all three independent experiments are shown. Six replicates per sample in each experiment were used. WST8 results comes from the averages combined three experiments, error bars are the standard deviation of the sample data.

Discussion

Possible explanations for non-significant changes due to CA1 expression

The results here have shown that while overall the cell viabilities have all decreased in the cells expressing CA1, the changes were not statistically significant. The possible explanations for this result can include: (but not exclusive to) 1) CA1 expression does not cause cell viability changes; 2) the levels of CA1 expressions in the cell lines are insufficient to cause cell viability changes; 3) 36hr time point is not optimal to see changes in cell viability.

Regarding the first possibility, it is certainly possible that increase in transient CA1 expression do not cause cellular viability changes. This is consistent with the observation from another study using a human osteosarcoma cell line (Chang et al., 2012). But on addition of a high level of concentration of acetazolamide (with the addition of the osteogenic media), a CA inhibitor which CA1 is relatively sensitive to, reduced the cell viabilities (Chang et al., 2012, Supuran et al., 2003). However, the addition of acetazolamide can inhibit other CA isoforms in the Saos-2 osteosarcoma cell line (which also endogenously expresses CA2 and CA9) (Müller et al., 2013). Furthermore, this study used the osteogenic media to induce bio-mineralization. With its extraneous effects that could increase CA2 and CA9 expressions may dampen CA1-associated changes in the cells. Currently, there is no data using the same approach as this study here.

With regards to the second and the third possibilities, they are the obvious limitations of the transient protein expression approach. Using cell line which has the *CA1* gene stably integrated into its genome and its protein expression is induced with the application of

doxycycline allows prolonged expression of CA1 to observe its effects on cellular viability within a longer time frame (Gossen and Bujard, 1992, Pluta et al., 2005, Freundlieb et al., 1999). Furthermore, the levels of CA1 expression should not decrease over time as is the case with transient expressions; with the addition of using virus particles to transduce cell lines with vectors containing *CA1* allows a higher percentage of cells to express CA1 proteins, thereby potentially increasing the amount of CA1 in the cells. However, even with higher and prolonged CA1 expressions they may not have any significant effect in cells. As results demonstrated from the Chang *et al* study mentioned above, the application of the osteogenic media increased CA1 protein expression by approximately 5-fold compared to the endogenous expression. In addition, the study observed the cell viability changes in these cells for 9 days, there was still no significant changes in the elevated CA1 expressing cells. On the other hand, the study differs from a pure CA1 expression study as they did not examine whether the expression of other CA isoforms have also been increased along with CA1 which may modify any CA1 associated effects as well as the additional cellular effects of the osteogenic media may have other than on CA expressions which included upregulation of other bio-mineralization genes (Chang et al., 2012).

Other isoforms of CA other than CA1 are also expressed in some of the cell lines used in this study. With regards to the MCF7 cell line, it expresses the CA2 and CA9 isoforms (Shareef et al., 2013, Kaluzová et al., 2004, Mallory et al., 2005). The HEK293 cell line has found to only expressing the CA2 isoform (Lankat-Buttgereit et al., 2004). No report in the literature was found that indicated COS7 cells endogenously express any CA isoforms. Expression of CA2 was tested in COS7 cells in this study using a human blood sample positive control, results show that as expected CA2 was detected strongly in human blood, however, it was not present in COS7

cells (the CA2 in the monkey species shares homology with the human CA2 epitope recognized by the antibody used (#EPR5195, Abcam, Cambridge, UK) (Supplementary figure). Due to its high levels of activity, the CA2 isoform may be the functioning CA in the cell lines maintaining the cellular pH and viabilities (Maren, 1967, Supuran et al, 2003). When a relatively low activity form of CA such as CA1 is transiently expressed in the cells, any effect associated with CA1 expression may not be as pronounced in CA2 expressing cells due to most of the functional activity has been taken over by CA2 (i.e. the HEK293 and MCF7 cell lines) as opposed to the non-CA2 expressing cells (i.e. the COS7 cell line). Although there are no significant differences in the cell viability changes between the three cell lines with increased CA1 expression, the reasons outlined above (i.e. prolonged expression CA1, increase in level of CA1 expression) calls for further investigation.

Discussion of the study approach

This study has applied the tetrazolium assay to examine the cell viabilities. It is the most widely used assay with high sensitivity for measuring cell viability changes (Berridge et al., 2005). Although using WST8 tetrazolium as opposed to the insoluble MTT salts has eliminated the limitations of solubilizing the formazan salts in the assay, there are some fundamental differences in the reduction process of these salts. Where the water soluble salts (including WST8) are reduced via NADH derived from the mitochondria, the MTT salts can be reduced in the cytoplasm, in the endosome/lysosome as well as in the mitochondria through other enzymes other than NADH (Liu et al., 1997). However, this is unlikely to mean that MTT assays

are more accurate than its water soluble derivatives; in fact, the opposite may be true. One reason is that monitoring cell viabilities using both MTT and WST salts are dependent on NADH being the responsible factor during reduction; therefore any additional factors may be irrelevant (Berridge and Tan, 1993). Furthermore, it has been found using the WST salts are more sensitive compared to the MTT assay (including other popularly used tetrazolium salts) tested in a variety of cell lines (Tominaga et al., 1999, Tiwari et al., 2015, Ginouves et al., 2014). Readings from the MTT assay has reported to be unstable causing it to be not as precise and accurate as using WST salts, possibly due to differences in the extent of solubilizing in the MTT assay during experimental handling and differences in the reagents used for solubilizing in different studies (Ginouves et al., 2014, van Tonder et al., 2015). The use of WST salts will eliminate these problems due to the lack of need for dissolving.

In summary, due to various factors as discussed above, these could diminish CA1-associated effects in this study such as insufficient levels and duration in CA1 expression leading to an absence of cell viabilities being observed. By using inducible CA1 stable cell lines and using different approaches in addition to WST8 to measure cell viability changes, it is possible any CA1-associated changes will be detected in a further study.

References:

BERRIDGE, M. V., HERST, P. M. & TAN, A. S. 2005. Tetrazolium dyes as tools in cell biology: new insights into their cellular reduction. *Biotechnol Annu Rev,* 11**,** 127-52.

BERRIDGE, M. V. & TAN, A. S. 1993. Characterization of the cellular reduction of 3-(4,5-dimethylthiazol-2-yl)-2,5-diphenyltetrazolium bromide (MTT): subcellular localization, substrate dependence, and involvement of mitochondrial electron transport in MTT reduction. *Arch Biochem Biophys,* 303**,** 474-82.

CHANG, X., HAN, J., ZHAO, Y., YAN, X., SUN, S. & CUI, Y. 2010. Increased expression of carbonic anhydrase I in the synovium of patients with ankylosing spondylitis. *BMC Musculoskeletal Disorders,* 11**,** 279.

CHANG, X., ZHENG, Y., YANG, Q., WANG, L., PAN, J., XIA, Y., YAN, X. & HAN, J. 2012. Carbonic anhydrase I (CA1) is involved in the process of bone formation and is susceptible to ankylosing spondylitis. *Arthritis Res Ther,* 14.

CHAPMAN, S. K. & MAREN, T. H. 1978. A search for the function of human carbonic anhydrase B. *Biochimica et Biophysica Acta (BBA) - Enzymology,* 527**,** 272-276.

CHEGWIDDEN, W. R. & CARTER, N. D. 2000. Introduction to the carbonic anhydrases. *Exs,* 90**,** 14-28.

CIANCHI, F., VINCI, M. C., SUPURAN, C. T., PERUZZI, B., DE GIULI, P., FASOLIS, G., PERIGLI, G., PASTOREKOVA, S., PAPUCCI, L., PINI, A., MASINI, E. & PUCCETTI, L. 2010. Selective Inhibition of Carbonic Anhydrase IX Decreases Cell Proliferation and Induces Ceramide-Mediated Apoptosis in Human Cancer Cells. *Journal of Pharmacology and Experimental Therapeutics,* 334**,** 710-719.

FONTI, R., LATELLA, G., CAPRILLI, R., FRIERI, G., MARCHEGGIANO, A. & SAMBUY, Y. 1998. Carbonic anhydrase I reduction in colonic mucosa of patients with active ulcerative colitis. *Dig Dis Sci,* 43**,** 2086-92.

FREUNDLIEB, S., SCHIRRA-MULLER, C. & BUJARD, H. 1999. A tetracycline controlled activation/repression system with increased potential for gene transfer into mammalian cells. *J Gene Med,* 1**,** 4-12.

GINOUVES, M., CARME, B., COUPPIE, P. & PREVOT, G. 2014. Comparison of Tetrazolium Salt Assays for Evaluation of Drug Activity against Leishmania spp. *Journal of Clinical Microbiology,* 52**,** 2131-2138.

GOSSEN, M. & BUJARD, H. 1992. Tight control of gene expression in mammalian cells by tetracycline-responsive promoters. *Proc Natl Acad Sci U S A,* 89**,** 5547-51.

KALUZOVÁ, M., KALUZ, S., LERMAN, M. I. & STANBRIDGE, E. J. 2004. DNA Damage Is a Prerequisite for p53-Mediated Proteasomal Degradation of HIF-1α in Hypoxic Cells and Downregulation of the Hypoxia Marker Carbonic Anhydrase IX. *Molecular and Cellular Biology,* 24**,** 5757-5766.

KENDALL, A. G. & TASHIAN, R. E. 1977. Erythrocyte carbonic anhydrase I: inherited deficiency in humans. *Science,* 197**,** 471-2.

LANKAT-BUTTGEREIT, B., GREGEL, C., KNOLLE, A., HASILIK, A., ARNOLD, R. & GOKE, R. 2004. Pdcd4 inhibits growth of tumor cells by suppression of carbonic anhydrase type II. *Mol Cell Endocrinol,* 214**,** 149-53.

LIU, Y., PETERSON, D. A., KIMURA, H. & SCHUBERT, D. 1997. Mechanism of cellular 3-(4,5-dimethylthiazol-2-yl)-2,5-diphenyltetrazolium bromide (MTT) reduction. *J Neurochem,* 69**,** 581-93.

LONNERHOLM, G., SELKING, O. & WISTRAND, P. J. 1985. Amount and distribution of carbonic anhydrases CA I and CA II in the gastrointestinal tract. *Gastroenterology,* 88**,** 1151-61.

MALLORY, J. C., CRUDDEN, G., OLIVA, A., SAUNDERS, C., STROMBERG, A. & CRAVEN, R. J. 2005. A Novel Group of Genes Regulates Susceptibility to Antineoplastic Drugs in Highly Tumorigenic Breast Cancer Cells. *Molecular Pharmacology,* 68**,** 1747-1756.

MAREN, T. H. 1967. Carbonic anhydrase: chemistry, physiology, and inhibition. *Physiol Rev,* 47**,** 595-781.

MAREN, T. H., RAYBURN, C. S. & LIDDELL, N. E. 1976. Inhibition by anions of human red cell carbonic anhydrase B: physiological and biochemical implications. *Science,* 191**,** 469-72.

MARQUES, S. M., ENYEDY, É. A., SUPURAN, C. T., KRUPENKO, N. I., KRUPENKO, S. A. & AMÉLIA SANTOS, M. 2010. Pteridine–sulfonamide conjugates as dual inhibitors of carbonic anhydrases and dihydrofolate reductase with potential antitumor activity. *Bioorganic & Medicinal Chemistry,* 18**,** 5081-5089.

MOSMANN, T. 1983. Rapid colorimetric assay for cellular growth and survival: application to proliferation and cytotoxicity assays. *J Immunol Methods,* 65**,** 55-63.

MÜLLER, W. E. G., SCHRÖDER, H. C., SCHLOSSMACHER, U., GREBENJUK, V. A., USHIJIMA, H. & WANG, X. 2013. Induction of carbonic anhydrase in SaOS-2 cells, exposed to bicarbonate and consequences for calcium phosphate crystal formation. *Biomaterials,* 34**,** 8671-8680.

PARKKILA, S. 2000. An overview of the distribution and function of carbonic anhydrase in mammals. *Exs,* 90**,** 79-93.

PARKKILA, S., PARKKILA, A. K., JUVONEN, T. & RAJANIEMI, H. 1994. Distribution of the carbonic anhydrase isoenzymes I, II, and VI in the human alimentary tract. *Gut,* 35**,** 646-650.

PENG, Y., LI, X., WU, M., YANG, J., LIU, M., ZHANG, W., XIANG, B., WANG, X., LI, G. & SHEN, S. 2012. New prognosis biomarkers identified by dynamic proteomic analysis of colorectal cancer. *Mol Biosyst,* 8**,** 3077-88.

PLUTA, K., LUCE, M. J., BAO, L., AGHA-MOHAMMADI, S. & REISER, J. 2005. Tight control of transgene expression by lentivirus vectors containing second-generation tetracycline-responsive promoters. *J Gene Med,* 7**,** 803-17.

SELLIN, J. H. & DESOIGNIE, R. 1990. Short-chain fatty acid absorption in rabbit colon *in vitro*. *Gastroenterology,* 99**,** 676-83.

SHAREEF, M. M., UDAYAKUMAR, T. S., SINHA, V. K., SALEEM, S. M. & GRIGGS, W. W. 2013. Interaction of HIF-1α and Notch3 Is Required for the Expression of Carbonic Anhydrase 9 in Breast Carcinoma Cells. *Genes & Cancer*.

SLY, W. S. & HU, P. Y. 1995. Human carbonic anhydrases and carbonic anhydrase deficiencies. *Annu Rev Biochem,* 64**,** 375-401.

SUPURAN, C. T. 2008. Carbonic anhydrases: novel therapeutic applications for inhibitors and activators. *Nat Rev Drug Discov,* 7**,** 168-181.

SUPURAN, C. T. 2011. Carbonic anhydrase inhibitors and activators for novel therapeutic applications. *Future Med Chem,* 3**,** 1165-80.

SUPURAN, C. T., SCOZZAFAVA, A. & CASINI, A. 2003. Carbonic anhydrase inhibitors. *Med Res Rev,* 23**,** 146-89.

TAKAKURA, M., YOKOMIZO, A., TANAKA, Y., KOBAYASHI, M., JUNG, G., BANNO, M., SAKUMA, T., IMADA, K., ODA, Y., KAMITA, M., HONDA, K., YAMADA, T., NAITO, S. & ONO, M. 2012. Carbonic anhydrase I as a new plasma biomarker for prostate cancer. *ISRN Oncol,* 768190**,** 19.

TIWARI, K., WAVDHANE, M., HAQUE, S., GOVENDER, T., KRUGER, H. G., MISHRA, M. K., CHANDRA, R. & TIWARI, D. 2015. A sensitive WST-8-based bioassay for PEGylated granulocyte colony stimulating factor using the NFS-60 cell line. *Pharmaceutical Biology,* 53**,** 849-854.

TOMINAGA, H., ISHIYAMA, M., OHSETO, F., SASAMOTO, K., HAMAMOTO, T., SUZUKI, K. & WATANABE, M. 1999. A water-soluble tetrazolium salt useful for colorimetric cell viability assay. *Analytical Communications,* 36**,** 47-50.

TORELLA, D., ELLISON, G. M., TORELLA, M., VICINANZA, C., AQUILA, I., IACONETTI, C., SCALISE, M., MARINO, F., HENNING, B. J., LEWIS, F. C., GARERI, C., LASCAR, N., CUDA, G., SALVATORE, T., NAPPI, G., INDOLFI, C., TORELLA, R., COZZOLINO, D. & SASSO, F. C. 2014. Carbonic anhydrase activation is associated with worsened pathological remodeling in human ischemic diabetic cardiomyopathy. *J Am Heart Assoc,* 3**,** 000434.

VAN TONDER, A., JOUBERT, A. M. & CROMARTY, A. D. 2015. Limitations of the 3-(4,5-dimethylthiazol-2-yl)-2,5-diphenyl-2H-tetrazolium bromide (MTT) assay when compared to three commonly used cell enumeration assays. *BMC Res Notes,* 8**,** 015-1000.

ZHENG, Y., WANG, L., ZHANG, W., XU, H. & CHANG, X. 2012. Transgenic mice over-expressing carbonic anhydrase I showed aggravated joint inflammation and tissue destruction. *BMC Musculoskelet Disord,* 13**,** 1471-2474.

Investigating the effect of CA1 in mammalian cells by induced stable expression

Introduction

CA isoforms and cell viability

Studying the role of CA in cellular apoptosis and proliferation has incorporated the use of cancer cells, where CA9 and CA12 have been the focus to develop prognostic markers and therapeutic agents for cancer (Chiche et al., 2009, Pastorekova et al., 2008, Gondi et al., 2013, Cianchi et al., 2010a). Other CA members have also been investigated including the role of CA3 in hydrogen peroxide-induced apoptosis, CA7 during oxidative stress damage, the mitochondrion CA5 during glucose mediated toxicity (Del Giudice et al., 2013, Raisanen et al., 1999, Patrick et al., 2015, Roy et al., 2010).

CA and optimization of intracellular pH

CA are important enzymes in the reversible hydration of CO_2 being converted into HCO_3^- and protons. Since this reaction involves the powerful CO_2/HCO_3^- buffer system in cells, CA enzymes play a critical role in maintaining the optimal pH and to dissipate clusters of concentrated pH gradients (Swietach et al., 2010, Boron, 2004). The protons are important signaling molecules in regulating cellular processes, however their levels need to be regulated (Highstein et al., 2014, Isom et al., 2013, Chiche et al., 2009). Since the physiological intracellular pH is slightly alkaline (around 7.3-7.4), cells have to deal with excessive protons produced from metabolic activities such as generation of ATP, oxidative phosphorylation, and

the uptake of protons via the transmembrane transporters (Swietach et al., 2010, Boron, 2004). pH regulation is crucial in maintaining cellular viability as cellular growth is dependent on slightly alkaline environments (Matsuyama et al., 2000, Gillies et al., 1990, Gillies et al., 1992).

To maintain the optimal intracellular pH levels, buffers are required to resist the intracellular pH changes (Boron, 2004, Roos and Boron, 1981). The CO_2/HCO_3^- buffer system forms the basis for the cellular buffering capacity to resist intracellular acidosis (Swietach et al., 2010, Swietach et al., 2007). As HCO_3^- are not permeable across the cell, this system is dependent upon the membrane transporters including the HCO_3^-/Na^+ and Cl^-/HCO_3^- co-transporters for HCO_3^- flux across the membrane barrier. The influx of HCO_3^- can react with intracellular protons forming CO_2 and H_2O thereby lowering intracellular pH; the reverse happens when the freely permeable CO_2 enters cells reacting with H_2O producing protons which decrease intracellular pH (Swietach et al., 2010, Boron, 2004). Without the catalysis of CA enzymes, the speed of buffering capacity will be limited by the slow kinetics of reversible CO_2 hydration hindering the pH regulatory mechanism.

CA1 and cell toxicity

One recent study showed that the increased CA1 protein level significantly induced apoptosis in human coronary endothelial cells, potentially exacerbating pathology seen in patients with diabetic cardiomyopathy (Torella et al., 2014). Another study has shown CA1 protein increased cerebral vessel leakage possibly due to vascular endothelial cell death by activating inflammatory pathways associated with CA1-induced alkalization (Gao et al., 2007).

One other study shows overexpression of CA1 causes significant tissue destruction of cartilage and joint tissues in joints of CA1 transgenic mice (Zheng et al., 2012). Although the number of available studies is limited, the consensus is that CA1 proteins can directly or indirectly cause cell death.

Data presented in chapter three have shown transient expression of wild-type CA1 proteins did not affect cell viability at 36hrs post-transfection. Due to the probable limitations of using transient expression systems significant effects were not observed. Using an unregulated stable cell line with the *CA1* gene integrated into its genome to observe effects of longer period of CA1 expression was not feasible as no stable cell lines can be obtained probably due to the fact that cells eventually died because of CA1-related toxicity (data not shown). To circumvent the problem, an inducible expression system was used in which the CA1 expression can be switched "off" to bypass the toxicity to allow the establishment of the stable cell line. Conversely, CA1 expression can be switched "on" to observe its effects in cells. The inducible expression was achieved by a lentiviral expression vector in this study.

Using the lentiviral inducible expression system for studying CA1

The inducible lentiviral expression vector system contains two components required for gene expression. The first is the trans-activator rtTA3 (reverse tetracycline trans-activator 3) which binds to the second component, the tetracycline response element (TRE) (Shin et al., 2006, Takiguchi et al., 2013). The TRE is essentially a string of operators that are fused to the vector promoter which regulates gene expression. However, without rtTA3 binding to the TRE,

the promoter cannot be activated to turn “on” gene expression. This binding action requires the presence of a tetracycline-based antibiotic (such as doxycycline used in this study) to first activate rtTA3, this then allows rtTA3 to bind to TRE activating gene expression.

Based on previous studies, the hypothesis is that expression of CA1 is toxic to cells activating apoptotic pathways, therefore reducing cell viabilities (Torella et al., 2014, Guo et al., 2012). Thus, with the ability of the inducible lentiviral expression system to temporarily switch off protein expression to avoid CA1-associated toxicity during the setting up stage and allow the observation into the effects of CA1 expression on cell viability and apoptosis. To test this hypothesis, two mammalian cell lines (HEK293 and COS7) were used to stably integrate the *CA1* gene (wild-type as well as Glu106Ile and Thr199Val mutants *CA1*) into the genomes to observe changes to their cellular viabilities using the WST8 method and apoptotic markers of both cleaved PARP-1 and activated Caspase3.

Materials and methods

Cell culture

COS7 (African green monkey kidney fibroblast-like cells), HEK293 (human embryonic kidney cells) were maintained at 37^{o}C and 5% CO_2. The cells were grown in Dulbecco's Modified Medium containing 1% L-Glutamine, 1% Penicillin-Streptomycin (100U/ml and 100mg/ml, respectively) and 10% heat-inactivated fetal bovine serum.

Lentiviral stable cell line production

Lentiviral particles were first produced in HEK293T cells. The cells were seeded 16hrs in 6cm^2 dishes prior to transfection in DMEM, 10% heat-inactivated FBS, 0.1% Penicillin-streptomycin at 37^{o}C and 5% CO_2. At approximately 50% to 70% cell confluency 900ng of pSPAX2 (lentivirus packaging vector) and 100ng of VSV-g (lentivirus envelope vector) and 1µg of pTRIPZ-CA1 or pTRIPZ spez eGFP expression vectors (the lentivirus packaging/envelop as well as the expression vectors were kindly provided by Dr. Ferdinand Kappes) were transfected into the HEK293T cells using 6µl of Lipofectamine 2000 transfection reagent (#11668019, Life technologies, USA) under the manufacturer's instructions. 18hrs post-transfection, the cell media was replaced with media containing 30% heat-inactivated FBS (DMEM, 30% heated inactivated FBS, 1% Penicillin-streptomycin). Forty hours post-transfection media containing the lentiviral particles were harvested and filter through .45µm filter for collect viral supernatant. Cells were replenished with fresh media containing 30% heat-inactivated FBS.

COS7 and HEK293 cells were seeded 24hrs prior to virus transduction in 10cm dishes, when they reached 10% to 30% cell confluency the cells were transduced with the viral supernatant for 6hrs with 8µl/ml of Polybrene (#H9268, Sigma, USA) and then was changed to normal cell growth media after transduction and incubated at 37^{o}C and 5% CO_2. At 12hr time-point, the viral media from the HEK293T cells was harvested and filtered again and used to transduce HEK293 and COS7 cells for another 6hrs. At the 18hr time-point, the viral media was replaced with normal cell media and incubated for another 6hrs. At the 24hrs time-point, the transduced cells were selected with Puromycin Dihydrochloride (Bio Basic, Canada) using 1µg/ml for transduced HEK293 cells and 2µg/ml for transduced COS7 cells. After 2 weeks, pure stable cell lines were obtained from transduced cell surviving from the puromycin selection. After the stable cell lines have been obtained, the cells were maintained in the growth media containing 0.25µg/ml and 0.5µg/ml of puromycin for HEK293 and COS7 cells respectively.

To induce protein expression in the stable cell lines, 0.25µg/ml of doxycycline (#D9891, Sigma, St Louis, USA) (powder diluted in sterilized water) was added to the cellular media. eGFP protein expression in cells transduced with lentiviruses containing the eGFP expression vector were induced at 48hrs, 96hrs and 144hrs of protein expression, expression levels were checked using a Nikon Eclipse Ti fluorescence imaging microscope under the blue fluorescence light at 200x magnification using 20x objective with 10x ocular magnifications. Media containing doxycycline were replenished every 48hrs.

Immunofluorescence

The following steps were carried out at room temperature. Cells were washed once with PBS and then fixed in 4% paraformaldehyde for 15mins. Cells were blocked in PBS buffer containing 1% Bovine Serum Albumin/ 0.3% Triton X-100 for 30mins before incubation with primary rabbit anti-CA1 antibody (#ab124976, Abcam, Cambridge, Massachusetts) diluted at 1:200 dilution in the blocking buffer for 1hr and Alexa Fluor 488 fluorophore (#ab150077, Abcam, Cambridge, Massachusetts) diluted in 1:200 in the blocking solution for 1hr. The cells were then washed with 1XPBS 3 times with 3-5mins incubation gently shaken on a plate shaker during each wash. The images were then taken using a Nikon Eclipse Ti imaging microscope under the blue fluorescence light at 200x magnification using 20x objective with 10x ocular magnifications.

Western blot analysis

Cells were lysed using 1X loading buffer (61.3mM Tris pH 8.0, 2% SDS, 10% glycerol, 0.0025% bromophenol blue, 2.5% β-mercaptoethanol) in 12 well plates. Proteins were collected in the supernatant by centrifuging the lysed cell samples at 10,000g for 30mins at 4^{o}C. Equal volumes of the protein were loaded onto 12% SDS-Polyacrylamide for gel electrophoresis. Proteins were transferred onto nitrocellulose membranes blocked with 5% milk solution (skimmed milk powder in PBS solution with 0.05% Tween-20) and then incubated with primary antibodies: rabbit monoclonal anti-human/mouse CA1 antibody (#ab124976, Abcam, Cambridge, Massachusetts) and human CA2 antibody (#EPR5195, Abcam, Cambridge, UK) and

anti-rabbit fluorescent secondary antibody (#9263223, Li-Cor Bioscience, Nebraska). Signals were visualized using the Odyssey Infra-red imager (Li-Cor Bioscience, Nebraska)

Cell viability assay

Cells were seeded in 96 well plates to carry out the assay for measuring cell viability using WST8 (Dojindo Laboratories, Japan). A total of 10µl of the WST8 reagent was added to each well with 100µl of the medium. After 2hrs incubation at 37^{o}C and 5% CO_2, absorbance readings at 450nm wavelength were read on a microplate reader (Biotek, Canada).

Flow cytometry analysis

Cells were trypsinized and pelleted by centrifugation at 500xG for 5mins. Cells were then re-suspended with PBS buffer containing 4% Paraformaldehyde at room temperature for 15mins. Cells were then pelleted and re-suspended in 90% methanol and 10% PBS solution and incubated at -20 ^{o}C for 30mins for cell permeabilization. Cells were then washed twice with freshly made PBS buffer containing 1% BSA. Cells were then blocked in the 1% BSA/PBS solution for 20mins at room temperature. After blocking, cells were washed with 1% BSA/PBS and then incubated with anti-Caspase-3-Alexa Fluor 647 (#560626, BD, San Diego, CA) or anti-PARP-1-Alexa Fluor 647 antibodies (#558710, BD, San Diego, CA). Fluorescence signals were collected in log mode using a FACSCalibur (BD, San Diego, CA) and data acquisition was done using the CellQuest Pro software (BD, San Diego, CA). Analysis of cell populations were performed on events gated according to forward light scatter/side scatter parameters.

Results

COS7 and HEK293 cells stably express eGFP and CA1 upon induction

COS7 and HEK293 cells stably expressing eGFP were made first by transducing the cells with lentiviruses which package the eGFP expression vector. 0.25μM of doxycycline was applied to the growth media to virus-transduced cells showing visible induced eGFP expression under fluorescent light. Figures 4.1 and 4.2 show eGFP expression can be seen in COS7 and HEK293 cells from 48hrs to 144hrs of protein expression (eGFP expression can be detected as early as 10-12 hours, data not shown). On the other hand, transduced cells without doxycycline induction showed no eGFP expression in the two figures shown.

Figure 4.3 shows wild-type, Glu106Ile and Thr199Val CA1 expressions were observed in both COS7 and HEK293 using 0.25μM of doxycycline to induce protein expressions for 96hrs. The figures show cells untransduced with lentiviruses (labelled as "untransduced") had no endogenous expression of CA1. Figure 4.3 also shows immunofluorescence assay results which confirm CA1 protein expression in HEK293 cells at 96hrs. In figure 4.3a, western analysis results showed a minor degree of leaky expression of Glu106Ile and Thr199Val CA1 in HEK293 cells, which was absent in COS7 in Figure 4.3b. Both Figure 4.3a and 4.3b show the levels of expression of wild-type and mutants CA1 were similar for both COS7 and HEK293 cells. Figure 4.3c shows similar degree of wild-type and mutants CA1 expressions in HEK293 cells at 96hrs were seen by immunofluorescent staining.

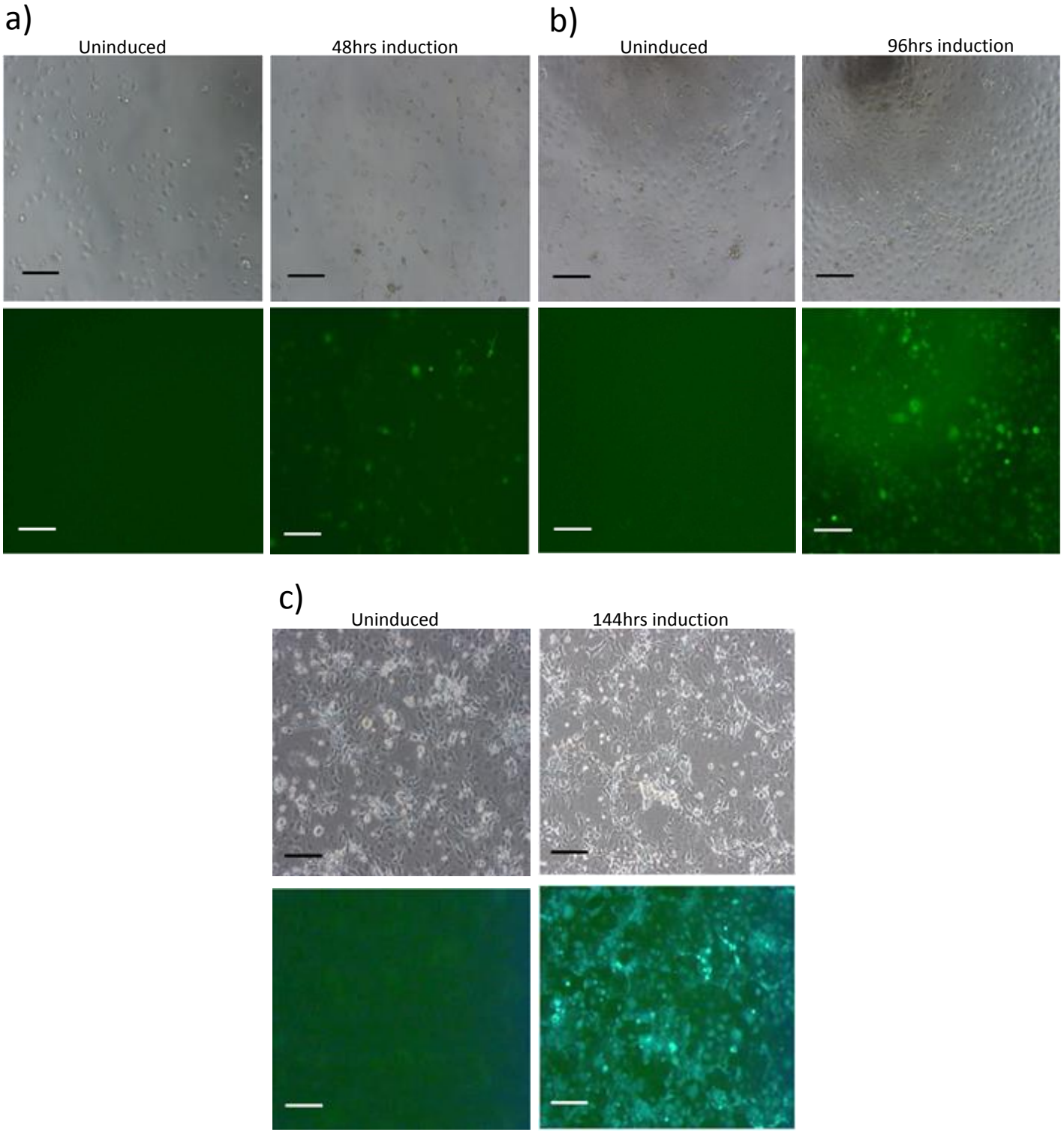

Figure 4.1. Transduced COS7 cells stably express eGFP. Green fluorescence showing eGFP expression was detected under white light blue fluorescence light in the presence of doxycycline for a) 48hrs, b) 96hrs and c) 144hrs. Cells transduced with eGFP vector lentivirus without doxycycline induction were used as comparative controls. Magnification = 200x. Scale bars = 50µm.

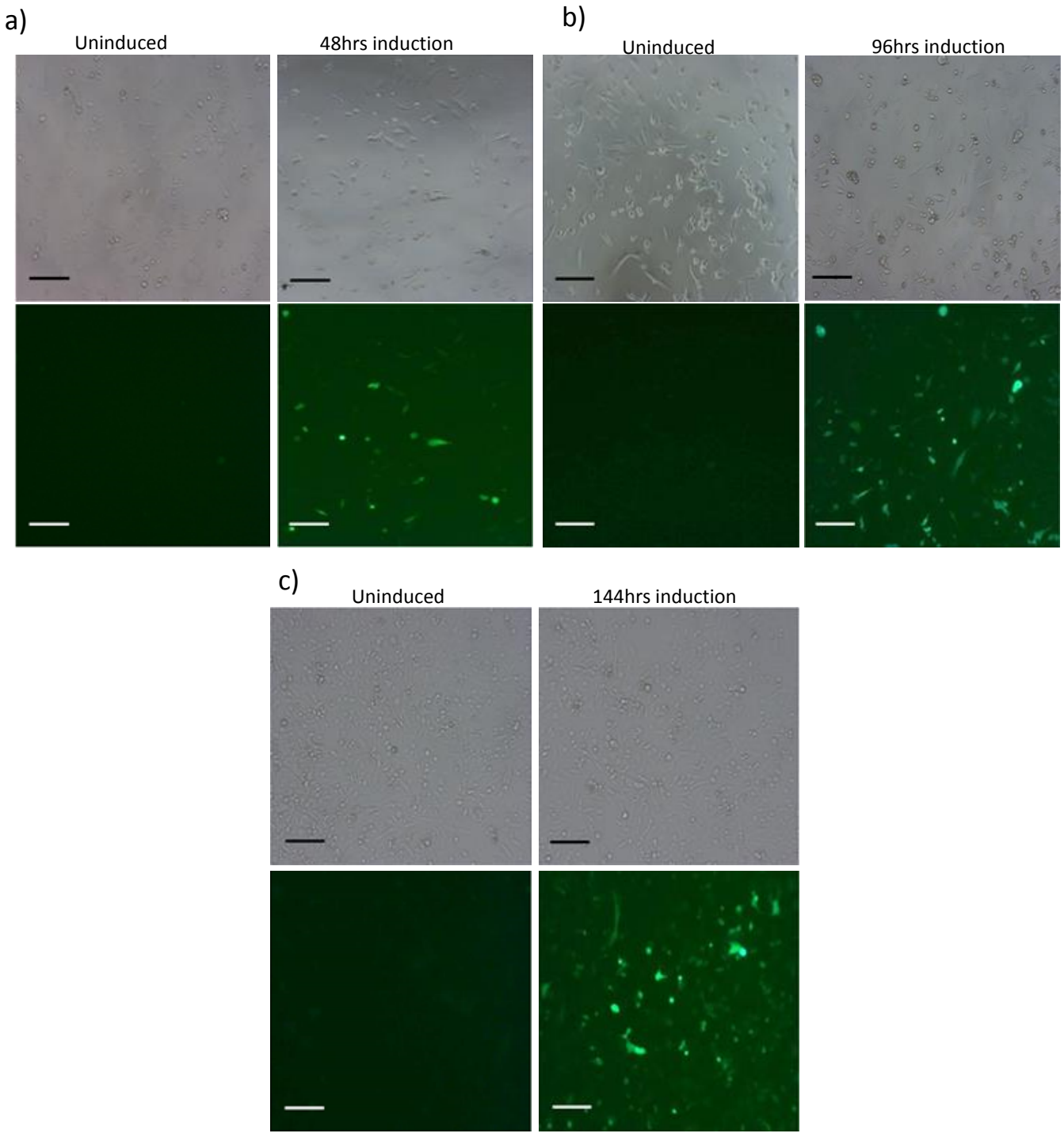

Figure 4.2. Transduced HEK293 cells stably express eGFP. Green fluorescence showing eGFP expression was detected under while light and blue fluorescence light in the presence of doxycycline for a) 48hrs, b) 96hrs and c) 144hrs. Cells transduced with eGFP vector lentivirus without doxycycline induction were used as comparative controls. Magnification = 200x. Scale bars = 50µm.

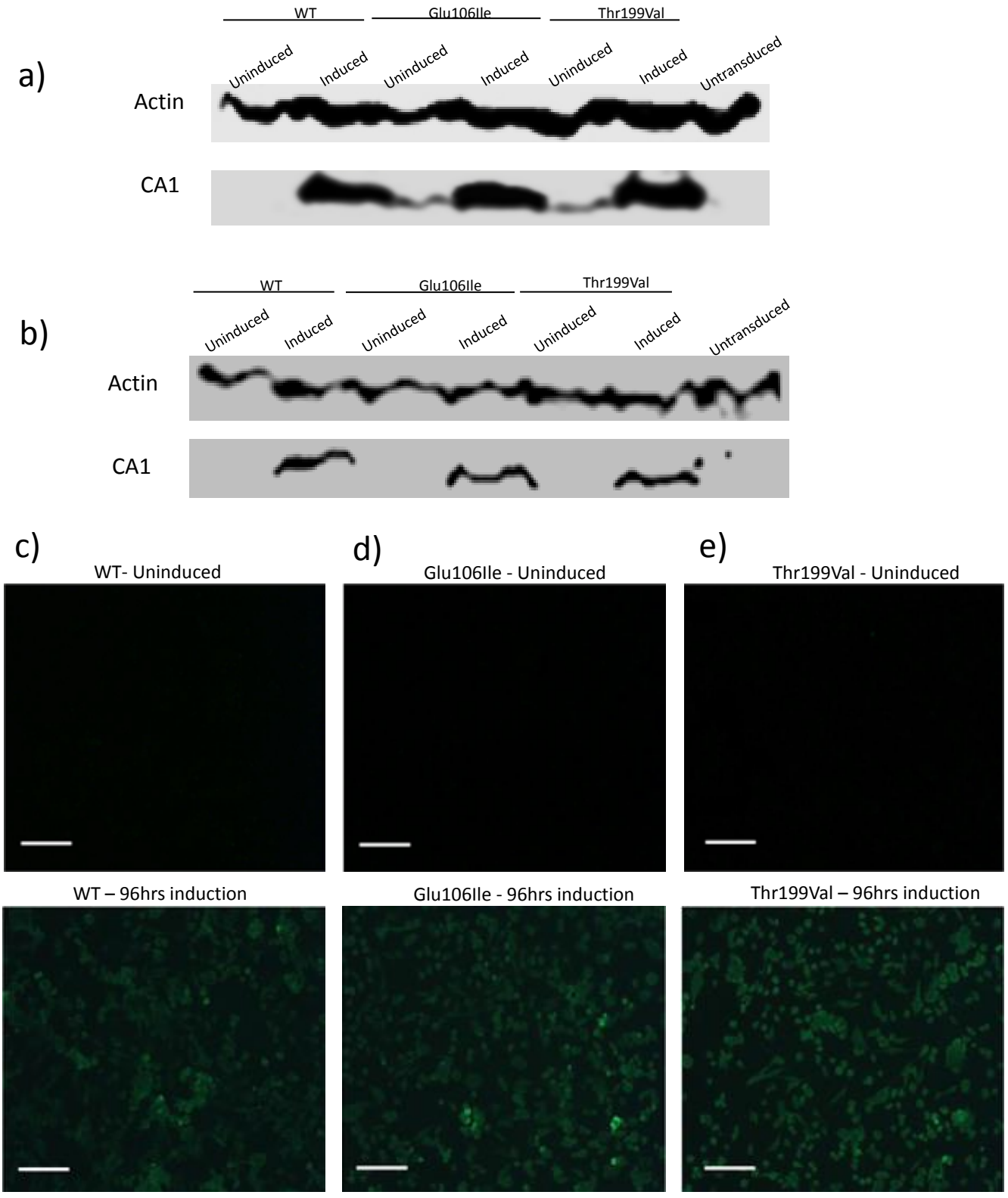

Figure 4.3. Transduced HEK293 and COS7 cells stably express CA1. CA1 protein expressions detected using western blotting in a) HEK293 and b) COS7 cells transduced with wild-type, Glu106Ile and Thr199Valal CA1 lentiviruses induced using doxycycline for 96hrs, Immunofluorescence confirmed CA1 expressions c), d), e) in HEK293 cells induced with doxycycline for 96hrs in green fluorescence. Untransduced cells with doxycycline and cells transduced with CA1 lentivirus without doxycycline induction were used as comparative controls as indicated. Magnification = 200x. Scale bars = 50µm.

Wild-type and mutant CA1 proteins induce toxicity in HEK293 cells

Cell viabilities in HEK293 induced by wild-type and Glu106Ile/Thr199Val mutant CA1 proteins were examined. Figures 4.4a, 4.4b and 4.4c show all three CA1 proteins caused moderate reductions in cell viabilities when compared to the un-induced cells. The levels of reduction were similar between the wild-type and the mutants as shown in Figures 4.4a, 4.4b and 4.4c (25% reduction for wild-type and 26%/19% reductions for Glu106Ile and Thr199Val, respectively at 96hrs; 28% reduction for wild-type and 24%/25% for Glu106Ile and Thr199Val respectively at 144hrs). However, only wild-type CA1 caused statistically significant reductions at both 96hrs and 144hrs compared to the un-induced cells in Figure 4.4a; whereas only Thr199Val mutant CA1-induced significant reduction at 144hrs in Figure 4.4c.

Figure 4.4d and 4.4e show neither general protein expression or addition of doxycycline were responsible for the reductions as no significant differences were observed in cells induced with eGFP expression or untransduced cells treated with doxycycline compared to cells with no doxycycline added.

Figure 4.4f shows when cell viabilities were compared between eGFP-induced sample and wild-type or mutants CA1, there were no statistical significant differences.

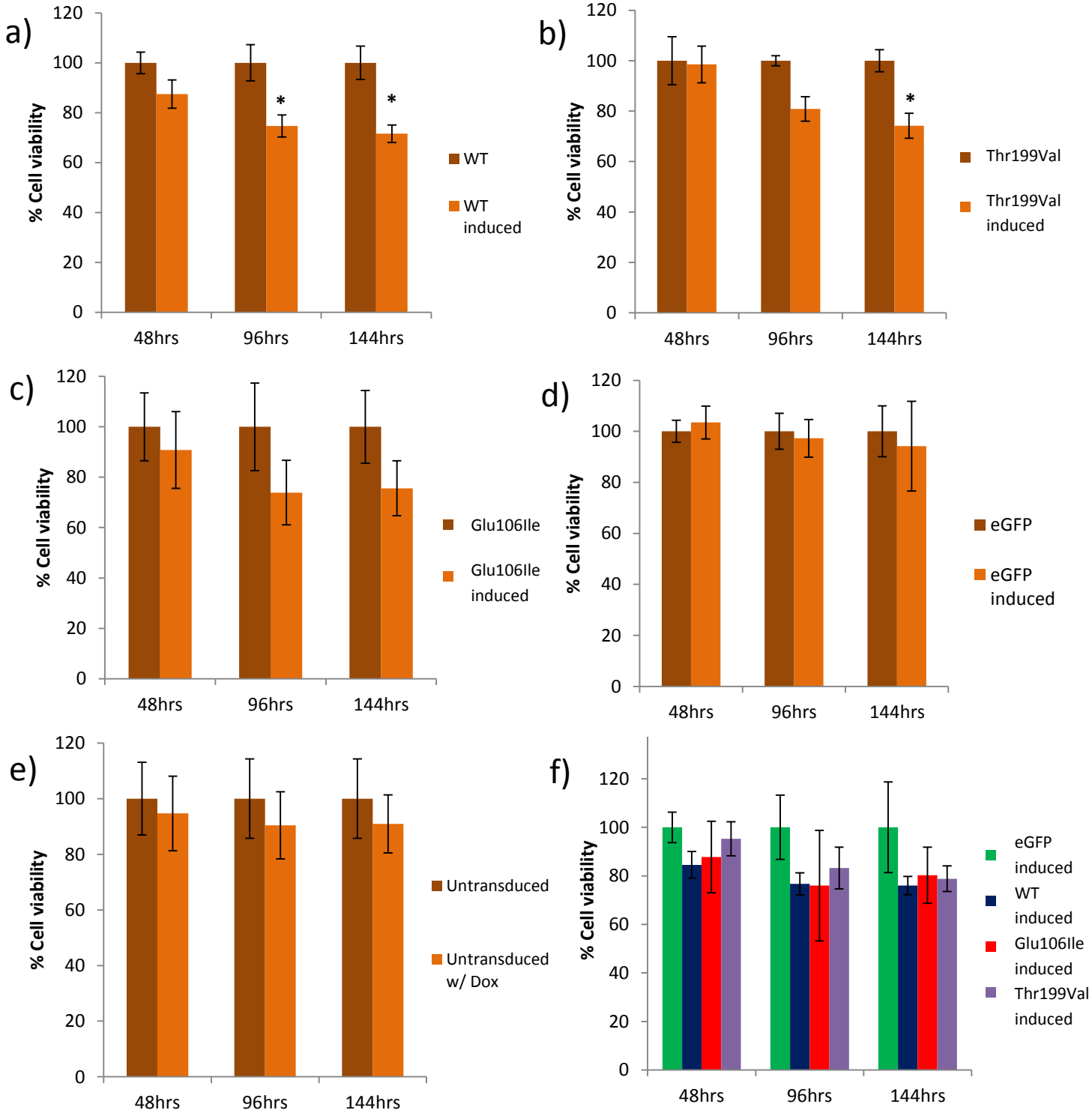

Figure 4.4. CA1 expression causes cell toxicity in HEK293 cells. Cell viabilities (WST8 assay) were examined in HEK293 cells induced with a) wild-type, b) Thr199Val c) Glu106Ile mutants CA1 and e) eGFP expression using 0.25µg/ml of doxycycline at 48hrs, 96hrs and 144hrs of induction. e) HEK293 cells untransduced with lentiviruses treated/not treated with doxycycline F) comparison between induced samples, relative to eGFP. All experiments were repeated as 3 independent experiments with each experiment having 6 independent sample replicates; the figure shows the averages of the 3 experiments, with error bars indicating standard deviations. All percentages were normalized relative to uninduced cell samples. Student's t-tests were done using Microsoft Excel; statistical significant results (with P value <0.05) are labeled with asterisks.

Doxycycline induced significant toxicity in COS7 cells

Figures 4.5d and 4.5e show that in eGFP and untransduced-COS7 cells, the added doxycycline had significantly reduced cell viabilities compared to non-doxycycline-treated cells. There were no significant differences between eGFP and untransduced cells (data analysis not shown); therefore, addition of doxycycline but not eGFP expression caused this toxicity.

Figures 4.5a, 4.5b and 4.5c show noticeable differences in cell viabilities between wild-type CA1 and Glu106Ile/Thr199Val data sets. Cell viabilities were reduced for all three CA1 proteins in induced vs. uninduced cells in the three figures at 144hrs of induction and only mutant CA1 protein induction caused significant loss in cell viabilities at 96hrs.

When normalized to cell viability in eGFP induced cells, figure 4.5f shows viability in wild-type CA1 induced cells was significantly higher at 96hrs; however, no changes were seen between eGFP and CA1 induced cells at 48hrs or 144hrs.

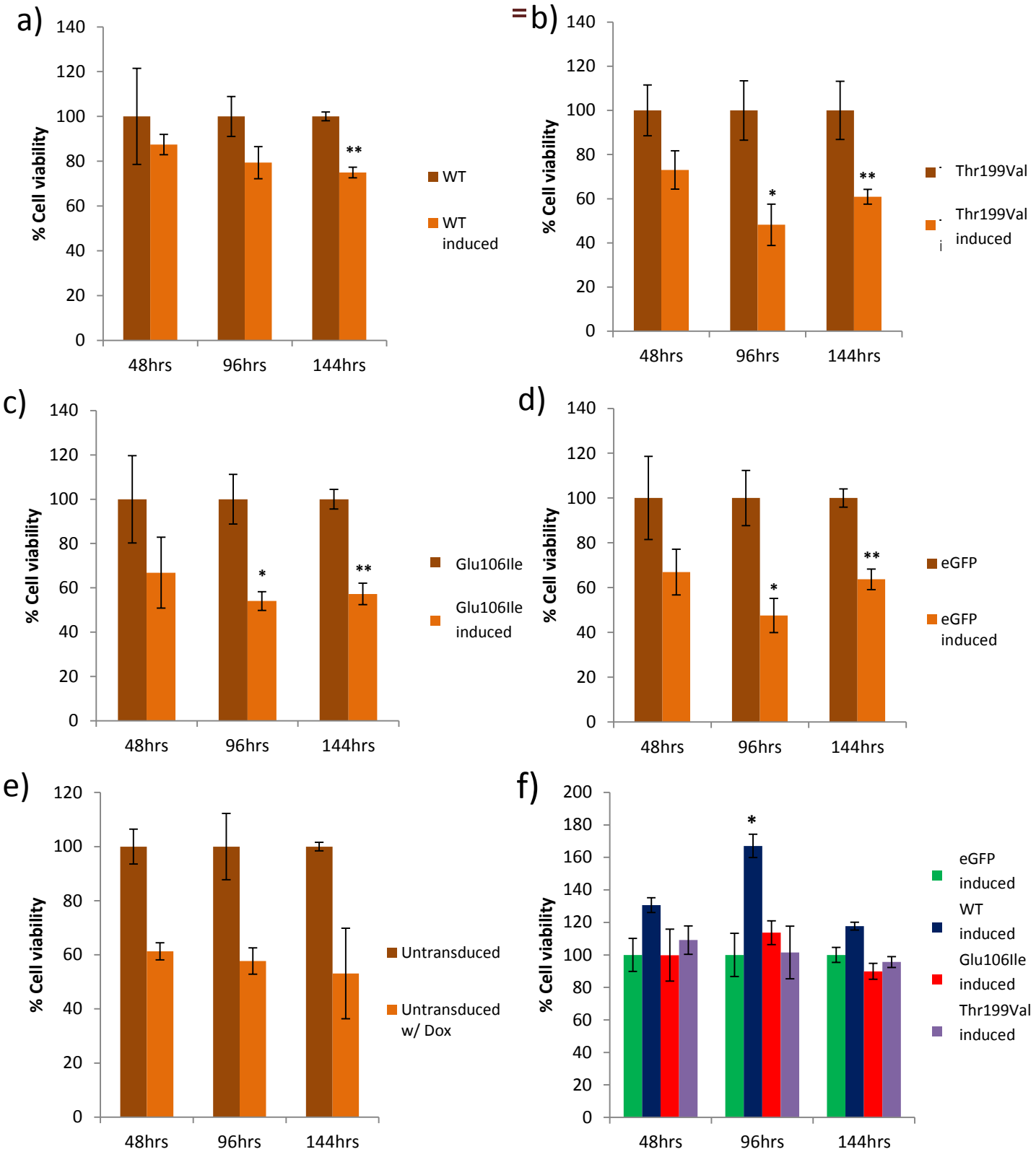

Figure 5.5. Doxycycline induced significant toxicity in COS7 cells. Cell viabilities in COS7 cells induced with a) wild-type, b) Thr199Val c) Glu106Ile mutants CA1 and d) eGFP using 0.25µg/ml of doxycycline at 48hrs, 96hrs and 144hrs of induction e) untransduced with treated/untreated with doxycycline. f) cell viability comparison between induced samples relative to eGFP. All experiments were repeated as 3 independent experiments with each experiment having 6 sample replicates wells; the figure shows the averages of the 3 experiments. All percentages were normalized relative to uninduced cell samples, with error bars indicate standard deviations. Student's t-tests were done using Microsoft Excel; statistical significant results (with P value <0.05) are labeled with asterisks.

Expression of CA1 proteins induces apoptosis in HEK293 cells

Cleavage of PARP-1 (Poly (ADP-Ribose) Polymerase 1) by caspases (cysteinyl-aspartate proteases) is one of the widely recognized hallmarks of apoptosis. It is carried out by Caspase-3 and Caspase-7 (which are activated via cleavage) under *in vivo* conditions and almost all members of caspase family under *in vitro* conditions (Chaitanya et al., 2010, D'Amours et al., 2001). Under low levels of stress, PARP-1 acts as a DNA damage repair protein to maintain genome integrity. However, when there is a high level of cell toxicity, PARP-1 is cleaved. PARP-1 is regulated this way to prevent it from rescuing cells and therefore to allow cells to enter apoptosis when there is a high level of stress; b) to prevent it from being "over-active" which consumes ATP and may activate necrotic processes (Chaitanya et al., 2010). Levels of cleaved Caspase-3 and cleaved PARP-1 were measured to observe apoptosis in HEK293 cells with induced CA1 expression.

As shown in Figure 4.4f, when protein expressions were induced in HEK293 cells, there were noticeable reduced cell viabilities in all CA1-induced cells (wild-type and the Glu106Ile/Thr199Val mutants) compared to eGFP-induced cells at all three time points of induction. Within the figure, it can be seen that the reduction was most obvious at 96hrs with between 20-24% of reductions seen in WST8 assay. Figure 4.6 shows the changes in activation of apoptosis when examined in wild-type and Glu106Ile CA1-induced HEK293 cells using eGFP as control.

Figures 4.6a and 4.6b show wild-type CA1-induced statistically significant increase in both Caspase-3 PARP-1 cleavage (cleaved Caspase-3 - 18% increase, P value = 0.0097; cleaved

PARP-1 - 16% increase, P value = 0.0149). In these two figures, for the Glu106Ile sample, there was statistically significant increase in cleaved Caspase-3 in the induced sample from the uninduced (8% increase, P value = 0.047), whereas the difference in cleaved PARP-1 was not statistically significant (8% increase, P value = 0.089). No noticeable differences were seen for either cleaved Caspase-3 or cleaved PARP-1 levels in eGFP-induced sample.

a)

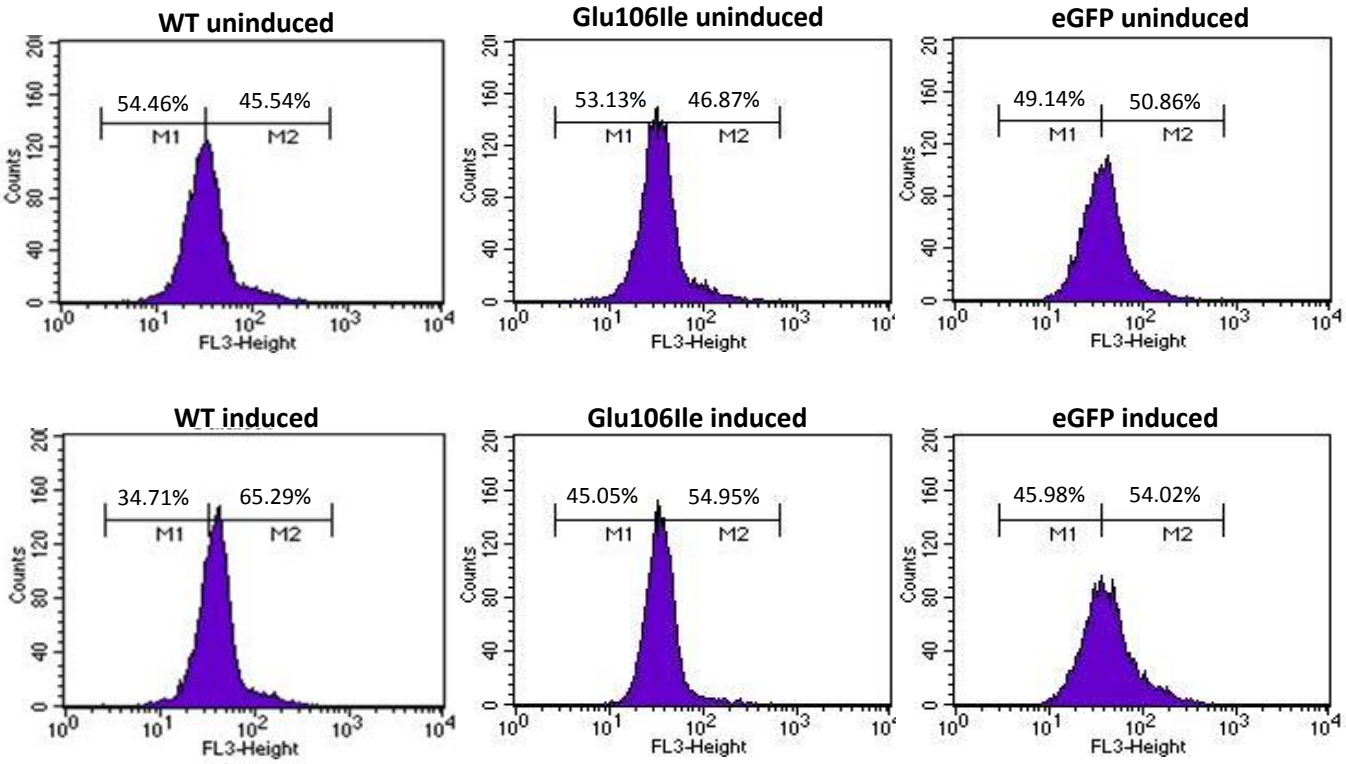

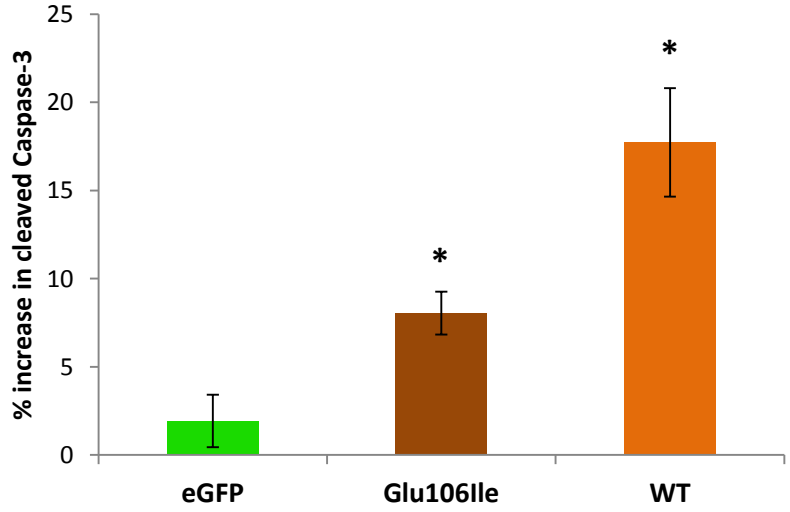

b)

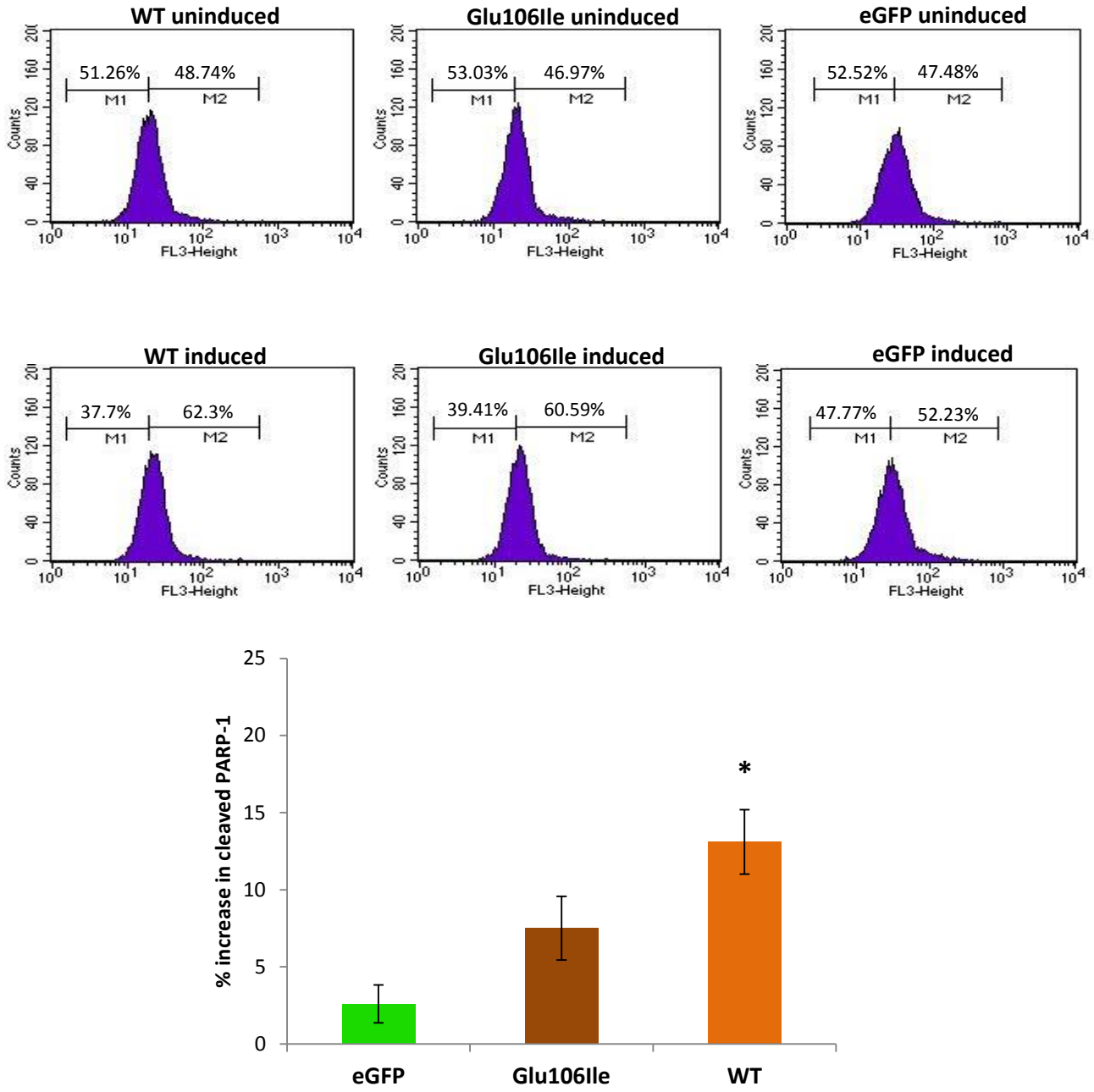

Figure 4.6. CA1 expression increases apoptosis activation in HEK293 cells. Expression of a) cleaved Caspase-3 and b) PARP-1 (flow cytometry assay) in HEK293 cells induced with wild-type, Glu106Ile mutants CA1 and eGFP expression. The histogram is plotted with the cleaved Caspase-3/PARP-1 fluorescence intensity (x-axis) against cell count (y-axis). M1 and M2 gates mark the cell population used to observe fluorescence shift across the x-axis. Bar graphs show percentages increase in induced samples relative to uninduced. All experiments were repeated as 3 independent experiments with each experiment having 3 independent sample replicates; the figure shows the averages of the 3 experiments, with error bars indicating standard deviations. Student's t-tests were done using Microsoft Excel; statistical significant results (with P value <0.05) are labeled with *.

Discussion

The main findings from the study in this chapter are (a) inducing CA1 expression (wild-type and Glu106Ile/Thr199Val mutants) caused reduction in HEK293 cell viabilities; b) wild-type CA1 expression protects COS7 from doxycycline induced cell toxicity; c) both wild-type and Glu106Ile CA1 increase activation of apoptosis in HEK293.

Novel discovery of intracellular CA1-induced toxicity in HEK293 cells

It is apparent that CA1–induced toxicity is not due to general protein expression or addition of doxycycline as eGFP expression as untransduced cells (with addition of doxycycline) did not significantly reduce cell viability at all three time-points (Figure 4.4d, 4.4e). On the other hand, CA1-induced toxicities were within ~25% and the cell viability reductions appeared to level out after 96hrs (Figure 4.4a, 4.4b, 4.4c). However, the effects were significant enough to induce apoptosis in HEK293 for both wild-type and Glu106Ile (Figure 4.6). This finding corroborates with a previous study showing increasing extracellular CA1 protein level elevates cellular apoptosis in human endothelial cells (Torella et al., 2014). Results from Torella *et al* were intriguing as (a) expression of transmembrane CA proteins (CA9 and CA12) functioning at the extracellular surface were believed to be protective (Supuran, 2008, Chiche et al., 2009, Swietach et al., 2007, Cianchi et al., 2010b); (b) this is the only study linking CA1 to apoptosis in a cellular environment as opposed to animal models (Zheng et al., 2012, Gao et al., 2007). However, the main difference between the Torella *et al* study and this study is the method of CA1 expression: the approach in this chapter expressed CA1 protein intracellularly as opposed

to adding CA1 protein directly to the extracellular media. Another previous study has found transmembrane CA4 which acts at the extracellular surface reduces cell viability in human colon epithelial and human colon cancer cells (Zhang et al., 2015a, Supuran, 2008). This difference between the intra- and extra- cellular milieu in which CA1 functions marks these results being the first time showing that intracellularly expressing CA1 is able to cause significant toxicity in mammalian cells.

Wild-type CA1 expression briefly mitigated doxycycline induced toxicity in COS7 cells

The used concentration of doxycycline in COS7 cells caused a significant level of toxicity cell viability (Figure 4.5). This toxicity was not due to general protein expression as cell viability changes in eGFP and untransduced cells were not significantly different (Figure 4.5d, 4.5e, data analysis not shown). Previous studies have demonstrated doxycycline is toxicity in human cell lines causing cell cycle arrest, decreasing cell viabilities and increasing cellular apoptosis; furthermore, the toxicity appears to be cell type-specific (Wu et al., 2006b, Sourdeval et al., 2006, Fife et al., 1997, Xie et al., 2008). Although wild-type CA1 expression mitigated the toxicity at 96hrs, it did not completely restore cells to their healthy states or did it have significant effect on cell viability loss at 144hrs suggesting that the effect was transient and not stable. On the other hand, Glu106Ile/Thr199Val mutants did not protect cells from doxycycline-induced toxicities suggesting that the effect seen at 96hrs could be CA1 activity dependent (Figure 4.5b, 4.5c, 4.5d).

Different response to CA1 may be due to differences in cell-environment

The difference in cellular response to wild-type CA1 expression in HEK293 and COS7 (i.e. CA1 is toxic to HEK293 cells versus being protective in COS7 cells) could be due to effects from CA1 being cell-type specific. However, due to the unwanted doxycycline-induced toxicity in COS7, differences in their CA expression profile (see discussions below and supplementary figure) and the absence of further observations into CA1 activity in the cells, they make speculations whether effects of CA1 are different in different cell lines difficult to consider. Another explanation is the different cellular environments in the two experiments (i.e. COS7 cells under severe toxicity from addition of doxycycline whereas HEK293 cells were not). As CA1 catalyzes the reversible hydration of CO_2 producing bicarbonates and protons, the main outcome of the reaction is the change in cellular pH. The CO_2 released by cell during respiration reaching the cellular membrane is restricted by its diffusion rate; when there is a large amount of CA activity CO_2 can be hydrated yielding protons and lowering intracellular pH (Swietach et al., 2007, Swietach et al., 2009). Therefore, it could be said that both accumulation of CO_2 and/or increase in intracellular CA activity could lower intracellular pH.

It was observed that wild-type CA1 was toxic in HEK293 at 96hrs but not 48hrs (nor at 36hrs of transient expression in chapter three). It is possible there was a rise in intracellular CO_2 from increased respiration due to increased cell densities (eGFP cells density increase in Figure 4.1 was comparable with CA1 sample sets, data not shown). Furthermore, it has been shown that HEK293 cells endogenously express CA2 proteins (Sterling et al., 2001, Lankat-Buttgereit et al., 2004). When a relatively high level of CA1 is also expressed (Figure 4.3) a potentially high

level of CA activity may amplify CO_2 hydration driving intracellular pH to become more acidic and activating apoptosis-associated with intracellular acidification (Barry and Eastman, 1992, Matsuyama et al., 2000).

On the other hand, in COS7 cells undergoing significant toxicity from doxycycline, its respiration level may decrease as previous studies have shown cells undergoing apoptosis have reduced respiration levels (Berghella and Ferraro, 2012, Zhu et al., 2012). The reduced CO_2 production would limit potential intracellular acidification associated with increased CA1 expression. As COS7 do not express the highly active CA2 (Supplementary figure), it would have a relatively lower level of intracellular CA activity to begin with thus further limiting any possible CA associated-acidification from CO_2. Whether the differences seen between the two cell lines are due to differences in cellular environment require further investigation in additional cell types and/or lowering doxycycline concentration to a non-toxic level in COS7 cells. However, lowering doxycycline may compromise its CA1 expression thus possibly limit the effect of CA1 expression.

CA1 mutants causing cellular toxicity and its implications

The speculation that increased CA activity is associated with HEK293 apoptosis is not completely without evidence as only in wild-type CA1 sample set was there significant reduction in cell viability in induced cells at 96hrs (Figure 4.4). However, the large degree of similarity between cell viabilities in wild-type and mutant CA1 sample sets makes it apparent that the mutants could cause a certain degree of toxicity.

Results showing CA1 mutant proteins decreasing HEK293 cell viability (as well as the Glu106Ile mutant increasing HEK293 apoptosis) was unexpected. Results from studies that have identified CA-induced apoptosis (either directly or indirectly) showed the effects were CA activity-dependent – the effects were either associated with CA-induced extracellular alkalinization or was mitigated by inhibition of CA activity (Gao et al., 2007, Shah et al., 2013, Zhang et al., 2015a). But the in vitro measurement of mutant CA1 clearly demonstrated that they do not possess catalytic activities as would have predicted from the literature (Figure 2.10). In addition, the data do suggest the mutants did not retain (or at least had reduced) enzyme activities as there were clear distinctions in cell viability between wild-type and mutant CA1-induced COS7 cells (wild-type CA1 protected cells against doxycycline-associated toxicity whereas the mutants did not). How much activity was reduced was not known; and subsequently how much CA1 activity was needed to induce HEK293 toxicity is not known. Due to the lack of previous studies on association with mutant CA and apoptosis, there is no clear indication of the relationship between CA activity and cell death.

Toxicity has been observed in CA mutants. Mis-folded missense mutants of CA4 induced apoptosis by upregulating endoplasmic reticulum (ER) stress in HEK293 cells (Datta et al., 2009). Furthermore, mutation at the 107 residue in CA2 has been found to mis-fold and prone to aggregation in marble brain syndrome (Almstedt et al., 2004). Whether the CA1 mutants used in this study are able to cause toxicity through aggregation and related ER stress is unknown as mutants at the Thr199 and Glu106 residues do not appear to significantly affect CA2 or CA1 protein folding (Xue et al., 1993a, Mohanty et al., 1998). Speculations on whether the Glu106Ile/Thr199Val CA1 mutants induce cell toxicity through mis-folding and subsequently

upregulated ER stress or the toxicity was enzyme activity-dependent requires further investigation.

To conclude, this study has shown wild-type and mutant CA1 expressions are toxic to HEK293 cells by reducing cell viabilities and inducing apoptosis. Conversely, wild-type not mutant CA1 proteins transiently stabilized doxycycline-induced toxicity in COS7 cells at one time-point and could be CA activity-dependent. However, whether the differences seen between the two cell lines were cellular environment-specific and whether CA1-induced toxicity seen HEK293 cells is CA activity-dependent require further investigation in other cell types and monitoring intracellular CA1 activity levels and ER stress.

References:

AIROLDI, C., COLOMBO, L., MANZONI, C., SIRONI, E., NATALELLO, A., DOGLIA, S. M., FORLONI, G., TAGLIAVINI, F., DEL FAVERO, E., CANTU, L., NICOTRA, F. & SALMONA, M. 2011. Tetracycline prevents A[small beta] oligomer toxicity through an atypical supramolecular interaction. *Organic & Biomolecular Chemistry,* 9**,** 463-472.

ALMSTEDT, K., LUNDQVIST, M., CARLSSON, J., KARLSSON, M., PERSSON, B., JONSSON, B. H., CARLSSON, U. & HAMMARSTROM, P. 2004. Unfolding a folding disease: folding, misfolding and aggregation of the marble brain syndrome-associated mutant H107Y of human carbonic anhydrase II. *J Mol Biol,* 342**,** 619-33.

BARRY, M. A. & EASTMAN, A. 1992. Endonuclease activation during apoptosis: The role of cytosolic Ca2+ and pH. *Biochemical and Biophysical Research Communications,* 186**,** 782-789.

BERGHELLA, L. & FERRARO, E. 2012. Early Decrease in Respiration and Uncoupling Event Independent of Cytochrome c Release in PC12 Cells Undergoing Apoptosis. *International Journal of Cell Biology,* 2012**,** 11.

BONANOMI, M., NATALELLO, A., VISENTIN, C., PASTORI, V., PENCO, A., CORNELLI, G., COLOMBO, G., MALABARBA, M. G., DOGLIA, S. M., RELINI, A., REGONESI, M. E. & TORTORA, P. 2014. Epigallocatechin-3-gallate and tetracycline differently affect ataxin-3 fibrillogenesis and reduce toxicity in spinocerebellar ataxia type 3 model. *Human Molecular Genetics,* 23**,** 6542-6552.

CARDOSO, I. & SARAIVA, M. J. 2006. Doxycycline disrupts transthyretin amyloid: evidence from studies in a FAP transgenic mice model. *The FASEB Journal,* 20**,** 234-239.

CHAITANYA, G. V., ALEXANDER, J. S. & BABU, P. P. 2010. PARP-1 cleavage fragments: signatures of cell-death proteases in neurodegeneration. *Cell Communication and Signaling,* 8**,** 1-11

CHICHE, J., ILC, K., LAFERRIERE, J., TROTTIER, E., DAYAN, F., MAZURE, N. M., BRAHIMI-HORN, M. C. & POUYSSEGUR, J. 2009. Hypoxia-inducible carbonic anhydrase IX and XII promote tumor cell growth by counteracting acidosis through the regulation of the intracellular pH. *Cancer Res,* 69**,** 358-68.

CIANCHI, F., VINCI, M. C., SUPURAN, C. T., PERUZZI, B., DE GIULI, P., FASOLIS, G., PERIGLI, G., PASTOREKOVA, S., PAPUCCI, L., PINI, A., MASINI, E. & PUCCETTI, L. 2010. Selective inhibition of carbonic anhydrase IX decreases cell proliferation and induces ceramide-mediated apoptosis in human cancer cells. *J Pharmacol Exp Ther,* 334**,** 710-9.

D'AMOURS, D., SALLMANN, F. R., DIXIT, V. M. & POIRIER, G. G. 2001. Gain-of-function of poly(ADP-ribose) polymerase-1 upon cleavage by apoptotic proteases: implications for apoptosis. *J Cell Sci,* 114**,** 3771-8.

DATTA, R., WAHEED, A., BONAPACE, G., SHAH, G. N. & SLY, W. S. 2009. Pathogenesis of retinitis pigmentosa associated with apoptosis-inducing mutations in carbonic anhydrase IV. *Proc Natl Acad Sci U S A,* 106**,** 3437-42.

DEL GIUDICE, R., MONTI, D. M., TRUPPO, E., ARCIELLO, A., SUPURAN, C. T., DE SIMONE, G. & MONTI, S. M. 2013. Human carbonic anhydrase VII protects cells from oxidative damage. *Biol Chem,* 394**,** 1343-8.

DIOMEDE, L., CASSATA, G., FIORDALISO, F., SALIO, M., AMI, D., NATALELLO, A., DOGLIA, S. M., DE LUIGI, A. & SALMONA, M. 2010. Tetracycline and its analogues protect Caenorhabditis elegans from β amyloid-induced toxicity by targeting oligomers. *Neurobiology of Disease,* 40**,** 424-431.

FIFE, R. S., ROUGRAFF, B. T., PROCTOR, C. & SLEDGE, G. W., JR. 1997. Inhibition of proliferation and induction of apoptosis by doxycycline in cultured human osteosarcoma cells. *J Lab Clin Med,* 130**,** 530-4.

GAO, B. B., CLERMONT, A., ROOK, S., FONDA, S. J., SRINIVASAN, V. J., WOJTKOWSKI, M., FUJIMOTO, J. G., AVERY, R. L., ARRIGG, P. G., BURSELL, S. E., AIELLO, L. P. & FEENER, E. P. 2007. Extracellular

carbonic anhydrase mediates hemorrhagic retinal and cerebral vascular permeability through prekallikrein activation. *Nat Med,* 13**,** 181-8.

LANKAT-BUTTGEREIT, B., GREGEL, C., KNOLLE, A., HASILIK, A., ARNOLD, R. & GOKE, R. 2004. Pdcd4 inhibits growth of tumor cells by suppression of carbonic anhydrase type II. *Mol Cell Endocrinol,* 214**,** 149-53.

MATSUYAMA, S., LLOPIS, J., DEVERAUX, Q. L., TSIEN, R. Y. & REED, J. C. 2000. Changes in intramitochondrial and cytosolic pH: early events that modulate caspase activation during apoptosis. *Nat Cell Biol,* 2**,** 318-325.

MOHANTY, KANNAN & MAHAJAN 1998. Human carbonic anhydrase I: Effect of specific site mutations on its function. *Journal of Biosciences* 23**,** 12.

MOULLAN, N., MOUCHIROUD, L., WANG, X., RYU, D., WILLIAMS, EVAN G., MOTTIS, A., JOVAISAITE, V., FROCHAUX, MICHAEL V., QUIROS, PEDRO M., DEPLANCKE, B., HOUTKOOPER, RIEKELT H. & AUWERX, J. 2015. Tetracyclines Disturb Mitochondrial Function across Eukaryotic Models: A Call for Caution in Biomedical Research. *Cell Reports,* 10**,** 1681-1691.

ONODA, T., ONO, T., DHAR, D. K., YAMANOI, A. & NAGASUE, N. 2006. Tetracycline analogues (doxycycline and COL-3) induce caspase-dependent and -independent apoptosis in human colon cancer cells. *Int J Cancer,* 118**,** 1309-15.

RAISANEN, S. R., LEHENKARI, P., TASANEN, M., RAHKILA, P., HARKONEN, P. L. & VAANANEN, H. K. 1999. Carbonic anhydrase III protects cells from hydrogen peroxide-induced apoptosis. *Faseb J,* 13**,** 513-22.

ROY, P., REAVEY, E., RAYNE, M., ROY, S., ABED EL BAKY, M., ISHII, Y. & BARTHOLOMEW, C. 2010. Enhanced sensitivity to hydrogen peroxide-induced apoptosis in Evi1 transformed Rat1 fibroblasts due to repression of carbonic anhydrase III. *Febs J,* 277**,** 441-52.

SHAH, G. N., PRICE, T. O., BANKS, W. A., MOROFUJI, Y., KOVAC, A., ERCAL, N., SORENSON, C. M., SHIN, E. S. & SHEIBANI, N. 2013. Pharmacological inhibition of mitochondrial carbonic anhydrases protects mouse cerebral pericytes from high glucose-induced oxidative stress and apoptosis. *J Pharmacol Exp Ther,* 344**,** 637-45.

SOURDEVAL, M., LEMAIRE, C., BRENNER, C., BOISVIEUX-ULRICH, E. & MARANO, F. 2006. Mechanisms of doxycycline-induced cytotoxicity on human bronchial epithelial cells. *Front Biosci,* 11**,** 3036-48.

STERLING, D., REITHMEIER, R. A. & CASEY, J. R. 2001. A transport metabolon. Functional interaction of carbonic anhydrase II and chloride/bicarbonate exchangers. *J Biol Chem,* 276**,** 47886-94.

SUPURAN, C. T. 2008. Carbonic anhydrases: novel therapeutic applications for inhibitors and activators. *Nat Rev Drug Discov,* 7**,** 168-81.

SWIETACH, P., PATIAR, S., SUPURAN, C. T., HARRIS, A. L. & VAUGHAN-JONES, R. D. 2009. The role of carbonic anhydrase 9 in regulating extracellular and intracellular ph in three-dimensional tumor cell growths. *J Biol Chem,* 284**,** 20299-310.

SWIETACH, P., VAUGHAN-JONES, R. D. & HARRIS, A. L. 2007. Regulation of tumor pH and the role of carbonic anhydrase 9. *Cancer Metastasis Rev,* 26**,** 299-310.

TORELLA, D., ELLISON, G. M., TORELLA, M., VICINANZA, C., AQUILA, I., IACONETTI, C., SCALISE, M., MARINO, F., HENNING, B. J., LEWIS, F. C., GARERI, C., LASCAR, N., CUDA, G., SALVATORE, T., NAPPI, G., INDOLFI, C., TORELLA, R., COZZOLINO, D. & SASSO, F. C. 2014. Carbonic anhydrase activation is associated with worsened pathological remodeling in human ischemic diabetic cardiomyopathy. *J Am Heart Assoc,* 3**,** 000434.

TRUPPO, E., SUPURAN, C. T., SANDOMENICO, A., VULLO, D., INNOCENTI, A., DI FIORE, A., ALTERIO, V., DE SIMONE, G. & MONTI, S. M. 2012. Carbonic anhydrase VII is S-glutathionylated without loss of catalytic activity and affinity for sulfonamide inhibitors. *Bioorg Med Chem Lett,* 22**,** 1560-4.

WU, J., LIU, T., XIE, J., XIN, F. & GUO, L. 2006. Mitochondria and calpains mediate caspase-dependent apoptosis induced by doxycycline in HeLa cells. *Cell Mol Life Sci,* 63**,** 949-57.

XIE, J., NAIR, A. & HERMISTON, T. W. 2008. A comparative study examining the cytotoxicity of inducible gene expression system ligands in different cell types. *Toxicology in Vitro,* 22**,** 261-266.

XUE, Y., LILJAS, A., JONSSON, B. H. & LINDSKOG, S. 1993. Structural analysis of the zinc hydroxide-Thr-199-Glu-106 hydrogen-bond network in human carbonic anhydrase II. *Proteins,* 17**,** 93-106.

YOON, J. M., KOPPULA, S., HUH, S. J., HUR, S. J. & KIM, C. G. 2015. Low concentrations of doxycycline attenuates FasL-induced apoptosis in HeLa cells. *Biological Research,* 48**,** 38.

ZHANG, J., TSOI, H., LI, X., WANG, H., GAO, J., WANG, K., GO, M. Y. Y., NG, S. C., CHAN, F. K. L., SUNG, J. J. Y. & YU, J. 2015. Carbonic anhydrase IV inhibits colon cancer development by inhibiting the Wnt signalling pathway through targeting the WTAP–WT1–TBL1 axis. *Gut*.

ZHENG, Y., WANG, L., ZHANG, W., XU, H. & CHANG, X. 2012. Transgenic mice over-expressing carbonic anhydrase I showed aggravated joint inflammation and tissue destruction. *BMC Musculoskelet Disord,* 13**,** 1471-2474.

ZHU, J. H., GUSDON, A. M., CIMEN, H., VAN HOUTEN, B., KOC, E. & CHU, C. T. 2012. Impaired mitochondrial biogenesis contributes to depletion of functional mitochondria in chronic MPP+ toxicity: dual roles for ERK1/2. *Cell Death Dis,* 3**,** e312.

Concluding Remarks: Improved understanding for the role of CA1 in human disease and ALS

Study objective and experimental approach

The investigation began with previously unpublished results showing around two-fold increase of CA1 protein in spinal cords of sporadic ALS patients (Figure 3.1). Whether the increase in expression was regulated or unregulated was unknown; and more importantly, how the increased level of CA1 protein will affect cells was unknown. If regulated, it implies the protein expression was "programmed", therefore likely to be protective under toxic conditions; whereas if unregulated i.e. not inherent and not controlled within the cellular response mechanism, it can escalate disease pathology and can be toxic. Due to the lack of studies that have directly examined the effect of increased CA1 expression in cells, the objective for this study was to examine whether increased CA1 expression will improve cell survival or is toxic leading to cellular death.

To investigate this, mammalian cell cultures were used in this study as they are easily maintained in laboratory conditions and they have high proliferative efficiency. As to the cell lines used, to investigate the role of elevated CA1 protein in cells, one can use cells that endogenously express CA1 and under conditions that may or may not mimic ALS pathology to observe changes to the cellular CA1 expressions. Another is to knock-down endogenous CA1 expression (or using inhibitors and activators to modify CA1 activity) and observe how cells respond to stress. Lastly, one can express CA1 exogenously in cells with the absence of endogenous CA1 expression to monitor changes to cell viability. In reality, all three paradigms

would be complimentary to one another to support this investigation. However, the exogenous expression route was chosen here due to available endogenous CA1 expressing cell lines being limited in number; furthermore, extensive testing has to be done to test numerous cell lines for endogenous CA1 expression dramatically limiting time and financial resources.

Brief summary of results presented in previous chapters

The data presented in chapter two to chapter four have centered around the effect of CA1 on cellular viability and apoptosis. Transient CA1 expression caused minor and non-significant reduction in cell viabilities in three different mammalian cell lines. However, longer time CA1 expression had more noticeable effects. Whereas expression of both wild-type and inactive mutant CA1 significantly reduced HEK293 cell viability, wild-type CA1 expression protected COS7 cells from doxycycline-induced cell toxicity and this protective effect was activity-dependent. Furthermore, the establishment of a simple yet effective immunofluorescence-based technique to measure CA anhydrase activity was also shown, getting around the need for more specialized equipment.

Increased CA1 expression can be toxic to healthy mammalian cells

Results from chapter four show CA1 expression reduced cell viability in HEK293 cells (Figure 4.4). This marks the results being the first time showing that intracellular expression of CA1 is able to cause significant toxicity in mammalian cells. As the physiological role of CA is pH

regulation, within chapter four it was speculated that CA1 hydrolyzed the accumulated intracellular CO_2 generating protons which caused the increase in apoptosis. Indeed, the rate of CO_2-induced intracellular acidification is dependent on CA hydration and the rate of intracellular acidification has been used to measure intracellular CA activity (Klier et al., 2014, Srinivas et al., 2002). Injections of both cytosolic CA2 and membrane-bound CA4 proteins have caused rapid increases in rates of CO_2-induced acidification in oocytes (Klier et al., 2014, Lu et al., 2006). From these results it has been shown that there was no significant CA1-induced toxicity at 36hrs using the transient expression system (Figures 3.2, 3.3 and 3.4). Using the inducible stable cell line system CA1 did not induce significant toxicity at 48hrs but at 96hrs and beyond (Figure 4.4). It appears that prolonged CA1 expression caused the toxicity. However, whether this is associated with CO_2-induced intracellular acidification requires further investigations into the intracellular pH changes under prolonged CA1 expression.

Mutant CA1 generated similar degrees of cell viability reductions in HEK293 as the wild-type (Figure 4.4), suggesting CA activity was not responsible for the toxicity. Indeed, in chapter two the results have shown both Thr199Val and Glu106Ile mutants do not retain any CA activity *in vitro* (Figure 2.10). However, it is possible that mutant CA1 proteins still retained intracellular enzyme activity. When observing CA activity in intact oocyte cells, CA2 His64Ala mutant retained most of its activity whereas the mutant has shown more than 10-fold decrease in turnover number *in vitro* (Tu et al., 1989, Schueler et al., 2011). Furthermore, both CA3 and CA1 have shown significant higher activity in proportion to CA2 in intact cells as compared to *in vitro* data (Becker and Deitmer, 2008, Becker et al., 2011). The possibility that protein expression itself unspecific to CA1 caused the toxicity is unlikely as eGFP expression did not cause changes

to the cell viability (Figure 4.4d). The similarity in the pattern of cell viability reductions in HEK293 cells between wild-type and mutant CA1 expressions suggest the toxicities were caused by the same mechanism (Figure 4.4). These results do suggest the mutants had reduced enzyme activities as wild-type CA1 protected COS7 cells against doxycycline induced toxicity whereas the mutants did not (Figure 4.5). The difference in enzyme activity may explain only wild-type CA1 significantly induced toxicity in HEK293 cells and not the mutants at 96hrs of induction (Figure 4.4).

As the cleavage of PARP-1 by activated Caspase-3 is one of the hallmarks of apoptosis, whether CA1 expression will affect this cellular pathway and if increased activation of apoptosis is associated with the reduced cell viabilities was observed next in the study (D'Amours et al., 2001, Chaitanya et al., 2010). Results from chapter four have shown CA1 expression increased apoptosis activation in HEK293 cells, increasing both Caspase-3 and PARP-1 cleavage at 96hrs of protein induction (Figure 4.6). Although evidence has shown CA inhibitors reduce cellular Caspase-3 activation after exposure to apoptotic agents, the results mark the first time showing CA1 expression is able to directly increase Caspase-3 activation and downstream PARP-1 cleavage (Wang et al., 2009, Fossati et al., 2016, Kniep et al., 2006). The levels of Caspase-3 activation and PARP-1 cleavage are consistently higher in wild-type CA1 compared to the Glu106Ile mutant (Figure 4.6c). However, the increases were modest and were not significant when compared between wild-type and Glu106Ile (data analysis not shown). Therefore, there is no strong evidence to suggest CA1-induced toxicity is activity dependent.

Previous studies have found CA-induced apoptosis activations that were independent of CA activity. Mutant CA4 proteins induced apoptosis in HEK293 and COS7 cells by increased ER stress activation (Datta et al., 2009, Rebello et al., 2004). Wild-type CA4 has shown to induce apoptosis in colon cancer cells by inhibition of the Wnt pathway through protein-protein interactions (Zhang et al., 2015a). To understand whether CA1-induced toxicity is dependent upon CA1 enzyme activity, further experiments that monitor intracellular CA1 activity will help to elucidate the mechanism behind this finding.

Increased CA1 expression can transiently mitigate doxycycline-induced stress

Several reports have demonstrated apoptosis activation in tumor cells exposed to doxycycline through activation of pro-apoptotic genes in the mitochondria (Son et al., 2009, Iwasaki et al., 2002, Wu et al., 2006). Doxycycline inhibits mitochondrial gene expression which disturbs mitochondria function in different eukaryotic cells (Moullan et al., 2015). This may lead to shift in energy production from oxidative phosphorylation to glycolysis, producing more lactate and consuming more glucose and less oxygen which slows proliferation in mammalian cells (Ahler et al., 2013). The lactate produced from increased glycolysis can dissociate into lactate anions and protons that accumulate within the cell to cause intracellular acidosis (Hertz and Dienel, 2005).

Results from chapter four has shown wild-type CA1 expression reduced doxycycline associated toxicity in COS7 cells whereas mutant CA1 expression did not at 96hrs of induction

(Figure 4.5). This suggests the protection is dependent upon CA1 enzyme activity – by eliminating the intracellular protons by speeding up its reaction with HCO_3^- to generate CO_2.

Previous study has shown COS7 express NBCe1 endogenously which responsible for HCO_3^- influx (Shirakabe et al., 2006). CA1 has been found to enhance the activity of the electrogenic Na^+-HCO_3^- cotransporter NBCe1 in the transmembrane of intact *Xenopus* oocytes (Schueler et al., 2011). NBCe1 is one of the main transporters in the cell transmembrane responsible for influx of HCO_3^- thus responsible for cellular alkalinization acting as acid extruders (Casey et al., 2010). With increased CA1 expression enhancing the action of NBCe1, it is possible that the exogenously expressed CA1 in the experiments mitigated the potential intracellular acidosis associated with doxycycline protecting the cells from toxicity (Figure 4.4) (Schueler et al., 2011). However, without endogenously expressing the highly active CA2 (Supplementary figure) the cells may not be restored to full viability. As glycolysis only generates 2 ATPs per glucose molecule, whereas oxidative phosphorylation generates up to 30 ATPs per glucose molecule, the inefficiency in ATP production may further hinder cells to restore to their healthy state (Berg et al., 2012). However, due to the results showing wild-type CA1 only stabilized cell viability at one time-point suggests the any effect associated with wild-type CA1 was transient.

Summary

In summary, the above has discussed the speculations as to how CA1 may protect COS7 cells from doxycycline induced toxicity and how CA1 may cause toxicity and increase apoptosis in HEK293 cells.

Within HEK293 cells, it was found for the first time induced CA1 expressions cause significantly reduced cell viability and cause significant increased activation of the Caspase-3 cascade which also led to significant increase in downstream PARP-1 cleavage. Within this chapter it was discussed whether the toxicity was CA1 catalytic activity dependent. From one perspective, the toxicity may be due to increased intracellular CO_2 from accumulated cell density producing protons at a faster rate. However, as the cell viability changes were similar between wild-type and mutant CA1-induced cells, there is no strong evidence to conclude whether the toxicities seen in HEK293 cells were CA1 catalytic activity dependent.

Within COS7 cells, CA1 expression may optimize cellular pH from possible doxycycline induced intracellular acidosis by increasing the rate of intracellular proton elimination as it speeds up the protons reacting with HCO_3^-. Furthermore, it may enhance the activity of NBCe1 bicarbonate co-transporters to increase cellular HCO_3^- influx. However, due to inefficient energy production via possible increased reliance upon glycolysis the cells were not able to restore their full viability.

Although the study has identified the mutant CA1 being catalytically inactive using the *in vitro* approach, by monitoring the intracellular CA1 activity would help to answer whether CA1 enzyme activity is associated with the toxic effects seen in HEK293 and will confirm the findings

in COS7 cells. To conclude, this study has highlighted the CA1 expression could transiently stabilize cell viability loss in mammalian cells from doxycycline-induced toxicity. In particular, the study for the first time shows intracellular CA1 expression is able to inflict significant toxicity in mammalian cells through increased activation of the Caspase-3 apoptosis cascade.

CA has been long been established to be central players in the nervous system, playing important roles in the maintenance of intracellular and extracellular neuronal pH and ion concentrations, propagation of neuron activities and central nervous system energy metabolism (Chesler and Kaila, 1992, Chesler, 2003, see "Role of CA in the nervous system" on Page 32). However, how CA affects the human neuro-muscular activities are not well documented and there is a general lack of understanding of the role of CA play in ALS. Preliminary data from Dr. Liu (Figure 3.1) showing increased CA1 expression in the spinal cords of ALS patients, and the lack of clear answers to the basic question of how CA1 can affect cell survival in cellular expression systems formed the basis for this study. Results presented here suggest when healthy cells express increased levels of CA1 it can lead to upregulation of downstream apoptosis; alternatively, when cells undergo stress CA1 can be protective to prevent further loss in cell viabilities. How these data will translate into ALS will require further investigation into the effect of CA1 in ALS-related cell types and disease environment. However, the results presented in this study calls for better understanding of CA1 in ALS, and its pH regulatory enzyme function in the disease.

References:

AHLER, E., SULLIVAN, W. J., CASS, A., BRAAS, D., YORK, A. G., BENSINGER, S. J., GRAEBER, T. G. & CHRISTOFK, H. R. 2013. Doxycycline Alters Metabolism and Proliferation of Human Cell Lines. *PLoS ONE,* 8**,** 645-61.

BECKER, H. M. & DEITMER, J. W. 2008. Nonenzymatic proton handling by carbonic anhydrase II during H+-lactate cotransport via monocarboxylate transporter 1. *J Biol Chem,* 283**,** 21655-67.

BECKER, H. M., KLIER, M., SCHÜLER, C., MCKENNA, R. & DEITMER, J. W. 2011. Intramolecular proton shuttle supports not only catalytic but also noncatalytic function of carbonic anhydrase II. *Proceedings of the National Academy of Sciences of the United States of America,* 108**,** 3071-3076.

BERG, J. M., TYMOCZKO, J. L. & STRYER, L. 2012. *Biochemistry,* New York, W. H. Freeman and Co., 7th edition, 468, 555

CASEY, J. R., GRINSTEIN, S. & ORLOWSKI, J. 2010. Sensors and regulators of intracellular pH. *Nat Rev Mol Cell Biol,* 11**,** 50-61.

CHAITANYA, G. V., ALEXANDER, J. S. & BABU, P. P. 2010. PARP-1 cleavage fragments: signatures of cell-death proteases in neurodegeneration. *Cell Communication and Signaling,* 8**,** 1-11.

CHESLER, M. 2003. Regulation and Modulation of pH in the Brain. *Physiological Reviews,* 83**,** 1183-1221.

CHESLER, M. & KAILA, K. 1992. Modulation of pH by neuronal activity. *Trends in Neurosciences,* 15**,** 396-402.

D'AMOURS, D., SALLMANN, F. R., DIXIT, V. M. & POIRIER, G. G. 2001. Gain-of-function of poly(ADP-ribose) polymerase-1 upon cleavage by apoptotic proteases: implications for apoptosis. *J Cell Sci,* 114**,** 3771-8.

DATTA, R., WAHEED, A., BONAPACE, G., SHAH, G. N. & SLY, W. S. 2009. Pathogenesis of retinitis pigmentosa associated with apoptosis-inducing mutations in carbonic anhydrase IV. *Proc Natl Acad Sci U S A,* 106**,** 3437-42.

FOSSATI, S., GIANNONI, P., SOLESIO, M. E., COCKLIN, S. L., CABRERA, E., GHISO, J. & ROSTAGNO, A. 2016. The carbonic anhydrase inhibitor methazolamide prevents amyloid beta-induced mitochondrial dysfunction and caspase activation protecting neuronal and glial cells *in vitro* and in the mouse brain. *Neurobiology of Disease,* 86**,** 29-40.

HERTZ, L. & DIENEL, G. A. 2005. Lactate transport and transporters: general principles and functional roles in brain cells. *J Neurosci Res,* 79**,** 11-8.

KLIER, M., ANDES, F. T., DEITMER, J. W. & BECKER, H. M. 2014. Intracellular and Extracellular Carbonic Anhydrases Cooperate Non-enzymatically to Enhance Activity of Monocarboxylate Transporters. *Journal of Biological Chemistry,* 289**,** 2765-2775.

KNIEP, E. M., ROEHLECKE, C., OZKUCUR, N., STEINBERG, A., REBER, F., KNELS, L. & FUNK, R. H. 2006. Inhibition of apoptosis and reduction of intracellular pH decrease in retinal neural cell cultures by a blocker of carbonic anhydrase. *Invest Ophthalmol Vis Sci,* 47**,** 1185-92.

LU, J., DALY, C. M., PARKER, M. D., GILL, H. S., PIERMARINI, P. M., PELLETIER, M. F. & BORON, W. F. 2006. Effect of Human Carbonic Anhydrase II on the Activity of the Human Electrogenic Na/HCO_3^- Cotransporter NBCe1-A in Xenopus Oocytes. *Journal of Biological Chemistry,* 281**,** 19241-19250.

REBELLO, G., RAMESAR, R., VORSTER, A., ROBERTS, L., EHRENREICH, L., OPPON, E., GAMA, D., BARDIEN, S., GREENBERG, J., BONAPACE, G., WAHEED, A., SHAH, G. N. & SLY, W. S. 2004. Apoptosis-inducing signal sequence mutation in carbonic anhydrase IV identified in patients with the RP17 form of retinitis pigmentosa. *Proc Natl Acad Sci U S A,* 101**,** 6617-22.

SCHUELER, C., BECKER, H. M., MCKENNA, R. & DEITMER, J. W. 2011. Transport Activity of the Sodium Bicarbonate Cotransporter NBCe1 Is Enhanced by Different Isoforms of Carbonic Anhydrase. *PLoS ONE,* 6**,** e27167.

SHIRAKABE, K., PRIORI, G., YAMADA, H., ANDO, H., HORITA, S., FUJITA, T., FUJIMOTO, I., MIZUTANI, A., SEKI, G. & MIKOSHIBA, K. 2006. IRBIT, an inositol 1,4,5-trisphosphate receptor-binding protein, specifically binds to and activates pancreas-type Na^+/HCO_3^- cotransporter 1 (pNBC1). *Proceedings of the National Academy of Sciences of the United States of America,* 103**,** 9542-9547.

SRINIVAS, S. P., ONG, A., ZHAI, C.-B. & BONANNO, J. A. 2002. Inhibition of Carbonic Anhydrase Activity in Cultured Bovine Corneal Endothelial Cells by Dorzolamide. *Investigative Ophthalmology & Visual Science,* 43**,** 3273-3278.

TU, C. K., SILVERMAN, D. N., FORSMAN, C., JONSSON, B. H. & LINDSKOG, S. 1989. Role of histidine 64 in the catalytic mechanism of human carbonic anhydrase II studied with a site-specific mutant. *Biochemistry,* 28**,** 7913-8.

WANG, X., FIGUEROA, B. E., STAVROVSKAYA, I. G., ZHANG, Y., SIRIANNI, A. C., ZHU, S., DAY, A. L., KRISTAL, B. S. & FRIEDLANDER, R. M. 2009. Methazolamide and Melatonin Inhibit Mitochondrial Cytochrome C Release and Are Neuroprotective in Experimental Models of Ischemic Injury. *Stroke; a journal of cerebral circulation,* 40**,** 1877-1885.

ZHANG, J., TSOI, H., LI, X., WANG, H., GAO, J., WANG, K., GO, M. Y. Y., NG, S. C., CHAN, F. K. L., SUNG, J. J. Y. & YU, J. 2015. Carbonic anhydrase IV inhibits colon cancer development by inhibiting the Wnt signalling pathway through targeting the WTAP–WT1–TBL1 axis. *Gut*. 2015; e-pub ahead of print 12 June 2015

SUPPLEMENTARY FIGURE

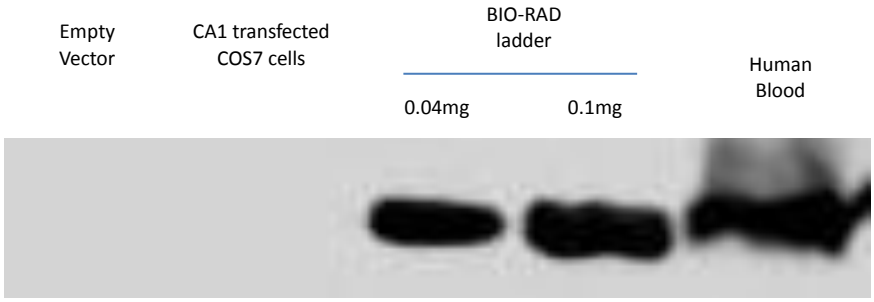

Supplementary figure. COS7 cells do not express detectable amount of endogenous CA2 proteins. Western blot analysis of COS7 cells transfected with empty pcDNA3.1 (+) vector (empty vector) and pcDNA3.1(+)-CA1 (human wild-type *CA1*) plasmid. CA1-transfected COS7 cells previously shown to express CA1 proteins were used as control for any cross-reactions between CA1 and CA2 antibodies. Bio-Rad molecular weight ladder containing bovine CA2 was used as the positive control for CA2 (0.04mg and 0.1mg indicate total amount of ladder protein loaded to the SDS gel, expected CA2 protein size is ~26kDa) (#161-0317, Bio-RaD, California, USA). 5µl of lysed human blood was loaded to the gel as the positive control for CA2 expression

APPENDICES

Primer names	Primer sequences
F1	5’-TACTGGCTTATCGAAATTAATACGACTCACTATAGGG-3’
R1	5’- TGGCAACTAGAAGGCACAGTCGAGG-3’
F2	5'-GAGCATGGTTCAatcCATACAGTGGATGG-3'
R2	5'-ATCCACTGTATGgatTGAACCATGCTCATT-3'
F3	5’-CCTGGCTCTCTGgtTCATCCTCCTC-3’
R3	5’-AAGAGGAGGATGAacCAGAGAGCCAGG-3’
F4	5’-TGAGCATGGTTCAcaaCATACAGTGG-3’
R4	5’-TCCACTGTATGttgTGAACCATGCTCA-3’

Appendix 1. Primer sequences for generating mutant CA1 plasmids. The mutants DNA sequences were generated *CA1* pcDNA3.1+ plasmid using the two round PCR approach shown above. The lower case letters show where the mutation is, and the primer sequences used are from Mohanty *et al* (Mohanty et al., 1998)

Primer name	Primer sequences
F5	5’-TGACCATATGGTGAGCAAGGGCGAG-3’
R5	5'TGACAAGCTTTCAATGATGATGATGATGATGAAATGAAGCTCTCACTG-3'

Appendix 2. Primer sequences for generating his-tagged wild-type and mutant CA1 proteins.

Plasmid name	Vector source	Insert	Size (bp)	Resistance
pcDNA3.1-CA1	Invitrogen	Human wild-type CA1	6810	Ampicillin
pcDNA3.1-CA1-Glu106Ile	Invitrogen	Human Glu106Ile CA1	6810	Ampicillin
pcDNA3.1-CA1-Thr199Val	Invitrogen	Human Thr199Val CA1	6810	Ampicillin
pcDNA3.1-CA1-Glu106Gln	Invitrogen	Human Glu106Gln CA1	6810	Ampicillin
pRSETC-CA1-His	Dr. Meng-Hue Lee	Human wild-type CA1-6xHistag	3717	Ampicillin
pRSETC-CA1-Glu106Ile	Dr. Meng-Hue Lee	Human Glu106Ile CA1-6xHistag	3717	Ampicillin
pRSETC-CA1-Thr199Val	Dr. Meng-Hue Lee	Human Thr199Val CA1-6xHistag	3717	Ampicillin
pRSETC-CA1-Glu106Gln	Dr. Meng-Hue Lee	Human Glu106Gln CA1-6xHistag	3717	Ampicillin
€885pTRIPZ spezial CA1 WT	Dr. Ferdinand Kappes	Human wild-type CA1	13800	Ampicillin
€885pTRIPZ spezial CA1 Glu106Ile	Dr. Ferdinand Kappes	Human Glu106Ile CA1	13800	Ampicillin
€885pTRIPZ spezial CA1 Thr199Val	Dr. Ferdinand Kappes	Human Thr199Val CA1	13800	Ampicillin
pTRIPZ spez eGFP CA1 WT	Dr. Ferdinand Kappes	Human wild-type CA1	13800	Ampicillin
pTRIPZ spez eGFP CA1 Glu106Ile	Dr. Ferdinand Kappes	Human Glu106Ile CA1	13800	Ampicillin
pTRIPZ spez eGFP CA1 Thr199Val	Dr. Ferdinand Kappes	Human Thr199Val CA1	13800	Ampicillin
psPAX2 – Lentiviral packaging plasmid	Dr. Ferdinand Kappes	N/A	10703	Ampicillin
VSV-G – Lentiviral envelope plasmid	Dr. Ferdinand Kappes	N/A	5824	Ampicillin

Appendix 3. Summary of plasmids.